Effects of hormones, genetics, and sex on typical and atypical brain organization

Richard Alexander Ingmar Bethlehem

Department of Psychiatry

University of Cambridge

This dissertation is submitted for the degree of

Doctor of Philosophy

King's College Cambridge May 2017

"Study the art of science. Develop your senses. Especially learn how to see. Realize that everything connects to everything else"

Leonardo Da Vinci

Declaration

I hereby declare that except where specific reference is made to the work of others, the contents of this dissertation are original and have not been submitted in whole or in part for consideration for any other degree or qualification in this, or any other University. This dissertation is the result of my own work except where specifically indicated in the text. This dissertation contains less than 65,000 words including appendices, bibliography, footnotes, tables and equations and has less than 150 figures. Due to the collaborative nature of science in general and the work presented here in particular the first-person plural ("we") is used throughout this thesis. Below is an overview of contributions to each chapter.

Chapter 2 of this thesis is the result of a collaboration with the Brain Mapping Unit. Specifically, Professors Ed Bullmore and Simon Baron-Cohen, Dr Rafael Romero-Garcia and Dr Elijah Mak. I initiated this collaboration, led the project, performed the analyses and wrote the manuscript. This chapter is also currently in revision at *Cerebral Cortex* and available on BiorXiv (Bethlehem, Romero-Garcia, Mak, Bullmore, & Baron-Cohen, 2017).

Chapter 3 of this thesis is a follow up to the collaboration of Chapter 2 and also included Professors Ed Bullmore and Simon Baron-Cohen, Dr. Rafael Romero-Garcia and Varun Warrier. Again, I led the project, performed the analyses and wrote the manuscript. This chapter has also been submitted as a stand-alone paper and is currently under review.

Chapter 4 of this thesis includes data obtained from the MRC-AIMS consortium collected at Kings College London and Cambridge University. This is a large collaboration that has since been extended across Europe (EU-AIMS). The data presented in this chapter were not collected by me. The study was designed by me, I performed all the analyses and wrote the manuscript.

Chapter 5 of this thesis is the result of a larger collaboration initiated by myself, Owen Parsons and Dr Jan Freyberg while we were all still graduate students at the Autism Research Centre in Cambridge. This project has since been extended to include data collection at the Centre for Research on Autism and Education (Dr. Anna Remmington), with plans to collect another dataset at Harvard University (Dr. Caroline Robertson). Data collection on this project is still ongoing and data presented here should be considered as preliminary pilot data. Again I led the project, collected the data, ran the analyses and wrote the manuscript.

Chapter 6 of this thesis was conducted in collaboration with multiple researchers affiliated with the Autism Research Centre in Cambridge (Drs. Michael Lombardo, Bonnie Auyeung, Meng-Chuan Lai and Professor Simon Baron-Cohen) and others in Cambridge and abroad (Drs. Valerie Voon, Prantik Kundu, Sentil Soubramanian, Akeem Sule and Julia Deakin). Again, I led the project, performed the analyses and wrote the manuscript. This chapter was recently published at *Translational Psychiatry* (Bethlehem et al., 2017).

Chapter 7 of this thesis is the direct result of a collaboration with the group of Professor Jack van Honk at Utrecht University and the University of Cape Town (Drs. Peter Bos and David Terburg and Professor Dan Stein). During my doctoral research I spent two months at the University of Cape Town conducting this study as part of an MRC partnership grant awarded to me in my second year. For this study I collected the resting-state imaging data, analysed all the connectivity data and co-wrote the manuscript with Dr. David Terburg and Sarah Heany. This chapter has also been submitted as a stand-alone paper and is currently under review.

Richard A.I. Bethlehem

May 2017

Acknowledgements

No thesis or research project is possible without the help of a lot of different people. First and foremost of course my supervisors: Simon and Jack. When I started at the ARC as a research intern it was Jack that helped me get a foot in the door by emailing Simon. Leaving me under the impression that they were already good friends, only to find out after I arrived that they had actually never met in person. Clearly this has not stood in the way of many years of fruitful collaboration by now, which I hope we can continue to keep going for the foreseeable future!

Simon, I am immensely grateful for all the support you have given me these past years. You have always made Cambridge feel like a second home to me. You are undoubtedly one of the kindest people I have ever met and I can not begin to thank you for the immense personal support you have given me at times when I struggled. I believe the surfing metaphor of "just riding it out" that you introduced has certainly helped me through tough times more than once. I can only hope that in our continuing conversations I can keep repaying you with the same kindness. As a researcher you have always given me complete autonomy, which I appreciate enormously and which I know is not always the case when people pursue a PhD. I would like to think this worked out well for the both of us, but it has certainly kept my motivation and enthusiasm for science going these past years. I hope we can keep this up for many years to come!

Jack, as I mentioned you were the person that got me into Cambridge in the first place. First as an intern and then with your immortal reference letter for my PhD application that only read: 'I hope Richard stays at Utrecht for his PhD'. I am quite sure that the application committee in

Cambridge has never seen such a short and powerful reference. As a researcher you have always kept me on my toes with a pleasant mix of slight madness and criticism that I believe led to two excellent papers on oxytocin. You were a very gracious host when I came to visit you in Cape Town and I still admire your enthusiasm for jumping into that insanely cold ocean and encouraging me to do the same to get over my jetlag only 3 hours after stepping of the plane. The research you are doing there is absolutely unique and fascinating and I hope we get more opportunities again in the future to collaborate on hormones and brains.

During my time at the ARC there have been a lot of different graduate students and post-docs that have helped me over the years and I am grateful to everyone there, but some deserve explicit mention.

Mike, when I started with an internship at the ARC you mentored me through many coding and statistics issues for which I am very grateful and which have proven invaluable skills these past years. I always appreciated the "my door is always open" policy and it is truly a shame we no longer share the same corridor for me to stroll down so I could start an hour long discussion on how to deal with some statistics issue. It is actually somewhat surprising that we had to wait till my third year as a graduate student before we actually wrote a paper together. I can wholeheartedly say that that has been an absolute pleasure and probably one of the smoothest co-writing processes I have ever gone through. There is definitely more data where that came from so I hope we can repeat that experience again in the near future!

Meng-Chuan, you were my daily supervisor during my internship but more than that you have been a great friend these past years. You were the first to induct me into the field of neuroimaging and I can only imagine how much patience that must have taken at times. You

have also always been a wealth of knowledge when it came to autism and/or gender differences in autism, an area of research you have truly taken to the next level. Luckily the world is a small place that allows regular trips across the big pond to catch up so I hope we will be seeing each other around and share many more interesting meals across the world.

Bonnie, we have been working on oxytocin for a while now and I still remember us haggling with pieces of tape, cloth and cardboard in an effort to get the most reliable setup for our eye-tracking interviews. Someone could have surely made a sketch of skype-conversations taking place between people in adjacent rooms just to test whether it was all working. All while we were perfectly able to just have the same conversation through the wall. You always took a lot of effort to make everyone feel at home at the ARC and to make sure everything was running smoothly. Something that you have, in my opinion, done an excellent job at! Thanks again for making the ARC such a fun place to be.

I am also very grateful to my two longest running office mates and fellow graduates: Varun and Jan. Jan, I can only admire your patience having to share an office with me. I am pretty sure not two days would go by without me turning around and starting a question with: “Jan, you are pretty good with Matlab right?”. I always enjoyed our chats and whiteboard scribbling’s. It was fun trying to figure out EEG analyses together and its nice to see that we have now both also developed an interest in using/learning Python. I am sure there will be a time in the future where we share an office again and my daily question will start with “Jan, you are pretty good with Python right?”.

Varun, you have inducted me into the wondrous world of genetics and transcriptomics and I can only hope I have given you a good flavor of neuroimaging. It was enormously fun to see

both our research interests develop in that direction and I am sure we will definitely have lots of successful and fun collaborative imaging genetics projects to work on in the future. The imaging genetics project we worked on as part of this thesis was probably the fastest and smoothest interdisciplinary project I have worked on. You definitely kept me sharp at times where I was getting fed up with the mathematics of it all and you insisted we meet with your housemates from the mathematics department to make sure we understood everything down to minute details. If there is anyone from our cohort of graduate students that I would predict to be a professor running his or her own group within the next ten years, it will certainly be you. Either that or we will see you winning University Challenge. Besides an amazing labmate you have also been a terrific travel buddy (have we not technically been on 4 continents now?). I thoroughly enjoyed you showing me around India and our trips to Morocco, Romania and the US!

Owen, we only shared an office for a short while before getting lost in an office reorganization. We did however travel quite a bit and just know that if I ever need a travel buddy to bring games you will be definitely the first person on my list! On our next trip we should definitely go surfing again, if only to wash away our near-drowning experience in San Diego.

Of course none of this work would have been possible without significant help from a lot of volunteers that donated their time and effort by taking part in my studies. I am immensely grateful to all of them. I would also not have been able to get this far without more than significant support from several funders. Not in the least the Autism Research Trust who graciously funded most of my oxytocin research and my current fellowship. I am also grateful to the Medical Research Council, Cambridge Trust and Pinsent Darwin Trust for funding me during my PhD.

Although the research that goes into a PhD took me 3,5 years, the journey that brought me here started much earlier. The reason I made it this far can undoubtedly be attributed to three very important people.

First of all, both of my parents. You always tell me that from the moment I could talk I never really stopped, other than to sleep or eat perhaps. As exhausting as that must have been you never failed to stimulate my curiosity for the world around us. You would never got annoyed with me asking endless questions and I honestly think that this is one of the most fundamental traits to be cherished in research. So thank you for nurturing that element in me! Both of you have of course also given me the confidence to make my own decisions and follow my own path. I am sure that my initial choice to study philosophy was probably not the first thing that would have come to mind as the degree you imagined your son to do. However, even if there was any doubt about its usefulness you always stood by me and gave me the freedom to chase my own dreams. Without that I would have never ended up where I am now.

Lastly, Claudia; you already know how important a contribution you have been to my personal, (and also professional) development as a more complete human being. From the moment I met you, you showed me a whole new side of humanity that can only be described as eye-opening and truly inspirational. At times you must have thought you were living with an emotionally immature child in what sometimes could have been described as a mental institution (from people in weird hotdog costumes, to housemates' borderline girlfriends or boyfriends and housemates slipping into gambling habits), but I like to think some of your strength has rubbed off on me over the years making me better person in the process. We met when I was still doing philosophy and trying to figure out what to do with my future. You were the first to recognize

my interest in the human psyche and encourage me to pursue a further degree in that direction. You have never shied away from being a critical thinker and you absolutely helped me become more self-critical as a person and a researcher. You also opened my eyes to the joys of having pets around and I am sure Mozart, Samson and Sylvester are still grateful to you for that. You are the most inspirational, caring, kind, creative, open-minded and strongest person I have ever met and I am sure that a bright future for you still lies ahead in whatever direction you decide to steer it.

Abstract

The first part of this thesis discusses developmental influences on the human connectome in relation to autism and attention deficit hyperactivity disorder (ADHD), conditions associated with alterations in brain connectivity and marked by social impairments. It reports an experiment investigating whether the connectomes of individuals with autism or ADHD differ from the connectome of neurotypical individuals, and what the underlying genetic basis could be for any differences in neural architecture. Chapter 2 reports an analysis of networks in children with autism or ADHD, using structural covariance magnetic resonance imaging (scMRI). We found overlapping as well as distinct network features across both conditions. Chapter 3 reports an analysis of how gene expression might be associated with the basic building blocs of these structural covariance networks. We found that synaptic and transcriptionally downregulated genes were replicably associated with cortical thickness differences in children with autism, but not in children with ADHD.

In addition, the first part also aims to elucidate the potential modulation effects of sex on autism neurobiology. Chapter 4 reports an analysis of structural covariance networks in male and female adults with and without autism. We found that biological sex is a modulator of neurobiological heterogeneity in autism. Chapter 5 reports pilot data aiming to identify an electrophysiological signature of these network properties using electroencephalography (EEG). We find little evidence for theories about network asymmetry, but indications of altered frontal network integration.

The second part of the thesis examines the acute effects of hormones on brain connectomics. Hormones are an integral part of the mechanism of social behaviour. In a series of hormone administration studies, we report experiments to test the acute effects of steroid and peptide hormones on brain functional connectivity (Chapters 6 and 7). Chapter 6 reports an oxytocin administration study that used a novel data-driven approach to assess resting-state fMRI connectivity in women. Although the number of fMRI studies on oxytocin have increased over past years, little is known about its effect on women. We found that oxytocin robustly enhances cortico-subcortical connectivity, and that this effect positively correlates with autistic traits. This is interesting given that oxytocin has been proposed as a potential therapeutic in autism. Chapter 7 reports an experiment testing if testosterone modulates connectivity in a specific social environment (a fear response). This was confirmed during the social task, but not during baseline resting-state, highlighting the role of testosterone in functional connectivity in this specific context.

Chapter 8 is the concluding chapter that integrates all the empirical findings in the thesis. We discuss their implications for our understanding of autism and ADHD, and of the role of steroid and peptide hormones in the typically and atypically developing connectome. Chapter 8 also reflects on the limitations of the experiments reported, and sets out future directions for research in this area.

Contents

List of Figures

List of Tables

Nomenclature

AAA – Adult Asperger Assessment questionnaire
ABIDE – Autism Brain Imaging Database Exchange
ADOS – Autism Diagnostic Observation Schedule
ADI-R – Autism Diagnostic Interview Revised
AIBS – Allen Institute for Brain Sciences
AQ – Autism Quotient
ARC – Autism Research Centre in Cambridge
Autism - Autism Spectrum Conditions/Autism Spectrum Disorders
BOLD – Blood Oxygen Level Dependent response
CARD - Cambridge Autism Research Database
Cases - individuals with a diagnosis of autism*
(*unless otherwise specified)
Controls – neurotypical individuals
CRAE – Centre for Research on Autism and Education in London
CT - Cortical Thickness
ΔCT - global differences in cortical thickness (e.g. autism - controls)
DMN – Default Mode Network
DPSS – Discrete Prolate Spheroidal Sequences
DTI – Diffusion Tensor Imaging
DWI – Diffusion Weighted Imaging
EEG – Electroencephalography
EMB – Extreme Male Brain theory
EU-AIMS – European Union Autism Imaging Multicentre Study
FAI – Frontal Asymmetry Index
FDR – False Discovery Rate
FFT – Fast Fourier Transform
FSPGR – Fast Spoiled Gradient Echo
GI – Gender Incoherence theory
GO – Gene Ontology
GTEx – Genotype Tissue Expression
GWAS – Genome Wide Association Study
GU – Georgetown University
HAR – Human Accelerated Region
ICA – Independent Component Analysis
ICN – Institute for Cognitive Neuroscience
IQ – Intelligence Quotient
KCL – Kings College London
KEGG – Kyoto Encyclopedia of Genes and Genomes 2016
KKI – Kennedy Krueger Institute
MAGMA – Mulit-marker Analysis of GenoMic Annotation
MRC – Medical Research Council
MRC-AIMS – MRC Autism Imaging Multicentre Study

MRI - Magnetic Resonance Imaging
MTFFT – Multi Taper Fast Fourier Transform
NT – Neurotypical
fMRI – functional Magnetic Resonance Imaging
OFC – Orbitofrontal cortex
OLS – Ordinary Least Squares
OR - Odds Ratio
OXT – Oxytocin
OXTR – Oxytocin Receptor
PCA – Principal Component Analysis
PLSR - Partial Least Squares Regression
Q-value - Benjamini-Hochberg FDR corrected P-value
RRHO – Rank-rank Hypergeometric Overlap
RS-fMRI – Resting-state fMRI
SNP – Single Nucleotide Polymorphism
TET – Threat Escape Task
ToM – Theory of Mind
TPJ – Temporo-Parietal Junction
VBM – Voxel Based Morphometry
VE – Von Economo
WCC – Weak Central Coherence
WPLI – Weighted Phase Lag Index
UCL – University College London

Chapter 1 Introduction

The idea of the brain as a network of constituent neuronal elements is not new. Already in the early 1900's Santiago Ramón y Cajal, considered one of the founding fathers of modern neuroscience, noticed the structured patterns of the human cortex (DeFelipe & Jones, 1988). Methods to study these fascinating patterns have evolved fast since the time of Golgi staining. Techniques such as fluorescence microscopy, electron microscopy but also magnetic resonance imaging (MRI), diffusion tensor imaging (DTI), and elecetroencephalography (EEG) are but a few examples of techniques that have made it possible to study neuronal and cortical structures at micro and macro scales. These advances combined with improvements in computational power are increasingly giving rise to a new field of neuroscientific study: network science and the study of the human connectome (Sporns, Tononi, & Kötter, 2005). In its broadest sense the human connectome is taken to mean: the network of connections between different parts of the brain.

Distinctions are often made between structural connectivity (e.g. physical connections) and functional connectivity (some statistical relation between activity in different brain regions). These networks are no longer being studied on a purely structural level or in vitro. There is an increased interest in the relation between the functioning of this network and the functioning on a more cognitive and behavioural level (Seung, 2011), as well as efforts to disentangle the mechanistic underpinning of the emergent network properties (Romme et al., 2016; Whitaker et al., 2016). Before moving on to combining cognitive and behavioural elements with brain organizational principles and investigating mechanistic organizational principles however it is

important to keep a number of key concepts in mind throughout this thesis. First and foremost, we need to distinguish between different types of connectivity analyses.

1.1 Structural connectivity

Structural connectivity refers to physical connections in the brain, either at the synaptic level, or at the level of axons or even the dense connection highway of the corpus callosum as a whole. Often these connections are investigated in humans in-vivo using some type of diffusion weighted imaging such as Diffusion Tensor Imaging (DTI). These techniques are generally intended to measure dispersion or diffusion of water molecules in order to visualize the white matter fibre structure (e.g. myelin) of brain connections. Assuming that connections in the brain are continuously forming and changing this is a valuable technique to study development of brain networks. Thus, this method can be particularly promising to study neurodevelopmental conditions such as autism or ADHD. Studies have for example found evidence that these white matter tracts might be developing along different trajectories in a neurodevelopmental condition such as autism (Courchesne, 2004; Courchesne et al., 2007; Courchesne, Campbell, & Solso, 2011). Specifically, that there might be an early overgrowth combined with later undergrowth, or even a regression (Courchesne, 2002, 2004; Courchesne et al., 2001; Courchesne, Carper, & Akshoomoff, 2003). Differences in growth patterns and in synaptic pruning (Craik & Bialystok, 2006; Low & Cheng, 2006) are likely to result in different structural neural networks.

Recent reviews of connectivity studies in autism suggest that there are indeed connectivity differences that might characterize the condition (Rane et al., 2015; Vissers, Cohen, & Geurts, 2012). The patterns that are mostly reported are of decreased connectivity and an increase in diffusivity, yet the overall picture seems heterogeneous and somewhat dependent on

methodologies (Vissers et al., 2012). Although the majority of connectivity research in autism has focused on functional connectivity it is likely that differences in structural connectivity could underlie differences in functional connectivity (Greicius, Supekar, Menon, & Dougherty, 2009).

1.2 Functional connectivity

Functional connectivity is best defined as a temporal correlation in the activity between two spatially different regions (Friston, Frith, Liddle, & Frackowiak, 1993; Zuo et al., 2010). When using fMRI this refers to a correlation in the blood oxygenated level dependent (BOLD) response between different brain regions. However, in an electrophysiological sense, this can also refer to phase lagged relations in electrical field potentials (such as measured with electroencephalography) over time between different recording sites. The complete functional architecture of the brain is often referred to as the brain's functional 'connectome' (Biswal, Eldreth, Motes, & Rypma, 2010; Seung, 2011). The general idea is that complex processing requires different brain regions to work together (e.g. synchronize or correlate their activity). In individuals with autism this type of integration of multiple systems might be affected or atypical (Belmonte et al., 2004). In a recent review of the literature on atypical functional in autism it was evident that, since connectivity was suggested as a target for research, there has been an explosion of connectivity theories concerning autism (Vissers et al., 2012). One prominent theory postulates that autism is characterized by local over-connectivity combined with global underconnectivity (Belmonte et al., 2004). Sadly, the methods and findings have been as heterogeneous as the spectrum itself (Vissers et al., 2012). What is clear is that there is a diverse pattern of connectivity differences that might not be fully captured solely in terms of "local" or "global" connectivity differences.

1.3 Structural covariance

There is also a third, somewhat intermediate, level of analysis called structural covariance analysis, which technically should not be considered connectivity in a pure sense, but which does tell us something about brain organization. This recently emerging method refers to the technique of covarying inter-individual differences in neural anatomy (Alexander-Bloch, Giedd, & Bullmore, 2013; Evans, 2013). Generally, a single (gray-matter based) anatomical property such as cortical thickness or regional volume is used to construct a correlation matrix for one or several groups by taking the cross correlation of that anatomical property for a single region with all other regions. This correlation thus reflects the extent to which the neuroanatomy of a certain region is related to the neuroanatomy of other regions. As such it serves as an intermediate method of network analysis between functional and structural connectivity. The obtained correlation matrices can subsequently be subjected to network analysis. Structural covariance networks, in a neurotypical population, have been shown to strongly overlap with networks derived from purely structural measures such as diffusion weighted imaging (Gong, He, Chen, & Evans, 2012). It is likely that these networks are strongly related to networks derived from functional connectivity analysis (Alexander-Bloch, Giedd, et al., 2013).

In addition, structural covariance networks have been shown to be partly heritable (Schmitt et al., 2009) and follow a pattern of coordinated maturation (Alexander-Bloch, Raznahan, Bullmore, & Giedd, 2013; Raznahan et al., 2011; Zielinski, Gennatas, Zhou, & Seeley, 2010). With respect to neurodevelopment, structural covariance networks might provide a relatively easy way to investigate potential differences in brain network development as any differences are likely the result of differing developmental trajectories (e.g. one is effectively measuring some stage of this shared developmental trajectory). This can be particularly interesting in

studying coordinated development of brain networks when for example comparing two neurodevelopmental groups. The advantage of structural covariance analysis is that it focuses on this coordinated structure of the entire brain as opposed to zooming in on a specific structure.

Furthermore, structural data on which these networks are based is much more widely available, analytically less computationally intensive and arguably less sensitive to noise compared to functional imaging (such as motion artefacts). For example, in autism, structural covariance analysis has shown that in regions relevant for social and sensorimotor processing there is a regional or nodal decrease in centrality (Balardin et al., 2015). Meaning that these regions are less strongly embedded in the global brain network in individuals with autism. Furthermore, speech and language impairments in autism have also been associated with differences in structural covariance properties (Sharda, Khundrakpam, Evans, & Singh, 2014).

A caveat of using structural covariance analysis that should be emphasized is that the resulting structural covariance network is based on the group-wise covariance. Thus, individual level data is lost at this point. Tools to assess individual level structural covariance are being developed but for the present work we focused on existing methodology. It should be noted however that the group-level networks derived from structural covariance analysis show high overlap with functional and structural connectivity derived networks (Alexander-Bloch, Giedd, et al., 2013). As new tools to assess individual level structural covariance become available they will be applied to the data outlined in this thesis as well.

Thus, there are a number of different ways to assess changes to the network of neural connections that is the human brain. In addition to the three broad domains described above

there are a number of methods to quantify organizational properties of brain networks. In this thesis we will mainly use two of those: graph theory and independent component analysis (ICA). Graph theory is described in detail elsewhere (Bullmore & Sporns, 2009; Mark Newman, 2010; Sporns, 2011) but a brief overview of the most commonly used measures and their mathematical underpinning is provided in the Supplementary material (Appendix A). Within ICA there are yet more different parameters and sub-domains. Throughout this thesis the most commonly used implementation by fsl (https://fsl.fmrib.ox.ac.uk/fsl/fslwiki/) is utilized. This implementation is described in more detail by Christian Beckman and colleagues (Beckmann, DeLuca, Devlin, & Smith, 2005). Where applicable each individual chapter describes the exact methods and parameters used.

Much like any other type of network, components of brain networks tend to be specialized to specific functions, yet they clearly do not operate in isolation. This is evident from our day to day interaction with the world around us. Human (social) behaviour undoubtedly arises as a complex interaction between a constantly changing environment and our responses to it. In such a dynamic and complex system, it seems unlikely that our responses are driven by a single specialized brain region, but more likely by a complex and dynamic system. Thus, the need to understand the brain as a complex network becomes ever more important. In that respect, there are numerous factors that could potentially influence the underlying architecture and subsequent emerging functionality of brain networks. Looking at three specific factors (coordinated developmental maturation, genetic contributions to cortical organization and the acute effects of hormones) this thesis examines the broad question of how brain network organization is affected in developmental psychopathology, specifically in relation to autism.

1.4 Brain morphology in atypical development

The first influence on brain networks addressed in this thesis is how coordinated maturation of different parts of the brain might give rise to altered morphology in two developmental conditions; autism and ADHD. These two conditions are of particular interest because, while they are considered distinct conditions from a diagnostic perspective, clinically they share phenotypic features and have high comorbidity and genetic overlap (Leitner, Neuroscience, & Leitner, 2014; Rommelse et al., 2010). Studying both conditions in conjunction might thus shed light on general principles of atypical development as well as unique features for both autism and ADHD. Regardless of this overlap, most studies have focused on only one condition, with considerable heterogeneity in their results. The rationale for combining the two was that a dual-condition approach might help elucidate the shared and distinct neural characteristics (Dougherty, Evans, Myers, Moore, & Michael, 2015).

Using structural covariance analysis, Chapter 2 discusses this overlap between autism and ADHD. In this chapter, we thus broadly address the question of whether there is a converging or a diverging pattern of coordinated developmental maturation between the two developmental conditions, with specific emphasis long-range and short-range connectivity patterns. It has been speculated that individuals with autism may have a disruption in the balance of these two types of connections (Belmonte et al., 2004). Specifically, it has been hypothesized that individuals with autism have increased local (short-range) connections at the expensive of global (long-range) connections. This hypothesis finds evidence from behavioural studies that for example show increased attention to detail at the expense of more global information integration (Frith & Happé, 1994). Although there are many studies that have reported inherent connectivity

differences that would point to a generally altered pattern of brain organization, to date these have not been captured in a single explanatory framework (Vissers, Cohen, & Geurts, 2012).

Several studies on ADHD also suggest alterations in cortical organization (Durston, Eickhoff, Konrad, & Eickhoff, 2010; Konrad & Eickhoff, 2010). Yet again, there does not appear to be clear uniform pattern in these findings. The idea of disruptions in long-range versus short-range connectivity is one of the few ideas that finds resonance in both conditions (Kern et al., 2015) and which might provide a more unified framework. To address this question, graph theory was used to analyse topological properties of structural covariance networks across both conditions and relative to a neurotypical (NT; n=87) group using data from the ABIDE (autism; n=62) and ADHD-200 datasets (ADHD; n=69). Regional cortical thickness was used to construct the structural covariance networks. In these covariance networks we studies the relationship between regional Euclidean distance and the relative extent of their group-wise covariance. The assumption here is that regions that share a developmental trajectory have higher group-wise covariance and that a shared developmental trajectory is a potential marker for underlying functional or structural coherence between regions.

Having examined structural covariance, based upon cortical thickness covariance networks in children with autism, we next turned our attention to study a group of adults with autism. Fortunately, the adult data-set that we are working with gives us the opportunity to answer an additional and vital question in autism research: is there a moderating effect of biological sex on these potentially altered developmental trajectories? There have been several theories that have aimed to capture the known male bias in autism diagnoses into a coherent framework (Baron-Cohen, 2002; Bejerot et al., 2012). On one hand, there is the theory of autism as being

an extreme form of the male brain (Baron-Cohen, 2002), which broadly states that normative neural and cognitive sex differences might be exaggerated towards the extreme male end in individuals with autism. On the other hand there is a more recent theory that describes autism in terms of gender incoherence (Bejerot et al., 2012). In this account individuals with autism would show a phenotype that falls in-between the normative sex differences (and to some extend perhaps even more closely resembles female patterns). Both accounts and their respective predictions for brain organization principles are described in more detail in Chapter 4. Thus, Chapter 4 discusses not only how some of the findings from Chapter 2 progress into adulthood, but also addresses the potential moderating effects of biological sex in adults with autism. A further question that emerges from the known male bias in autism and the resulting relation to social behaviour is how sex hormones come into play. This question is addressed in more detail in Chapters 6 and 7.

1.5 Genetic contributions to altered brain morphology

Chapter 3 builds on work done in Chapter 2 and extensively addresses how (and which) genetic risk factors for autism are associated with the underlying differences in cortical morphology. We specifically asked how genes contribute to differences in cortical thickness in autism. Differences in cortical morphology - in particular cortical volume, thickness and surface area - have been reported extensively in individuals with autism (Ecker, 2016; Ecker, Ginestet, Feng, Johnston, Lombardo, Lai, Suckling, Palaniyappan, Daly, Murphy, Williams, Bullmore, Baron-Cohen, Brammer, & Murphy, 2013; Ecker, Ronan, et al., 2013; Lai et al., 2014) and they are the building blocks on which the structural covariance analysis of Chapters 2 and 4 are effectively based. However, it is unclear what genetic variants implicated in autism contribute

to these differences. Here, we ask: what are the genetic determinants of global cortical thickness differences (ΔCT) in children with autism? We used Partial Least Squares Regression (PLSR) on structural MRI data from 62 children with autism (cases) and 87 matched typically developing control individuals (controls) and cortical gene expression data from the Allen Institute for Brain Science (AIBS) to identify genes that contribute to global differences in cortical thickness in autism. This data-driven approach provides weights for the association of each gene with ΔCT. Analysing these gene weights we explored enrichment with a number of different classes of genetic risk in autism. Given the data-driven nature of this approach we also validated our discovery findings in two independent MRI datasets from the second release of ABIDE.

1.6 Brain Function

Although not a major part of this thesis atypical brain function in autism is also briefly explored by means of EEG. Several studies have shown atypical power spectral density patterns in the EEG frequency bands of individuals with autism. We hypothesized that altered morphology, as outlined in Chapters 2-4, would ultimately lead to alterations in functional organization. In addition, we speculated that the spectral density differences observed in the autism literature might in fact be sustained by alterations in functional connectivity. There is a large and growing body of literature outlining theories of altered functional connectivity in autism that has been reviewed in detail elsewhere (Vissers et al., 2012). In the present study, we utilized EEG to study potential difference in connectivity, as measured by the weighted phase lag index (WPLI), as a potential underlying mechanism for altered power spectral density.

1.7 Acute effect of hormones on intrinsic brain functioning

The third factor, that of hormonal influences, is addressed in Chapters 6 and 7. As briefly discussed in Chapter 4 in relation to effects of biological sex, hormones might play a pivotal role in autism. They have however, a much wider role to play social behaviour. We focused specifically on two hormones and their effects on functional connectivity: oxytocin and testosterone.

The peptide hormone oxytocin has often been speculated as a 'natural' treatment for namely the social difficulties associated with autism (Meyer-Lindenberg, Domes, Kirsch, & Heinrichs, 2011). In popular culture it has even been termed the 'love', 'trust' or 'cuddle' hormone. Although early studies have shown some generally positive effects to social behaviour in autism (Auyeung et al., 2015), the field in general is riddled with paradoxes of positive and negative effects (Bethlehem, Baron-Cohen, van Honk, Auyeung, & Bos, 2014). Part of this heterogeneity and apparent contradictory body of work might be resolved by gaining a better understanding of oxytocins baseline effect on the brain. Specifically, it may influence various human behaviours by altering brain network dynamics (Bethlehem, van Honk, Auyeung, & Baron-Cohen, 2013). Previous oxytocin studies are largely male-biased and often constrained by task-based inferences. In Chapter 6 we thus investigated the impact of oxytocin on resting state connectivity between subcortical and cortical networks in women. We collected resting state fMRI data on 26 typically-developing women 40 minutes following intranasal oxytocin administration using a double-blind placebo-controlled crossover design. Independent components analysis (ICA) was applied to examine connectivity between networks. An independent analysis of oxytocin receptor (*OXTR*) gene expression in human subcortical and cortical areas was carried out to determine plausibility of direct oxytocin effects on *OXTR*

The second hormone we investigated was testosterone. Testosterone has often been speculated to play an important role in autism given that the condition is male based and finds some indications of what could be described as 'extremely male brain phenotype' (Baron-Cohen, 2002). It was recently shown that part of these characteristics might be driven by prenatal over-exposure to steroidogenic hormones such as testosterone (Baron-Cohen et al., 2015). Within the framework of the present research it was unfortunately not possible to specifically investigate the direct effect of pre-natal testosterone on brain morphology. However, others have already shown that it can have profound effects on grey matter morphology in a sexually dimorphic way (Auyeung, Lombardo, & Baron-cohen, 2013; Lombardo, Ashwin, Auyeung, Chakrabarti, Taylor, et al., 2012) as well as more general effect on brain connectivity and organization (Koolschijn, Peper, & Crone, 2014; Peper, Koolschijn, & Ce, 2012; Peper, van den Heuvel, Mandl, Pol, & van Honk, 2011). Outside of the influence during brain development testosterone is known to have acute effects on social behaviour (Bos, Panksepp, Bluthé, & van Honk, 2012; Van Honk et al., 2012; van Honk, Bos, & Terburg, 2014). Within the framework of the present research it is interesting to note that testosterone and oxytocin have been speculated to have broadly opposing effects on brain dynamics (Bos et al., 2012). Specifically, recent evidence suggests that testosterone can decrease the functional coupling between orbitofrontal cortex (OFC) and amygdala (van Wingen, Mattern, Verkes, Buitelaar, & Fernández, 2010; Volman et al., 2016; Volman, Toni, Verhagen, & Roelofs, 2011). Theoretically this decoupling has been linked to a testosterone-driven increase of goal-directed behaviour in case of threat, but this has never been studied directly. In addition, much like oxytocin, testosterones effects have often been speculated to be context dependent (van Honk, Terburg, et al., 2011). Thus, in addition to studying testosterone in this very specific context of

goal-directed threat behaviour, we also sought to assess its basic effect on resting-state brain activation and connectivity in a placebo-controlled crossover administration study.

1.8 Framework

As disparate as these three factors (genetic, hormones and sex) might seem they are all interconnected. Like cogs in the big wheel of human behaviour (Figure 1.1). Neurodevelopmental conditions such as autism or ADHD provide a unique window into these interactions as they show where some interactions might have been atypical. Although it is beyond the scope of any thesis to analyse the totality of this framework and all its interactions we sought to highlight some of them.

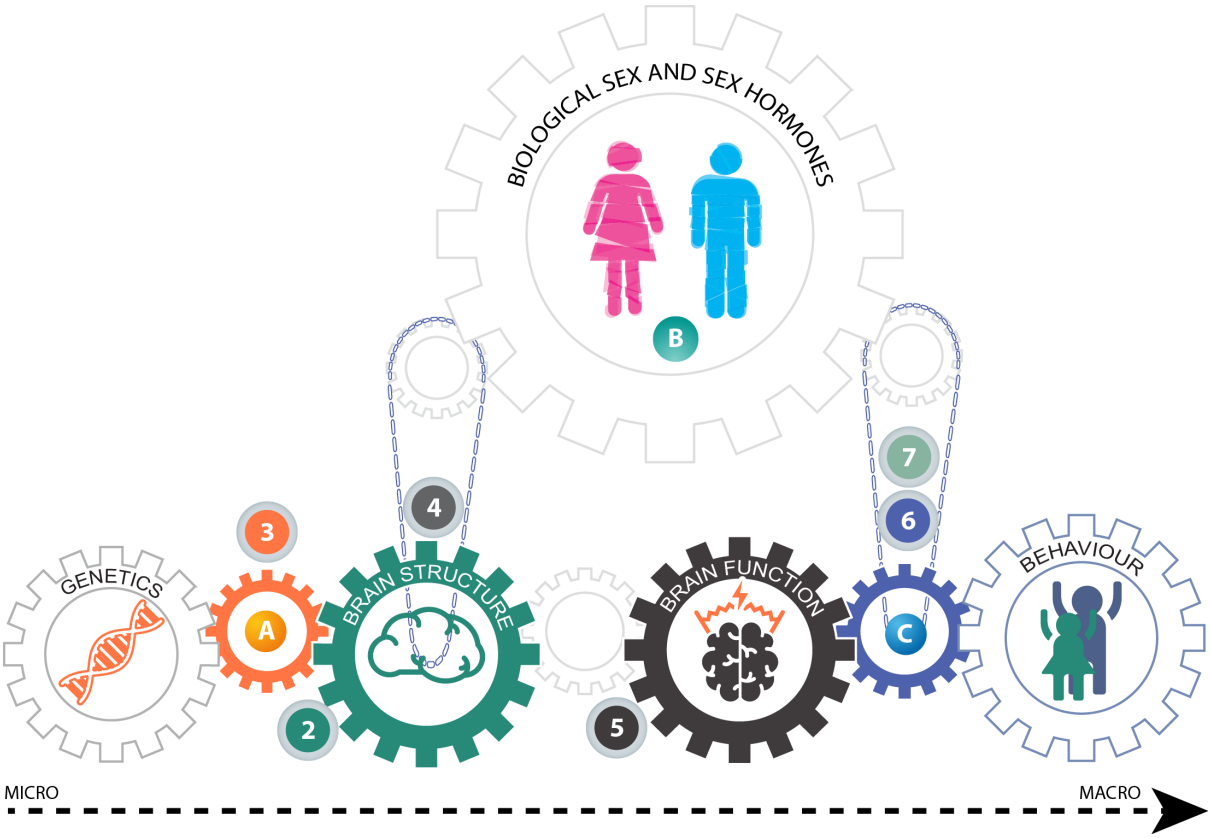

Figure 1.1: Framework

Numbers denote chapters in this thesis, letters denote the 3 main elements of the framework presently being discussed (A: Genes B: Gender C: Hormones). Thus; Chapter 2 discussed brain morphology in atypical

development, Chapter 3 discusses the influences of genes on this altered morphology, Chapter 4 discusses the interaction between biological sex and atypical development, Chapter 5 discusses potential altered brain function in atypical development, Chapter 6 discusses how hormones interaction with brain function to potentially alter behaviour in a manner that interacts with atypical development, and lastly Chapter 7 discusses how hormones can operate in a narrow and specific context to modify behaviour.

Chapter 2 Altered structural brain organization in atypical development

2.1 Introduction

Autism is characterized by deficits in social communication alongside unusually restricted interests and repetitive behaviours, difficulties adjusting to unexpected change, and sensory hypersensitivity (American Psychiatric Association, 2013). Despite a large body of research to understand its underlying neurobiology (Loth et al., 2015), no distinct set of biomarkers for autism has yet been established. With respect to the neuroimaging literature and specifically network organization, several authors have suggested potential differences in brain organization in autism compared to neurotypical control groups with little consensus. There is for example debate about whether autism is characterized by neural over- or under-connectivity (Belmonte et al., 2004; Brock, Brown, Boucher, & Rippon, 2002; Courchesne & Pierce, 2005; Just, Cherkassky, Keller, & Minshew, 2004; Rubenstein & Merzenich, 2003). A now widely discussed hypothesis is that people with autism suffer from atypical connectivity (Assaf et al., 2010; Cherkassky, Kana, Keller, & Just, 2006; Courchesne & Pierce, 2005; Just, Cherkassky, Keller, Kana, & Minshew, 2007). Specifically, there is a tendency for autism to be associated with excess local or short-range connectivity, relating to enhanced local processing. This is thought to be accompanied by decreased global or long-range connectivity, relating to impaired integration as manifested in 'weak central coherence'. Thus, a prominent theory of neural connectivity in autism is of global under- and local over-connectivity (Belmonte et al., 2004; Vissers et al., 2012). Other, more recent theories have pointed towards more network dependent

levels of dysconnectivity. Zielinski et al. (2012) reported a connectivity reduction in the salience network and posterior regions of the DMN, whereas they report frontal DMN regions to be over-connected. This notion of network dependent alterations was recently confirmed by a large structural covariance study in the ABIDE dataset (Long, Duan, Chen, Zhang, & Chen, 2016). Interestingly, Long and colleagues also show how this network dependency seems to change with age. Lastly, regional covariance alterations in autism have also been demonstrated to persist in white matter microstructure (Dean et al., 2016). Dean and colleagues show an overall decreased coherence in individuals with autism that might suggest a broader pattern of dysconnectivity.

ADHD on the other hand is characterised by a triad of symptoms: hyperactivity, impulsive behaviour and inattentiveness (American Psychiatric Association, 2013). Studies using connectivity analyses have attempted to shed light on its underlying neurobiology and have found both decreased and increased functional connectivity in specific networks (Tomasi & Volkow, 2012), altered connectivity in the default mode network (DMN) (Fair et al., 2010) and differences in cross-network interactions (Cai, Chen, Szegletes, Supekar, & Menon, 2015). These effects might be smaller than the literature suggests (Mostert et al., 2016).

Autism and ADHD show high comorbidity and phenotypic overlap (Leitner et al., 2014; Rommelse et al., 2010; Rommelse, Geurts, Franke, Buitelaar, & Hartman, 2011), and are both also potentially marked by differences in connectivity. There have even been suggestions that these connectivity differences lie on a similar dimension of local and global connectivity imbalances (Kern et al., 2015). In addition, both conditions have been associated with alterations in cortical development (Hardan, Libove, Keshavan, Melhem, & Minshew, 2009;

Shaw et al., 2007) that could in turn give rise to differences in the topological organisation of brain networks. In the present study, we aimed to identify distinct as well as overlapping patterns of brain organisation that might shed a light on the underlying architecture of both conditions, giving rise to divergent yet related findings using structural covariance analyses.

Structural covariance analysis involves covarying inter-individual differences (i.e. coordinated variations in grey matter morphology) in neural anatomy across groups (Alexander-Bloch *et al.*, 2013; Evans, 2013) and is emerging as an efficient approach for assessing structural brain organization. A key assumption underlying this methodology is that morphological correlations are related to axonal connectivity between brain regions, with shared trophic, genetic, and neurodevelopmental influences (Alexander-Bloch *et al.*, 2013). Thus, structural covariance network analysis is not the same as analysis of functional connectivity or structural networks obtained with diffusion imaging, yet it has shown moderately strong overlap with both (Alexander-Bloch *et al.*, 2013; Gong *et al.*, 2012). In addition, structural covariance networks are highly heritable (Schmitt et al., 2009) and follow a pattern of coordinated maturation (Alexander-Bloch *et al.*, 2013; Raznahan *et al.*, 2011; Zielinski *et al.*, 2010). With respect to neurodevelopmental conditions, structural covariance networks might provide a way to investigate potential differences in brain network development. Differences between neurotypical individuals and individuals with a developmental condition are likely the result of divergent developmental trajectories in coordinated development of different brain networks. The advantage of structural covariance analysis is that it focuses on this coordinated structure of the entire brain as opposed to focusing on a specific structure. In addition, structural data on which these networks are based are widely available, analysis is less computationally intensive and arguably less sensitive to noise, compared to functional imaging.

Previous investigations of structural covariance in autism have shown regional or nodal decrease in centrality, particularly in key regions subserving social and sensorimotor processing, compared to neurotypical individuals (Balardin et al., 2015). Furthermore, speech and language impairments in autism have been associated with differences in structural covariance properties (Sharda, Khundrakpam, Evans, & Singh, 2014). Studies of functional connectivity networks in autism are more abundant (Vissers et al., 2012). In ADHD, structural covariance analyses have been scarce. A study that specifically investigated structural covariance in drug-naïve adolescent males found that grey matter volume covariance was significantly reduced between multiple brain regions including: insula and right hippocampus, and between the orbito-frontal cortices (OFC) and bilateral caudate (Li et al., 2015). Similar to the autism literature, studies that have explored functional connectivity differences in ADHD are more abundant (Konrad & Eickhoff, 2010).

While autism and ADHD are considered distinct conditions from a diagnostic perspective, clinically they share some common phenotypic features (such as social difficulties, atypical attentional patterns, and executive dysfunction) and have high comorbidity (Leitner et al., 2014; Rommelse et al., 2010, 2011). DSM-5 (American Psychiatric Association, 2013) now allows comorbid diagnosis of autism and ADHD, acknowledging the common co-occurrence of these conditions. Regardless, most studies to date have focused on each condition separately, with considerable heterogeneity in results. Taking a dual-condition approach might help elucidate shared and distinct neural characteristics. The proposal for a dual-condition approach is supported by a recent review that found both distinct as well as overlapping neural characteristics between autism and ADHD (Dougherty et al., 2015). There is also increasing

interest in the clinical and research communities to investigate autism and ADHD along a continuum of atypical neural connectivity (Kern et al., 2015).

In the present study, we used the graph theoretical framework to analyse properties of structural covariance networks across autism and ADHD, relative to an age and gender matched neurotypical control (NT) group. One study has taken a similar approach using resting-state fMRI and diffusion weighted tractography and reported marked connectivity differences between network hubs, indicating a disruption in rich-club topology. Rich-clubs are defined as highly connected parts of a network that tend to connect to other highly connected parts. Specifically, Ray and colleagues (Ray et al., 2014) report a decrease in connectivity within the rich-club but increased connectivity outside the rich-club in ADHD. The autism group showed an opposite pattern of increased connectivity within rich-club connectivity. These findings may fit with the idea of increased local connectivity in autism (i.e., increased within rich-club connectivity), with ADHD showing the opposite pattern. Yet, these findings could also mediate increased strength in long-range connections within the rich-club. In the present study we aimed to further investigate the relation between distance and connectivity by looking at group-wise cortical thickness covariance as a function of Euclidean distance. In addition, we investigate potential overlap in modular and hub organization as assessed by structural covariance network analyses.

2.2 Methods

2.2.1 Image processing

Structural T1-weighted MPRAGE images were collected from two publically available datasets: ABIDE (http://fcon_1000.projects.nitrc.org/indi/abide/) and ADHD-200 (http://fcon_1000.projects.nitrc.org/indi/adhd200/). From these datasets, 3 diagnostic groups (autism, ADHD and neurotypical individuals) of males between the ages of 8 and 12 years old were selected. The initial sample consisted of 348 eligible individuals. The structural T1-MPRAGE data were pre-processed using Freesurfer *v5.3* to estimate regional cortical thickness. Cortical reconstructions were checked by three experienced independent researchers. Images were included in the analyses only when a consensus on the data quality was reached (see Supplementary Materials for more details on data selection). The cortical thickness maps were automatically parcellated into 308 equally sized cortical regions of $500mm^2$ that were constrained by the anatomical boundaries defined in the Desikan-Killiany atlas (Desikan et al., 2006; Romero-garcia, Atienza, Clemmensen, & Cantero, 2012). The backtracking algorithm grows subparcels by placing seeds at random peripheral locations of the standard atlas regions and joining them up until a standard pre-determined subparcel size is reached (Romero-garcia et al., 2012). It does this reiteratively (i.e., it restarts at new random positions if it fails to cover an entire atlas region) until the entire atlas region is covered. Individual parcellation templates were created by warping this standard template containing 308 cortical regions to each individual MPRAGE image in native space. A key advantage of warping of the segmentation map to the native space relates to the attenuation of possible distortions from warping images to a standard space that is normally needed for group comparisons. Lastly, average cortical thickness was extracted for each of the 308 cortical regions in each individual participant.

As a secondary post-hoc step in quality control, individuals that had an average variability in cortical thickness of more than two standard deviations away from the group mean were removed from further analysis. After quality control and matching on age and IQ, our final sample consisted of 218 participants: ADHD (n=69, age = 9.99 ±1.17, IQ = 107.95 ±14.18), autism (n=62 age=10.07 ±1.11, IQ = 108.86 ±16.94) and NT (n=87, age = 10.04 ±1.13, IQ = 110.89 ±10.39). See supplementary Figure B.1 for an overview and Table B.1 for details on scanner site and matching procedure. Scanner site was regressed out from raw cortical thickness estimates across groups. To aid interpretation of the cortical thickness estimates, the residuals from this regression where added to the sample mean. Group-wise structural covariance matrices were then computed by taking the inter-regional Pearson correlation of these parcel-wise cortical thickness estimations. This was done within each group to create group-wise structural covariance matrices.

2.3 Data Analysis

2.3.1 Group differences of distance effects in CT covariance

To determine potential group effects on the CT covariance for short and long-range associations, we investigated the linear slope differences in the relationship between correlation strength and Euclidean distance between nodal centroids. Consequently, one-way analysis of covariance (ANCOVA) was performed with the diagnosis group as a factor and Euclidean inter-regional distance as a covariate. For significant group effects, post-hoc paired t-tests were used to identify which slopes were significantly different from each other.

2.3.2 Graphs

To construct adjacency matrices for graph analyses, the minimal spanning tree (van Wijk et al., 2010) was used as the threshold starting point for building covariance networks at a representative density of 10%. The density of a network relates to the fraction of edges present in the network compared to the maximum possible number of edges. Graph analyses were performed across densities (0-15%) and between-group differences were compared using non-parametric permutation tests on paired group comparisons (1000 permutations). Thus, permuted networks were constructed by permuting the underlying cortical thickness estimates for each group and subsequently constructing adjacency matrices for each permutation to create a null distribution. In view of the large number of comparisons across the 308 nodes, differences in local measures were subjected to a False Discover Rate (FDR) non-linear multiple comparison correction with alpha set at < 0.025 to allow simultaneous correction for two-tailed testing (Benjamini & Hochberg, 1995).

2.3.3 Degree, cortical thickness and wiring cost analysis

Nodal degree reflects the number of edges connecting each node. Nodes with the highest degree of the network are defined as hubs. The present study considered a wide range of degree thresholds to reduce bias related to the choice of an arbitrary set of hubs (ranging from 0 to 100% of the nodes). Thus, group differences in degree and CT of the hubs of the networks were evaluated for each degree threshold. To decrease the noise effect, we calculated the cumulative degree distribution as $P(k) = \sum_{k' \geq k} p(k')$.

Inter-regional distance (d_{ij}) between two nodes *i* and *j* was estimated as the Euclidean distance between the centroids, $d_{ij} = \sqrt{(x_i - x_j)^2 + (y_i - y_j)^2 + (z - z_j)^2}$, where *x*, *y* and *z* represent the coordinates of the centroid of each region in MNI space. The mean connection distance or wiring cost (W_c) of a network was computed as, $W_c = (\sum_{i,j} net_{ij} * d_{ij})/N$, where *net(i,j)* is equal to 1 if regions *i* and *j* are connected, 0 otherwise and *N* is the total number of connections of the network.

2.3.4 Modular agreement

Modular agreement was evaluated by quantifying the proportion of pairs of regions that were classified within the same module in community partitions (using iterating Louvain clustering to obtain modular partitions) associated with different diagnostic groups. Thus, two groups will show high modular agreement if network modules mainly include the same set of brain regions in both groups. As modular agreement is highly affected by intrinsic trivial characteristics of the modular partition, z-scores were used as a measure of how over- or under- represented a given metric was compared with random community partitions.

In order to test against appropriately designed surrogate data, statistical significance was assessed against a null distribution built from metric values computed in 1000 random communities generated by preserving the number of modules, size of the modules, spatial contiguity and hemispheric symmetry of the real community partition. The 95th quantile of the resulting distribution was used as a statistical threshold to retain or reject the null hypothesis of no significant modular agreement between diagnostic groups. Moreover, differences in modular agreement between pairs of groups were statistically tested using a similar procedure. Indices of modular agreement of each pair of groups were subtracted and compared with the differences

of modular agreement derived from the 1000 random communities in each pair of groups. Similarly, the 95th quantile of the resulting distribution was used as a statistical threshold to retain or reject the null hypothesis of no modular agreement differences between pairs of diagnostic groups. Significant results were corrected for multiple comparisons using FDR (Benjamini & Hochberg, 1995).

2.4 Results

2.4.1 Distance covariance topology

In all groups the group-wise correlation strength decreased with increased anatomical distance. Results from the analysis of variance show a main effect of group $F(2,141828) = 2192.76$, $p<0.0001$. Post-hoc analyses indicated that all three groups had a small but significantly different slope: ADHD < Neurotypical (p-value < 10^{-15}), Autism < Neurotypical (p-value < 0.005) and ADHD < Autism (p-value < 10^{-15}). Figure 2.1 shows the linear relation of the inter-regional correlation as a function of Euclidean distance and the mean and confidence intervals of the slope estimates. In the ADHD group, inter-regional correlation decreased the fastest whereas the neurotypical group shows the smallest decrease. This result shows that both autism and ADHD have relatively weaker long-range covariance and stronger local covariance. Compared to the neurotypical group both groups show a balance that more strongly favors short-range over long-range covariance.

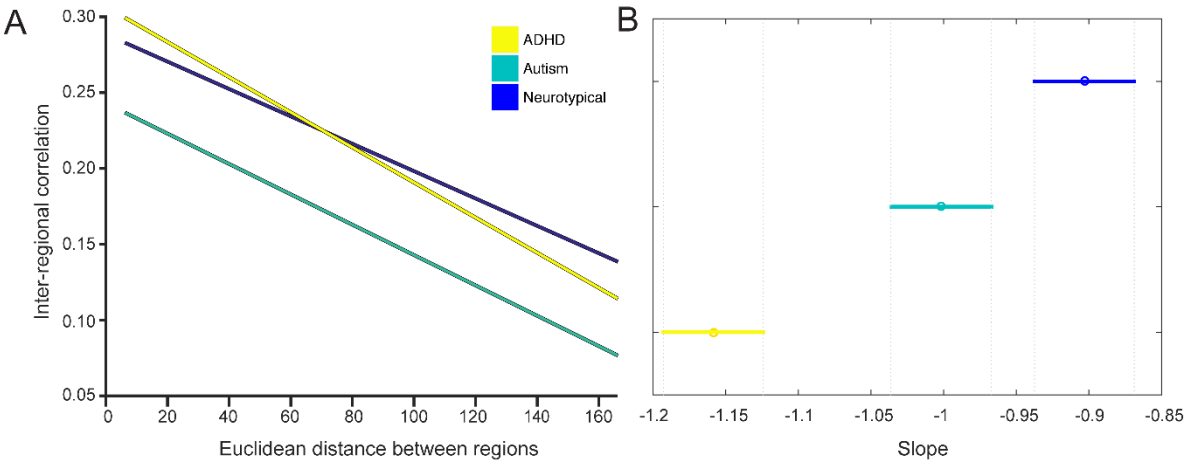

Figure 2.1: Inter-regional correlation strength as a function of Euclidean distance.
Panel A shows the inter-regional correlation over the entire distance range. Panel B shows the mean slope for each group and the 95% confidence interval of the mean slope.

2.4.2 Degree

After constructing the covariance matrices (Figure 2.2A), the degree of each node was computed (Figure 2.2B) and the top 10% nodes with highest degree were retained as hubs for visualization (Figure 2.2C). Most of the hubs were located within frontal and parietal cortices in the three groups. In contrast, nodes with lower degree were mainly placed in the occipital cortex. There were several nodes that showed degree differences between groups, but these were not consistent across degree densities. We did however observe marked differences between groups in the overall degree distribution. Figure 2.3 show the cumulative degree distribution of each group. Interestingly, hubs of the autism group exhibited significantly lower degree than both neurotypical ($p < 0.025$; for degree values from 83 to 88) and ADHD ($p < 0.025$; for degree values from 64 to 89). These difference were corrected for multiple comparisons for the range of higher degree nodes (FDR correction in the degree range from 50 to 90).

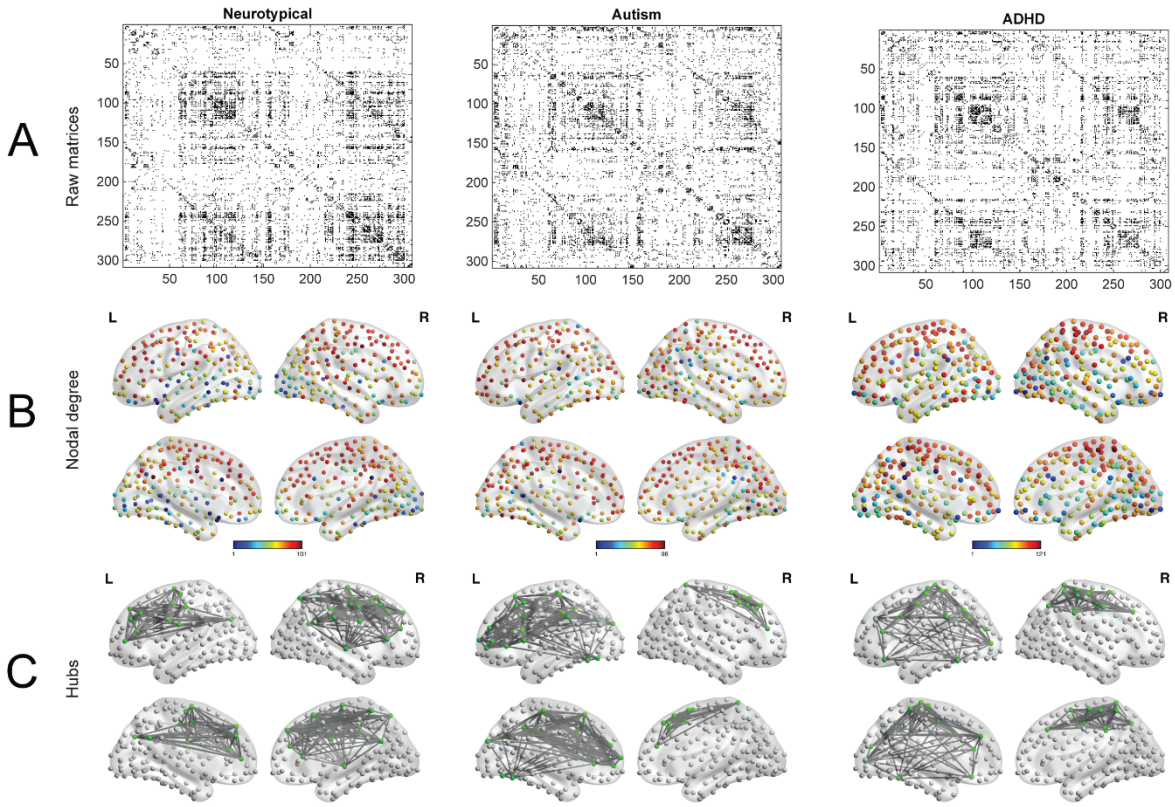

Figure 2.2*:* Overview of procedure and metrics.

Panel A shows the binary adjacency matrices for the three groups thresholded at 10% above the minimal spanning tree. Subsequent graph construction is based on these thresholded matrices. **Panel B** display the topological distribution of nodal degree at 10% density. **Panel C** illustrates the networks with nodes that have the highest degree (top 10%).

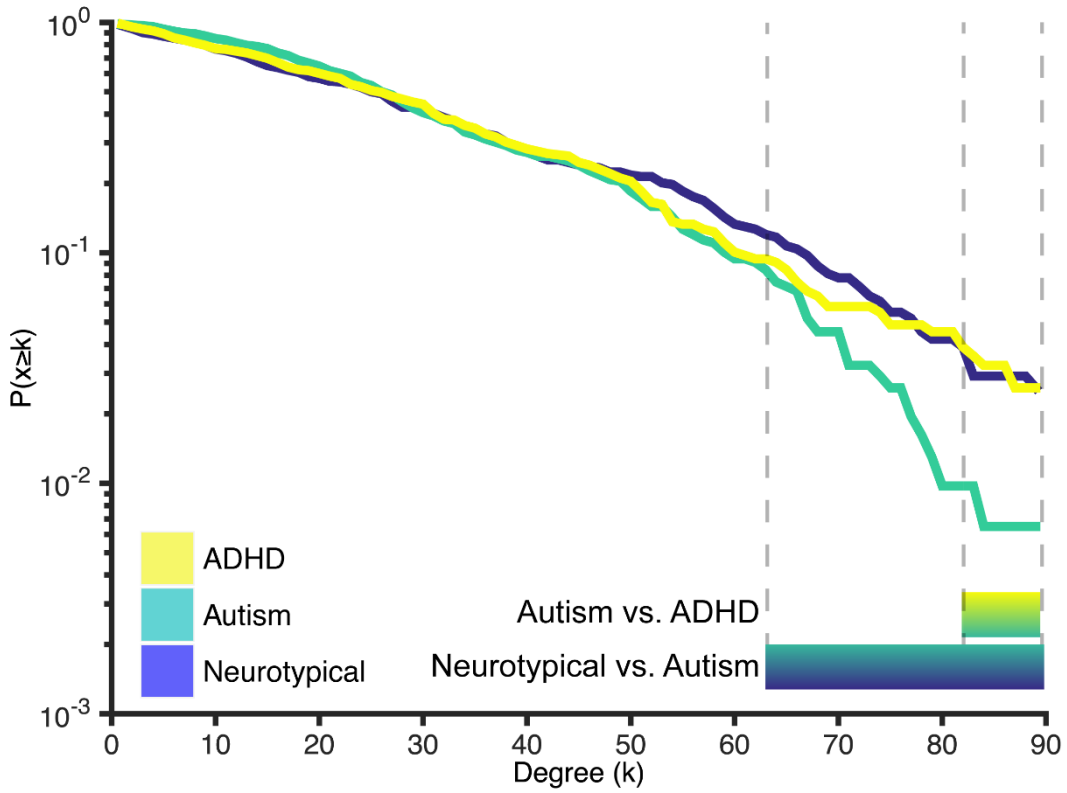

Figure 2.3**:** Cumulative degree distribution**.**

Lines represent the proportion of nodes in the network with a degree higher than k (hubs) in each group. Bars below the figure represent the areas where there is a significant difference between the groups. Hubs of the autism group showed significantly lower degree compared to the ADHD group (k-range: 83-88) and compared to the neurotypical group (k-range: 64-89).

2.4.3 Wiring cost

In line with the group differences observed in the decay of cortical thickness correlation as a function of the inter-regional distance described above, the wiring cost analysis showed a significant decrease of the average distance between connected regions in the ADHD group compared with neurotypical (Figure 2.4; $p < 0.008$), revealing a reduction of long range connections in the ADHD network. It should be noted however that there was an extremely large overlap between all three groups.

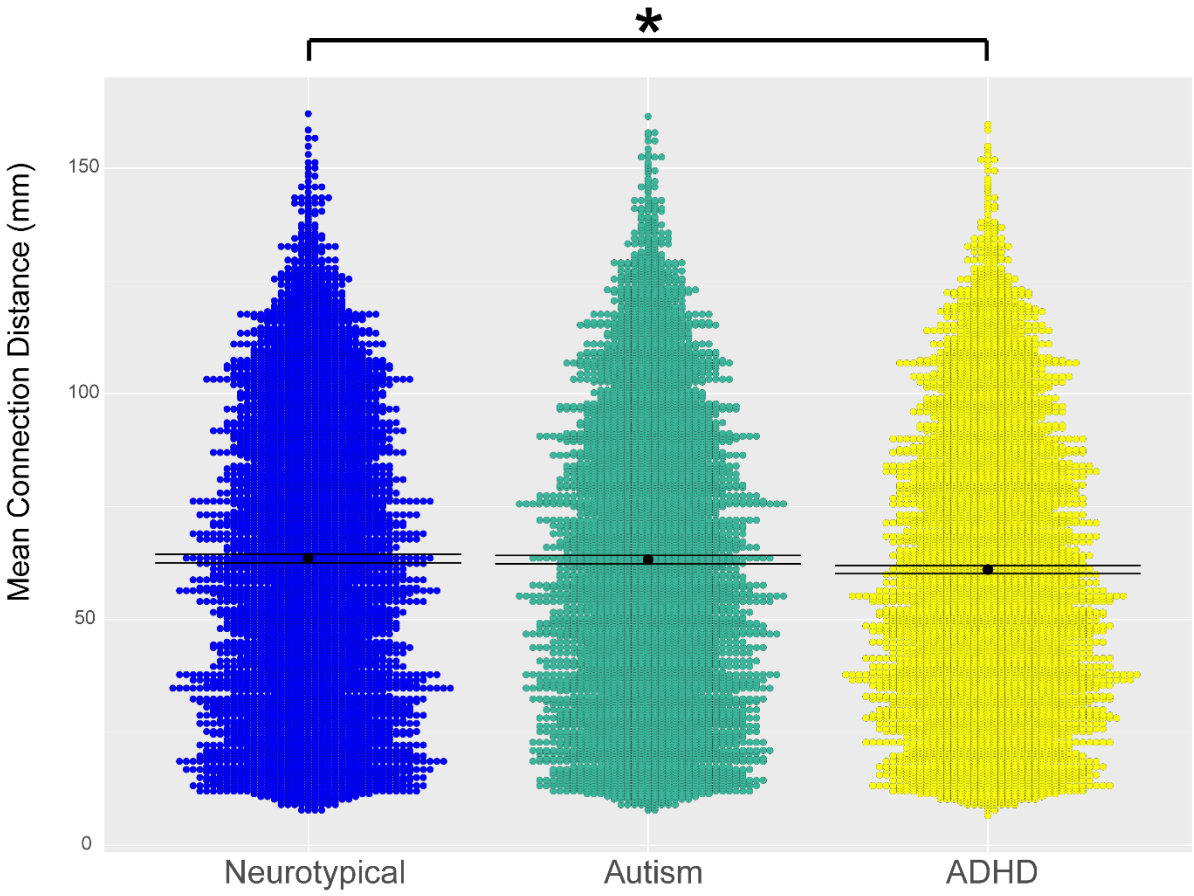

Figure 2.4: Violin representation of the mean inter-regional distance.
The ADHD group has significantly lower connection distance compared to the neurotypical group. Mean is shown as a black dot with error bars representing 95% confidence intervals

2.4.4 Cortical thickness as a function of degree

Given that there were notable differences in degree distributions (i.e. hubs in the autism group had lower degree than the other groups; Figure 2.2) we chose to analyze both the absolute degree distribution and take a percentile that was based on the group itself. Although the autism and neurotypical group showed little difference in cortical thickness across the entire range of degrees with both methods, high degree nodes had significantly reduced cortical thickness in

the ADHD group (Figure 2.5). This suggests that there might be increased synaptic pruning in these hub regions in the ADHD group.

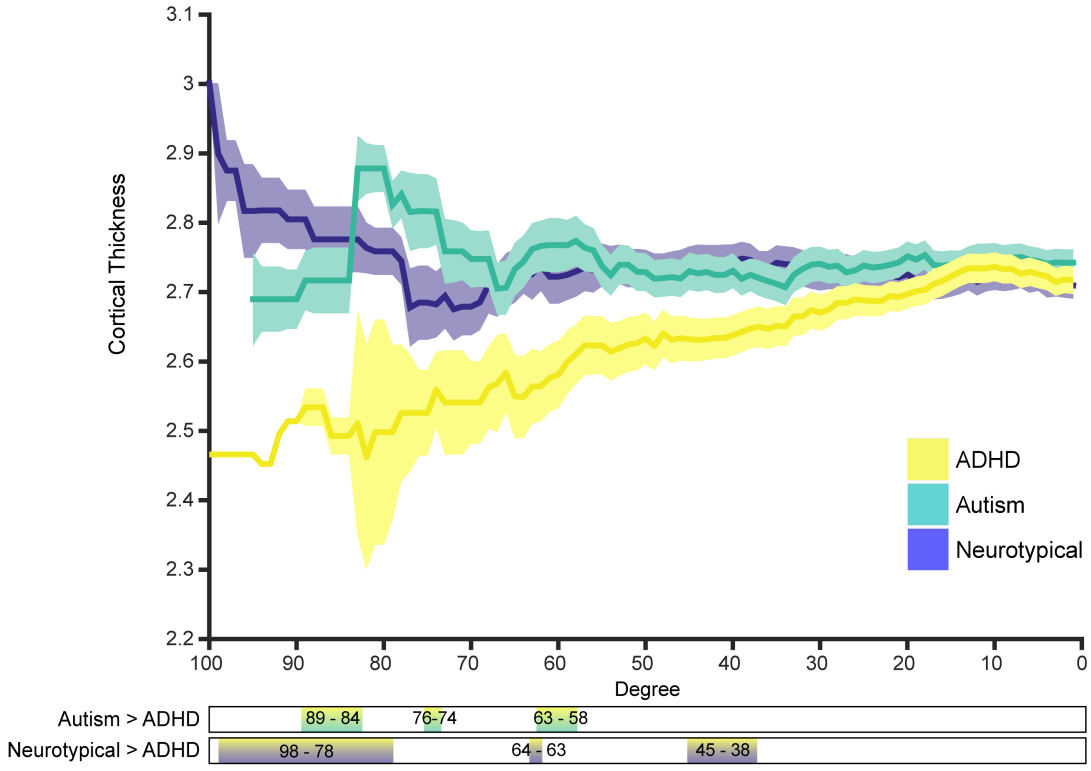

Figure 2.5: Cortical thickness as a function of degree.
Bars below the figure show the degree ranges where there is a significant difference between the respective groups.

2.4.5 Modular consistency and clustering

To investigate similarities in global topology, we further evaluated the modular overlap between the community structure of the three groups. The modular overlap between all group-wise comparisons were significantly higher than expected by chance (Figure 2.6), suggesting that a global scale there were no marked differences in structural covariance community structure. However, the Autism-ADHD group overlap was significantly lower than the Neurotypical-ADHD overlap ($p < 10^{-3}$). There was also a small non-significant effect for the Neurotypical-ADHD overlap compared to Neurotypical-Autism ($p = 0.04$). This indicates that

although there were perhaps no massive topological differences in community structure, the autism and ADHD group differ more from one another than they do from the neurotypical group (i.e. there was lower modular agreement between autism and ADHD then there was between the other groups).

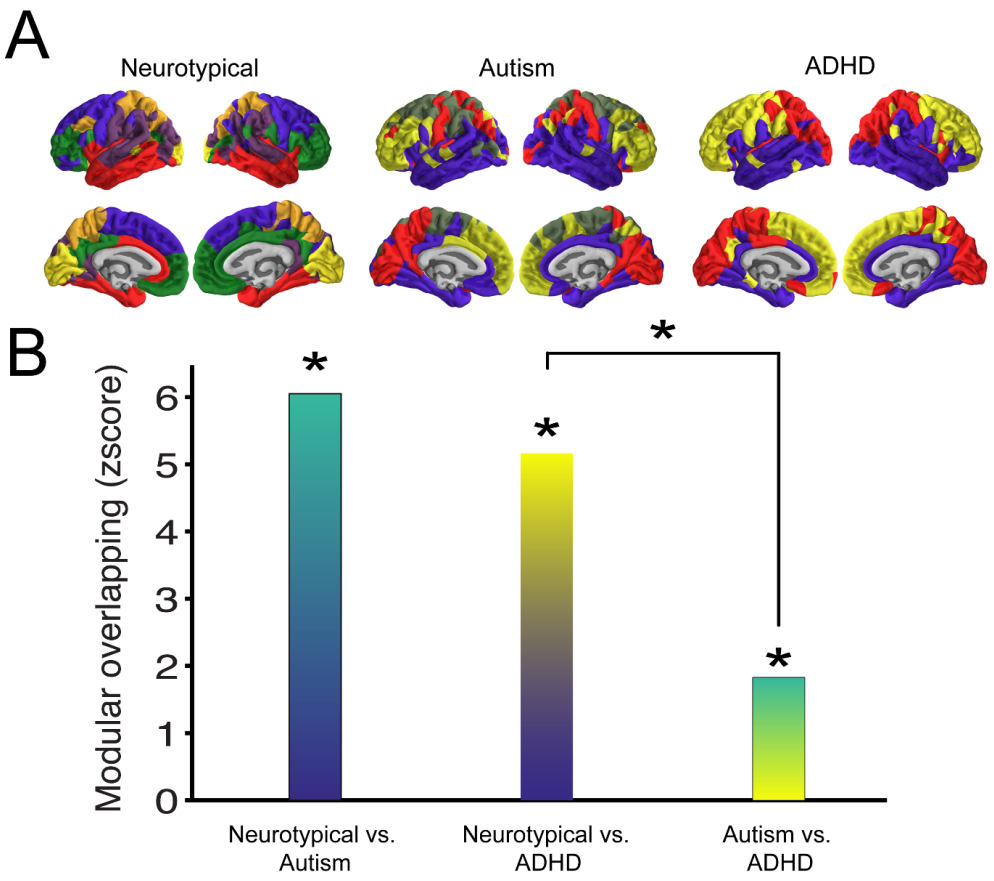

Figure 2.6*:* Similarities in community structure across groups.

Panel **A** illustrates the modular organization of the structural covariance network derived from each group. The colours show association of the region with a certain module. These colours are set for each group individually as not all groups have the same number of modules. Panel **B** displays the z-transformed modular overlap for each group-wise comparison, colour meshes are chosen to represent the group comparison. All overlap scores are significantly different from zero, indicating that nodes in one module are most likely part of the same module in both groups. Note that Autism-ADHD overlap was reduced compared to the NT-ADHD overlap.

Lastly, we extended our main findings using covariance networks based on inter-regional correlation of the Local Gyrification Index (LGI). Structural covariance network based on LGI also showed a significant reduction of the nodal degree in highly connected nodes in Autism

compared with Neurotypical group (See Figure B.4). In line with the reduction of CT in the hubs of Autism and ADHD compared to Neurotypical groups described in Figure 2.5, we found a reduction of LGI in ADHD compared to Neurotypical groups for highly connected nodes. Overall, these results suggest that both thickness and gyrification of high degree nodes are particularly affected in these conditions.

2.5 Discussion

Comparing autism and ADHD, our findings reveal a complex topology of convergent yet distinct patterns of brain network organization. At a global level of community structure all groups show a significant degree of overlap, however the autism and ADHD group showed less similarity than they do compared to the neurotypical control group. The decay of cortical thickness correlation strength as a function of inter-regional distance was also markedly different for both clinical groups. Fitting with the idea of a local vs global connectivity difference in developmental conditions both the autism and ADHD group showed a pattern that diverges from the neurotypical control group. Yet, they do not appear to be in opposing direction. Both groups showed a significantly stronger decrease in correlation strength with increased distance relative to a control group.

These finding suggest that in both conditions the topology favours short-range correlations over long-range correlations. This idea is prominent in the autism literature, but less so in the ADHD literature. For example, Schaer and colleagues observed increased covariance in cortical folding in individuals with autism in short-range but not in long-range connections (Schaer et al., 2013). It will be interesting for future studies on different modalities such as resting-state or DTI

imaging to see if potential connectivity differences follow a pattern similar to the present structural covariance properties. In addition, we found that the ADHD group had a marked decrease in cortical thickness in high degree regions compared to the other two groups. A previous study showed that children with ADHD exhibited reduced CT in fronto-parietal regions, but increased CT in occipital regions (Almeida Montes et al., 2013). In the present analysis cortical hubs were mainly located in fronto-parietal networks, thus this finding fits with the idea of overall reduced CT in those areas. Interestingly, Almeida-Montes and colleagues also show that some of these differences increase with age. This would also fit with previous work showing some delay in cortical maturation of cerebrum and specifically prefrontal cortex in children with ADHD (Shaw et al., 2007).

A previous study indicated that wiring costs in autism might also fit in a model of increased local connectivity and decreased global connectivity in grey matter connections (Ecker, Ronan, et al., 2013). Thus, we extended our local versus global analysis to include wiring cost characteristics. We found that the ADHD group showed significantly reduced wiring cost. This is consistent with the notion of a network shift towards increased segregation (i.e. more local connections) at the expense of global integration (Deco, Tononi, Boly, & Kringelbach, 2015). We did not find a significant difference in the wiring cost for the autism group. The present approach to assess wiring costs differs significantly from the one taken by Ecker et al. (Ecker, Ronan, et al., 2013) (e.g., we use Euclidean distance between centroids of anatomically derived nodes compared to a measure of mean separation distance on the cortical sheet). It is possible that our approach might be too coarse to pick up wiring cost differences in the autism group. Our results do indicate a sharp reduction in the number of connections of the hubs regions in the autism network. Under-connected hubs could indicate a reduced capability of integrating

information over the long-range and across modalities, something that has often been speculated to be the case in autism (Happé & Frith, 2006). Again, future studies will have to show whether these patterns also emerge from connectomic data.

Since changes in structural covariance are postulated to be a result of a prolonged developmental process, our findings also provide emerging evidence for a systematic difference in the developmental trajectory/profile of brain organization between these groups. However, a recent large cross condition analysis of potential genetic relationship showed only moderate genetic overlap between autism and ADHD (Lee et al., 2013). Thus, the true underlying cause for these differences is likely more indirect and could emerge from long-term differences in brain function. In relation to that, phenotypic overlap might perhaps also be sought in a more indirect causal relationship. Unfortunately, the present data does not allow a detailed analysis of phenotypic or trait overlap (due to the lack of overlapping measures between the two datasets). Leitner (2014) lists a number of converging point in ADHD and autism aetiology, perhaps most strikingly the difficulties with social interaction. Although the profile, and possibly the cause, of social difficulties likely differs between children with autism or ADHD problems with social interaction are found in both (Leitner et al., 2014). Perhaps these have a concordant effects on brain networks as this is a critical element of brain development (Blakemore, 2010).

Contrary to our predictions, and in contrast to a previous study (Ray et al., 2014) that used a different imaging modality, we did not find any significant differences in rich-club topology between any of the groups. The rich-club coefficient indicates that high degree nodes are more likely to connect to other high-degree nodes (sometimes summarised as ‘the rich cling

together'). Although the structural covariance networks were constructed from T1-MPRAGE data, we had expected to find overlap between the fMRI, DTI and our current results. It would be highly interesting to see how these differences develop further. Connectivity findings in adult autism and ADHD are notoriously heterogeneous (Konrad & Eickhoff, 2010; Vissers et al., 2012), and some developmental neuroanatomical differences might gradually change with age. The present data was restricted to a very specific age group and developmental changes continue long after this time frame. It would be interesting to see whether the currently observed lack of differences in structural covariance topology propagate in the same direction. More research is needed to assess these potential longitudinal changes in this population.

Modular organization of the network of the three groups revealed no significant differences, but instead showed significant overlap. Therefore, network nodes belonging to one module in one group are likely to belong to the same module in the other group. Considered in the clinical context of overlapping phenotypes and high comorbidity, the present results strengthen the notion that these two conditions should not be studied in isolation. However, the two clinical groups (despite being significantly similar) show less modular similarity to one another than they do compared to a neurotypical group. However, both groups also showed significant overlap with the neurotypical group, suggesting that the neuroanatomical differences between the clinical and control groups operate on more fine-grained scales (such as might be observed in graph theoretical measures). This finding shows that when these groups are studied solely in contrast with a neurotypical group no difference might be observed on this metric.

There are some caveats surrounding the current study. First, and in contrast to some studies, we used cortical thickness estimates to construct our structural covariance network, thereby

excluding sub-cortical regions from network analysis. Separate analyses of subcortical volumetric and covariance differences for the present data are however included in the supplementary materials. To be able to combine cortical and subcortical regions, some studies have used covariance of grey matter volume instead (Balardin et al., 2015). However, grey matter volume relies on the relationship between two different morphometric parameters, cortical thickness and surface area. Cortical thickness and surface area are both highly heritable but are unrelated genetically (Panizzon et al., 2009), leading to different developmental trajectories across childhood and adolescence (Herting, Gautam, Spielberg, Dahl, & Sowell, 2015). The combination of at least two different sources of genetic and maturational influence into a unique descriptor of cortical volume may act as a confounding factor that hinders a clear interpretation in the context of cortical covariance based networks. This is particularly relevant in conditions such as autism and ADHD where differences in cortical thickness, cortical volume and surface area are highly heterogeneous (Ecker, Ginestet, Feng, Johnston, Lombardo, Lai, Suckling, Palaniyappan, Daly, Murphy, Williams, Bullmore, Baron-Cohen, Brammer, Murphy, et al., 2013; Wolosin, Richardson, Hennessey, Denckla, & Mostofsky, 2009).

Furthermore, as outlined in the introduction, structural covariance analysis is based on group-level data and we could thus not investigate any direct brain-behaviour relationship. In addition, although both the ABIDE and ADHD-200 are generally well phenotyped they do not share many overlapping behavioural measures that would allow more detailed analysis of potentially overlapping symptomatology. It could be the case that some of the findings here are in fact driven by subgroups within each condition that drive the group mean differences. Unfortunately, due to the nature of structural covariance analysis we are unable to fully disentangle that possibility.

Another potential caveat in clinical imaging studies is the interaction with medication. In the present sample only a small proportion of included subjects were reported to be on active medication (<5%). In the autism group these were predominantly anti-depressants (e.g. Fluoxetine), anti-psychotics (e.g. Risperidone) and in some cases psycho-stimulants (e.g. Methylphenidate). In the ADHD group these were predominantly psycho-stimulants (e.g. Methylphenidate). No information was available on the length of use or dosage. Although it seems unlikely that in this young age range there will have already been a sustained effect of medication use on cortical thickness, this cannot be fully ruled out in the present study. For reasons outlined above, structural covariance analysis does not lend itself to the analysis of small sub-groups.

In light of the recent proliferation in graph theoretical studies, several semantic caveats should also be clarified to facilitate cross-comparisons of findings. While we have adopted the term "structural covariance" to characterise the macroscale connectome, the same terminology has also been used to describe structural networks that are indicative of atrophy patterns in neurodegenerative conditions (Seeley, Crawford, Zhou, Miller, & Greicius, 2009). In the latter approach, the covariance networks are typically derived from voxel-wise seed-based correlations, the seed being defined as a focal site of atrophy as found using voxel-based morphometry (VBM). Distinct from these restricted patterns of pathology-related networks, other studies have derived whole-brain networks on the basis of pairwise correlations between the structural morphology (i.e. volume, thickness, gyrification) across brain regions (Alexander-Bloch, Giedd, et al., 2013; Lerch et al., 2006; Mak, Colloby, Thomas, & O'Brien, 2016). The second difference concerns the morphology of interest in deriving the structural networks. For instance, volume-based intensities are inherently limited by the geometric

convergence of surface area and cortical thickness (Ashburner & Friston, 2000), both of which may be underpinned by distinct genetic and developmental factors. In contrast, cortical thickness provides a physical property of the cortical mantle by explicitly modeling the boundaries between the white matter and pial surface (Fischl & Dale, 2000). Despite the differences in the construction of the networks, both approaches are similar in that the networks are derived at the group-level, thereby precluding single-subject analyses and/or correlations against clinical data. The central tenet of both approaches similarly rests upon the assumption that strong correlations - particularly those that exceed an arbitrary threshold - reflect underlying connectivity between regions (Alexander-Bloch et al., 2013).

Secondly, it is possible that in both publically available datasets, some participants might have been comorbid for the other condition (e.g., individuals in the ABIDE might have had comorbid ADHD, and *vice versa*). Although all individuals in these data-sets were diagnosed under the DSM-IV criteria, which does not allow this type of comorbidity, without the availability of more detailed diagnostic data, comorbidity or general phenotypic overlap cannot be ruled out completely. In addition, sample size restrictions would not allow a further subdivision within the presentation type of the ADHD group, which could be an interesting avenue for future research. Yet the primary aim of this study was to investigate overlap between the two conditions. If the present results were due to the individuals that shared this comorbidity, this would still support a common underlying neural architecture. Nonetheless, future longitudinal studies need to disentangle this overlap more precisely and in relation to specific phenotypic overlap as well as the trajectory of topological changes over time.

In sum, we found convergence between autism and ADHD, where both conditions show stronger decrease in covariance with increased Euclidean distance between centroids compared to a neurotypical population. The two conditions also show divergence. Namely, there is less modular overlap between the two conditions then there is between each condition and the neurotypical group. The ADHD group also showed reduced cortical thickness and higher degree in hubs regions compared to the autism group. Lastly, the ADHD group also showed reduced wiring costs compared to the autism group. Future research investigating these patterns in functional and structural connectivity and relating findings to behavioural or phenotypic data will hopefully shed light on the convergent and divergent neural substrates of autism and ADHD. Our findings do support the notion that both developmental conditions involve a shift in network topology that might be characterized as favouring local over global patterns. Lastly, they highlight the value of taking an integrated approach across conditions.

Chapter 3 Genetic origins of atypical brain organization

3.1 Introduction

In addition to behavioural, clinical differences, differences in cortical morphology between individuals with autism compared to typical controls have been reported (Ecker, 2016; Ecker, Ginestet, Feng, Johnston, Lombardo, Lai, Suckling, Palaniyappan, Daly, Murphy, Williams, Bullmore, Baron-Cohen, Brammer, Murphy, et al., 2013; Lai et al., 2014; Mensen et al., 2016). While heterogenous, recent studies have reported increased cortical volumes in the first years of life with autism compared to controls, with accelerated decline or arrest in growth in adolescents (Ecker, 2016; Mensen et al., 2016). Changes in cortical volume may be attributed to changes in cortical thickness (CT), changes in surface area, or both (Ecker, 2016).

In support of this, studies have separately identified differences in both surface area (Hazlett et al., 2017) and cortical thickness (CT) (E. Smith et al., 2016) in children with autism. Despite significant heterogeneity in cortical morphology, recent studies have indicated alterations in areas associated with higher cognition (e.g., language, social perception and self-referential processing) (E. Smith et al., 2016; Yang, Beam, Pelphrey, Abdullahi, & Jou, 2016). This has been supported by observed differences in cortical minicolumns in association areas in individuals with autism (McKavanagh, Buckley, & Chance, 2015).

It is unclear what contributes to these differences in cortical morphology in individuals with autism. Genetic factors play a major role in the development of brain networks and volumes in typically developing individuals (Elman et al., 2017; Hibar et al., 2015; Whitaker et al., 2016). For instance, twin heritability of cortical thickness measures suggest modest to high heritability for most regions of the brain (Eyler et al., 2012). In parallel, the contribution of genetic factors for autism has been estimated between 50-80% (Bourgeron, 2016; Gaugler et al., 2014; Tick, Bolton, Happé, Rutter, & Rijsdijk, 2016). Different classes of genetic variation have been associated with risk for autism. Several recent studies have identified a significant contribution of rare, *de novo*, putative loss-of-function mutations for autism (Kosmicki et al., 2016; Sanders et al., 2015; Stessman et al., 2017; Wang et al., 2013; Yuen et al., 2016). In addition, analyses of narrow-sense additive heritability has identified that common genetic variants, cumulatively, account for approximately half of the total variance in risk for autism (Gaugler et al., 2014).

Recent studies have also identified genes dysregulated in the autism post-mortem cortex (Gupta et al., 2014; Parikshak, Swarup, Belgard, Irimia, Ramaswami, Gandal, Hartl, Leppa, Ubieta, et al., 2016; Voineagu et al., 2011). Studies have replicably shown that genes involved in synaptic transmission and related neuronal processes are downregulated in the autism postmortem cortex, and genes involved in astrocytes and microglial pathways are upregulated (Parikshak, Swarup, Belgard, Irimia, Ramaswami, Gandal, Hartl, Leppa, Ubieta, et al., 2016; Voineagu et al., 2011). These dysregulated genes may either represent causal mechanisms for risk or compensatory mechanisms as a result of upstream biological and cellular changes. Genes dysregulated in the autism postmortem cortex are also enriched in specific gene-coexpression modules identified using both adult (Gupta et al., 2014; Parikshak, Swarup, Belgard, Irimia,

Ramaswami, Gandal, Hartl, Leppa, Ubieta, et al., 2016; Voineagu et al., 2011) and fetal (Parikshak et al., 2013) cortical postmortem samples.

Despite considerable progress in understanding neuroanatomical and genetic risk for autism, several questions remain. Mechanistically, it is likely that genetic risk variants alter neuroanatomical structural and functional properties, which ultimately contributes to the behavioural and clinical phenotypes. It is then pertinent to ask how genetic risk for autism contributes to differences in cortical morphology observed in individuals with autism. To our knowledge, no study has extensively investigated the association between autism risk genes and global changes in cortical morphology. Focusing on CT, we ask 3 specific questions: Q1) Which genes and biological pathways contribute to global differences in cortical thickness (ΔCT) in children with autism? Q2) What is the spatial expression profile of genes associated with ΔCT? and Q3) Are these genes enriched for three different classes of risk factors associated with autism: rare, *de novo* variants, common genetic variants, and/or dysregulated genes in the post-mortem cortex? We address these questions by combining analysis of ΔCT in autism as measured with MRI with gene expression postmortem data provided by the Allen Institute for Brain Science (AIBS; (Hawrylycz et al., 2012)). Similar, approaches have recently been used with the AIBS data in relation to schizophrenia (Romme et al., 2016) and myelination during development (Whitaker et al., 2016).

3.2 Methods

3.2.1 Overview

We first assessed differences in CT (ΔCT) across 308 cortical regions in individuals with autism by extracting cortical thickness estimates for 62 children with autism (cases) and 87 matched typically developing individuals (controls) from the ABIDE-I (Discovery dataset). Using median gene expression of 20,737 genes from 6 postmortem cortical brain samples (Hawrylycz et al., 2012), we conduct a Partial Least Squares regression (PLSR), a data reduction and regression technique, to identify significant genes and enriched pathways that contribute to ΔCT (Q1). We next quantify the expression of the same significant genes in terms of their spatial profile by comparing them across the different brain regions and Von Economo classes (Von Economo and Koskinas, 2008), which provides a way of assessing the hypothesis that there would be a global differentiation between higher order cognitive processing and more primary sensory processing (Q2). We test any significant genes for enrichment for 5 different sources of risk for autism (Q3):

1. Genes dysregulated in the autism postmortem cortex.
2. Adult cortical gene co-expression modules associated with dysregulated genes in the autism postmortem cortex.
3. Fetal cortical gene co-expression modules associated with dysregulated genes in the autism postmortem cortex.
4. Genes enriched for rare, de novo loss of function mutations in autism.
5. Common genetic variants associated with autism.

To assess the replicability of the discovery findings we validated the results using two independent datasets from ABIDE-II: Validation 1 with 48 cases and 54 controls and Validation 2 with 56 cases and 154 controls. In parallel, we also used a second list of genes

dysregulated in autism identified using a partially-overlapping cortical gene expression dataset autism and control post-mortem brain samples to validate the enrichment analysis within the original discovery dataset (validation autism gene expression dataset). To assess specificity of our results, we furthermore sought to answer these questions in a matched MRI dataset of children with ADHD, another childhood psychiatric condition. A schematic overview of the study protocol is provided in Figure 3.1.

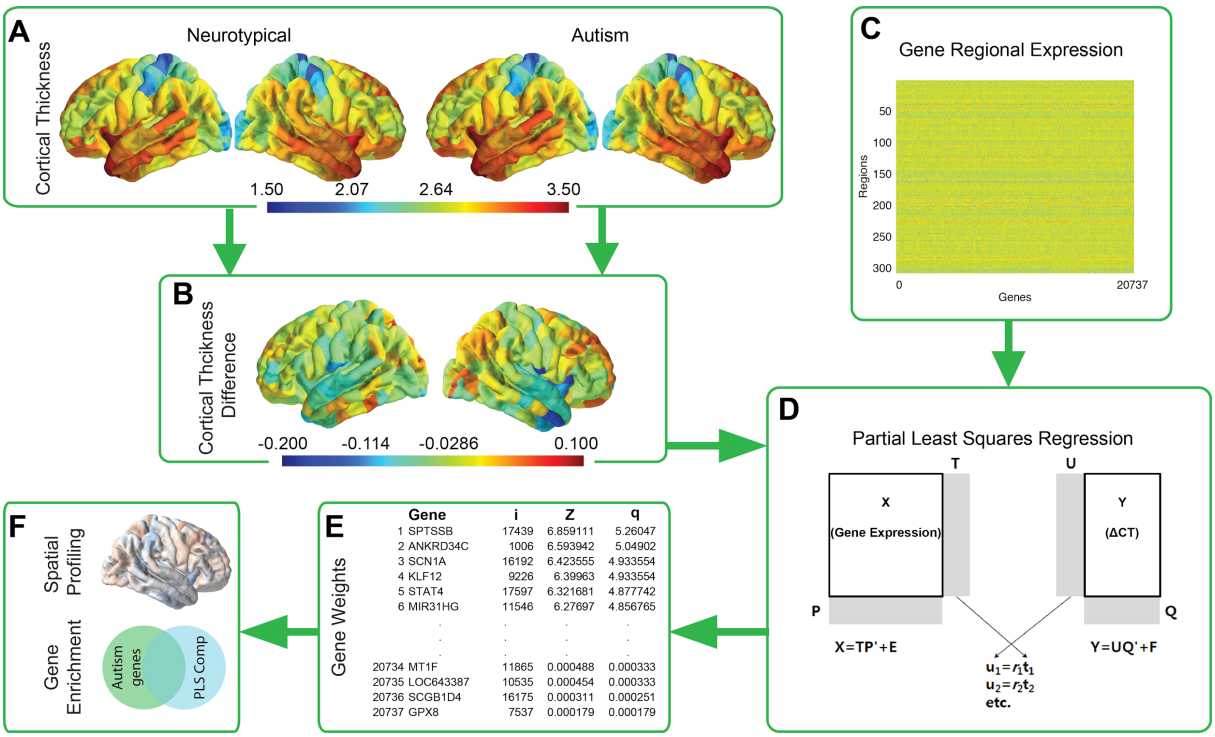

Figure 3.1: Schematic overview of the methodology

Mean cortical thickness was extracted for both the autism and the neurotypical groups across 308 cortical nodes (Panel A). A difference score in cortical thickness (ΔCT; autism - neurotypical) was calculated between these two groups (Panel B). In parallel the median AIBS gene expression profiles for 20,737 genes were calculated across the same 308 cortical nodes used in the imaging analysis (Panel C). Both these streams were included in a bootstrapped PLSR analysis that used the gene expression profiles as predictors and the ΔCT as response variable (Panel D). The PLSR assigns weights to each gene in terms of its contribution to the overall model in each component. Bootstrapped standard errors were derived and the gene weights were Z-transformed and corrected for multiple comparison using a Benjamini and Hochberg FDR correction (Panel E; i = gene index number, z = z-score for that gene's association and q = FDR corrected z-score). Genes that were significant after FDR correction (z-score>1.96) were analysed in terms of their spatial expression as well as tested for enrichment against three classes of risk for autism: dysregulated autism genes in the postmortem cortex, genes harbouring rare de-novo variants, and common genetic variants in autism (Panel F).

3.2.2 Discovery dataset

3.2.2.1 Neuroimaging

Imaging data used for discovery in this study are described in detail in the Supplementary Note and elsewhere (Bethlehem, Romero-Garcia, et al., 2017). In short, structural T1 weighted MPRAGE images were obtained from the ABIDE I database (http://fcon_1000.projects.nitrc.org/indi/abide/, selecting participants in the age range from 9-11, all males. All subjects were matched on age, and IQ between groups (see Table 1; Discovery Column). CT estimates were extracted using freesurfer and visually inspected for quality of segmentation by two independent researchers. Only when there was consensus on the quality were images included in the final sample. Next, images were parcellated into 308 cortical regions and mean CT for these regions was extracted. All groups were matched across scanner sites for mean CT. Scanning sites that had more than 10 individuals of only one group (Control/Autism) were excluded to avoid regressing out the group effect by regressing out site. In addition, scanner site was regressed out from CT estimates and the residuals were added to the group mean to allow for easier interpretation. The final discovery dataset consisted of 62 children with autism (cases) and 87 matched neurotypical individuals (controls).

3.2.2.2 Regional gene expression

We used the transcriptomic dataset of the adult human brain created by the Allen Institute for Brain Science (http://human.brain-map.org) (Hawrylycz et al., 2012). The AIBS dataset includes six donors, three Caucasian, two African-American and one Hispanic. Their ages were 57, 55, 49, 39, 31 and 24 years. Further details on microarray analysis are available from the Allen Institute (www.brain-map.org). As different cRNA hybridization probes were used to identify the expression level of the same gene, expression values from multiple probes were

averaged for each gene. Probes that were not matched to gene symbols in the AIBS data were excluded, resulting in 20,737 genes expression values that were evaluated in 3,702 brain samples. Due to the similarity of gene expression between hemispheres, the AIBS only sampled two of the four donors in the right hemisphere. In order to increase the number of AIBS samples per cortical region, all samples were pooled between hemispheres.

The anatomical structure associated to each tissue sample was determined using the MRI data provided by the AIBS for each donor. T1-images of the six donors were processed following the Freesurfer pipeline. The high-resolution parcellation with 308 cortical regions, employed in the neuroimaging dataset, was warped from the anatomical space of the average subject provided by FreeSurfer (fsaverage) into the surface reconstruction of each AIBS donor brain. Surface-based parcellation of each donor brain was transformed into a volumetric parcellation that covered the whole cortical mantle. 73% of the total AIBS cortical samples were located within the resulting volumetric parcels. To improve on this, the parcellation scheme was expanded 2 mm into the WM, resulting in a final AIBS sample coverage of 91%. Gene expression values for each cortical parcel were computed as the median gene expression of all the samples falling within the parcel from all six donors. Expression values had very different scales across genes, for that reason the regional expression values of each gene were normalized by taking a z-score across regions. The final regional gene expression values were represented as a 308x20737 matrix that contained the whole-genome expression data for the 308 MRI regions of interest.

3.2.2.3 PLSR analysis

PLSR was used to determine the relation between gene-expression and ΔCT (CT autism – CT NT). Partial least squares regression or PLSR is a data reduction technique closely related to principal component analysis (PCA) and ordinary least squares (OLS) regression. PLSR projects both the independent and dependent variable into a new space and identifies components that explain the maximum covariance between the independent and dependent variables. Principle component regression on the other hand, extracts components or factors with a view of maximizing the covariance only between the independent variables. As a result of the difference in methods, the components extracted in PLSR are more likely to explain the variance in the dependant variable. There are a few advantages of PLSR over OLS regression or PCA. First, it allows correlated variables in its predictor matrix (Wold, Sjöström, & Eriksson, 2001), with no assumption made about the distribution. Second, the precision of the PLSR model increases with an increasing number of relevant variables (Wold et al., 2001). Third, it can find a parsimonious model when the predictors are highly correlated, thus avoiding the problem of multicollinearity in OLS regression. Fourth, by projecting both the independent and dependent variable onto a new space, it extracts components in the independent variable that better explains the variance in the dependent variable, unlike PCA regression.

We used the SIMPLS algorithm (de Jong, 1993) to conduct PLSR in Matlab with median gene expression of 20,737 genes across 308 cortical nodes as the independent variable and ΔCT across the same 308 cortical nodes as the dependent variable. We identified the number of optimal components for PLSR using cross-validation (plsdepot package in R: https://cran.r-project.org/web/packages/plsdepot/index.html), and used the highest cumulative predictive error sum of squares to identify the number of components in the model with the best fit. To

assess significance of the contribution to the variance explained for each component we created a bootstrapped null-distribution for the variance of each of those components (10,000 resamples). We focused our analyses only on components that explained a significant proportion of the variance, and explained at least 10% of the variance.

Standard deviation for gene weights (or loadings) in each component were identified by bootstrapping (1000 bootstraps), and the weights for each gene were Z transformed after dividing them by the standard deviation. Significant genes in each component were identified after correcting for multiple testing using the Benjamini-Hochberg (Benjamini & Hochberg, 1995) FDR method (FDR-adjusted p or $q < 0.05$). We used significant genes with both negative and positive weights in our analysis. As our dependent variable, ΔCT, had both positive and negative values, weights are not informative about directionality in the analysis. A detailed description of the PLSR regression and the rationale behind choosing the unsigned weights is provided in the Supplementary Material.

3.2.2.4 Topographical enrichment analyses

Topographical (or anatomical) expression patterns of the significant genes in each component over the different cortical classes defined in the Von Economo (VE) atlas (Von Economo & Koskinas, 2008) were conducted after creating a resampling based null distribution (10,000 resamples). Z-scores for the differential expression across all 7 VE classes were computed and permuted to test their significant deviation from the null distribution.

3.2.2.5 Genetic modules and enrichment analyses

We used Enrichr (http://amp.pharm.mssm.edu/Enrichr) (Chen et al., 2013; Kuleshov et al., 2016) to investigate the enrichment of significant PLSR genes for each component against Gene Ontology Biological Processes. We also investigated the enrichment in different classes of autism risk genes using logistic regression:

1. *Transcriptionally dysregulated genes* (n = 1143, 584 upregulated and 558 downregulated in the autism cortex) were identified from Parikshak *et al*. (2016) (48 autism donors and 49 neurotypical donors). We used genes that were transcriptionally dysregulated in the postmortem cortex with FDR adjusted P-values < 0.05. We also separated the genes into transcriptionally downregulated and transcriptionally upregulated and tested enrichment separately to see if either upregulated or downregulated genes drive the enrichment with the dysregulated genes.
2. Adult gene co-expression modules: Transcriptionally dysregulated genes are likely to represent a number of different biological processes. To further understand what processes they contribute to, we can investigate specific gene co-expression modules associated with transcriptionally dysregulated genes. Gene co-expression modules are thought to represent clusters of genes that co-express, and are under common co-regulatory mechanisms and which, ultimately contribute to common function. We investigated enrichment in six-postmortem cortical weighted gene co-expression modules that were significantly associated with the dysregulated genes: Modules M9, M19, and M20 (associated with transcriptionally upregulated genes in autism compared to control cortex) and modules M4, M10, and M16 (associated with transcriptionally downregulated genes in autism compared to cortex) (Parikshak et al., 2016).
3. Fetal gene co-expression modules: As autism is a neurodevelopmental condition we

also investigated if significant PLSR genes for each component were enriched for specific developmental cortical weighted gene co-expression modules that are associated with either rare, *de novo* variants in autism (Mdev2 and Mdev3) or with transcriptionally dysregulated genes in the autism post-mortem cortex (Mdev13, Mdev16, and Mdev17) (Parikshak et al., 2013).

4. *Genes harbouring rare, de novo, putative loss of function variants* (rare, de novo genes, n = 65) were identified from Sanders et al., (2015).
5. *Common genetic variants* associated with autism were downloaded from the latest data freeze from the Psychiatric Genomics Consortium (5,305 cases and 5,305 pseudocontrols). Gene based P-values and Z scores were obtained using MAGMA for each gene (de Leeuw et al., 2015).

Enrichment analyses for the different classes of autism risk genes were done using logistic regression after accounting for gene length as a covariate. Enrichments are reported as significant if they had a Benjamini-Hochberg FDR adjusted P-value < 0.05 (Benjamini & Hochberg, 1995) and if they have an enrichment odds ratio (OR) > 1. The Supplementary Material provides further details about the gene sets and the methods used.

3.2.3 Autism structural MRI validation dataset

To validate our initial findings two additional MRI imaging datasets were obtained from the ABIDE-II: ABIDE-GU (Georgetown University), consisting of 51 children with autism and 55 typically developing children (Validation 1) and ABIDE-KKI (Kennedy Krieger Institute) that included 56 children with autism and 155 neurotypical controls (Validation 2). After quality control, we excluded 3 cases and 1 typical control from ABIDE-GU and 2 controls for ABIDE-

KKI, as they were outliers for global CT. This resulted in a final sample of 48 cases and 54 controls for Validation 1 and 56 cases and 154 controls for Validation 2 (see Table 3.1; Validation columns). PLSR analyses were performed using the same methods in the discovery dataset (more details on this dataset are provided in a Supplementary Note). As only the first component significantly explained the variance ($P < 0.00001$, 10,000 bootstraps), we focused subsequent analysis on the first component. GO term enrichment, pathway, and gene enrichment analyses were performed as described for the discovery dataset. Gene enrichment analyses that were significant in the discovery dataset were validated against the validation MRI datasets using the following genes of interest: Transcriptionally downregulated genes from adult postmortem brain tissues (Parikshak, Swarup, Belgard, Irimia, Ramaswami, Gandal, Hartl, Leppa, Ubieta, et al., 2016); adult gene-coexpression modules associated with transcriptionally downregulated genes in autism (M4, M10, M16, and M20) (Parikshak, Swarup, Belgard, Irimia, Ramaswami, Gandal, Hartl, Leppa, Ubieta, et al., 2016);; and developmental cortex gene-coexpression modules associated with transcriptionally dysregulated genes (Mdev13 and Mdev17). We again corrected for all the tests conducted in each validation dataset using Benjamini-Hochberg FDR. In addition to validation using independent MRI data, we performed validation of the enrichment for downregulated genes using a partially overlapping gene-expression dataset (33 autism donors and 38 control donors; 13 autism donors and 14 control donors overlap) (Gandal et al., 2016). We investigated if the significant PLSR genes identified in all three MRI datasets (Discovery, Validation 1, and Validation 2) were enriched for downregulated genes identified from the Validation autism gene expression dataset. Further details on this are provided in the Supplementary Material.

3.2.4 ADHD structural MRI dataset

To investigate the selectiveness for autism we also ran the PLSR analysis for ΔCT in a matched group of children with and without ADHD, another childhood condition, selected from the ADHD-200 database (http://fcon_1000.projects.nitrc.org/indi/adhd200/). This is the same group as described elsewhere (Bethlehem, Romero-Garcia, et al., 2017) with the control groups being identical to the above described control group in the discovery dataset (see Table 3.1; Discovery Column and Validation 2 Column). Selection and all analysis on the ADHD dataset follow the same pipeline as the autism discovery dataset and are included in the Supplementary Material. The ADHD group was also matched to the discovery autism and neurotypical groups with regards to age, IQ and mean cortical thickness across scanner sites. Matching of the groups and regression of cortical thickness was done simultaneously with the above described discovery dataset to ensure a valid comparison between both groups could be made.

Table 3.1: Descriptive statistics for all three datasets

	Discovery		**Validation 1**		**Validation 2**		**ADHD**	
	Autism	**Controls***	**Autism**	**Controls**	**Autism**	**Controls**	**ADHD**	**Controls***
n	62	87	48	54	56	154	69	87
	(0 F)	(0 F)	(8 F)	(27 F)	(15 F)	(56 F)	(0 F)	(0 F)
Age	10.07	10.04	10.98	10.43	10.32	10.34	9.99	10.04
	(±1.11)	(±1.13)	(±1.53)	(±1.71)	(±1.51)	(±1.20)	(±1.17)	(±1.13)
FIQ	108.86	110.98	118.68	122.04	103.42	114.4	107.95	110.98
	(±16.94)	(±10.39)	(±15.01)	(±13.27)	(±15.99)	(±10.55)	(±14.18)	(±10.39)

The Discovery cohort was obtained from ABIDE-I. The validation cohorts were obtained from the ABIDE-II (Validation 1: Georgetown University, Validation 2: Kennedy Kreiger Institute). The n-row denotes the number of subjects with the number of females (F) provided in parenthesis, FIQ denotes the full-scale IQ, with standard deviations in parenthesis below. *Indicates that the same controls were used for both the

Autism Discovery and the ADHD datasets. Further details on the Discovery and ADHD datasets are described elsewhere (Bethlehem, Romero-Garcia, et al., 2017).

3.3 Results

3.3.1 Autism discovery MRI dataset

3.3.1.1 PLSR analyses and characterization

Cross-validation using an initial 35 component analyses identified that a 13-component model had the best fit (Supplementary Table C.1) Thus, PLSR was run using a 13-component model. Four components (Components 1, 3, 4 and 6) explained more than 10% of the variance in the total model (Supplementary Figure C.1). However, variance in ΔCT explained by PLS components was higher than expected by chance only for the first component ($p = 0.009$, 10,000 permutations) but not for the remaining components ($p = 0.303$, $p = 0.693$ and $p = 0.394$, for components 3, 4 and 6, respectively). We first conducted pathway and ontology based enrichment analyses to characterize the first component. Supplementary Table C.2, shows the top ten pathways at the Kyoto Encyclopedia of Genes and Genomes (KEGG) for the first component. Only the GO term "Synaptic Transmission" in component 1 (PLSR1) survived FDR correction for multiple comparisons (q-value = 0.00006). PLSR1 was also significantly enriched for 11 pathways (Table C.2). As only PLSR1 had clear biological underpinnings and was significantly associated with CT variance, we thus focused on PLSR1 for subsequent enrichment analyses. There was a significant positive correlation between ΔCT and the scores of PLSR1 ($r = 0.32$; $P = 4.15x10\text{-}9$; Figure 3.3G)

3.3.1.2 Topographical enrichment analyses

We next conducted spatial characterization of PLSR1 across all 5 VE classes (Von Economo & Koskinas, 2008) as well as an additional 2 subtype classes covering limbic regions and allocortex (class 6) and insular cortex (class 7) (Whitaker et al., 2016; Zilles & Amunts, 2012). As described above, we expected a potential differentiation between higher order cognitive processing and more primary sensory processing. The genes in PLSR1 are significantly over-expressed in secondary sensory and association cortices (VE classes 2, 3 and 4: all $P_{corrected} < 0.01$) compared to a null distribution. In limbic and insular regions however these genes appear to be under-expressed (VE classes 6 and 7: all $P_{corrected} < 0.01$). However, they also appear to be over-expressed in granular and primary motor cortices (VE Class 1). Figure 3.2 shows the results from the spatial characterization of the first component across all VE classes. Von Economo expression profiles in the two validation datasets largely resemble the pattern of over-expression in association cortices observed in the discovery dataset (Supplementary Materials and Supplementary Figure C.5). The validation datasets additionally revealed a significant under-expression of the PLSR1 in primary sensory areas (classes 1 and 5; $P_{corrected} < 10^{-4}$).

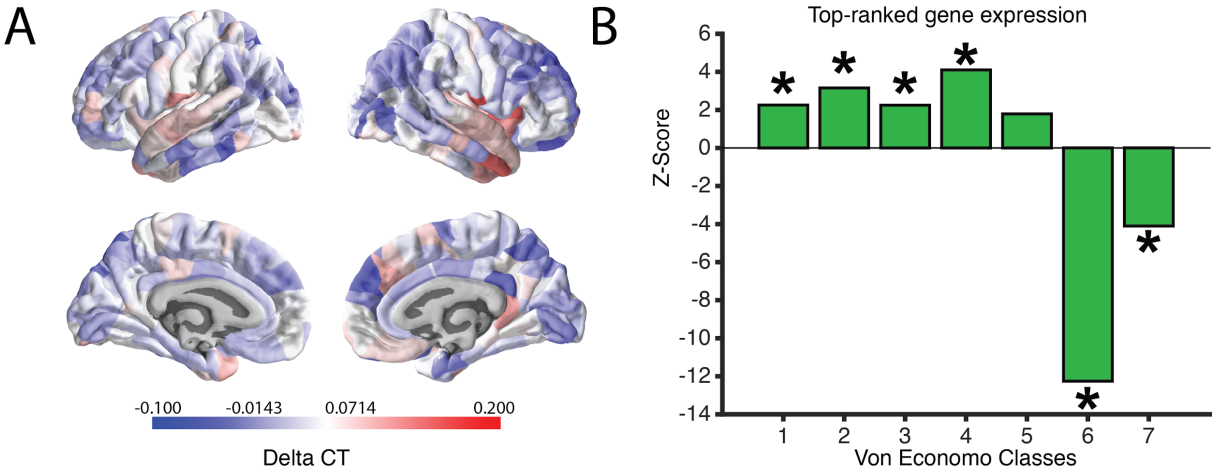

Figure 3.2: Expression and Von Economo classification for PLSR1

The heatmap in panel A shows the ΔCT distribution across all 308 cortical regions. The barplot in panel B shows the z-scores of the mean distribution across the different Von Economo Classes (Class 1: granular cortex, primary motor cortex. Class 2: association cortex. Class 3: association cortex. Class 4: dysgranular cortex, secondary sensory cortex. Class 5: agranular cortex, primary sensory cortex. Class 6: limbic regions, allocortex. Class 7: insular cortex.). All significant over- or under-expression classes are marked with an asterisk. To determine significance, we used permutation testing and an FDR corrected p-value < 0.025 to fully account for two-tailed testing.

3.3.1.3 Gene enrichment analyses

We first investigated if the significant genes in the PLSR1 component were enriched for genes that are differentially expressed in the autism cortex. We identified a significant enrichment for genes that are dysregulated in the autism post-mortem cortex (OR = 1.21; $P_{corrected} < 2.81x10^{-15}$). This was driven entirely by genes downregulated in autism cortex in comparison to control cortex (OR = 1.87; $P_{corrected} < 3.55x10^{-16}$). In comparison, there was no enrichment for upregulated genes (OR = 1.01; $P_{corrected} = 0.49$). The downregulated genes have been previously reported to be enriched for several GO terms including synaptic transmission (Parikshak, Swarup, Belgard, Irimia, Ramaswami, Gandal, Hartl, Leppa, Ubieta, et al., 2016).

Transcriptionally dysregulated genes can reflect several different underlying processes. To provide better resolution of the processes involved, we next investigated if this enrichment was associated with six adult co-expression modules associated with dysregulated autism genes. Three of these were associated with genes downregulated in the autism postmortem cortex (M4, M10, M19), and three were enriched for genes upregulated in the autism postmortem cortex (M9, M19, and M20) compared to controls. As we had identified a significant enrichment for downregulated autism genes but not for the upregulated autism genes, we hypothesized that gene co-expression modules associated with downregulated genes would also be enriched for association with PLSR1 genes. Indeed, PLSR1 was enriched for all three downregulated

modules (M4: OR = 1.07; $P_{corrected} < 3.55x10^{-16}$; M10: OR = 1.07; $P_{corrected} < 3.55x10^{-16}$; M16: OR = 1.07; $P_{corrected} < 3.55x10^{-16}$) but none of the 3 upregulated modules (M20) (M20: OR = 0.96; $P_{corrected} < 7.655x10^{-5}$; M9: OR = 0.93; $P_{corrected} = 2.92x10^{-14}$; M19: OR = 0.93; $P_{corrected} < 3.55x10^{-16}$).

We next investigated if the significant genes in PLSR1 are also enriched in specific cortical developmental modules constructed from gene expression dataset of fetal or early postnatal brains. We focused our investigation on 5 modules with evidence of association with different classes of autism risk genes (Parikshak et al., 2013). The Mdev13, Mdev16, and the Mdev17 modules are enriched for transcriptionally dysregulated genes in autism postmortem frontal and temporal cortices (Parikshak et al., 2013). The Mdev2 and the Mdev3 modules are enriched for rare variants identified in autism (Parikshak et al., 2013). We reasoned that our PLSR1 component would be enriched for the three modules also enriched for transcriptionally dysregulated autism genes, but not for the two modules enriched for rare de novo variants associated with autism, in line with previous enrichment analyses. We identified significant enrichment for Mdev13 (OR = 1.04; $P_{corrected} < 3.55x10^{-16}$), Mdev 16 (OR = 1.05; $P_{corrected} < 3.55x10^{-16}$) and Mdev17 (OR = 1.04; $P_{corrected} < 3.55x10^{-16}$). For the two modules associated with rare, *de novo* variants, we identified fewer PLSR1 genes than expected by chance (Mdev2: OR = 0.9659; $P_{corrected} = 1.70x10^{-11}$; Mdev3: OR = 0.961; $P_{corrected} < 3.55x10^{-16}$).

We did not identify a significant enrichment for rare, *de novo* genes (OR = 0.96; $P_{corrected} = 0.27$). We also did not identify a significant enrichment for common variants using MAGMA to collapse SNP based P-values to gene based P-values (OR = 1.00; $P_{corrected} = 0.29$). Results of the gene enrichment analysis are provided in Figure 3.3J and Supplementary Table C.6.

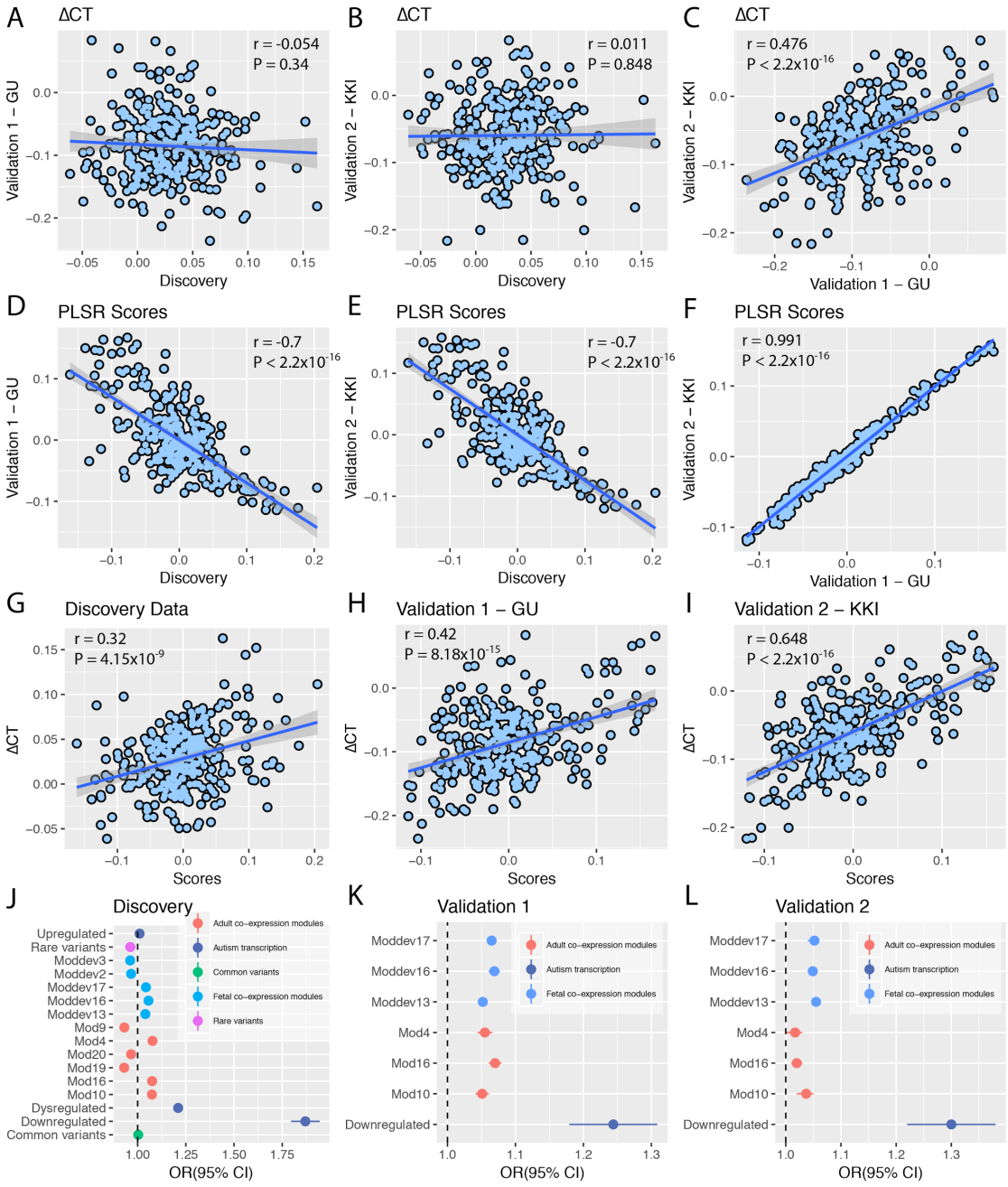

Figure 3.3: Dataset comparisons

Panels A-C show the correlation between ΔCT in the three datasets. Panels D-F show the correlation between the PLSR scores of all three datasets. Panels G-I show the correlation between ΔCT and the PLSR scores in all three datasets (indicating that increased scores are strongly correlated with increased ΔCT). Panel J shows the odds ratios for the gene-enrichment analysis in the discovery dataset. All significantly enriched modules were replicated in the validation datasets (panels K and L) apart from module 4 of the adult co-expression modules. Pearson correlation coefficient and P-values of the correlations are provided in the top of the respective panels.

3.3.2 Autism validation MRI dataset

3.3.2.1 PLSR analyses and characterization

We conducted validation of all the significant enrichment analyses using ΔCT from two independent cohorts (Validation 1 and Validation 2). Both the validation samples include males and females, though of a similar age range, whereas, the discovery dataset included only males. We first investigated the correlations in ΔCT between the three datasets. There was a non-significant correlation between the discovery and the two validation datasets (Figure 3.3A and 3.3B). This can be explained by a number of factors such as the inclusion of females in the second dataset (though the supplementary materials includes an analysis to rule this factor out), heterogeneity due to scanner sites in the discovery dataset, age of onset of puberty, and clinical conditions. However, there was a significant positive correlation in ΔCT between the two validation datasets ($r = 0.476$; $P < 2.2x10\text{-}16$).

Variance in ΔCT explained by PLS components was again significant only for the first component (PLSR1-validation) ($P < 10^{-14}$, 10,000 permutations) for both validation datasets (Supplementary Figure C.2). Subsequent analysis focused only on this component (PLSR1). The first component explained 14% of the total variance in Validation 1 and 42% of the total variance in Validation 2. There was also a significant positive correlation between ΔCT and the gene expression scores in both validation datasets (Figures 3.3H and 3.3I) as was the case in the discovery dataset (Figure 3.3.G). Further, PLSR1 was also enriched for the GO term 'Synaptic transmission' ($P_{corrected} = 0.0001$ for both Validation 1 and Validation 2). In addition, for Validation 2, the PSLR component was also enriched for the GO term 'Membrane depolarization' ($P_{corrected} = 0.0007$). Enrichment in KEGG pathways for both the validation datasets are provided in Supplementary Tables C.3 and C.4.

Despite the lack of correlation between ΔCT in the Discovery and the two validation datasets, there was significant correlation in the gene scores (Figures 3.3D to 3.3F and Figure 3.4 A to C) and gene loadings (Supplementary Figure C.3). Despite the different correlations in ΔCT between the datasets, PLSR identifies highly correlated gene expression scores, with similar gene weights, suggesting that a highly similar set of genes contribute to ΔCT in autism in the three different datasets. This was further supported by a high degree of rank-rank overlap in the Z scores of the PLSR1 components of the three datasets (Supplementary Figure C.7 and Supplementary Materials). We note that the while the discovery dataset comprises only male participants, both Validation 1 and Validation 2 comprises male and female participants. We investigated if the removal of female participants increased the correlation in ΔCT, gene loadings, and gene scores (Supplementary Materials). We did not find any evidence of improved correlations after removing the female participants (Supplementary Figure C.4). Thus it seems unlikely that biological sex is the main contributor to this noise. As the datasets mainly differ on multi-site versus single-site it seemd plausible that some of the noise might be explained by the fact that different scanners were involved to cllect the datat from the discovery data.

3.3.2.2 Topographical enrichment analyses of PLS scores

We also explored the topographical pattern of the PLSR scores. The areas that show particularly high scores are extremely robust across datasets (as would be expected from the highly significant correlations). This was particularly evident in areas around the temporo-parietal junction (both left and right), left and right temporal lobe and some smaller effects around frontal and anterior cingulate regions. Although this analysis should be considered

exploratory it is interesting to note that they are all regions that are specifically implicated in autism (Lombardo et al., 2011; Lombardo & Baron-Cohen, 2011).

Figure 3.4: PLS Scores for all autism datasets

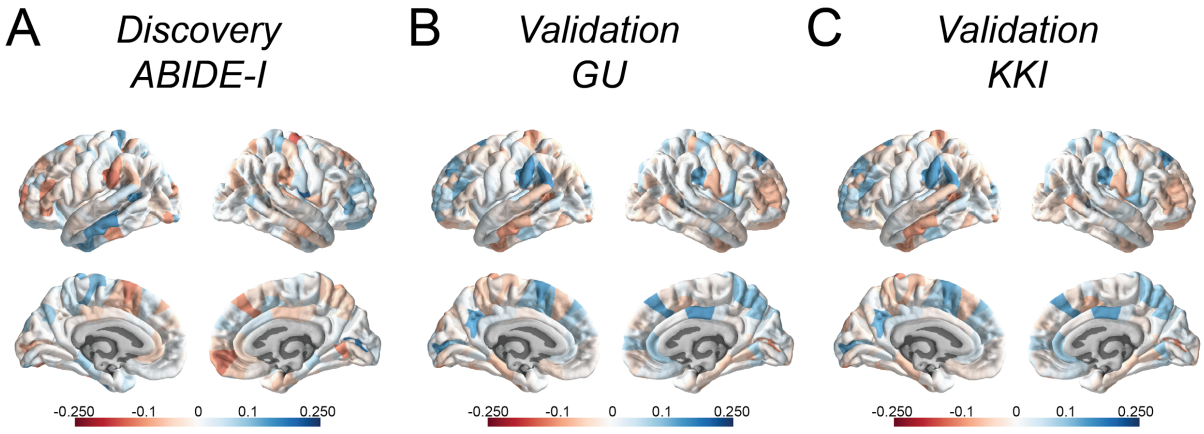

3.3.2.3 Gene enrichment analyses

We next sought to replicate the significant genetic enrichments observed in the analyses using the discovery dataset. We identified a significant enrichment of transcriptionally downregulated genes in the autism post mortem cortex (Validation 1: OR = 1.24; $P_{corrected}$ = 0.004; Validation 2: OR = 1.3; $P_{corrected}$ = 0.001), providing confidence in the robustness of our initial results (Figure 3.3K and L).

Mirroring the enrichment with the downregulated genes in the autism post-mortem cortex, we also identified enrichment for the three adult gene co-expression modules that are enriched for downregulated genes in Validation 1 (M4, M10, and M16) and two of the three (M10 and M16) adult gene co-expression modules for Validation 2 (Figure 3.3K and L, Supplementary Table C.6). We were able to also replicate the enrichment for the three fetal gene co-expression

modules (Mdev13, Mdev16, and Mdev17) for both the validation datasets (Figures 3.3K and 3.3L, Supplementary Table C.6).

3.3.3 Secondary validation analyses

Our primary validation used an independent MRI dataset. However, we also sought to validate our results using a partially overlapping post-mortem gene-expression dataset from individuals with autism and controls (Gandal et al., 2016). Some cortical tissue samples overlap with discovery post-mortem gene expression dataset from Parikshak et al., 2016, details of which are provided in the Supplementary Materials. This provides a second list of genes downregulated in the autism post-mortem cortex. We focused only on the genes downregulated in the autism post-mortem cortex as this was driving the enrichment identified in the discovery and validation MRI datasets. Using significant PLSR1 genes from the discovery MRI dataset we identified a significant enrichment for the new list of downregulated genes (OR = 1.39, $P_{corrected} = 1.86x10^{-7}$). We identified a similar enrichment using significant PLSR1 genes from both the validation datasets (Validation 1: OR = 1.35; $P_{corrected} = 0.005$; Validation 2: OR = 1.30; $P_{corrected} = 0.019$). This validation using a partially overlapping gene expression dataset provides further robustness to the results.

3.3.4 Comparison with ADHD

We also wanted to investigate if the enrichment was specific to autism or whether there was a similar mechanism in other neuropsychiatric conditions. To make the analysis comparable to the autism analysis, we focused on ADHD, another developmental neuropsychiatric condition affecting children. There are significant phenotypic and genetic correlations between the two

conditions, and we had access to matched MRI data from children with ADHD. PLSR analysis of ΔCT in ADHD data did not identify any components that significantly explained the variance in ΔCT (Supplementary Table C.5). Thus, we did not consider the ADHD dataset for further analyses. Details of the number of components, the model fit, and the variance explained are provided in the Supplementary Material.

3.4 Discussion

We report the association of transcriptionally downregulated genes in the autism postmortem cortex with global differences in cortical thickness in 166 children with autism and 295 neurotypical children. Using partial least squares regression on a discovery dataset of 62 cases and 87 controls, we identify one component (PLSR1) that explains a significant proportion of variance in ΔCT and is enriched for the GO term 'Synaptic Transmission'. This component was enriched for genes downregulated in the autism post-mortem cortex, which we validated using two independent structural MRI datasets and a quasi-independent autism post-mortem gene expression dataset. However, we did not find an enrichment for either common variants or rare, *de novo* variants associated with autism in the current study. We also identify that the PLSR1 genes are enriched for fetal and adult developmental cortical modules that have been previously reported to be enriched for transcriptionally dysregulated genes in the postmortem autism cortex and for genes involved in synaptic transmission (Parikshak et al., 2013; Parikshak, Swarup, Belgard, Irimia, Ramaswami, Gandal, Hartl, Leppa, Ubieta, et al., 2016). In contrast we did not find an enrichment for developmental cortical modules enriched for rare variants associated with autism, underscoring the role of transcriptionally dysregulated genes but not rare de novo variants associated with autism. We were unable to identify genes that contribute to ΔCT in ADHD, another childhood condition. Our study provides robust

evidence linking large-scale differences in CT to synaptic genes and dysregulated genes in the autism postmortem cortex.

The validation using two independent autism MRI datasets, this time comprising MRI data from both male and female children with and without autism suggests a few things. First, the results are valid even using MRI data from different cohorts. The results were also valid despite non-significant correlations in global ΔCT between the discovery and the two validation datasets. Second, our results suggest that the same sets of genes contribute to ΔCT regardless of sex. Studies have identified differences in cortical morphology between neurotypical males and females and between males and females with autism (Lai, Lombardo, Suckling, et al., 2013; Sowell et al., 2007). We furthermore identified a high correlation between a males-only dataset and two males and females combined MRI datasets for the gene weights and gene scores in the first PLS component.

Previous studies have identified a role for the genes involved in synaptic transmission and neuronal signaling in brain networks (Whitaker et al., 2016). Changes in CT may be due to a host of factors such as changes in myelination, synaptic pruning, and dendritic arborization (Dube et al., 2015; Fjell et al., 2015). The enrichment of genes involved in synaptic transmission with genes that contribute to differences in cortical thickness may, thus, reflect these underlying processes. Evidence from rare genetic variants (Bourgeron, 2009, 2015) and transcriptionally dysregulated genes in autism have highlighted a role for synaptic transmission in the aetiology of autism (Parikshak, Swarup, Belgard, Irimia, Ramaswami, Gandal, Hartl, Leppa, Ubieta, et al., 2016; Voineagu et al., 2011). We find an enrichment for transcriptionally dysregulated genes in CT differences in autism, but have not identified an enrichment for rare, *de novo* loss

of function genes or common variants implicated in autism. The lack of enrichment with rare, *de novo* loss of function genes may be due to both the relative low frequencies of such variants and small proportion of variance in liability explained by rare de novo variants (Gaugler et al., 2014). In contrast, the lack of enrichment with common variants may be explained by the lack of statistical power of even the largest available autism GWAS dataset.

The current study does not directly describe a mechanism that links dysregulation in synaptic genes and cortical thickness differences. However, animal studies have shown that several candidate genes for autism risk are regulated by synaptic activity, leading to the hypothesis that dysregulation in synaptic homeostasis is a major risk for autism (Bourgeron, 2015). The effects of this can contribute to both processing of cognitive and non-cognitive input, and to more morphological changes in neuroanatomy via processes such as activity dependent synaptic pruning and dendritic arborization. Post-mortem studies on the brains of children and adolescents with autism have indicated a lack of synaptic pruning (Tang et al., 2014). Investigating the specific role of synaptic genes in altering neural circuitry and cortical morphology will help elucidate the precise molecular mechanisms underlying cortical thickness differences seen in autism.

There are, however, some caveats that need to be taken into consideration while interpreting these results. While we have used the largest sample of MRI data in children with autism available to us, the sample size is still not ideal to capture the high heterogeneity in the condition. We deliberately focused on a narrow age range to reduce age-related variability at the cost of increasing the number of samples. Second, gene expression data was derived from only six postmortem adult brain samples (which is the largest and most detailed currently

available). Gene expression is known to vary with age (Glass et al., 2013; Somel et al., 2010). Unfortunately, we are restricted in using the adult gene expression data from the AIBS for several reasons. First, this is the most spatially detailed dataset of gene expression. Second, the availability of MNI coordinates in the adult gene expression datasets allows for mapping of gene expression in distinct brain regions to cortical thickness differences extracted from MRI scans. Third, gene expression changes with age are limited and restricted to specific brain regions. A recent study identified only 9 genes significantly altered globally across the 10 regions investigated in post-mortem tissue samples (Soreq et al., 2017), largely driven by glial genes. Cell specific enrichment in our dataset implicated neuronal genes only. Fourth, as autism is a developmental condition, investigating differences in cortical morphology at an early age is important to limit the role of environmental factors that contribute to differences in cortical morphology later in life (Lange et al., 2015; B. a. Zielinski et al., 2014). Fifth, enrichment for gene expression modules associated with autism risk in the developing cortex provides further confidence that the genes identified here are relevant across the age-spectrum. We do acknowledge that investigating a paediatric specific gene-expression dataset will help further refine the analyses, once this data becomes available.

Third, we focused on a specific age-range for the current study. Longitudinal changes in autistic individuals have been observed (Hazlett et al., 2017; Lange et al., 2015), and different genes and pathways may contribute to cortical morphology at different ages. Further, the age of onset of puberty varies between individuals and we note that, particularly for the older children in our datasets, puberty may influence morphology (Koolschijn et al., 2014). Finally, transcriptional dysregulation may reflect both a causative risk mechanism for autism, or a compensatory consequence of genetic, hormonal, and environmental risk for autism. We were

unable to disentangle if transcriptionally dysregulated genes causally contribute to cortical morphology changes, or if they are both downstream of a common risk mechanism, or both.

To our knowledge, this is the first study linking different genetic risk mechanisms in autism with changes in cortical morphology. In sum, we have shown that genes that are enriched for synaptic transmission and downregulated in individuals with autism are significantly associated with global changes in cortical thickness. We also show that these genes are generally overexpressed in association cortices. We were able to validate the results in an independent MRI dataset and quasi-independent gene expression dataset but not in a matched MRI dataset that included individuals with ADHD, showing both replicability as well as selectivity.

Chapter 4 Altered structural brain organization in adults with autism

4.1 Introduction

Neuroscientific, psychological, genetic and biological research into mental health is marked by a search for commonalities in the underlying neurobiology. In some conditions however, this is easier said than done. Autism is one such condition that is difficult to capture in a concise way while doing justice to the breadth of the spectrum. It is for example not uncommon to speak of the 'autisms' rather than of autism as a single type of condition. DSM-V defines autism as a developmental disorder marked by qualitative impairments in social interaction and communication combined with repetitive and stereotyped behaviour (American Psychiatric Association, 2013). This categorical definition however might not fully capture the wide phenotypic variety seen in the autistic spectrum. Indeed, DSM 5 now defines conditions on a spectrum or scale rather than as a category. The heterogeneity of the condition is strongly reflected in the diversity and variability of research findings. Some have even characterized the field as "a fragmented tapestry stitched from differing analytical threads and theoretical patterns" (Belmonte et al., 2004). Nonetheless there have been some promising results in the search for an underlying framework that can characterize the specificity of autism while still applying to the whole spectrum. One particularly promising and interesting approach has been that of brain connectivity or network analyses.

4.1.1 Cognitive processing styles in autism

There are several theories describing specific aspects of the autism spectrum and its traits and behaviours. Some prominent theories include that of hyper-systemizing (Baron-Cohen, Ashwin, Ashwin, Tavassoli, & Chakrabarti, 2009; Baron-Cohen, Hoekstra, Knickmeyer, & Wheelwright, 2006) and enhanced perception (Ashwin, Ashwin, Rhydderch, Howells, & Baron-cohen, 2009; Plaisted Grant, Davis, Grant, & Davis, 2009). The theory of hyper-systemizing, for example, proposes that people with autism have a strong drive to search for repeating patterns or rules to understand a system. Enhanced perception theory argues that sensory experience is heightened allowing the development of specific talents seen in autistic individuals (Ashwin et al., 2009; Plaisted Grant et al., 2009). Hyper-systemizing and enhanced perception are not incompatible and might in fact complement one another. What separates these two theories from most others is that they focus on the possible over-development of a specific trait, perhaps giving rise to talent. In contrast, other prominent theories have focused more on deficits in cognitive processing. Examples include deficits in executive functioning (Ozonoff, Pennington, & Rogers, 1991) complex information processing (Minshew, Goldstein, & Siegel, 1997) and empathy (Baron-cohen, Richler, Bisarya, Gurunathan, & Wheelwright, 2003; Baron-Cohen & Wheelwright, 2004). Since their postulation, several studies have provided support for differences in cognitive processing (Happé, 1999; Happé & Frith, 2006).

Two prominent theories have sought a more integrated approach to unifying some of the heterogeneity in autism by taking a broader perspective. The Weak-Central Coherence (Happé & Frith, 2006) (WCC) theory of autism proposes that people with autism have a cognitive style that involves a preference for processing local details over the global picture. In people diagnosed with autism this theory has often been used to explain a dichotomy between

difficulties in social interaction combined with an excellent eye for detail. Social interaction requires people to take into account the overall context, being relatively flexible, not rigidly systemizing and not only focusing on specific sensory details.

A second theory that takes a broader perspective is the extreme male brain theory (EMB) (Baron-Cohen, 2002). Stemming from the fact that autism is much more common in males (with estimated ratios ranging from 1 in 4 to 1 in 2). Baron-Cohen proposed that autism or autistic traits show a pattern of extreme masculinization, where any typical sex difference is exaggerated in autism. For example, if males on average perform worse than females on tasks intended to measure theory of mind capacity, then EMB predicts that men with autism would score lower than neurotypical men. In addition, the EMB theory also suggests involvement of prenatal sex steroid pathways, since hormones are one of the most important drivers of neurobiological sex differences. This notion found support in a large scale epidemiological study of prenatal steroids such as testosterone being elevated in children later diagnosed with autism (Baron-Cohen et al., 2015). It is well-known that there are sex differences in neuroanatomy of neurotypical individuals (Ruigrok et al., 2014). Sadly, most research and diagnostic tools in autism research are largely focused on males, despite increasing evidence of biological sex modulating its aetiology (Frazier, Georgiades, Bishop, & Hardan, 2014; Lai, Lombardo, Suckling, et al., 2013; Lai, Lombardo, Auyeung, Chakrabarti, & Baron-cohen, 2015). Interestingly, there have been reports of substantial neuroanatomical sex differences in the neurotypical and autism groups that are relevant to the EMB theory (Lai, Lombardo, Suckling, et al., 2013). Specifically, females with autism show a neuroanatomical pattern of masculinization that is not apparent in males with autim (Lai, Lombardo, Suckling, et al., 2013).

Perhaps closely related to EMB theory and particularly relevant to this sex difference in ASC has been the postulation of potential gender incoherence (GI) effects (Bejerot et al., 2012). Bejerot and colleagues noted that individuals with autism often show androgynous facial features. They showed that to some degree women with autism showed masculinization whereas men on the spectrum showed a tendency towards feminization. The notion that women with autism would show masculinization is not in direct conflict with the notion that autism is an extreme form of the male brain, but they differ perhaps mostly in their extent EMB would predict; female controls < male controls < autism (or in the opposite direction). Whereas GI would predict; male autism = female controls < male controls = female autism (or female controls < male autism < female autism < male controls).

4.1.2 Hypothesis and chapter outline

To assess network differences in autism and across biological sex we utilized graph theory (Bullmore & Sporns, 2009; Mark Newman, 2010; Stam & Reijneveld, 2007). Graph theory allows us to study different modalities of network data within the same mathematical framework. Graph theory has been proven to be an extremely useful mathematical framework to quantify network properties of complex biological systems, especially the brain (Bullmore & Sporns, 2009). Appendix A gives a detailed overview some of the background and mathematical methods that have been adopted from graph theory to study human brain neural networks. Details of the metrics can also be found elsewhere (Mark Newman, 2010; Stam & Reijneveld, 2007). In the present study we focused on global network properties of characteristic path length, normalized clustering coefficients (e.g. transitivity), assortativity (as a measure of the ability of a network to rapidly propagate information) and efficiency (e.g. the

ratio between strength and number of connections needed to connect the entire network). We also explored local or nodal measures of degree (the number of connections of each node), clustering (the level to which nodes are part of local clusters), betweenness centrality (to evaluate the importance of a networks node in the transfer of information) and local efficiency (how 'efficiently' information from one node can propagate throughout the network).

The WCC may provide an intuitive framework in relation to studying network organization. One can for example hypothesize that difficulties with information integration or lack of central coherence might be related to an overall disrupted brain network that impedes these two phenotypic factors. The theory however does not provide a clearly testable hypothesis as any group difference in any direction can be interpreted as atypical and thus evidence for weak central coherence. It also does not speculate on potential sex differences within and between the spectrum. However, the EMB theory also provides an intuitive, but more clearly testable hypothesis to assess potential network abnormalities in autism and across biological sex, namely that network metrics from the autism group would be an extreme of the typical male pattern of sex differences. This would predict a linear rank order of:

Female Control - Male Control - Autism

Thus, in order to test this theory we stratified the analyses over two groups as was done previously in a similar study of sex modulated effects in autism (Lai, Lombardo, Suckling, et al., 2013). In analysis Group 1 we entered both neurotypical groups and the female autism group. In analysis Group 2 we entered both neurotypical groups and the male autism group. Interestingly, this approach also allows me to test for potential gender incoherence effects by

looking at regions where the autism group does not differ from the opposites sex neurotypical group even when there is a neurotypical sex difference. This stratification allowed us to test for potential gender incoherence as post-hoc testing would reveal whether the female autism group would more closely resemble the male control group and/or whether the male autism group would more closely resemble the female control group.

4.2 Methods

4.2.1 Participants

A total of 133 adult participants were recruited as part of the Medical Research Council Autism Imaging Multicentre Study (MRC-AIMS). Diagnosis of Autism was confirmed for 30 male autistic participants using the Autism Diagnostic Interview-Revised (ADI-R) (Lord, Rutter, & Le Couteur, 1994). An additional three participants who scored 1 point below threshold on the repetitive behaviour domain of the ADI-R were also included because they met Autism Diagnostic Observation Schedule (ADOS) (Lord et al., 2000) criteria for autism spectrum and were diagnosed by experienced clinicians. Autism diagnosis was also confirmed for 30 female autistic participants using the ADI-R (Lord et al., 1994). Another three females, though not having ADI-R data available (because their childhood caregivers were not able to be interviewed), were also included for the reasons that one scored above the cut-off for 'autism spectrum' on the Autism Diagnostic Observation Schedule (ADOS), one previously received a diagnosis using the Adult Asperger Assessment (AAA) (Baron-Cohen, Wheelwright, Robinson, & Woodbury-Smith, 2005) which had incorporated care-giver reports on childhood behaviours, and one had been diagnosed by an expert clinician (Professor Digby Tantam, University of Sheffield) with assessments including comprehensive childhood developmental

history. Neurotypical (NT) volunteers (33 male, 34 female) were recruited through local advertisements and satisfied the same inclusion criteria as the autism groups, except that they did not have autism themselves or in their family history. Exclusion criteria for both groups included current or historical psychotic disorders, substance-use disorders, medical disorders associated with autism (e.g., tuberous sclerosis, fragile X syndrome), intellectual disability, epilepsy, hyperkinetic disorder, Tourette's syndrome, and current use of antipsychotic medication. Data from 3 male autistic participants was excluded (two due to incomplete brain coverage during scanning and one due to neuro-radiological diagnosis of agenesis of corpus callosum), leaving 30 male autistic participants for subsequent analysis. For the female autism cohort, data from three women was excluded (two with incomplete brain coverage and one with marked motion artefact), leaving 30 available for subsequent analysis. Informed written consent was obtained for all participants in accord with procedures approved by the Suffolk Research Ethics Committee.

4.2.2 Motion assessment

It was recently shown that head motion in the scanner may significantly confound functional connectivity measurements in functional MRI (Power, Barnes, Snyder, Schlaggar, & Petersen, 2012; Van Dijk, Sabuncu, & Buckner, 2012). Although this is not an issue for structural covariance analysis, we intend to use the same groups for functional connectivity analysis at a later stage and matched all groups based on in-scanner head motion of their functional imaging session.

Small jerky head movements can produce changes in the BOLD time-series that subsequently lead to systematic changes in the correlation structure when estimating functional connectivity

(Power et al., 2012; Van Dijk et al., 2012). Power et al. (2012) show that this may trigger a shift in long and short range functional coupling, effectively increasing overall (anatomically) short-range correlations and decreasing long-range correlations. Both studies (Power et al., 2012; Van Dijk et al., 2012) show how this effect persists despite spatial registration and co-varying or regressing out motion altogether. They furthermore suggest that specific groups of individuals might show larger in-scanner motion. Specifically Power et al. (2012) show that this effect is strongest in children, intermediate in adolescents and weakest in adults. It is very well possible that people with autism might show more in-scanner head motion. Motion analysis of our original sample indeed indicated possible group differences in in-scanner motion. Therefore we chose to match our groups based on motion as well as on age and IQ, for both the structural covariance as well as the functional connectivity analysis.

Three measures were calculated based on the reallignment parameters obtained during pre-processing using scripts described in Wilke (Wilke, 2012) as part of a motion fingerprint analysis (http://www.medizin.uni-tuebingen.de/kinder/en/research/neuroimaging/software/): average scan-to-scan displacement, number of scan-to-scan displacements larger then 1mm in Euclidean distance (i.e., 'jerky' movement), and maximum scan-to-scan displacement (Power et al., 2012; Wilke, 2012). Participants showing more than 10 jerky movements (more than 1.6% in the total number of time points) larger than 1mm in Euclidean distance, as well as the extreme outliers on the other two measures, were excluded from subsequent analyses (4 participants in the male autistic group, 1 participant in the female neurotypical group). This removal of motion outliers resulted in the four groups pair-wise matched on all three motion descriptors, as well as ensuring subject images most liable to motion confounding effects were

removed from subsequent analyses. The final cohort, group-wise matched for motion, age and full-scale IQ, consisted of 117 participants (Table 4.1).

Table 4.1: Descriptive statistics

	MC (N=33)	MA (N=25)	FC (N=29)	FA (N=30)	Statistics
	Mean (SD) [1st – 3th quartile]	Mean (SD) [1st – 3th quartile]	Mean (SD) [1st – 3th quartile]	Mean (SD) [1st – 3th quartile]	
Age (Years)	28.4 (6.1)	27.8 (7.4)	27.6 (6.5)	28.0 (8.3)	ns
Verbal IQ	110.8 (12.0)	114.4 (12.7)	118.1 (9.6)	113.5 (12.3)	FC>MC (p = .010)
Performance IQ	118.5 (11.4)	113.8 (15.3)	116.0 (8.9)	109.9 (18.0)	MC>FA (p = .030) *
Full-scale IQ	116.3 (11.6)	115.8 (13.8)	119.5 (7.7)	113.3 (16.6)	ns
Motion					
Average scan-to-scan displacement	0.10 [0.08 – 0.13]	0.11 [0.09 – 0.16]	0.90 [0.08 – 0.11]	0.10 [0.09 – 0.12]	ns**
Displacements larger than 1mm Euclidean distance	0 [0 – 0]	0 [0 – 1]	0 [0 - 0]	0 [0 - 1]	ns**
Maximum scan-to-scan displacement	0.38 [0.34 – 0.65]	0.60 [0.31 – 1.11]	0.56 [0.28 – 0.74]	0.53 [0.37 – 1.07]	ns**
AQ	15.2 (6.9)	32.8 (8.2)	11.9 (4.7)	37.9 (6.8)	***
ADI-R					
Social	-	16.0 [13.0 -21.5]	-	17.0 [12.0 – 21.0]	ns****
Communication	-	15.0 [12.0 – 17.5]	-	13.0 [10.0 – 17.0]	ns****
RSB	-	5.0 [3.0 – 7.5]	-	5.0 [3.0 – 5.0]	ns****
ADOS					
S + C	–	7.0 [4.0 – 12.0]	–	3.5 [1.75 – 6.25]	MA>FA (p = .013) ****
RSB	–	1 [0 – 2]	–	0 [0 – 0]	MA>FA (p < .001) ****

*: Independent Samples T-Test, Levene's Test for Equality of Variances showed significant non-equal variances, therefore equal variance was not assumed in the statistical tests.

: **No main effect on Kruskal Wallis Test & **no** significant difference in post-hoc Mann-Whitney Tests between pairs of groups.

***: Significant main effects for diagnosis and gender as well as interaction. Post-Hoc uncorrected: MC<MA (p < .001), FC<FA (p < .001), MA<FA (p = .052), MC>FC (p = .007), MA>FC (p < .001) & FA>MC (p < .001).

****: Mann-Whitney U Test

MC = (neuro) typical control group male adults; **MA** = male adults with autism; **FC** = (neuro) typical control group female adults; **FA** = female adults with autism; **SD** = standard deviation; **ns** = non-significant (p > 0.05); **AQ** = Autism Spectrum Quotient; **ADI-R** = Autism Diagnostic Interview-Revised; **RSB**: repetitive, restrictive and stereotyped behaviour; **ADOS**: Autism Diagnostic Observation Schedule; **S + C**: ADOS "social interaction + communication" total scores.

4.2.3 Image processing

Freesurfer (http://surfer.nmr.mgh.harvard.edu/) was used to segment individual T1-weighted fast spoiled gradient echo (FSPGR) structural images and obtain information on individual cortical thickness maps. All Freesurfer obtained estimations of white-grey matter boundaries were visually inspected for accuracy. To create a consistent parcellation template for both the structural covariance matrix as well as the functional resting-state data a method developed by Romero-Garcia and colleagues (Romero-garcia et al., 2012) was used. This method uses a backtracking algorithm to subparcellate the standard Desikan-Killiany atlas (Desikan et al., 2006) into 308 cortical and 41 sub-cortical regions. The standard Desikan-Killiany atlas subdivides the cortex into 66 standard gyral-based cortical regions. There are however two good reasons for subparcellating the data beyond that. First, the sub-parcellation provides a better resolution and it seems reasonable to assume that some anatomically defined brain regions have relevant functional subdivisions. Functional neuroimaging studies will seldom show activation effects for an entire anatomically bound region. Ideally these meaningful sub-divisions are known, but as this is unfortunately not the case the second best approach might be to randomly sub-parcellate while keeping anatomical boundaries in place. A second, and perhaps more important, reason for sub-parcellating, is that it allows for networks to be constructed from similar sized nodes. When only anatomically defined regions are used some regions will be much larger (e.g. contains many more voxels). This might result in a somewhat unbalanced graph as the contribution of each node to the overall graph metrics is not weighted by a nodes anatomical size. Sub-parcellating into similar sized regions makes that a redundant issue and ensures balanced networks while retaining potentially meaningful a-priori anatomical information.

The backtracking algorithm used, grows subparcels by placing seeds at random peripheral locations of the standard atlas regions and joining them up until a standard pre-determined subparcel size is reached. It does this reiteratively (i.e. it restarts at new random positions if it fails to cover an entire atlas region) until the entire atlas region is covered. Individual parcellation templates were created by warping this standard template containing 349 regions to each individuals' subject space FSPGR image. Warping of the segmentation map to the individuals subject space has the advantage of avoiding possible distortions from warping images to a standard space that is normally needed for group comparisons. Lastly, average cortical thickness was extracted for each of the 308 cortical regions in each individual subject and these formed the basis for creating group based adjacency matrices of structural covariance.

4.2.4 Graph construction

Age was linearly regressed out of the cortical thickness estimates as variation in structural measurements is likely to be strongly related to age especially when it concerns cortical thickness (Alexander-Bloch, Giedd, et al., 2013) and more so if the age range is considerable (as was the case in the present data). There is considerable variety in literature with regards to including total grey matter volume as a covariate. In autism it is known that total grey matter volume may be correlated with the main factor of biological sex (Lai, Lombardo, Suckling, et al., 2013) and including it as a covariate would likely remove a lot of variance explained by that target independent variable. For this reason, it was decided not to include grey matter volume as a covariate.

Graph analyses were done using custom Matlab code, combined with functions from the Brain Connectivity Toolbox (https://sites.google.com/site/bctnet/) for computing graph metrics.

Graphs were constructed from the residual cortical thickness measures by taking the Pearson correlation coefficients between atlas regions across individuals within one group, resulting in 4 matrices of 308 by 308 correlation values. For all graph metrics the minimum density was estimated as the starting point for computing metrics over a range of densities. The minimum density is the minimum threshold for including nodes in the network at a level at which all nodes are still connected. This is done to ensure that the graphs that are compared across groups have the same degree, as different degrees will likely bias any group comparisons (van Wijk et al., 2010). Subsequently all global graph metrics were computed between 1% and 20% densities, analogous to previous literature (Alexander-Bloch, Giedd, et al., 2013) and representative of plausible biological networks. Local graph metrics were computed for representative densities of 2, 5 and 10% and only consistent effects were entered into a post-hoc analysis. Figure 4.1 gives an overview of the graph construction procedure, the raw group-wise adjacency matrices and the binary matrix thresholded at 10% density for representation.

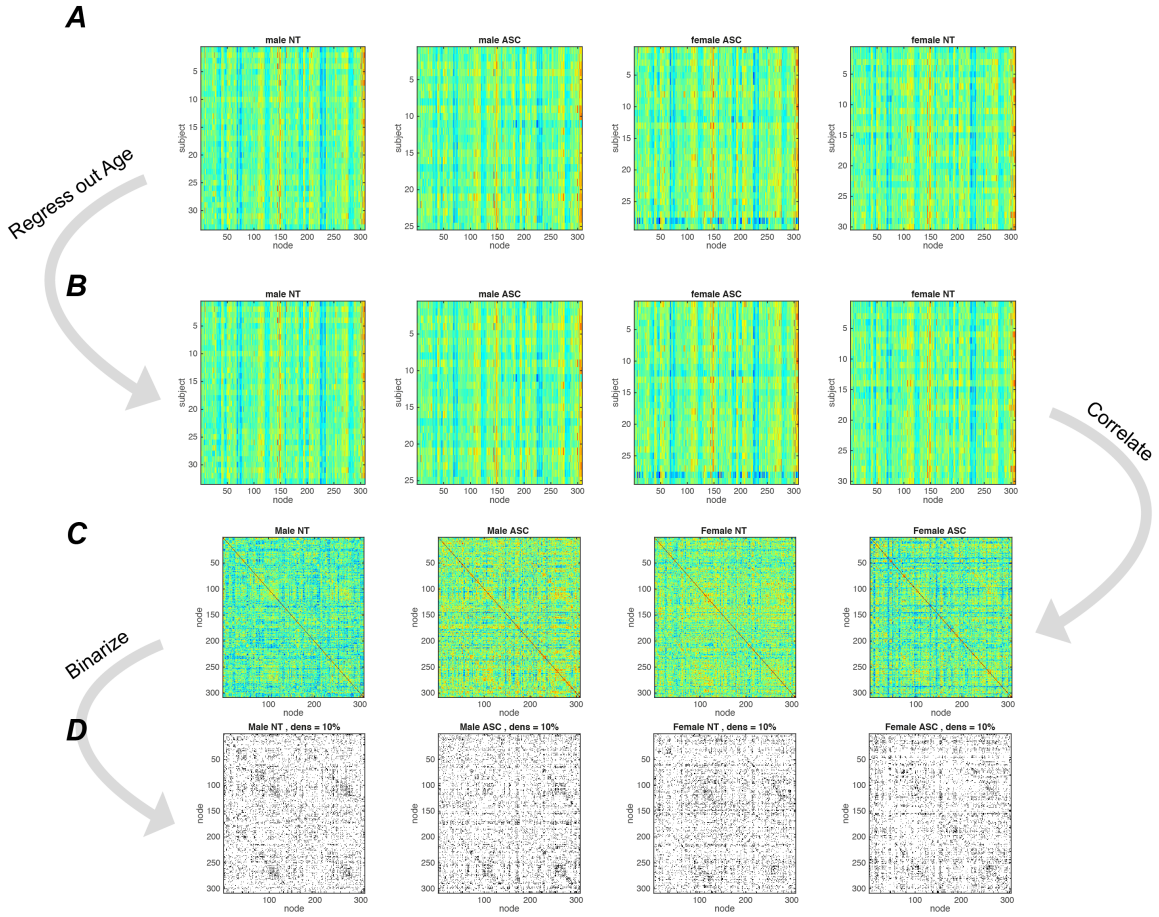

Figure 4.1**:** Methods overview

Panel **A** shows the original cortical thickness data for each subject across all the parcellated nodes. From these images it is also apparent that in the female ASC group there is one participant (28) for which the Freesurfer segmentation failed. This subject was subsequently removed from further analysis, and its removal did not affect the group matching reported earlier. Panel **B** shows the same cortical thickness measurements after age is regressed out. This also indicates that the overall structure of cortical thickness across nodes remains relatively intact. Panel **C** shows the group-wise raw adjacency matrix. Panel **D** shows the binary matrix thresholded at 10% density.

4.2.5 Data analysis

As only a single adjacency matrix for each group is obtained and not one for each individual, group comparisons rely on reconstructing a confidence interval or distribution for each group based on its original values. To test for group-wise differences in graph topological measures we bootstrapped (50 iterations with replacement) each matrix within each group to obtain confidence intervals on the estimates in the same fashion as done elsewhere (Alexander-Bloch,

Giedd, et al., 2013). In principal, increasing the number of bootstraps would generally increase the reliability of the estimated confidence intervals. In practice, using a large number of bootstraps potentially threatens the validity of statistical tests when comparing across the bootstrapped group distributions as it increases the degrees of freedom disproportionally to the original group size. Bootstrapping a sample by a factor of 500 results in 499 degrees of freedom, which is disproportional to the original sample size of the groups from which the measures were obtained[1]. Thus, in the present study we used a small number of bootstrap iterations (e.g. 50) that was close to the original sample size. This number of bootstraps showed robustness over several independent runs (e.g. there was no difference in obtained metrics in 5 independent runs).

First, global metrics were investigated by calculating each metric over a range of costs and subsequently testing for the linearly expected rank-order. In order to test for expected rank differences the Jonckheere-Terpstra test was used (Jonckheere, 1954). The Jonckheere-Terpstra test provides more statistical power than the conventional Kruskal-Wallis or Mann-Whitney rank order test in cases where there are more than two groups. We used a matlab based implementation of this rank-order test (Cardillo G. (2008) Jonckheere-Terpstra test: A nonparametric Test for Trends http://www.mathworks.com/matlabcentral/fileexchange/22159). Obtained test-statistics were corrected for multiple comparisons using a non-linear false-discovery rate (FDR) correction (Chumbley & Friston, 2009) with *alpha* set at $p<0.05$.

[1] Note that this is only an issue when the bootstrapped confidence intervals are subsequently used for parametric testing of linear effects as was done in the present sample.

Second, individual nodal properties of each parcellation node were assessed by specifically looking at expected rank-order in local metrics (degree, clustering, betweenness centrality and local efficiency) using the Jonckheere-Terpstra test (Jonckheere, 1954) for expected rank order. As mentioned before the analysis was stratified on biological sex for the autism groups. All p-values resulting from this analysis were FDR corrected (Chumbley & Friston, 2009) using a stringent non-parametric FDR correction set at $p<0.01$. All local metrics were computed at representative densities of 2, 5 and 10 percent. The Jonckheere-Terpstra test does not test the direction of the linear rank and also allows for individual pairs in the rank to not be significantly different (e.g. group1>group2=group3 will also result in a significant effect of rank order). Thus this test is only suitable to test a main two-tailed effect of rank order and pairwise post-hoc tests were used to assess the direction and individual contribution of group pairs. Only nodes showing a significant main effect were entered into the post-hoc analyses.

4.3 Results

The distribution of Pearson correlation coefficients of stuctural was similar across all four groups and as expected was slightly skewed towards positive correlations (Figure 4.2). Although there appears to be a small difference between the two male groups, two-sample Kolomogorov-Smirnov tests did not indicate any significant differences between any of the two pairs. This suggests that there is no clear a-priori bias in constructing graph metrics based on a global difference in connectivity structure. As the interpretation of a difference in negative and positive correlations in (f)MRI constructed graphs is unclear (and the mean of the distribution is influenced by pre-processing, especially by different kinds of regression and thus partially arbitrary) it is common practice to base graph construction on the absolute correlation values. The same was done in constructing the adjacency matrices for structural covariance networks.

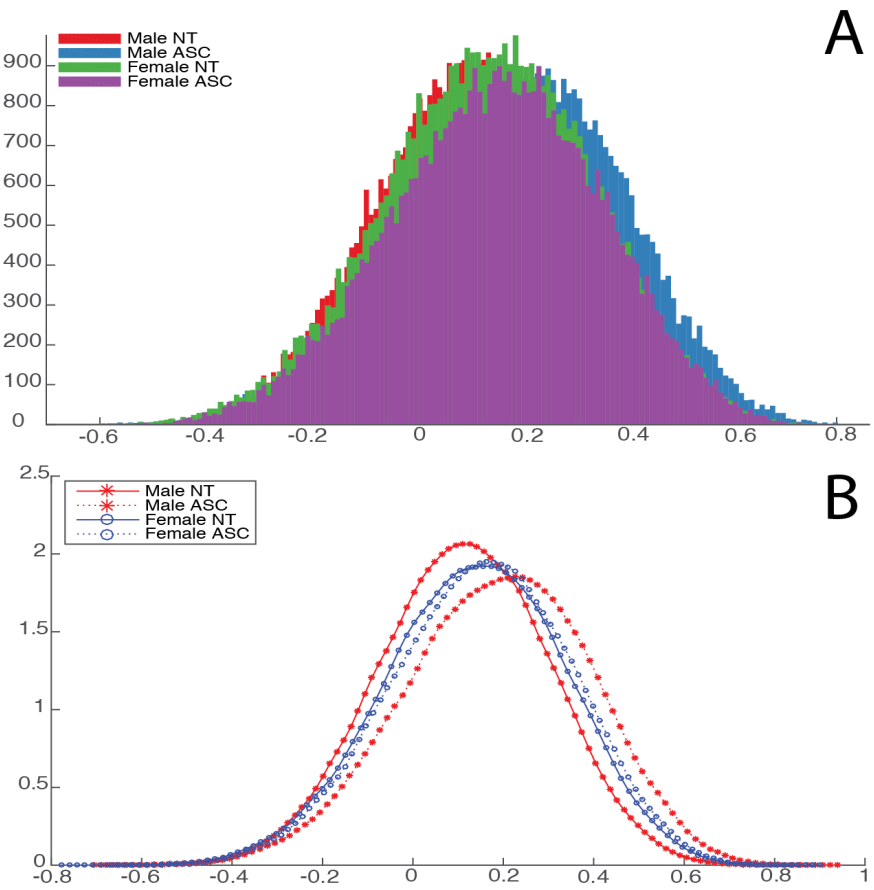

Figure 4.2: Correlation distribution

Panel A shows the Pearson correlation estimates of structural covariance for all four groups. Panel B shows the probability density for these distributions.

4.3.1 Global measures

First, whole brain measures were explored at representative network densities of 2, 5 and 10 percent (Alexander-Bloch, Giedd, et al., 2013). Degree is perhaps the most fundamental graph theoretical measure, representing the number of connections that each node has. Figure 4.3A shows the degree distribution of all four groups across representative densities. As would be expected in a non-random biological network all the distributions show a positive skewness (Sporns, 2011). There were no significant differences in the underlying degree distributions of the four groups. They all show a comparable level of skewness, although at increasing density

the male neurotypical group shows a slightly narrower distribution. Nonetheless, the degree distributions confirm that the constructed networks are biologically plausible and give a certain degree of confidence that the network construction was done appropriately.

Secondly, a number of measures were explored at a range of costs (Figure 4.3, Panel B) and the Jonckheere-Terpstra test for linear rank order was performed on the stratified groups. Characteristic path length is arguably one of the most fundamental metrics in graphs as most subsequent measures are based on this (second perhaps only to degree). Path length represents the average distance between two nodes in a network (e.g. the number of paths you have to travel on average to reach another node from any given node). In the present sample no differences were observed in characteristic path length across the investigated densities. Although the female autism group slightly deviated from the other groups for some densities, these differences did not show a significant linear rank order effect that survived multiple comparison correction across costs. Global efficiency of the networks also showed no significant rank order effects. Again, the female autism group seems to deviate slightly from the other groups at some cost points but none of these were enough to show a significant rank order effect.

As regions are further separated in a physical distance some the functional connectivity properties are likely to diminish as well (Sporns, 2011). To evaluate the extend to which the network might subdivide into local sub-networks one can look at clustering properties of individual nodes (e.g. the extend to which nodes connect to close neighbours). When looking at global clustering properties (e.g. the average of local clustering) the metric might be biased towards nodes that have a relatively high clustering coefficient. Transitivity provides a

normalized measure of this clustering index that does not suffer from the same bias (Mark Newman, 2010; Sporns, 2011). As can be seen in Figure 4.3, panel B there are some group differences in transitivity across the four groups, especially at densities above 10%. The rank order of these differences however does not follow the EMB or GI expected order (and thus the Jonckheere-Terpstra test detected no significant main differences for that group). There appears to be a sex difference in the neurotypical group. This difference, although perhaps 'extreme' in the sense that it goes beyond the neurotypical sex difference, was not significant for either the male or the female autism group and furthermore would be extreme in the opposite direction (towards 'extreme female').

Positive assortativity is essentially a measure of the degree to which high-degree nodes connect to other high degree nodes (and negative assortativity is indicative of low-degree nodes connecting to other low degree nodes) (Mark Newman, 2010; Sporns, 2011). The measure is adopted mostly from epidemiology where it is used to model the potential spread of disease using the assumption that networks with high assortativity are more prone to a quick spread (e.g. information propagates faster in networks where high degree nodes connect to other high degree nodes). In brain networks it can be taken as a proxy for studying the potential of information spread where highly assortative brain networks would be able to propagate information more easily. In general, positive assortativity is indicative of a network that is not dispersed or disconnected but instead has relatively good coherence (Sporns, 2011). Brain networks in general always show positive assortativity. In the present dataset differences in assortativity could be observed across all four group but these differ depending on the density at which the network is thresholded. Above 10% density only the female autism group showed somewhat higher assortativity. None of these differences show a clear rank order effect as

predicted by EMB or GI theory nor do they appear very consistent at lower densities. In short, most of our global measures show fairly consistent patterns that seem robust across the four groups. It could be that looking at whole-brain measures might be too coarse an approach to pick up diagnostic or sex differences in these groups.

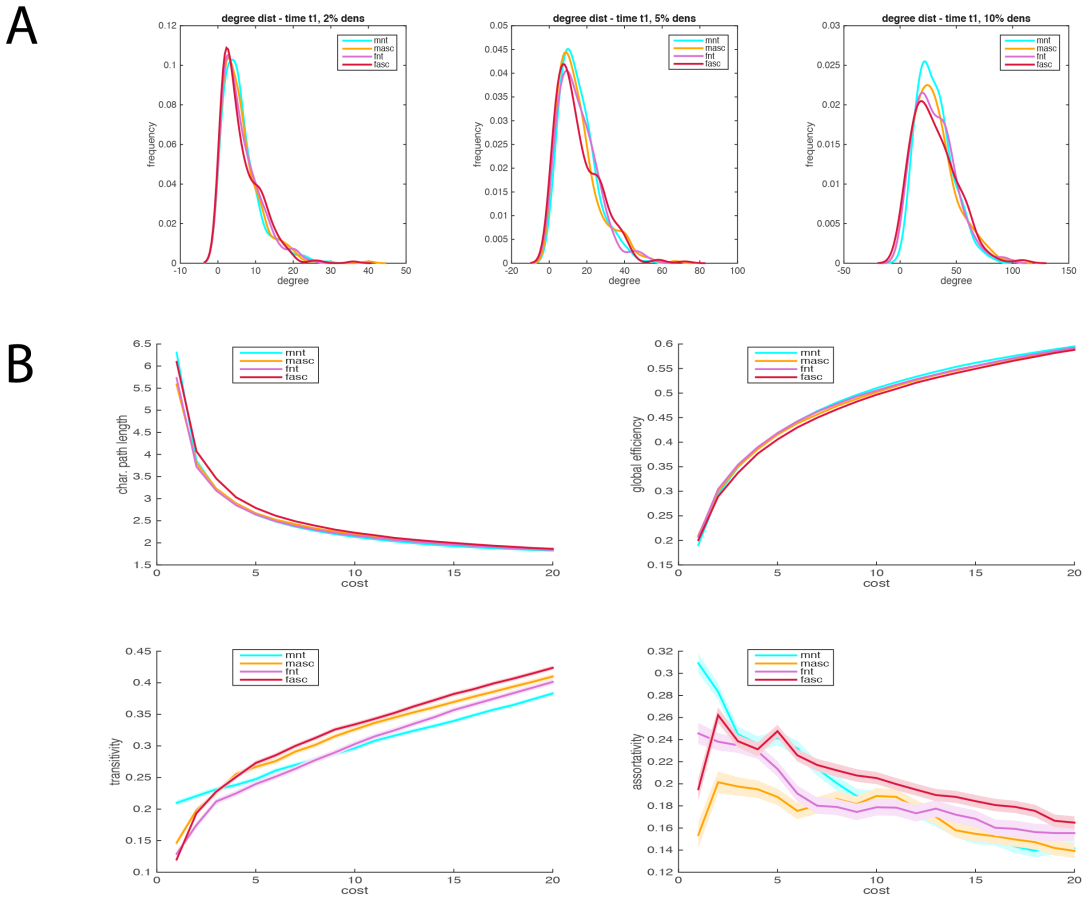

Figure 4.3**:** Graph metrics

Panel A shows the degree distributions for the 4 groups over the three different costs. Panel B shows results for global measures of path length, efficiency, transitivity and assortativity. Shaded areas show the standard error of the mean as based on the bootstrapping procedure described above.

4.3.2 Local measures; main effects

Investigating nodal or local effects of degree, clustering, betweenness centrality and efficiency there are a number of regions that show a linear rank order main effect in each group (Figure

4.4). Specifically, for degree and centrality a number of regions frequently associated with autism in particular and social cognitive functioning in general stand out. Namely, the anterior insula, anterior and mid cingulate cortex, areas around the right temporo-parietal junction (rTPJ), the middle frontal gyrus and dorso-lateral prefrontal cortex, the left middle and superior temporal gyrus, posterior parts of the fusiform gyrus and occipito-temporal areas.

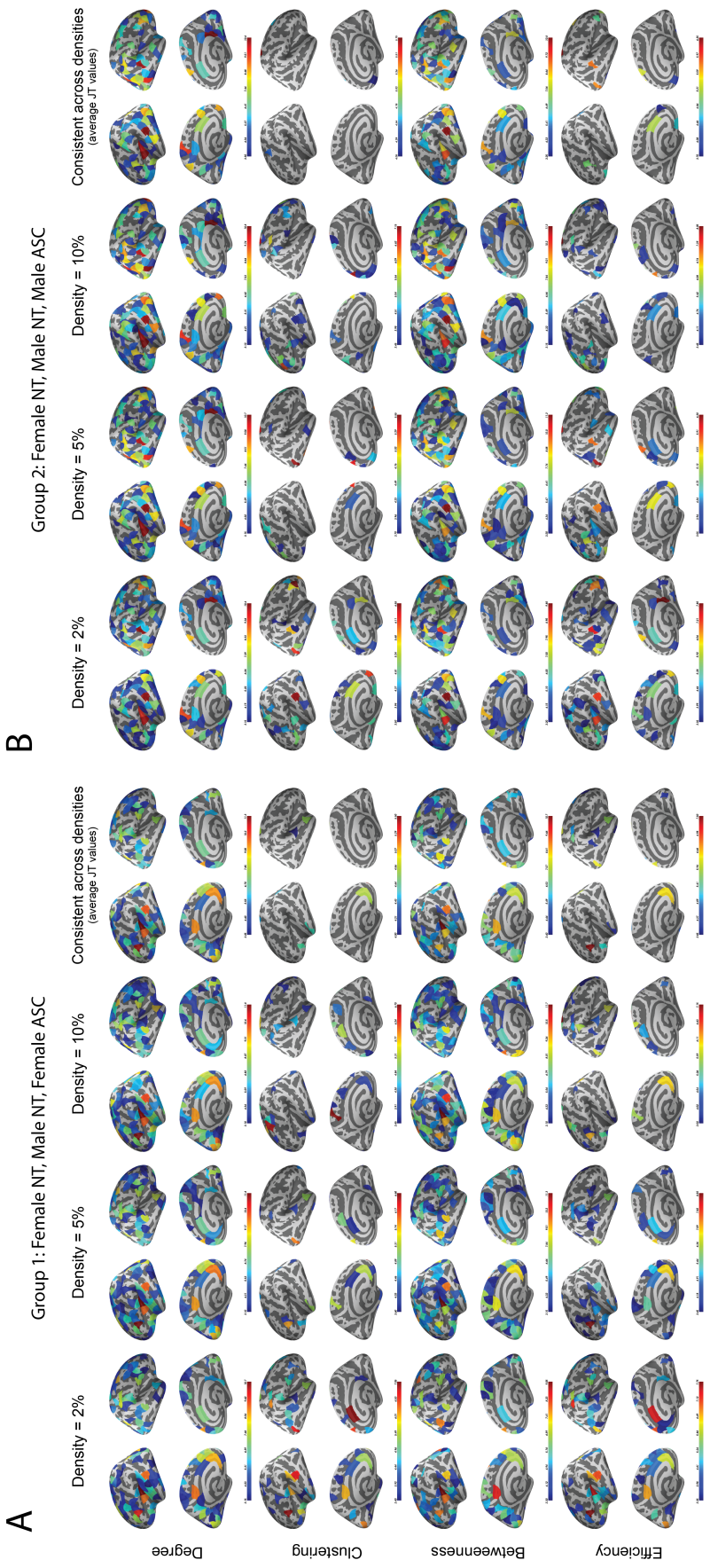
A
Group 1: Female NT, Male NT, Female ASC
Density = 2%
Density = 5%
Density = 10%
Consistent across densities
(average JT values)
B
Group 2: Female NT, Male NT, Male ASC
Density = 2%
Density = 5%
Density = 10%
Consistent across densities
(average JT values)
Degree
Clustering
Betweenness
Efficiency

Figure 4.4: Topological effects
Topological distribution of local main effects for Degree, Clustering, Betweenness Centrality and Efficiency at densities of 2, 5, and 10 percent as well as an overview of consistent local differences across all densities. Only significant nodes are shown ($p<0.05$) corrected for multiple comparisons across all 308 nodes using a non-linear FDR correction set at $p<0.01$. Colour indicates relative value of the Jonckheere-Terpstra test statistic (comparable to a conventional F-value). For the columns indicating where effects where consistent across all densities the average JT test-statistic is presented. Panel A shows the results for analysis group 1, Panel B shows the results for analysis group 2.

As the Jonckheere-Terpstra test allows for non significant differences within individual pairs and only tests the overall linear rank order (e.g. it is a two-tailed test) we subsequently conducted two-tailed Post-Hoc independent samples t-tests (with *alpha* set $p<0.05$) for each node of each pair of the expected rank. These tests were conducted on the networks weighted at 10% density and only areas that had previously shown consistent main effect differences for the respective measure and analysis group were included. As with the main rank order tests all resulting p-values were corrected for multiple comparisons using a non-linear FDR correction of $p<0.01$ (taking into account all 308 nodes). As with the analyses above these were stratified for the two analysis groups as well.

4.3.2.1 Local measures: analysis Group 1

As can be expected from the minimally consistent regions showing main rank order effects on clustering and local efficiency not all the individual comparisons contained regions that survived multiple comparison corrections on these two measures in the post-hoc tests. In both cases the aforementioned main effects were apparent mostly between the two neurotypical groups. Thus, only the other two local measures of degree and betweenness centrality are discussed in more detail below (Figure 4.5, Tables 4.2 and 4.3).

The measure of nodal degree showed differences across all three post-hoc tests. Differences were heterogeneous, but were mostly visible around left lateral occipital areas, right fusiform gyrus, lingual (occipital part), superior frontal and right supramargincal gyrus. Betweenness centrality is one of the few measures that has previously been studied in autism (Balardin et al., 2015). Balardin and colleagues report differences in medial frontal, parietal and temporal-occipital regions showing reduced betweenness centrality in autism. Our approach is slightly different; we investigated EMB and/or GI rank order effects, used a different more fine-grained parcellation scheme and used cortical thickness as opposed to GM volume. we also find areas of decreased betweenness that partially overlap with those findings. Interestingly we also observe some areas showing a pattern of increased centrality. Namely in left superior frontal, the rostral part of the middle frontal lobe, left postcentral gyrus, lingual areas and parts of the supramarginal gyrus.

With respect to expected EMB rank order we found a number of regions that follow this pattern in either direction (decrease or increase). Most notably the anterior insula showed a positive EMB effect on both the degree and centrality measures. The same was true for left superior frontal areas and left anterior (rostral) cingulate. In addition, our analysis also highlights a number of regions where there seems to be some masculinization of the female profile in the sense that the neurotypical sex differences did not propagate to the female autism versus male neurotypical comparison. This was most apparent in bilateral superior and middle frontal areas (around Brodmann area 10), in lateral occipital areas and in parts of the precuneus.

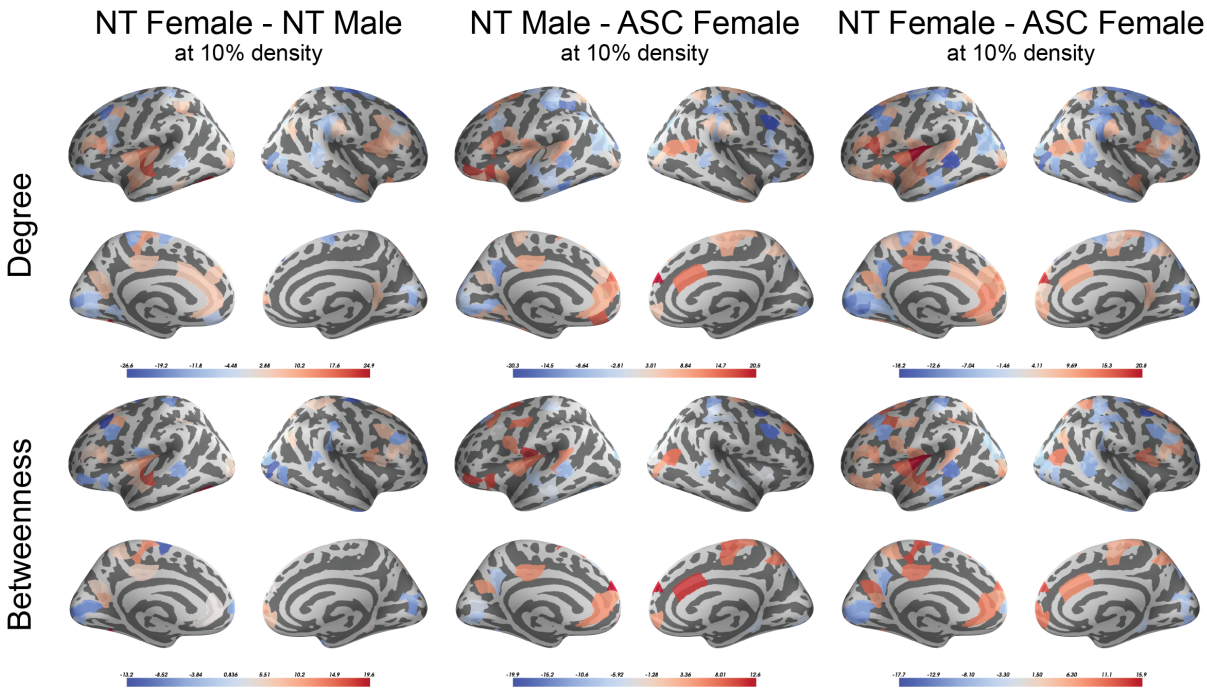

Figure 4.5: Group 1 local effects

T-maps of nodes showing increased (negative/blue) or decreased (positive/red) degree and centrality relative to the first mentioned group on the three Post-Hoc tests. For example, in the first column the red colours represent areas where NT Male < NT Female, and blue colours represent the opposite. Areas where the direction of differences for a specific region is consistent can be considered to follow an EMB pattern. Areas where there was a sex difference in the neurotypical groups, between the neurotypical and autism groups, but not between the male neurotypical group and the female autism group can be considered example of a GI rank order.

Table 4.2: Post-Hoc comparisons group 1.

Regions showing either EMB effects or GI effects on Degree.

Degree			
Extreme Male Brain			
Node	**FC - MC** (T-score)	**MC - FA** (T-score)	**FC - FA** (T-Score)
lh_bankssts_part1	-5.32	-11.37	-18.17
lh_caudalmiddlefrontal_part3	-4.95	-3.45	-8.63
lh_fusiform_part3	4.52	4.38	8.00
lh_inferiorparietal_part4	-5.76	-5.89	-10.61
lh_lateraloccipital_part9	5.56	3.96	10.16
lh_lingual_part2	-3.53	-8.06	-10.39
lh_lingual_part4	-7.19	-7.58	-13.02
lh_parsopercularis_part1	11.21	7.97	17.59
lh_pericalcarine_part1	-13.64	-3.54	-11.63
lh_postcentral_part3	-6.93	-3.97	-10.69
lh_posteriorcingulate_part1	5.31	7.94	12.87
lh_precuneus_part3	4.49	3.63	9.43
lh_rostralanteriorcingulate_part1	5.17	7.81	12.89
lh_superiorfrontal_part7	5.14	4.17	8.54
lh_superiorfrontal_part11	-6.00	-6.71	-12.75
lh_insula_part1	14.21	7.80	20.81
lh_insula_part3	8.60	6.75	15.04
rh_bankssts_part1	-4.72	-4.85	-8.98
rh_inferiorparietal_part4	-5.07	-6.71	-11.33
rh_postcentral_part8	-5.02	-4.35	-7.81
rh_superiortemporal_part3	7.30	4.37	12.36
rh_supramarginal_part4	3.80	3.60	7.24
rh_supramarginal_part7	-5.00	-4.65	-9.80
Gender Incoherence			
Node	**FC - MC** (T-score)	**MC - FA** (T-score)	**FC - FA** (T-Score)
lh_caudalanteriorcingulate_part1	4.64	*NS*	6.84
lh_caudalmiddlefrontal_part4	7.42	*NS*	6.90
lh_inferiortemporal_part3	-6.10	*NS*	-7.20
lh_lateraloccipital_part7	6.22	*NS*	5.30
lh_paracentral_part3	10.67	*NS*	9.46
lh_pericalcarine_part2	-7.54	*NS*	-7.35
lh_precentral_part6	-9.11	*NS*	-8.89
lh_precuneus_part1	6.14	*NS*	5.82
lh_rostralmiddlefrontal_part1	6.40	*NS*	9.33
lh_superiorfrontal_part2	-9.56	*NS*	-10.63
lh_superiortemporal_part4	9.67	*NS*	9.72
lh_superiortemporal_part7	5.42	*NS*	8.54
lh_supramarginal_part1	6.70	*NS*	4.98
lh_transversetemporal_part1	7.35	*NS*	4.53
rh_bankssts_part2	-7.69	*NS*	-7.05
rh_cuneus_part3	-4.68	*NS*	-6.90
rh_inferiorparietal_part10	5.17	*NS*	3.63
rh_inferiortemporal_part3	-10.00	*NS*	-7.96
rh_isthmuscingulate_part1	5.68	*NS*	6.98
rh_lateraloccipital_part2	-6.77	*NS*	-6.14
rh_parsopercularis_part1	9.06	*NS*	8.75
rh_parsopercularis_part2	7.03	*NS*	8.21
rh_pericalcarine_part3	-11.36	*NS*	-10.55
rh_precentral_part1	11.22	*NS*	13.98
rh_rostralmiddlefrontal_part5	-3.73	*NS*	-6.60
rh_rostralmiddlefrontal_part6	-4.74	*NS*	-5.75
rh_rostralmiddlefrontal_part7	4.55	*NS*	3.96
rh_rostralmiddlefrontal_part8	-3.76	*NS*	-4.20
rh_superiorfrontal_part2	8.80	*NS*	7.34
rh_superiorfrontal_part5	-10.88	*NS*	-9.06
rh_superiorparietal_part2	-4.82	*NS*	-7.13
rh_superiorparietal_part7	9.60	*NS*	8.46

Table 4.3: Post-Hoc comparisons group 1.

Regions showing either EMB effects or GI effects on Betweenness Centrality

Betweenness Centrality			
	Extreme Male Brain		
Node	**FC - MC** (T-score)	**MC - FA** (T-score)	**FC - FA** (T-Score)
lh_bankssts_part1	-5.57	-9.52	-13.84
lh_caudalmiddlefrontal_part3	-5.01	-3.68	-8.83
lh_lingual_part2	-3.69	-6.68	-10.08
lh_pericalcarine_part2	-7.49	-4.94	-9.54
lh_postcentral_part3	-7.60	-4.17	-10.71
lh_posteriorcingulate_part1	5.39	5.08	10.11
lh_precuneus_part3	5.23	4.29	11.44
lh_rostralanteriorcingulate_part1	3.61	5.38	9.65
lh_superiorfrontal_part12	5.68	8.51	11.80
lh_insula_part1	11.15	7.91	15.87
lh_insula_part3	7.41	5.10	11.79
rh_lateraloccipital_part6	-4.06	-3.75	-6.78
rh_medialorbitofrontal_part1	6.69	3.69	9.78
rh_superiorfrontal_part6	3.67	12.36	13.20
	Gender Incoherence		
Node	**FC - MC** (T-score)	**MC - FA** (T-score)	**FC - FA** (T-Score)
lh_caudalmiddlefrontal_part4	9.37	*NS*	11.79
lh_lateraloccipital_part7	6.69	*NS*	4.14
lh_lateraloccipital_part9	4.79	*NS*	7.47
lh_paracentral_part3	12.09	*NS*	13.35
lh_parsopercularis_part1	7.67	*NS*	7.75
lh_pericalcarine_part1	-7.28	*NS*	-8.45
lh_precuneus_part1	8.58	*NS*	6.87
lh_precuneus_part2	5.79	*NS*	6.26
lh_rostralmiddlefrontal_part1	5.01	*NS*	4.97
lh_rostralmiddlefrontal_part3	4.27	*NS*	5.11
lh_superiorfrontal_part1	-5.08	*NS*	-5.16
lh_superiorfrontal_part2	-10.98	*NS*	-10.91
lh_superiortemporal_part7	6.07	*NS*	7.81
lh_supramarginal_part1	4.76	*NS*	7.29
rh_bankssts_part2	-4.42	*NS*	-6.62
rh_cuneus_part3	-4.77	*NS*	-7.43
rh_inferiorparietal_part10	5.83	*NS*	4.88
rh_inferiortemporal_part1	-8.39	*NS*	-7.26
rh_lateraloccipital_part2	-6.45	*NS*	-5.02
rh_parsopercularis_part1	6.33	*NS*	8.50
rh_parsopercularis_part2	6.56	*NS*	3.82
rh_pericalcarine_part3	-6.72	*NS*	-4.13
rh_precentral_part1	10.71	*NS*	10.44
rh_rostralmiddlefrontal_part5	-4.83	*NS*	-4.72
rh_rostralmiddlefrontal_part6	-3.66	*NS*	-6.27
rh_rostralmiddlefrontal_part7	5.84	*NS*	6.56
rh_superiorfrontal_part2	9.52	*NS*	10.23
rh_superiorfrontal_part9	7.69	*NS*	7.35
rh_superiorparietal_part6	5.56	*NS*	7.45
rh_superiorparietal_part7	9.87	*NS*	7.91
rh_supramarginal_part7	-4.54	*NS*	-6.11
rh_frontalpole_part1	4.43	*NS*	5.13

4.3.2.2 Local measures: analysis Group 2

As with the analysis of group 1 clustering nor local efficiency showed consistent post-hoc effects. Again degree and betweenness centrality are the measures showing the strongest effects (Figure 4.6, Tables 4.4 and 4.5). Most consistently are differences in degree as well betweenness centrality in regions around the right temporo-parietal junction (rTPJ), temporal occipital and supramarginal areas. Left anterior insula also showed a consistent difference. With respect to expected rank order order these regions all follow the order as predicted by the EMB theory. The direction of this EMB order did differ between sub-regions. For example, one part of the supramarginal gyrus showed a positive effect (NT Female<NT Male<Autism Male), and another showed a negative EMB order (NT Female>NT Male>Autism Male). Apart from one sub-region in inferior parietal cortex there were no regions showing a GI effect in analysis group 2. Thus, there were no regions that showed a feminization of the male autism group.

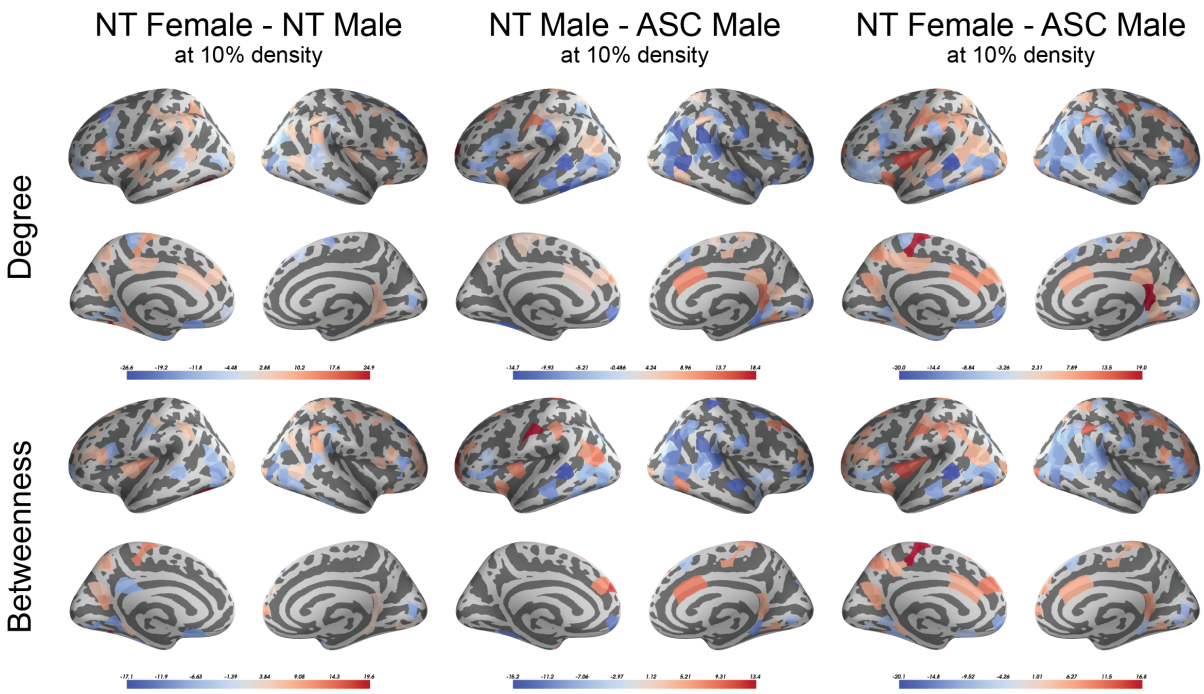

Figure 4.6: Group 2 local effects

T-maps of nodes showing increased (negative or blue) or decreased (positive or red) degree and centrality relative to the first mentioned group on the three Post-Hoc tests. For example, in the first column the red colours represent areas where NT Male < NT Female, and blue colours represent the opposite. Areas where the direction of differences for a specific region is consistent can be considered to follow an EMB pattern. Areas where there was a sex difference in the neurotypical groups, between the neurotypical male and male autism groups, but not between the female neurotypical group and the male autism group can be considered example of a GI rank order.

Table 4.4: Post-Hoc comparisons group 2.

Regions showing an EMB effect in Group 2. There were no regions showing GI patterns in this group.

Degree			
Extreme Male Brain			
Node	**FC - MC** (T-score)	**MC - MA** (T-score)	**FC - MA** (T-Score)
lh_bankssts_part1	-5.32	-13.04	-19.99
lh_caudalanteriorcingulate_part1	4.64	4.36	9.59
lh_inferiorparietal_part4	-5.76	-5.40	-10.34
lh_lateraloccipital_part4	-8.63	-4.97	-12.13
lh_medialorbitofrontal_part2	-3.89	-9.34	-12.77
lh_paracentral_part3	10.67	4.46	18.38
lh_parsopercularis_part3	-6.23	-3.96	-9.98
lh_postcentral_part8	4.74	4.00	9.01
lh_precuneus_part6	6.33	4.68	9.69
lh_superiorfrontal_part7	5.14	5.02	9.66
lh_supramarginal_part6	4.25	4.02	8.15
lh_insula_part1	14.21	3.60	15.06
lh_insula_part3	8.60	8.31	16.87
rh_bankssts_part2	-7.69	-7.79	-14.09
rh_inferiorparietal_part4	-5.07	-10.89	-16.72
rh_inferiorparietal_part7	-8.41	-3.74	-12.61
rh_isthmuscingulate_part1	5.68	12.74	19.04
rh_lateraloccipital_part2	-6.77	-10.08	-15.02
rh_lateraloccipital_part8	4.03	4.91	9.17
rh_rostralmiddlefrontal_part2	-5.04	-11.30	-15.22
rh_superiorfrontal_part11	-4.87	-5.42	-11.14
rh_supramarginal_part3	5.20	5.78	11.70
rh_supramarginal_part7	-5.00	-5.52	-10.87

Table 4.5: Post-Hoc comparisons group 2.

Post-Hoc comparisons of regions showing an EMB effect in Group 2. There was only one region showing a GI effect

Betweenness Centrality			
Extreme Male Brain			
Node	**FC - MC** (T-score)	**MC - MA** (T-score)	**FC - MA** (T-Score)
lh_bankssts_part1	-5.57	-15.24	-20.01
lh_insula_part3	7.41	7.72	14.01
rh_bankssts_part2	-4.42	-8.65	-12.02
rh_isthmuscingulate_part1	3.82	4.94	7.89
rh_lateraloccipital_part2	-6.45	-9.41	-13.16
rh_lateraloccipital_part7	3.66	4.26	8.39
rh_lateraloccipital_part8	6.98	3.96	10.43
rh_rostralmiddlefrontal_part9	4.71	4.49	9.02
rh_supramarginal_part7	-4.54	-6.02	-9.77
Gender Incoherence			
Node	**FC - MC** (T-score)	**MC - MA** (T-score)	**FC - MA** (T-Score)
rh_inferiortemporal_part2	-4.70	7.04	*NS*

4.4 Discussion

The present results further reinforce the importance of accounting for biological sex in studying the neurobiology of autism. We found main effects of biological sex in all the measures that were investigated in the neurotypical groups. This in itself was not the main purpose of the present study and our findings would need to be replicated in a study designed to test normative sex differences and larger samples, they do however reinforce the importance of taking into account biological sex in neuroimaging (Ruigrok et al., 2014). Interestingly, and of particular interest in this study, was the fact that biological sex seems to affect autism differentially. Both in female and male groups of individuals with autism did we find extremes of the neurotypical sex difference as well as indications of gender incoherence. Our results also show a heterogeneous pattern of decreases and increases of nodal degree and betweenness centrality that follows similar patterns of exaggerated neurotypical sex differences as well as gender incoherence.

4.4.1 Global

At a global scale, and specifically in relation to transitivity, the connectivity pattern does not completely fit with the EMB theory but at times more closely resembles an account of gender incoherence (Bejerot et al., 2012). In contrast to the EMB theory, this account suggests that females with autism would show masculinisation (e.g. are closer to neurotypical males than females) and the male autism group might show feminization (e.g. be closer to neurotypical females). The sparse collection of neuroimaging studies that investigated female autism indeed find those patterns (Alaerts, Swinnen, & Wenderoth, 2016; Lai, Lombardo, Suckling, et al., 2013). The present global clustering effects on structural covariance however present a somewhat intermediate pattern where the autism groups appear to be more of an extreme in the

direction of feminization. As none of the global measures showed clear significant rank order effects in either of the analysis groups this suggestion is something that would require further study. The relatively small effects reported here can not be taken as conclusive evidence for either GI or EMB.

4.4.2 Local

At the nodal level there were a number of regions that showed EMB linear rank order effects in both stratified groups, most notably the anterior insula. Across both analysis groups the anterior insula showed decreased degree in the autism groups compared to the control groups. This region has often been associated with hypo-activation and hypo-connectivity in autism (Caria, de Falco, Falco, & Caria, 2015; Uddin, Supekar, & Menon, 2010), but also with language delay and GM volume differences (Lai et al., 2014). Perhaps unsurprisingly this region also shows decreased regional cerebral blood flow (rCBF) (Ohnishi et al., 2000). Activation (as measured with BOLD fMRI), rCBF and disconnectivity are likely to be related or at least to be measuring similar underlying neural constructs. Furthermore, Nordahl and colleagues (Nordahl et al., 2007) showed that this area also exhibited abnormal cortical folding in children with autism. Thus, there is some converging evidence to suggest that this region might develop differently in individuals with autism that causes both functional as well as structural covariance network changes. As with all network analysis the link to a clear behavioural talent or deficit remains speculative, but as this region is strongly involved in agency and self-other distinctions (Craig, 2009) it is tentative to suggest that it might be linked to that aspect of the autism phenotype.

In addition to the anterior insula, inferior temporal gyri and temporal-occipital areas showed main linear rank order effects. These areas have been implicated in autism mostly with respect to the processing of faces (Pierce, Müller, Ambrose, Allen, & Courchesne, 2001). Studies routinely show that individuals with autism process faces differently and Pierce and colleagues (2001) showed that they might in fact use different underlying neural systems to do so. The current differences in structural covariance might reflect this behavioural and neural difference. If these regions are consistently differentially activated during development than it seems plausible that their structural covariance might differ as well. In other words differentially activated and functionally related areas could results in different patterns of synaptogenesis (Katz & Shatz, 1996). However, the difference in areas recruited for face-processing could also be the result of an early neuroanatomical difference. In that logic, the structural covariance difference observed reflects the result of a different developmental trajectory that might not be driven by functional activation (but perhaps by genetics as noted in the previous chapter).

Perhaps the most interesting area to show a main rank order effect is the area around the rTPJ. This region is often associated with mentalizing, theory of mind, self-other distinctions and social impairments in autism (Lombardo et al., 2011). It has been a region of interest in many neuroimaging studies looking into theory of mind (ToM) deficits in autism (Kaiser et al., 2016; Kana, Keller, Cherkassky, Minshew, & Just, 2009; Lombardo et al., 2011). In a previous study investigating precisely a ToM network of brain regions it was shown that individuals with autism show reduced covariance in TPJ regions (Bernhardt, Valk, et al., 2014; Bernhardt, Klimecki, Leiberg, & Singer, 2014). The present findings fit well with the idea of a disruption in this region that might be further modulated by biological sex.

When zooming in on the female autism group analysis it is most interesting to note that a large number of brain regions tend to show a pattern of masculinization that fits with earlier research on sex differences in autism neuroanatomy (Lai, Lombardo, Suckling, et al., 2013). Moreover, the opposing feminization of the male autism group was not apparent and this strengthens the notion that biological sex might influence autism neuroanatomy differentially. The analysis group that included the female autism group also showed areas that follow an extreme male brain pattern most notably in the anterior insula.

When looking at the male autism group there were almost no regions showing gender incoherence effects. This suggests that there is no pattern of feminization of the male autism group. In contrast, there were a number of areas that showed effects that fit the EMB account. Again this included the anterior insula, but also the lateral occipital and supramarginal areas. As with the anterior insula these regions have been associated previously with differences in self-other distinctions (Salmi et al., 2013). They also partially overlap with findings of structural abnormalities across autism and ADHD (Brieber et al., 2007). Given this regions' involvement in language processing it is also tentative to speculate on its relation to potential differences in language processing (Lai et al., 2014). However, further studies are needed to establish a clear behavioural link between the present structural covariance differences and behavioural traits.

Overall the post-hoc analyses revealed that both in the female as well as the male autism groups there are patterns that are in line with the EMB theory. We also found regions that fit with the notion of GI theory, but only in the female ASC group. How these differences in structural covariance might relate back to behavioural differences between the four groups remains to be understood and this should be an important target for future research. Combining structural

neuroanatomical measures with functional measures would be a step forward in better understanding the neurobiology of autism. It also seems apparent that network differences across sex and diagnosis are not easily captured in terms of hypo- or hyper-connectivity or increase or decrease of a certain feature. The overall picture is much more heterogeneous and depending on the region both increases as well as decreases in nodal and global network properties are found. Regardless of the direction, a large proportion of these effects are captured by a linear order such as EMB or GI would predict.

Lastly, the present study strongly reinforces the notion that it is of the utmost importance that stratification by biological sex be considered in moving autism research forward. We find diverging patterns of structural covariance when stratifying the analyses by biological sex and these differences are not fully captured by just one overall theory. Taking into account biological sex will furthermore reduce the heterogeneity of an otherwise very heterogeneous group and will hopefully lead to a more targeted approach in understanding and studying the neurobiology of autism.

Chapter 5 Altered functional brain organization in autism

5.1 Introduction

In recent years resting-state fMRI and diffusion tensor imaging have become the tools of choice for researchers studying the organisation of the human brain (Bullmore & Sporns, 2009). For much longer however researchers have been using electroencephalography (EEG) as a method to investigate cortical connectivity and organizational patterns (Thatcher, Krause, & Hrybyk, 1986). Although EEG suffers from an obvious lack in spatial resolution it makes up for this in temporal resolution with some systems now allowing recording speeds of over 4K Hz. This higher temporal resolution also allows one to study other characteristics on the measured signal such as power spectral densities of certain frequencies, phase amplitudes and other frequency information.

For autism research, EEG has mostly been used in paediatric samples (Billeci et al., 2013), most likely because it is less invasive than MRI, arguably less sensitive to physiological noise (such as motion) and likely more cost effective. Most of these studies have focused on posterior or anterior asymmetries in power spectral density (Burnette et al., 2011; Gabard-durnam, Tierney, Vogel-Farley, Tager-Flusberg, & Nelson, 2013; Stroganova et al., 2007). This is perhaps not surprising given the wide body of literature on possible abnormalities in the corpus callosum, the main inter-hemispheric communication fibre bundle, in individuals with autism (Paul, Corsello, Kennedy, & Adolphs, 2014). For example, Stroganova and colleagues (2007) report

a relative increased leftward asymmetry in boys with autism compared to a neurotypical control group and absence of a normally present leftward mu rhythm asymmetry. In addition, they showed that age and developmental delay were significant predictors for the alterations in EEG patterns.

However, it is difficult to tease apart the exact contribution of namely developmental delay as this variable is likely linked to the diagnosis itself. Interestingly though, Gabardine-Durnam and colleagues (2013) also show a relation between the development of EEG asymmetry patterns and risk for autism. Using groups divided into high and low-risk for autism and focussing specifically on previously reported frontal alpha asymmetries, they show that these two groups show different asymmetry trajectories over the course of development. Here, children with a low risk for developing autism show a relative rightward asymmetry of frontal alpha power as opposed to the high-risk group showing no clear asymmetrical power distribution in these frontal networks. Over the course of development however these patterns appear to crossover, with the low risk group slowly getting a less negative asymmetry and the high group slowly changing to a more negatively directed asymmetry pattern. Furthermore, left frontal asymmetry has been associated with decreased symptomatology and a later onset of symptoms (Burnette et al., 2011). In sum, these findings may suggest EEG asymmetry to be a potential biomarker.

In addition, it has been suggested that left frontal cortical activity underlies positive emotions and approach motivation, whereas right frontal cortical activity would be related to negative emotions and withdrawal motivation (Harmon-Jones, 2003). However, it is important to bear in mind that approach direction and emotional valence are not always associated (e.g. anger,

greed or lust are usually linked to approach behaviour, though often triggering negative emotions and undesired consequences). Furthermore, greater left than right frontal cortical activity measured by resting EEG has been found to correlate with trait anger (Harmon-Jones, 2003; Harmon-Jones & Allen, 1998), suicidal tendencies (Rohlfs & Ramírez, 2006), impulsive aggression in adolescents with affective and disruptive behaviour disorders (Rybak, Crayton, Young, Herba, & Konopka, 2006) or in persistently violent psychiatric patients (Convit, Czobor, & Volavka, 1991). This might fit with the social communication element in autism. Namely, right frontal asymmetry as an indicator of increased withdrawal could be a result of impaired or stressful social communication. Vice versa, if increased left frontal asymmetry is a marker for positive emotions and approach motivation this could also be marker for behavioural elements that might add some resilience in the case of autism.

In most studies there is however also heterogeneity in findings about power spectral asymmetries (Wang et al., 2013). In large parts this heterogeneity might be the result of differing age groups and testing conditions (task or no task, eyes-closed or open etc.). In order to ensure robustness of findings it is thus paramount to ensure a well-matched sample of neurotypical and autistic participants and ensure testing conditions are consistent between testing sessions. In addition to these measures the current study also used a small independent replication dataset collected at the Centre for Research on Autism and Education.

Although there have been numerous indications of altered cortical organisation in autism, as highlighted in the introduction (Belmonte et al., 2004; Vissers et al., 2012) no clear pattern has emerged and the asymmetry hypothesis seems possibly somewhat of an oversimplification. Few studies to date have made use of the rich information in resting-state EEG signals to

reconstruct potential network alterations at a whole brain level (Fallani et al., 2010). Especially in paediatric samples, EEG can be a less invasive method. Additionally, due to its high temporal resolution, EEG resting-state recordings only require a few minutes of data collection and are arguably less sensitive to noise resulting from head motion. In the present study we used high temporal resolution resting-state EEG (recorded at 2048 Hz) to assess differences in functional cortical organization of individuals with and without autism. In addition, we used a more robust measure of connectivity (as opposed to coherence or correlation); the weighted phase lag index (WPLI) (Stam, Nolte, & Daffertshofer, 2007; Vinck, Oostenveld, Van Wingerden, Battaglia, & Pennartz, 2011). Given that EEG is a relatively untouched tool to assess brain network alterations in autism we gathered two separate datasets. The first dataset is being collected at the Autism Research Centre in Cambridge (ARC) and serves as a discovery dataset. The second dataset is collected at the Centre for Research on Autism and Education (CRAE) at University College London and serves as a replication dataset. Data collection at both sites is ongoing and as previously mentioned the analysis presented here should be considered pilot data.

5.2 Methods

5.2.1 Participants: Autism Research Centre – University of Cambridge

A total of 58 participants were recruited as part of a larger EEG study that included resting-state EEG at the start of every session and a further additional 4 computerized tasks not described here. Recruitment was conducted via the Cambridge Autism Research Database (CARD) that also includes neurotypical individuals, as well as via online advertisements. A total of 14 individuals had previously been diagnosed with an autism spectrum condition took part (age: 38.85±11.69). The remaining 44 participants had never received a diagnosis of autism (age: 37.57±9.31). Prior to taking part all participants provided written informed consent and

completed a digital health screening assessment as well as the autism spectrum quotient questionnaire (Baron-Cohen, Wheelwright, Skinner, Martin, & Clubley, 2001) (AQ) online. Both groups were matched on age using a non-parametric Wilcoxon signed rank test (W: 395, p = 0.115) and differed significantly on the AQ (W: 579, p = $8.62*10^{-7}$). Boxplots on both metrics are shown in figure 1 below.

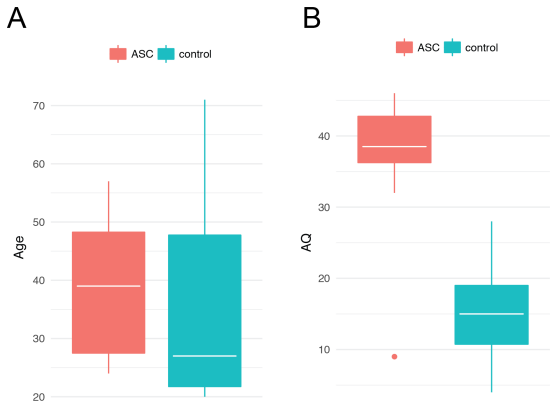

Figure 5.1: Descriptive statistics

Panel A shows the mean age of participants from both groups, panel B shows their AQ scores. White lines within the barplots represent the group mean, error bars represent standard deviations, participants who deviated more than 2 standard deviations from the mean are noted individuals.

5.2.2 Participants: Centre for Research in Autism Education

A total of 32 participants were recruited as part of a larger EEG study that included resting-state EEG at the start of every session and a further computerized task not described here. Recruitment was conducted via flyers around UCL (University College London) campus, social media advertisement (i.e Facebook, Twitter) and through the ICN (Institute of Cognitive Neuroscience, UCL) database. A total of 13 individuals had previously been diagnosed with an autism spectrum condition took part (age: 30.42±11.98). The remaining 19 participants had never received a diagnosis of autism (age: 35.54±15.17). Prior to taking part all participants provided written informed consent and completed a brief health screening assessment.

5.2.3 Recording procedure

Participants were seated in a comfortable adjustable chair, their head circumference was measured to determine the appropriate cap size and participants were asked to put on a BioSemi EEG cap themselves. Next, two researchers placed all electrodes onto the caps. EEG was recorded using 64 scalp Ag/AgCl tipped electrodes in accordance with the International 10/20 system, using an ActiveTwo EEG system from BioSemi (BioSemi, Amsterdam, The Netherlands). External electrodes were placed on the mastoid for post-hoc signal referencing and around the eyes to allow optional post-hoc eye-blink assessment.

After inserting all electrodes, they were all visually inspected online for potential line noise by a trained researcher and adjusted (increasing the amount of conductance gel or replacing the electrode) appropriately. Resting-state EEG was recorded during a four-minute session, divided in four one-minute periods for; eyes-open, eyes-closed, eyes-open and eyes-closed. Participants received a written instruction on the screen and could start the resting-state period themselves by pressing any key on the keyboard in front of them. They were subsequently cued with a short non-obtrusive sound when the first minute had passed. Only eyes-closed segments were analysed to maximally avoid artefacts from eye-blinks. As this study was part of a larger EEG study in which participants also took part in a number of tasks, the resting-state recording was always done at the start of the procedure.

5.2.4 Pre-processing

Brain oscillations, as measured with EEG, are the result of the continued waxing and waning of electric field potentials generated simultaneously in a large number of vertically oriented apical dendrites of pyramidal nerve cells in the cerebral cortex (Silva, 1999). As a result,

changes in lower subcortical brain systems, will likely spread to cortical regions and can then indirectly be picked up by electroencephalography. A major issue in EEG connectivity studies, in contrast to functional magnetic resonance imaging, is the fact that electrical signals measured through the scalp conduct through the same scalp. This means that the primary source of the electrical activity conduct through a larger volume, making it difficult to differentiate primary signals using sensors that are placed in close proximity to each other (as is the case in EEG electrode placement). This problem in EEG is commonly known as the volume conduction problem (Cohen, 2014).

Normally, when one estimates functional connectivity between signals from two different recording sites or nodes, Pearson correlations are used as a proxy for functional connectivity. Due to volume conduction however, the two signals from EEG electrodes are extremely likely to share a common source and will thus show high Pearson correlations that might be more related to Euclidean distance between electrodes than actual underlying connectivity. This would result in spurious high local functional connectivity between electrodes that are located in close proximity. To avoid the volume conduction bias in estimating functional connectivity between two time-varying signals one can instead use connectivity measures that are based on the phase or lag of the two signals. In the present data the weighted phase lag index (WPLI) was used as a measure of connectivity (Stam et al., 2007; Vinck et al., 2011). The phase lag index is a measure of the asymmetry of the distribution of phase differences. Stam et al. (2007) showed that in both real and simulated data this measure is much less affected by common sources (e.g. as a result of volume conduction) and active reference electrodes (as is the case with the BioSemi setup). The weighted variant (WPLI) provides a more reliable estimate across trials that is useful for subsequent graph analysis (Ortiz et al., 2012).

All pre-processing was carried out using fieldtrip (www.fieldtriptoolbox.org) using a similar pipeline as has been used before with the WPLI (Ortiz et al., 2012). All code used for the pre-processing and subsequent analyses are available on GitHub and include detailed documentation on its usage: (http://bit.ly/2i2T8Un). The following basic pre-processing steps were carried out on each individual dataset; eyes-closed segments were selected, raw timeseries were re-referenced to a mastoid reference electrode, signal was de-trended (to remove linear trends), demeaned and bandpass filtered (<60Hz lowpass filter) and a discrete Fourier transform filter was used to remove potential 50Hz line-noise (van Diessen et al., 2014). Next, independent component analysis (ICA) was used to decompose the pre-processed time-series into maximally independent components (Hyvärinen, 1999a). These components were visually inspected for artefacts such as eye-blinks, heartbeats and other unclassified noise, which were subsequently removed from the signal (Figure 5.2).

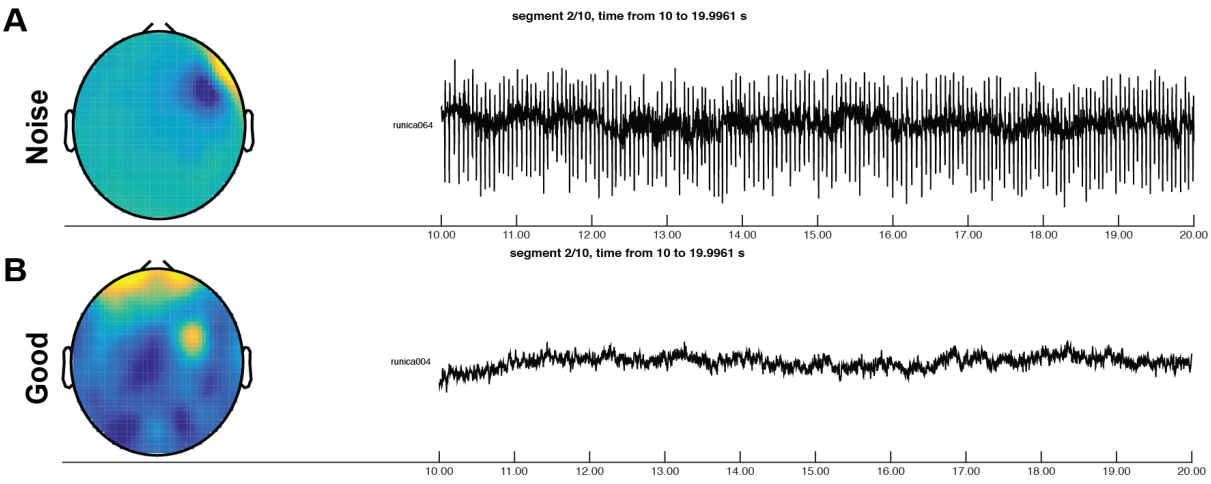

Figure 5.2: Example of ICA decomposition

Panel A shows an example of a component containing signal from a predominantly noisy electrode in frontal parietal cortex. Panel B shows and example of a component that would be classified as true signal.

The non-noise ICA components were back-projected into the original signal space. The recording was segmented into 4-second segments and the first and last epoch were removed to avoid any potential interference from the open and closing of eyes between the one minute segments. To obtain power and cross spectra we used the fieldtrip multi-taper fast Fourier transform function (MTFFT). Multi-tapering is essentially a windowed Fast Fourier Transform (FFT) method designed to minimize spectral leakage (Harris, 1978). Spectral leakage occurs during normal FFT because it samples continuous data discretely whereas energy from other non-measured frequencies might spread their energy into the sampled frequencies. Multi-tapering limits this effect by fitting multiple (usually Slepian) sequences to the cross-spectrum. This effectively smooths the power spectral estimate to include leakage and thus give a more accurate estimate of a specific frequency especially at the borders. However, using too many tapers risks over-smoothing the data and thereby including non-present frequency energy from neighbouring frequencies.

For broad frequency spectra (such as alpha, beta and gamma) this is not an issue as the leakage is relatively small compared to the overall frequency bandwidth. For narrow frequency bands however using too many tapers has an increased risk of confounding the spectral estimate from neighbouring frequencies. In the present study a Hanning window tapering (with more discrete edges and thus less smoothing) was used for the low frequencies and fieldtrips default discrete prolate spheroidal sequence (DPSS; a set of Slepian sequences) was used for the other frequencies. Thus, during spectral density estimation the time-series were simultaneously split into the 5 well-known frequency bands: delta [2-4Hz], theta [4-7Hz], alpha [7-13Hz], beta [13-30Hz] and gamma [30-60Hz].

5.2.5 Asymmetry analyses

To analyze inter- and intra-hemispheric asymmetry the power spectra density estimate of each electrode was used from the MTFFT estimate. To compute frontal asymmetry ratios, the following electrodes were chosen: Fc1, Fc2, Fc3, Fc4, Fc5, Fc6, F1, F2, F3, F4, F5, F6, F7, F8, AF3, AF4, AF7, AF8, Fp1 and Fp2. Uneven numbered electrodes present left hemisphere and even electrodes right hemisphere. A normalized frontal asymmetry index (FAI) was calculated by taking the mean power spectra of all left and right hemisphere electrodes respectively and combined using the following formula: [right-left]/[right+left]. To compute intra-hemispheric asymmetry left and right hemisphere were analyzed separately. Anterior electrodes included: F1, F2, F3, F4, F5, F6, F7, F8, AF3, AF4, AF7, AF8, Fp1 and FP2. Posterior electrodes included: O1, O2, PO3, PO4, PO7, PO8, P1, P2, P3, P4, P5, P6, P7, P8, P9 and P10. Again ratios were computed using: [anterior-posterior]/[anterior+posterior]. Although this is a relatively high number of electrodes, the inclusion of more channels/electrodes results in more reliable estimations of asymmetry (Kähkönen, Komssi, Wilenius, & Ilmoniemi, 2005; Schutter, de Weijer, Meuwese, Morgan, & van Honk, 2008). All computations were done in each of the 5 separate frequency bands. Statistical group comparisons were carried out using non-parametric permutation test (with 10.000 permutations, alpha set at $p<0.05$ and using the Welsh T-distribution) from the R Deducer package (http://www.deducer.org/).

5.2.6 Connectivity analyses

Pairwise weighted phase lag indices (WPLI) formed the basis for reconstructing graph matrices for each of the five frequency bands across all electrodes. The main basic metrics of interest were: inter-hemispheric connectivity, path length, centrality and modular structure, and small-world coefficient. To compare overall connectivity every connection was compared between

groups using a non-parametric two-tailed permutation test (using 10000 permutations) and the resulting p-value matrix was subsequently corrected for multiple comparison using FDR correction with alpha set at <0.05 (Benjamini & Hochberg, 1995). This FDR correction is arguably quite lenient for the present data. However, given the exploratory nature of the present analysis we chose a lenient threshold. For inter-hemispheric connectivity, the median (due to a non-normal distribution) absolute WPLI for all connections between left and right hemisphere was taken and compared between subjects. Graph metrics (Rubinov & Sporns, 2010) were computed on weighted binary matrices within a cost range of 0-30%. As a starting point to compute these the minimal spanning tree (MST) of the graph was used (Tewarie, van Dellen, Hillebrand, & Stam, 2015). The MST is the minimum set of connections needed to connect all electrodes. Only metrics that showed a consistent significant difference across multiple cost points were considered to be robust.

5.3 Results: ARC Data

5.3.1 Asymmetry analysis

Analyses of frontal cortical asymmetry indices (FAI) indicated no significant differences between the two groups as assessed using permutation testing in any of the 5 frequency bands (Figure 5.3). Visual inspection of power spectral density across the entire cortical region indicated no clear pattern differences between the two groups across the scalp, indicating that the lack of a difference is unlikely to be the result of the electrode selection. Across the frequency bands there does appear to be a slight trend towards positive indices for the autism group, whereas in the neurotypical group a more neutral pattern emerges. In the theta band for the autism group the FAI differs significantly from zero ($t=2.888$, $p=0.013$), which is not the

case for any of the frequency bands in the neurotypical group. This might suggest that the lack of effect studies might be more related to sample size and the number of outliers in both groups.

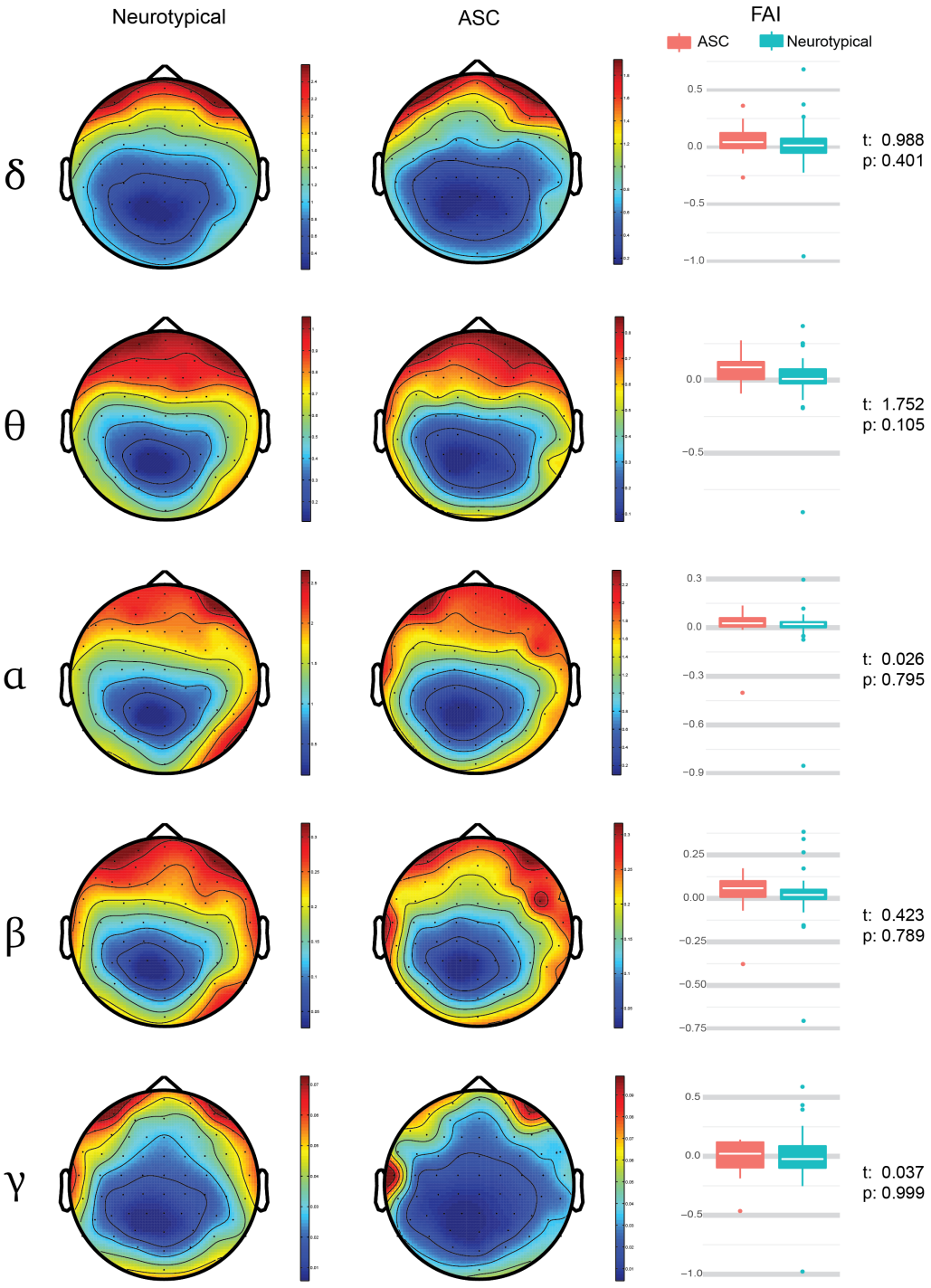

Figure 5.3: Median power and group-comparison for each frequency band

The left column shows the group median power spectral density for each frequency in the neurotypical group. The middle column shows the same information from the autism group. The right column shows the frontal asymmetry index (FAI) for each group as well as the t-statistic and p-value of the permutation test comparing each group.

5.3.2 Overall connectivity analysis

Comparing overall connectivity between groups revealed a number of connections that appeared different (Figure 5.4). The most prominent differences were observed in the beta and theta bands. This in contrast to previous studies that have mostly focus on alpha band activity. In the beta band it was mostly right frontal (F8), right frontal-central (FC4, FC2) and right temporo-parietal (TP8) electrodes that showed consistent median under-connectivity in the autism group. Most of these connections were to left-frontal electrode sites (F1, AF7, F7, FC5, FC1, C3, C5) but also to more parietal (CP1, P3, P7) and temporal electrodes (T7). In all cases the median difference indicated reduced connectivity in the autism group. Interestingly, the inter-hemispheric connectivity ratio showed no group differences in any of the frequency bands. Given that there were some electrode specific connectivity differences in mainly a select set of frontal electrodes it is possible that an overall inter-hemispheric connectivity measure is too broad. In the present sample power spectral density gave no indication of specific frontal differences, but follow-up research should perhaps focus on more specific frontal networks.

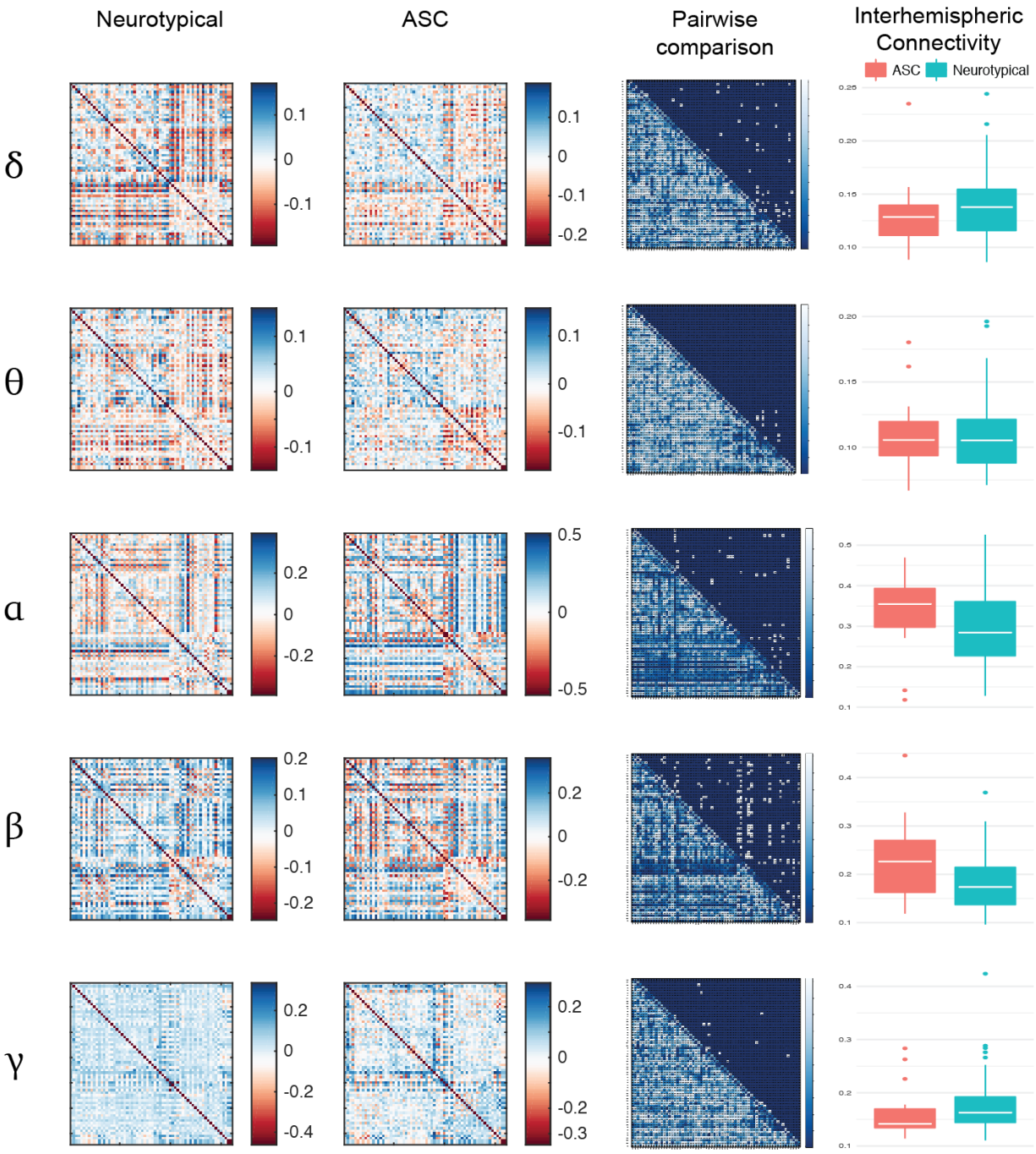

Figure 5.4: Adjacency matrices and inter-hemispheric connectivity

Left column show the median pairwise WPLI for the neurotypical group across all 64 electrodes. The second column shows the same matrices for the autism group. The third column shows the group-wise comparisons. The right panel show boxplots for the inter-hemispheric connectivity. Interactive high resolution matrices can be viewed on: http://bit.ly/2jPq7sw. The group-wise median differences are also displayed there.

5.3.3 Graph analysis

Graph analysis of common measures such as path length, betweenness centrality, modularity and small-worldness revealed no clear group-wise differences in any of the frequency bands (Figure 5.5). Similar to the analysis of the overall connectivity pattern it is likely that any potential group differences are masked by the fact that the present measures reflect a global (e.g. whole-brain) network property. At the same time the present sample might be too small to detect changes on such a broad summary measure.

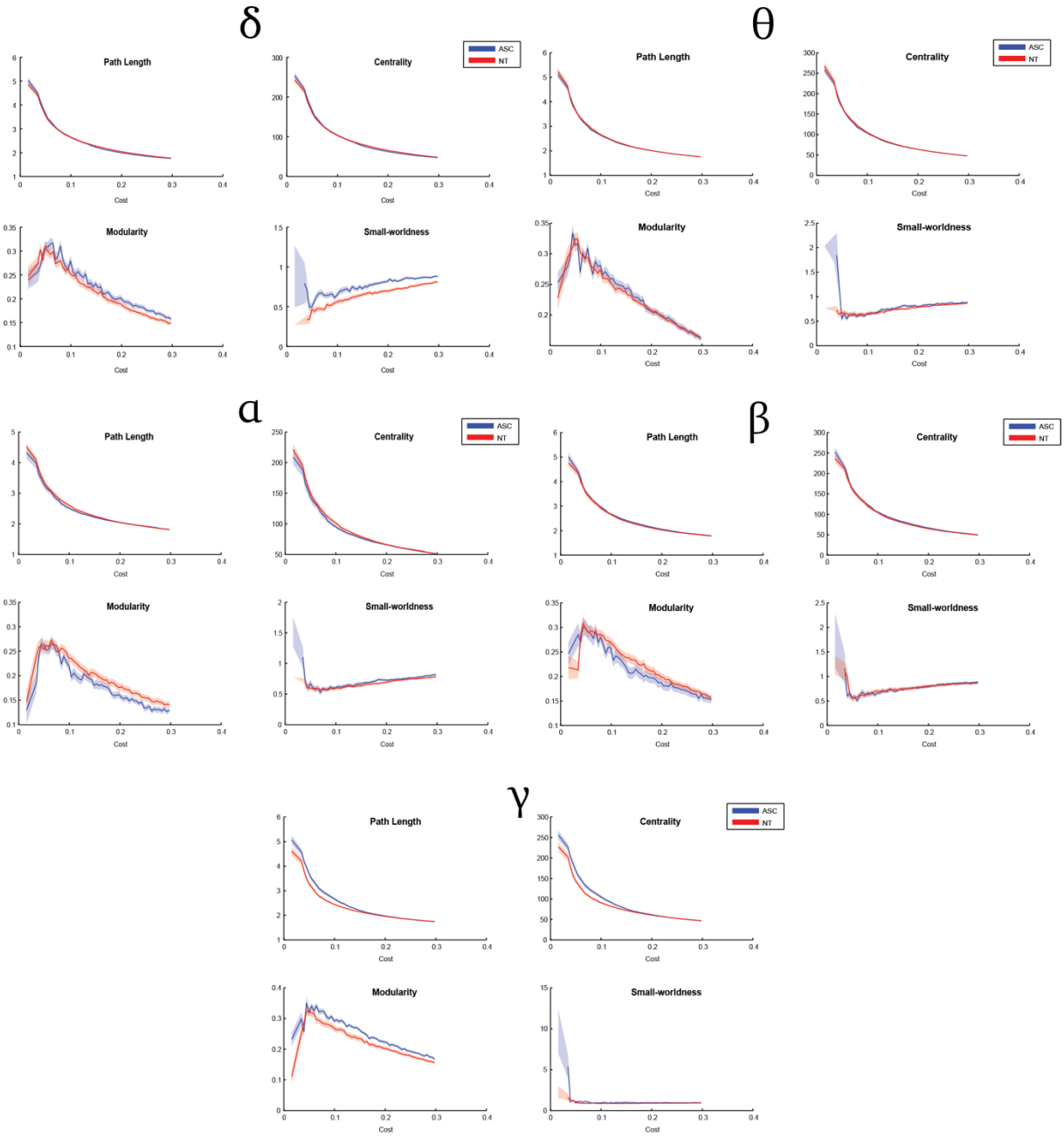

Figure 5.5: Graph theory metrics.

Lines in each plot represent the group mean at that specific cost. Cost indicates the level above the minimal spanning tree (e.g. a cost of 0.1 reflect the MST + the top 10% of all connections). The shaded areas around the lines indicate the standard error of the mean for the respective group. High resolution plots can be viewed on: http://bit.ly/2jPq7sw

5.4 Results: CRAE Data

All analyses conducted on the Cambridge ARC dataset were repeated for the data obtained from the Centre for Research on Autism and Education.

5.4.1 Asymmetry analysis

Similar to the Cambridge data, the asymmetry analysis revealed no effects that survived multiple comparisons. Interestingly, the mean difference even seemed to be in opposite direction as the discovery data.

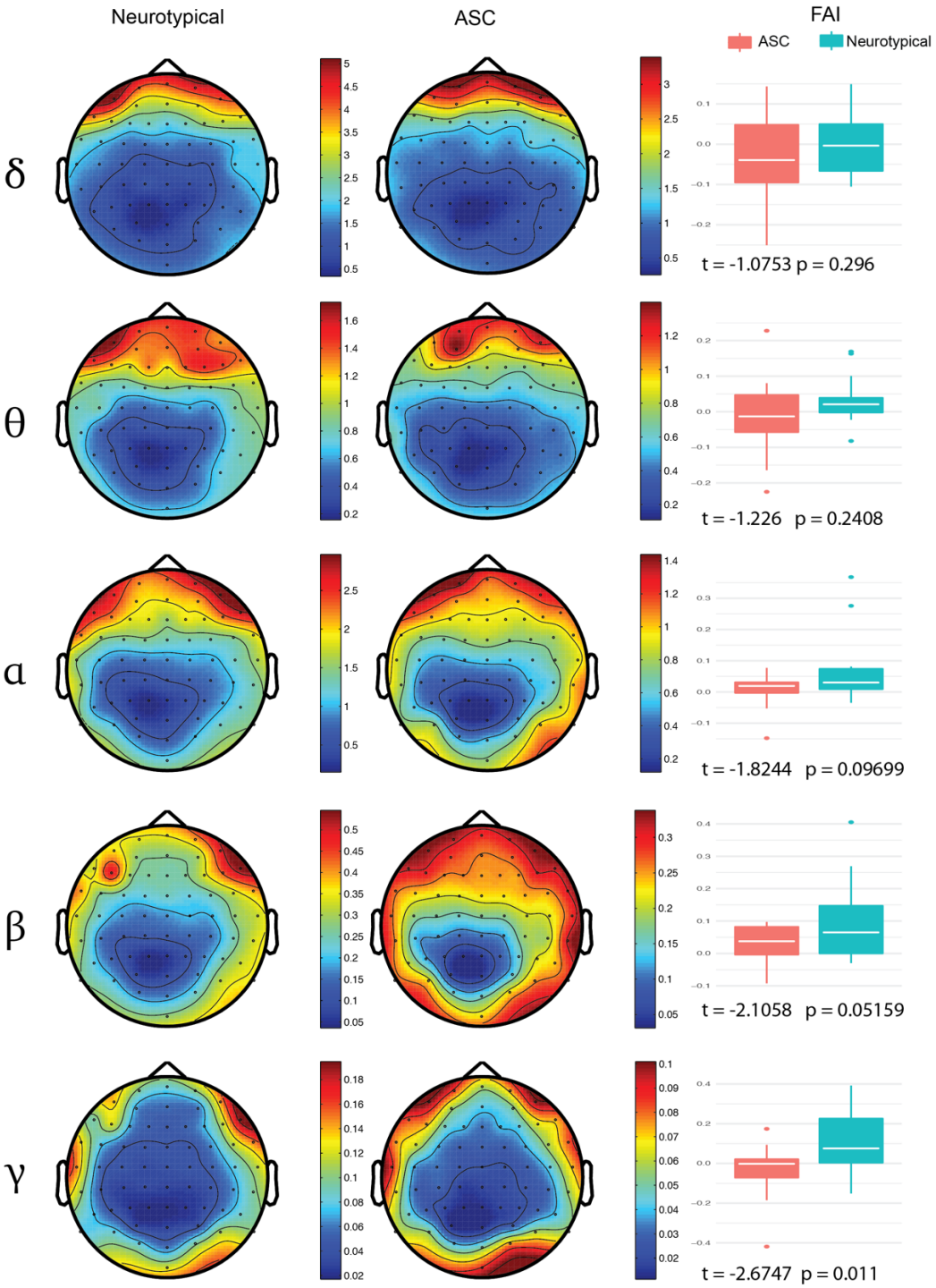

Figure 5.6: Median power and group-comparison for each frequency band

The left column shows the group median power spectral density for each frequency in the neurotypical group. The middle column shows the same information from the autism group. The right column shows the frontal asymmetry index (FAI) for each group as well as the t-statistic and p-value of the permutation test comparing each group.

5.4.2 Overall connectivity analysis

Analysis of the overall connectivity pattern revealed a number of electrode pairs with significantly altered connectivity between them. Although these electrodes do not perfectly overlap a pattern is emerging of mainly disconnected frontal electrode sites. (Figure 5.7)

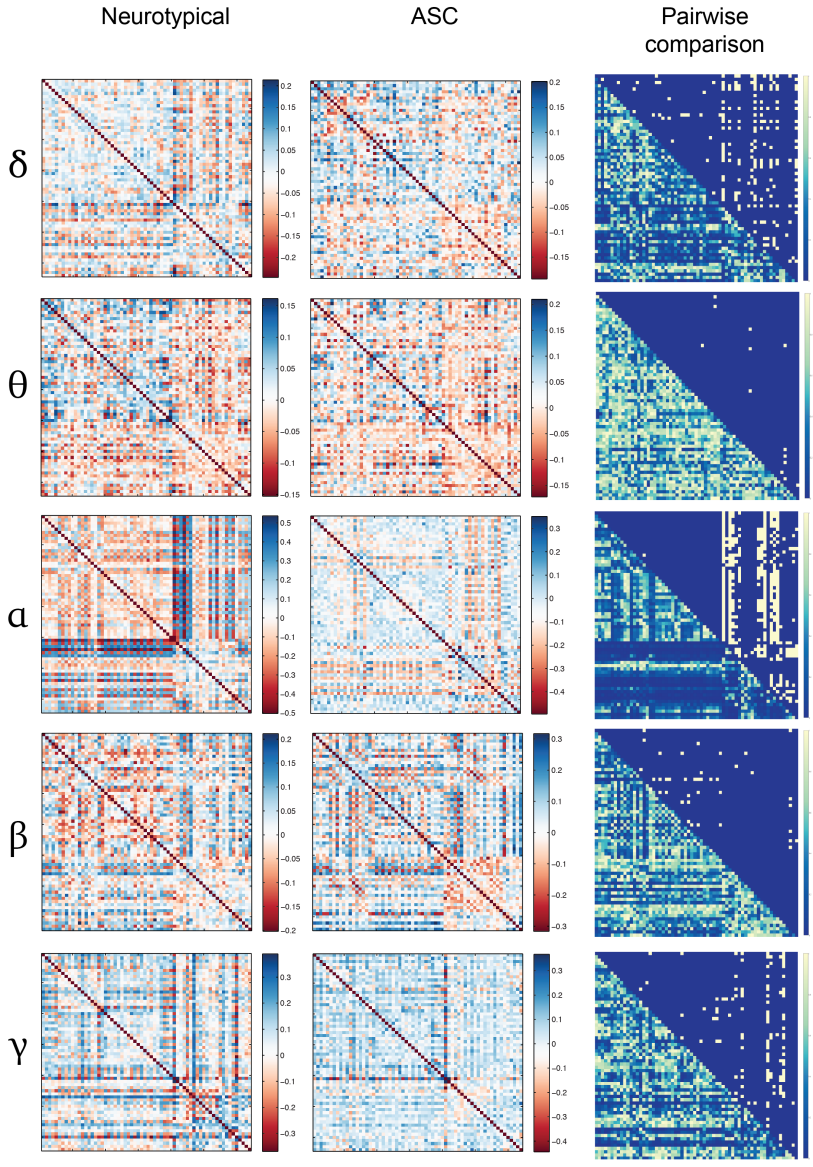

Figure 5.7**:** Adjacency matrices and inter-hemispheric connectivity

Left column show the median pairwise WPLI for the neurotypical group across all 64 electrodes. The second column shows the same matrices for the autism group. The third column shows the group-wise comparisons that survive FDR correction.

5.4.3 Graph theory analysis

Analysis of graph theoretical properties revealed no significant differences between the two groups (Figure 5.8).

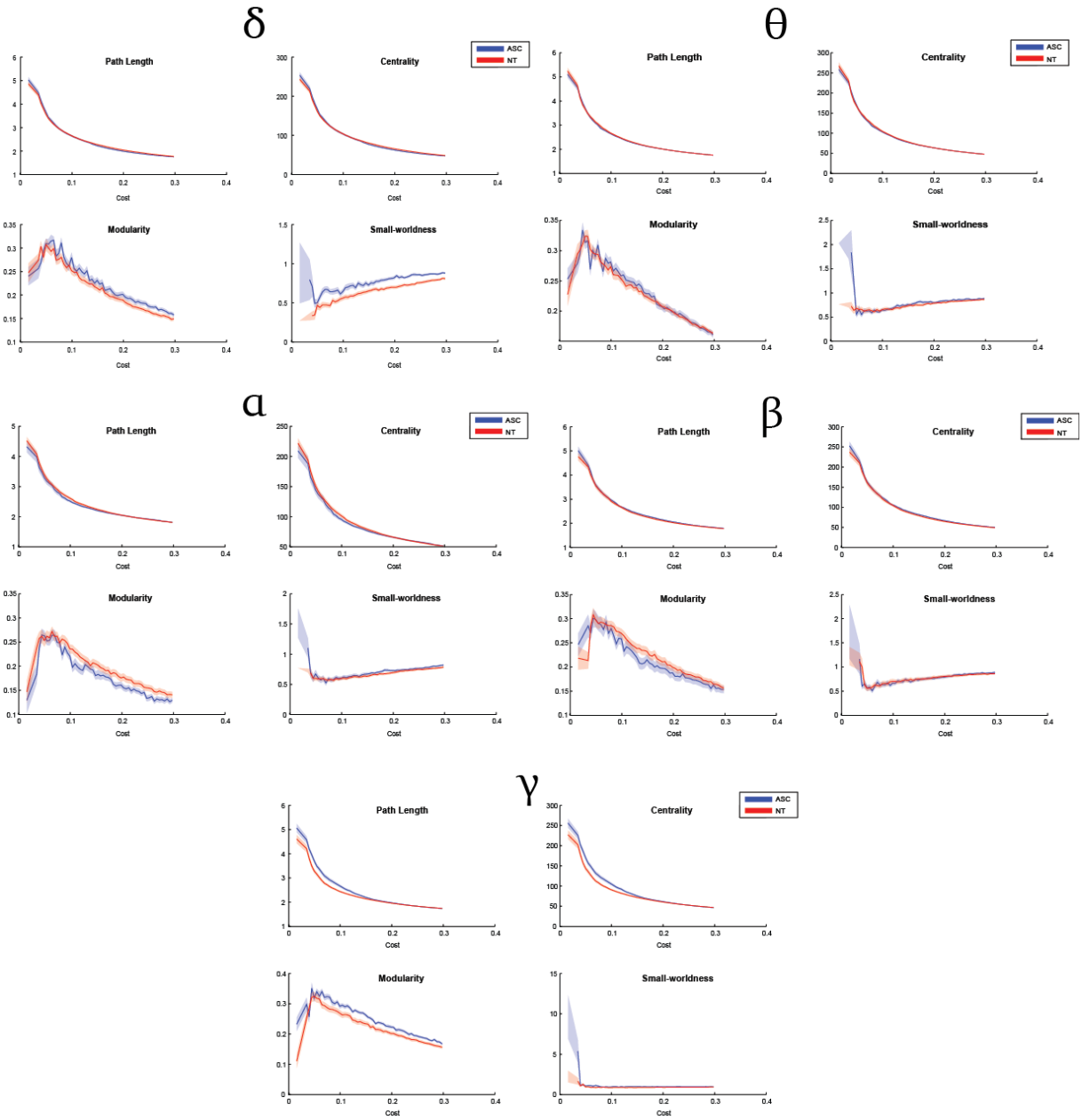

Figure 5.8**:** Graph theory metrics.

Lines in each plot represent the group mean at that specific cost. Cost indicates the level above the minimal spanning tree (e.g. a cost of 0.1 reflect the MST + the top 10% of all connections). The shaded areas around the lines indicate the standard error of the mean for the respective group.

5.5 Discussion

Functional interpretations of the asymmetry indices include predictions and inferences regarding psychopathology and dispositional styles, often focusing on the link between personality traits, social behaviour and resting baseline asymmetry (Harmon-Jones, Gable, & Peterson, 2010). Most research on asymmetry of spectral density in autism tends to find effects in alpha and beta frequency bandwidths. In the present pilot study we chose to extend our analyses to all five frequency bands given the somewhat heterogeneous findings in autism (Wang et al., 2013), and the exploratory nature of the present study. Although in the CRAE dataset there seemed to be two nominally significant differences in frontal asymmetry in the beta and gamma bands these did not survive multiple comparison correction across the five bands nor did they replicate in the Cambridge dataset. In fact the median frontal asymmetry indices for those two frequency bands showed opposite differences in the two datasets. This is most likely caused by three issues.

First, the sample sizes for both datasets is at present too small to draw any definitive conclusions. Group-wise figures presented in this chapter represent medians of each group as there was considerable variability in both the neurotypical as well as the autism group. As data collection at both sites is still ongoing (and a third site might be added in the near future), this is hopefully an issue that will be resolved in the long-term. It should be noted that previous studies on resting-state EEG asymmetry have had large variation in samples sizes, ranging from an upper bound of 463 individuals with a diagnosis to a lower bound of 9 (Billeci et al., 2013). Some of the heterogeneity in published literature might indeed also be attributable to power issues.

Secondly, and related to the former issue, the present datasets are too small to effectively account for potential confounds such as age, biological sex and IQ. As alluded to in the introduction of this chapter these factors are known to influence EEG asymmetry patterns as well as modulate effects within autism (Lai et al., 2015). A more exhaustive dataset would allow us to include those factors as potential mediators or covariates.

Thirdly, the current frontal asymmetry indices are based on the ratio between a cluster of frontal electrodes that all represent specific locations. In the literature there is considerable heterogeneity in terms of electrodes included in these ratios (Wang et al., 2013). Furthermore, when individual connections were pairwise compared between the two groups there were a range of connections that survived FDR correction in both datasets and across frequency bands (Figures 5.4 and 5.7). Again, due to sample size constraints no definitive conclusions can be drawn from that at this time, but it is noteworthy to point out that most of the connections that differed between the two groups were inter-hemispheric frontal connections. If we assume that balance in spectral density asymmetry is sustained by functional connections operating in the same frequency band it might be interesting to focus on the asymmetry of those connections specifically. Based on the present data this would constitute a certain circularity in the analysis as the selection of electrodes would be based on the same data and at present there might not even be enough consistency in which electrodes pass FDR correction across datasets. However, with the possible addition of a third site we plan to compute frontal spectral density asymmetries based on frontal electrodes that show a consistent connectivity difference across the two datasets described here.

As a novel extension the present study also explored the use of graph theoretical measures to assess potential whole-brain differences in functional connectivity. Across densities, bandwidths and datasets there were no significant differences in any of the main graph measures explored here. Again, sample size and sample heterogeneity might be factors contributing to this lack of differences. However, it is also very well possible that the complex and various differences that might exists in the functional connectome between individuals with autism and neurotypical individuals is not well captured by measures that describe overall brain connectivity in a singular vector. All research in autism connectivity, whether using functional magnetic resonance imaging (Vissers et al., 2012) or EEG (Wang et al., 2013), indicates a strong heterogeneity in its findings at both regional brain levels as well as in overall brain organization.

Lastly, there is of course another possibility. Assuming Occam's Razor of the most parsimonious explanation being the most likely, it might very well be the case that there simply are little to no differences in functional connectivity and asymmetry between individuals with autism and neurotypical individuals. Although literature would suggest that some differences should be expected there is a real possibility that this literature suffers to some extend from the well known publication bias of positive findings leading to potential type-I-errors (Sterling, 1959). Again the sample size of the present data does not allow any definitive conclusions. Hopefully the addition of more data and a third data collection site will add to the strength of the present findings, allowing for a more definitive conclusion.

Chapter 6 Effects of intranasal oxytocin on functional connectivity in women

6.1 Introduction

Oxytocin is a neuropeptide hormone involved in sexual intercourse, childbirth and parent-infant bonding, affecting reward processing, anxiety and social salience (Bethlehem et al., 2014). Oxytocin is not necessarily a 'pro-social' hormone, as effects are highly context- and person-dependent (Bartz, Zaki, Bolger, & Ochsner, 2011; Bethlehem et al., 2014). Oxytocin has received substantial interest as a potential treatment for psychiatric conditions such as autism (Meyer-Lindenberg, 2008), although clinical trials show modest effects (Watanabe et al., 2013, 2015; Yatawara, Einfeld, Hickie, Davenport, & Guastella, 2015). Given the marked heterogeneity in autism (Lai, Lombardo, Chakrabarti, & Baron-Cohen, 2013) it is possible that the benefits of oxytocin may vary substantially between individuals. For example, on-average intranasal oxytocin improves eye contact during naturalistic social interaction, but the largest effects occur for individuals who typically make the least amount of eye contact (Auyeung et al., 2015). Thus, in evaluating oxytocin's therapeutic potential, we must move towards a more precise understanding of how its effects may vary across individuals.

We have theorized that the widespread effects of oxytocin on complex human social behaviour may be due to distributed influence at a neural circuit level (Bethlehem et al., 2013). Although oxytocin acts directly at a local level via the oxytocin receptor (*OXTR*), it can potentially affect widespread circuit-level dynamics via connections to areas that are densely populated with

OXTR. One way to test the hypothesis that oxytocin affects circuit-level organization in the human brain is through oxytocin-administration studies within the context of in-vivo measurement of intrinsic functional brain organization (i.e. connectome or brain network organization) with resting state fMRI (rsfMRI) data. While there are a number of existing neuroimaging oxytocin-administration studies (Bethlehem et al., 2013), most have relied on task-based fMRI paradigms and largely focus on males. In the oxytocin literature there is a prominent bias towards males, and one that affects much of neuroscience and medical research (Beery & Zucker, 2011). Sex differences in the *OXTR* system are documented (Dumais & Veenema, 2015; Ebner et al., 2016; Kramer, Cushing, Carter, Wu, & Ottinger, 2004), suggesting that findings in males may not generalize to females. Furthermore, task-based fMRI has often shown opposite findings in males and females namely in terms of amygdala activation (Domes et al., 2010; Lischke et al., 2012).

Because oxytocin is viewed as a potential pharmacotherapy for conditions like autism, and given that sex may play a large moderating roles in drug effectiveness (Zagni, Simoni, & Colombo, 2016), it is essential to begin examining how oxytocin operates in the female brain. In addition, although there is a strong male bias in autism diagnoses (Baron-Cohen et al., 2011) there is reason to believe that females are strongly underrepresented that may have increased the male-biased understanding of autism (Lai et al., 2015). Given the lack of prior literature on oxytocin's network level effects on brain connectivity in women we chose to use a robust data-driven (hypothesis-free) approach to assess potential connectivity differences.

The majority of studies investigating how oxytocin affects the human brain use task-based fMRI paradigms. While task-based studies are important for targeting specific psychological

processes, examination of oxytocin-related effects may, as a result, be neuroanatomically constrained to specific circuits related to those tasks. Examination of functional connectivity using rsfMRI data allows for task-independent assessment of oxytocin's effect on intrinsic functional brain organization across the entire connectome. Furthermore, the small number of existing rsfMRI oxytocin-administration studies (Ebner et al., 2016; Koch et al., 2016; Sripada et al., 2013; Watanabe et al., 2015) use seed-based analyses that do not allow for hypothesis-free examination across the connectome. Thus, a more unconstrained approach could provide novel insights into oxytocin-related effects on connectome organization, especially when little to no prior hypothesis can be derived from existing literature.

Here we use independent components analysis (ICA) to examine how connectivity between-circuits (i.e. between-component connectivity) (Smith et al., 2013, 2015) differs across oxytocin and placebo. To facilitate our understanding of oxytocin-effects on connectivity in the human brain we analysed two publicly available post-mortem human brain gene expression datasets to answer the question of how the oxytocin receptor (*OXTR*) is expressed across a variety of subcortical and cortical areas in the human brain. To date, information on OXTR expression has largely been confined to animal studies and translation from that is problematic (Young, 2015). We predicted that oxytocin would have largest impact on connectivity between the densely *OXTR*-populated striatum and cortical circuits. Furthermore, we predicted that impact of oxytocin on connectivity would vary as a function of variation in autistic traits, with larger effects for individuals with higher levels of autistic traits (Auyeung et al., 2015).

6.2 Methods

6.2.1 Participants

All research was conducted in accordance with the Declaration of Helsinki and the study had received ethical approval from the NHS Research Ethics Service (NRES Committee East of England – Cambridge Central; REC reference number 14/EE/0202). This study was exempt from clinical trials status by the UK Medicines and Healthcare Regulatory Agency (MHRA).

In a double-blind randomized placebo-controlled cross-over design, 26 women (age: 23.6±4.6 years, range [21-50]) received an oxytocin nasal spray (24 IU, 40.32 µg, Syntocinon-spray; Novartis, Switzerland, pump-actuated) in one session and placebo (the same solution except for the active oxytocin) in the other session in a counterbalanced order. After instruction by a trained medical doctor the sprays were self-administered 40 minutes prior (Born et al., 2002) to undergoing resting-state fMRI imaging. Participants confirmed no nasal congestion or obstruction on the day of testing. This timing and dosage are by far the most commonly used in oxytocin administration studies to date (E. MacDonald et al., 2011). Sessions were separated by at least one week (to ensure full wash-out from the first administration) when participants were on hormonal contraceptive (19/26). When participants were not on hormonal contraceptive (7/26) both sessions took place in the early follicular phase of the menstrual cycle to ensure similar hormone levels between sessions.

Exclusion criteria included pregnancy; smoking; a diagnosis of bipolar, obsessive-compulsive, panic or psychotic disorder; use of any psychoactive medication within one year prior to the study; substance dependence; epilepsy; and being post-menopausal. These criteria were

assessed by self-report and participants' general practitioners were given the full protocol prior to participation and asked to notify the research term if they thought there was any reason for exclusion. More details on the testing procedure and sample are provided in the supplementary information and supplementary table (D.1). Briefly; all subjects completed the Wechsler Abbreviated Scale of Intelligence (Wechsler, 1999) (mean 115.3±13.19), Empathy Quotient (EQ) (Baron-Cohen & Wheelwright, 2004) (mean 55.6±14.53)) and Autism Quotient (AQ) (Baron-Cohen et al., 2001) (mean 14.4±7.32) questionnaires prior to the first scanning session. None of the participants had received a formal diagnosis of autism nor did they give any indication that they may have gone undiagnosed. We acknowledge no assessment was done to formally rule this out. They were instructed to refrain from alcohol or caffeine on the day of testing and from food and drink 2 hours prior to testing (except for water).

To understand whether oxytocin or some other placebo-related effect that explains any drug-related differences in connectivity, we utilized an independent dataset of age-matched typical females in order to ascertain what are the normative baseline between-component connectivity effects. Our logic here is that if normative connectivity looks similar to patterns we see during placebo, then we can reasonably infer that oxytocin is the primary reason for the induced change in connectivity and not due to some placebo-related change and no effect of oxytocin. This independent dataset consisted of 50 females whom were slightly older but did not statistically differ in age (mean age 31.6±12.2, Wilcoxon rank-sum test: $W = 764.5$, $p = 0.117$) collected on the same scanner and which used a similar multi-echo EPI sequence for data collection (see Morris *et al*, 2016 for full details).

6.2.2 Image acquisition and pre-processing

MRI scanning was done on a 3T Siemens MAGNETOM Tim Trio MRI scanner at the Wolfson Brain Imaging Centre in Cambridge, UK. For the oxytocin-dataset, a total of 270 resting-state functional volumes (eyes-open, with fixation cross) were acquired with a multi-echo EPI (Kundu, Inati, Evans, Luh, & Bandettini, 2012) sequence with online reconstruction (repetition time (TR), 2300 ms; field-of-view (FOV), 240 mm; 33 oblique slices, alternating slice acquisition, slice thickness 3.8 mm, 11% slice gap; 3 echoes at TE = 12, 29, and 46 ms, GRAPPA acceleration factor 2, BW=2368 Hz/pixel, flip angle, 80°). Anatomical images were acquired using a T1-weighted magnetization prepared rapid gradient echo (MPRAGE) sequence (TR, 2250 ms; TI, 900 ms; TE, 2.98 ms; flip angle, 9°; matrix 256×256×256, FOV 256 mm). For the independent rsfMRI dataset on age-matched females, data was acquired on the same 3T scanner and with a multi-echo EPI sequence that was similar to the oxytocin-dataset (TR, 2470 ms; FOV, 240 mm; 32 oblique slices, alternating slice acquisition, slice thickness 3.75 mm, 10% slice gap; 4 echoes at TE = 12, 28, 44, and 60 ms, GRAPPA acceleration factor 3, BW=1698 Hz/pixel, flip angle, 78°). Multi-echo functional images were pre-processed and denoised using the AFNI integrated multi-echo independent component analysis (ME-ICA, meica.py v3, beta1; http://afni.nimh.nih.gov) pipeline (Kundu et al., 2013), details on this procedure are outlined in the supplementary materials (Appendix D).

6.2.3 Gene expression analysis

To better characterize subcortical and cortical brain regions in terms of *OXTR* gene expression, we analyzed RNAseq data in the Allen Institute BrainSpan atlas (http://www.brainspan.org) and the Genotype-Tissue Expression (GTEx) consortium dataset (http://www.gtexportal.org/home/). The BrainSpan atlas covers a number of cortical areas the

might provide insights into potential cortical targets of oxytocin expression, whereas the GTEx dataset does not have many regionally-specific areas of the cortex (only BA9 and BA24) and mostly includes more detailed information on several subcortical brain regions. In these analyses we used all postnatal (birth to 79 yrs.) samples in each dataset, stratified by biological sex. *OXTR* was isolated and plots were produced to descriptively indicate expression levels across brain regions. Expression levels in both datasets were summarized as Reads Per Kilobase of transcript per Million mapped reads (RPKM). Full details for the BrainSpan and GTEx procedures are available in their white papers: http://bit.ly/2dqRF47 and http://bit.ly/2e8o1W2 respectively. To examine whether *OXTR* expression levels were significantly elevated in each brain region, we compared expression levels against zero and, as a more conservative test, against another tissue from GTEx where we would not expect *OXTR* to be expressed (i.e. skin). These tests were carried out using permutation t-tests (1000 permutations) implemented with the perm.t.test function in R.

6.2.4 Group Independent Components Analysis and Dual Regression

To assess large-scale intrinsic functional organization of the brain we first utilized the unsupervised data-driven method of independent component analysis (ICA) to conduct a group-ICA followed by a dual regression to back-project spatial maps and individual time series for each component and subject. Both group-ICA and dual regression were implemented with FSL's MELODIC and Dual Regression tools (www.fmrib.ox.ac.uk/fsl). For group-ICA, we constrained the dimensionality estimate to 30, as in most cases with low-dimensional ICA, the number of meaningful components can be anywhere from 10-30 (S. M. Smith et al., 2013).

Some components were localized primarily to white matter and although likely may be driven by true BOLD-related signal (due to high ME-ICA kappa weighting), were not considered in any further analyses. 22 out of 30 components were manually classified as primarily localized to grey matter and were clearly not noise-driven components. Correlation matrices were constructed for all component pairs, these were assessed for significance using paired sampled t-tests and resulting p-values were corrected for multiple comparisons using Bonferroni correction at a family-wise error rate of 5%. Difference scores were computed for pairs that survived FWE correction on the Fisher z-transformed correlation scores (Steiger, 1980) and entered into robust regression (for insensitivity to outliers) (Wager, Keller, Lacey, & Jonides, 2005) with AQ scores. For more details see the supplementary information.

6.2.5 Large-Scale Reverse Inference with NeuroSynth

To better characterize the components showing an oxytocin-related effect on connectivity we used the decoder function in NeuroSynth (Yarkoni, Poldrack, Nichols, Van Essen, & Wager, 2011) to compare the whole-brain component maps with large-scale automated meta-analysis maps within NeuroSynth. The top 100 terms (excluding terms for brain regions) ranked by the correlation strength between the component map and the meta-analytic map were visualized as a word cloud using the wordcloud library in R, with the size of the font scaled by correlation strength.

6.3 Results

6.3.1 Oxytocin Receptor (*OXTR*) Gene Expression

Expression profiles of *OXTR* in women derived from the GTEx dataset reveal broad expression across subcortical regions, but with notable enrichments particularly in nucleus accumbens,

substantia nigra, and the hypothalamus (Figure 6.1). All regions showed *OXTR* expression that was significantly above 0 and critically, was also significantly stronger than expression in a tissue we would expect to show little expression (i.e. skin) (Table D.2). Cortical regions from the BrainSpan dataset also exhibit significant *OXTR* expression (above 0 and when compared to skin; Table D.2), albeit at much more modest levels than some subcortical regions. This modest degree of *OXTR* expression may be particularly relevant given studies that show broad oxytocin-related effects on complex human social behaviour, social communication, and social cognition that affects distributed cortical regions (e.g., superior temporal gyrus, medial prefrontal cortex (MFC)). However, there is a lack of specificity apparent in *OXTR* expression in cortex, as most regions show similar levels of expression.

As a whole, these data indicate that oxytocin could have potent direct effects on *OXTR* within subcortical circuitry, particularly areas of the striatum and midbrain, but may also have similar *OXTR*-driven effects to a lesser extent across most cortical areas where *OXTR* expression is modest. Given the lack of specificity within cortex, these data also support an approach for examining oxytocin-related effects on intrinsic functional connectivity that examines all between-networks connections, as all may be susceptible to plausible effects. However, given the enrichment particularly in striatal and midbrain regions, it is likely that oxytocin-related effects on connectivity may particularly affect connections between cortex and the densely *OXTR*-populated striatum and midbrain. We also carried out exploratory analyses on gender differences in OXTR expression and these are included in the supplementary information (Figure D.1).

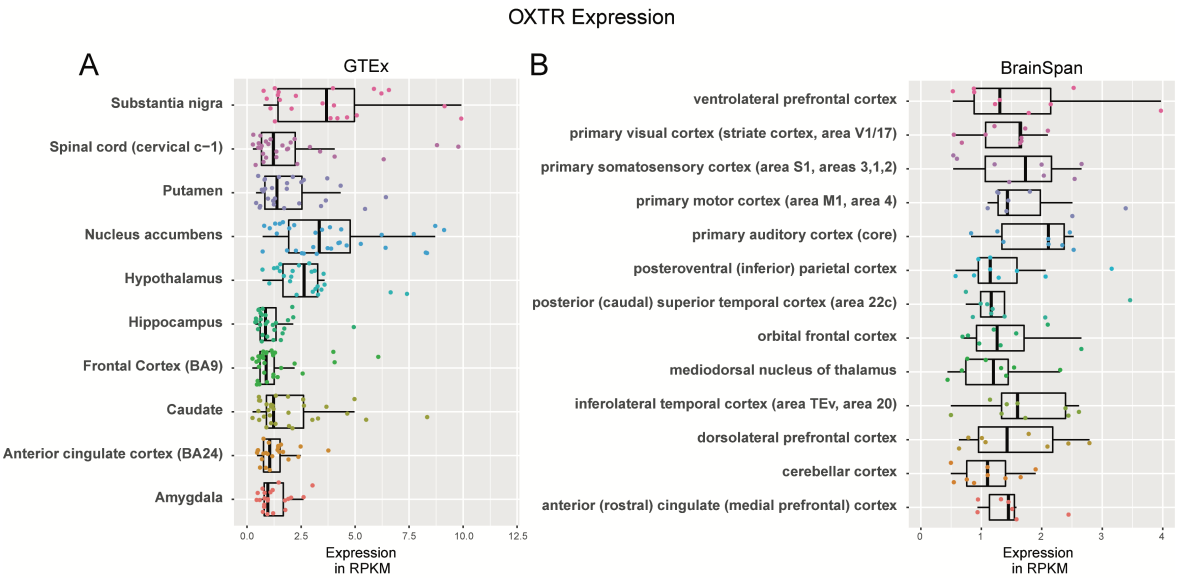

Figure 6.1: Oxytocin receptor (*OXTR*) gene expression in the female human brain.
This figure illustrates *OXTR* gene expression measured via RNAseq in BrainSpan (http://www.brainspan.org) and GTEx (http://www.gtexportal.org/home/) datasets. Panel A shows expression for all subcortical regions available in the GTEx dataset in women. All brain regions show significant expression of *OXTR* above 0 and compared to expression in non-brain (skin) tissue. On-average, *OXTR* expression is particularly enriched in ventral striatum (Nucleus Accumbens), substantia nigra, and hypothalamus. Panel B shows expression for all cortical areas and the thalamus available in the BrainSpan atlas in women. All areas also show significant, albeit modest, levels of *OXTR* expression compared to 0 and non-brain (skin) tissue.

6.3.2 Oxytocin-Related Between-Component Connectivity Differences

Analyses of all pairwise comparisons of between-component connectivity differences as a function of oxytocin administration revealed only one pair of components, IC11 and IC21 (Figure 6.2, panels A and B), whose connectivity was substantially affected by oxytocin (*t(24)* = 6.99, *p* = 3.10e-7, effect size d = 1.39, 95% CI [0.96 to 1.86]) and survived after Bonferroni correction (FWE p<0.05) for multiple comparisons. The full pairwise correlation matrix is provided in Supplementary Figure D.2. As shown in Fig 6.2E, all but 2 participants (92%; 23/25) showed evidence of a non-zero oxytocin-related boost in connectivity over the placebo condition (Figure 6.2, panel E). Within the placebo condition alone, connectivity was not

different from 0 (*t(24)* = -0.86, *p* = 0.39). However, within the oxytocin condition, connectivity was substantially elevated above 0 (*t(24)* = 6.22, *p* = 1.95e-6).

The IC11 component comprised regions in primary auditory cortex, middle and posterior divisions of the insula, superior temporal gyrus, posterior superior temporal sulcus, middle and posterior cingulate cortex, ventromedial prefrontal cortex, amygdala, and superior parietal lobe. These brain regions overlap with areas typically considered important in processes such as language, social-communication, self-referential and social cognition, pain, and emotion (Amodio & Frith, 2006; Friederici, 2012; Hickok & Poeppel, 2007; Wager et al., 2013; Yang, Rosenblau, Keifer, & Pelphrey, 2015). NeuroSynth decoding revealed that most of the terms with the highest correlation with IC11 were predominantly terms referring to pain-related, motor-related, or language/speech-related processes (Figure 6.2, panel C). The IC21 component was comprised entirely of subcortical regions such as the striatum, basal ganglia, amygdala, thalamus, midbrain, and brainstem. These regions, particularly the striatum, midbrain, and amygdala, are typically considered highly involved in reward and emotion-related processes (Haber & Knutson, 2010; Kober et al., 2008; Lindquist, Wager, Kober, Bliss-Moreau, & Barrett, 2012). This was again confirmed with NeuroSynth decoding showing a predominance of reward, motivation, and affective terms (Figure 6.2, panel D).

Next, we examined whether individual differences in autistic traits accounted for variability in oxytocin-related effects on connectivity between these networks in an exploratory analysis. Given prior work suggesting that oxytocin may have its largest effect on individuals who show the most atypical social behaviour (Auyeung et al., 2015), we hypothesized that oxytocin may have the largest effects on connectivity in individuals with the highest degree of autistic traits.

Here we found evidence confirming this hypothesis, as oxytocin's effect on between-component connectivity appeared to increase with increased degree of autistic traits: r = 0.41, one-tailed $p = 0.0351$ (Figure 6.2, panel F).

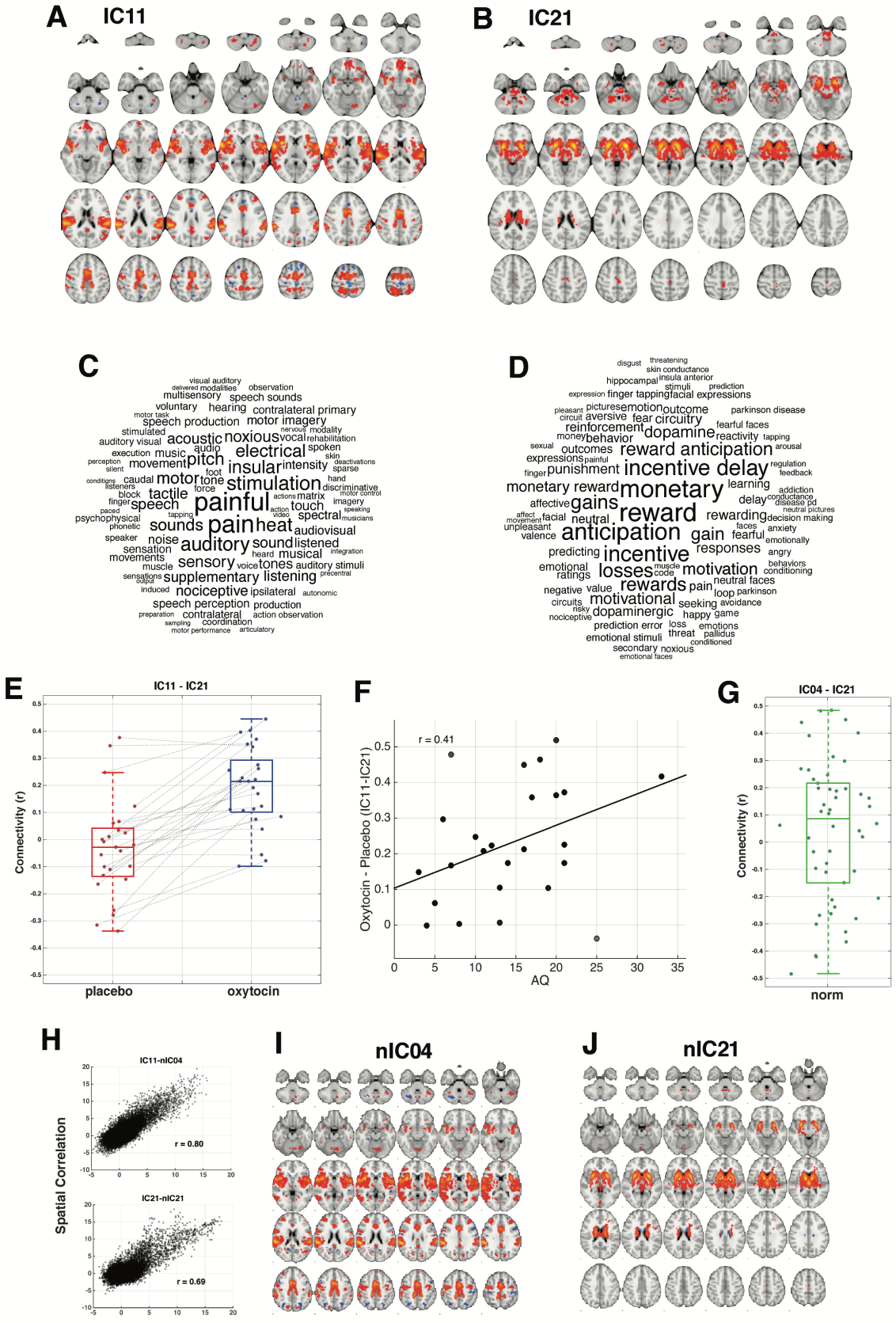

Figure 6.2: Oxytocin-related enhancement of intrinsic functional connectivity.

Panel A shows the spatial map of component IC11. Voxels are coloured by Z-statistics indicating how well each voxel's time series fits the component's time series. **Panel B** shows the same information for component IC21. **Panel C** shows the top 100 terms associated with component IC11 based on NeuroSynth decoding and font size represents relative correlation strength of that term to the component. **Panel D** shows the same information for component IC21. **Panel E** shows connectivity between IC11 and IC21 for each subject during placebo or oxytocin administration. Dots represent individual subjects and the lines connect each individual's data under placebo and oxytocin, with the positive slopes indicating an enhancement of connectivity after oxytocin administration. Underneath the individual-level data are boxplots that indicate the median, interquartile range, and outer fences. Interestingly, the two individuals who would be considered outliers in the placebo condition are the minority of individuals showing no enhancement of connectivity as a function of oxytocin. **Panel F** shows the relationship between oxytocin-related effects on connectivity and continuous variation in autistic traits as measured by the AQ. **Panel G** shows the between component connectivity of between comparable components of the normative dataset. **Panel H** shows the spatial correlation between the oxytocin data components and the two normative components that were selected. **Panels I and J** show the normative components spatial maps.

Finally, we ran further analyses to aid the interpretation of such an effect. One interpretation could be that oxytocin is the primary driver of enhanced connectivity between these components. However, the alternative could be that oxytocin has no effect on connectivity, and that the placebo might somehow induce a decrease in connectivity between these components. To tease apart these different interpretations, we looked to an independent dataset of rsfMRI to ascertain what the normative connectivity strength is between these two components. If oxytocin was truly enhancing connectivity between these components, we would predict that connectivity between these components under normative conditions would be similar to those seen under placebo. That is, normative connectivity effects between these components should manifest similarly to placebo and on average show no difference from 0.

We identified two components that were spatially nearly identical to the component pair we observed an oxytocin effect in; nIC4 and nIC21 (Figure 6.2I & 6.2J). Quantitatively confirming this similarity, we find very large correlations between the spatial component maps of the normative and oxytocin/placebo datasets (nIC4-IC11, r = 0.80; nIC21-IC21, r = 0.69, see Figure

6.2H). No other components showed any significant correlations (all $r < 0.2$). Similar to our placebo condition, this component-pair showed connectivity that was not significantly different from zero: $t(49) = 1.23$, $p = 0.22$ (Figure 6.2G). Furthermore, comparisons between normative connectivity and connectivity during placebo revealed no statistical difference (t-test with unequal variance assumed and degrees of freedom estimated using Satterthwaite's approximation; $t(64.6) = -1.507$, $p = 0.1370$). This further clarifies our interpretation that it is indeed the oxytocin condition that drives enhancements in connectivity between these components and that the placebo condition is a good approximation of normative functional connectivity effects within this corticostriatal circuit.

6.4 Discussion

This is the first study to investigate how oxytocin affects intrinsic functional organization of the human brain at the level of between-network interactions. We discovered a specific corticostriatal network implicated in social-communicative, motivational, and affective processes that is significantly affected by oxytocin. Under oxytocin the connectivity between these two components was substantially elevated, on-average, and an oxytocin-related boost was observed in almost all participants. The fact that these corticostriatal connections are not particularly strong under normative conditions and with the administration of placebo, but become increasingly coordinated under oxytocin may be important for understanding how oxytocin influences cognition and behaviour.

Future work is needed to examine oxytocin-related strengthening of connectivity between these circuits and its effect on specific cognitive and behavioural processes. For example, these corticostriatal connections under pain or social-communication processes may illuminate

important brain-behavior links that are affected by oxytocin. These results also illustrate how oxytocin is likely to extend beyond certain brain regions traditionally thought to be important (Meyer-Lindenberg et al., 2011). For example, previous neuroimaging studies in humans have largely focused on amygdala-related effects and to a lesser extent on striatal regions. The current study suggests oxytocin's effects may extend well beyond the amygdala and striatum, and most importantly, may incorporate interactions between subcortical striatal regions with cortical areas.

The degree to which oxytocin enhanced connectivity was also associated with continuous variation in autistic traits, such that those with the highest levels of autistic traits showed the largest oxytocin-related effect on connectivity. These results may point towards the idea that oxytocin may have varying impact on different subsets of individuals. Individuals with the highest levels of autistic traits seem to show the largest oxytocin-related connectivity boost. It will be important to extend these ideas into neuropsychiatric conditions such as autism Oxytocin is hypothesized to be of some potential value therapeutically for autism (Meyer-Lindenberg et al., 2011). However, given the large degree of heterogeneity in autism (Lai, Lombardo, Chakrabarti, et al., 2013) and the knowledge that therapies may work well for some individuals and not others, it will be of the utmost importance to examine how oxytocin may or may not work well on specific subsets of affected individuals.

Supporting the plausibility of oxytocin-related effects on connectivity between these circuits, we also showed evidence supporting the idea that many of the brain regions involved in both IC11 and IC21 maps show some degree of *OXTR* expression. For instance, it is well known from non-human animal work that the striatum and regions within the midbrain are highly

populated with oxytocin receptors (Insel & Shapiro, 1992; King, Walum, Inoue, Eyrich, & Young, 2015). We confirmed such findings with evidence from *OXTR* expression in the brain in human females and furthered a proof-of-concept evidence that oxytocin may leverage this enrichment in *OXTR* to influence neural circuits connected to the striatum. We also discovered that there are modest levels of *OXTR* expression throughout many cortical areas. Given the lack of cortical specificity for *OXTR* enrichment, it remains possible that the observed connectivity effects with rsfMRI may not necessarily be mediated by direct action of oxytocin on *OXTR* in specific cortical regions. Rather, oxytocin could exert such effects via other indirect routes, perhaps originating in striatal circuitry where there is high enrichment in *OXTR* or via other mechanisms of action (Bethlehem et al., 2013). Although expression patterns of *OXTR* were not specific to cortical regions it may be that more fine-grained spatial maps of *OXTR* might provide a clearer picture. For example, the development of a PET ligand could certainly further advance our understanding of *OXTR* distribution in-vivo in the human brain.

This study has several novel elements that need to be highlighted. Specifically, this study focusses specifically on oxytocin-related resting-state effects in women. There are notable male biases throughout neuroscience and medical research and this bias may explain why studies looking at the effects of drugs tend to miss many adverse effects or show a lack of efficacy when applied to females (Beery & Zucker, 2011; McCarthy, Arnold, Ball, Blaustein, & De Vries, 2012). This bias can be observed in much of the prior work on oxytocin in humans as well, with some neuroimaging studies indicating potential differences in the oxytocin system between sexes (Domes et al., 2010; Ebner et al., 2016; Gao et al., 2016; Riem et al., 2012; Rilling et al., 2013). Part of this bias in oxytocin research might be explained by the higher risk of side-effects (e.g. lactation in mothers, abnormal uterine contractions and elevated blood

pressure), though the intranasal administration has proven to be a safe method of administration (E. MacDonald et al., 2011). There have been a few studies that assessed the effect of gender in oxytocin administration. For example, previous studies examining functional connectivity during tasks show enhanced connectivity in women but decreased connectivity in men (Riem et al., 2012; Wittfoth-Schardt et al., 2012). Although our study was not explicitly set to examine sex differences in the effects of oxytocin, future research should focus on how oxytocin may have different effects across males and females.

Second, surpassing much of the existing neuroimaging work on oxytocin, our study is the first to take a whole-brain, unsupervised approach to examine connectivity between neural networks. The small number of studies examining in-vivo oxytocin-related changes to functional connectivity in humans utilized a seed-based connectivity approach. This approach elucidates effects of oxytocin on connectivity with the pre-selected seed region, but is limited by the a priori selection. As we have shown with the analysis of OXTR expression much of the prior work is not necessarily informed by this expression pattern. It partly lacks specificity for certain regions and the present data suggest that other brain regions, not traditionally reported in oxytocin administration literature, might also have OXTR expression that would make it a potential target for administration. Rather, prior work tends to be heavily directed to regions that are justified based on their role in psychological processes that are linked to oxytocin (e.g., amygdala). In our work, we have taken an unbiased approach to provide insight into oxytocin's effect on corticostriatal connectivity. These circuits might not have been identified with an approach constrained by task-based activation or seed-based connectivity based on this task-related activation.

The highlighted effect places emphasis on striatal interactions with cortical areas that are associated with pain processing. These results are interesting in light of work showing that oxytocin can not only act as an anxiolytic (Churchland & Winkielman, 2012; K. MacDonald & Feifel, 2014), but can also act as a painkiller (Rash, Aguirre-Camacho, & Campbell, 2013). It should be noted that the anxiolytic effect might not fully explain oxytocins effect on behaviour as benzodiazepines do not show a similar behavioural effect.

To our knowledge, there is little neuroimaging work in females focusing on oxytocin and its influence on neural systems for pain processing, as most published work is exclusively on males and/or is focused on empathy for pain (Bos, Montoya, Hermans, Keysers, & van Honk, 2015; Paloyelis et al., 2016; Singer et al., 2008; Zunhammer, Geis, Busch, Greenlee, & Eichhammer, 2015). Similar to oxytocin research, research on pain has traditionally been heavily male biased (Zagni et al., 2016), while women tend to suffer more from acute and chronic pain (Mogil, 2012). Our results suggest that future work is needed in this area, particularly on oxytocin's effect on pain and how such corticostriatal networks may be involved. In addition, areas identified by this data-driven approach show that key areas in the brains reward circuitry are modulated by oxytocin administration. It has been previously hypothesized that oxytocin exerts its effect on social salience and social cognition by modulating stress and reward processing (Bethlehem et al., 2014). The present study also highlights neural systems underlying these cognitive processes as key target for oxytocin administration. Further research into how oxytocin specifically modulates social reward processing might shed further light on its potential to more broadly modulate social cognition.

There are some caveats and limitations to keep in mind. First, the sample size is moderate and potentially provides low power to detect small effects. However, our multi-echo fMRI approach is a strength that could help counteract issues associated with statistical power. Multi-echo EPI acquisition and the ME-ICA denoising technique employed here is known to greatly enhance temporal signal-to-noise ratio (tSNR) and allow for enhanced ability to reduce false positives (Kundu et al., 2013). These enhancements tied to principled elimination of non-BOLD noise in rsfMRI could be beneficial for power because reduction in noise potentially increases observable effect sizes (Lombardo et al., 2016), and reduce effect size estimates for false positive effects.

Future work collecting larger samples to replicate and extend these findings would be facilitated by characterizing individuals in continuous variation in autistic traits. Our study indicates that oxytocin-related effects tend to be stronger in individuals with more autistic traits. As noted in the points about sex and gender, future work should also examine whether similar or different effects are present in males. It would also be important to further extend this work in clinically diagnosed individuals with autism. Our exploratory analysis revealed a potential correlation with autistic traits that may suggest that oxytocin could facilitate corticostriatal connectivity in clinically diagnosed patients. If such a relationship extends into the clinically diagnosed population of the autism spectrum, we may expect to see that oxytocin provides the largest enhancements to the most affected individuals (Auyeung et al., 2015). This should however at this point be considered exploratory.

Furthermore, there has been some debate in recent years about the extent to which oxytocin crosses the blood brain barrier (Leng & Ludwig, 2016). A recent study that assessed CSF and

plasma concentrations after intranasal administration found elevated levels in plasma after 15 minutes and a peak in CSF elevation at 75 minutes (Striepens et al., 2013). By far most studies have used the 24IU dose and timing of 40 minutes to show behavioural effects (Bethlehem et al., 2013; E. MacDonald et al., 2011; Meyer-Lindenberg et al., 2011). Yet, it is possible some behavioural effects might originate from peripheral elevation as opposed to a central effect (Leng & Ludwig, 2016). Nonetheless, a recent review on the issue suggests that the intranasal route is likely still the best candidate for administration and found no effects from intravenous administration (Quintana, Guastella, Westlye, & Andreassen, 2016). The relation between increased CSF oxytocin and timing of potential behavioural effect also remains unclear. The present study was not set out to determine the best dose or timing or to assess whether oxytocin could cross the blood-brain barrier. Unfortunately, there is currently no PET-ligand available to definitively assess the timing and central binding of intranasal oxytocin, though animal work on this is progressing (A. L. Smith, Barnhart, et al., 2013; A. L. Smith, Freeman, Voll, Young, & Goodman, 2013). Thus, in order to be able to compare the present findings to existing literature, we chose to use the same timing and dosage.

Finally, underpowered studies are common amongst oxytocin administration studies (Walum, Waldman, & Young, 2016). The observed effect here between IC11 and IC21 is large. For the current sample size, the minimum effect size achieving 80% power at an alpha of 0.05 is d = 0.6. An effect this low or lower was never observed in our bootstrapping analysis to estimate variability in the IC11-IC21 effect (see Supplemental Figure D.3). Therefore, we can reason that we had sufficient power to detect such an effect at the current sample size. As for other subtler effects, our report here is likely underpowered to detect such effects and much larger studies are likely needed to detect such smaller effects. Since this is the first work on the topic

of between-component connectivity in a female rsfMRI oxytocin administration study, we have provided effect sizes estimates for all IC comparisons to aid others in future power calculations (Supplementary Figure D.4). Each of the corresponding 22 IC maps can be viewed on and downloaded from NeuroVault (http://neurovault.org/collections/2154/).

In conclusion, we have discovered that oxytocin enhances corticostriatal connectivity in women. These corticostriatal networks play roles in social-communicative, motivational, and affective processes and the results may be particularly important for understanding how oxytocin changes neurodynamics that may be relevant for many neuropsychiatric conditions with deficits in those domains and neural circuits. Future work examining these effects in males as well as clinically diagnosed samples will be important, as will be the examination of what subsets of individuals may benefit most from oxytocin-related changes in between-network connectivity.

Chapter 7 Altered functional connectivity after testosterone administration

7.1 Introduction

The sex ratio in autism discussed earlier in this thesis has also been linked another hormone testosterone (T). Specifically prenatal testosterone has been shown to contribute to the risk of developing autism (Baron-Cohen et al., 2015;Baron-Cohen, 2002). Interestingly, early animal research showed that administration of T recovers loss of OXT receptors in areas important in social cognition (Arsenijevic & Tribollet, 1998; Bale & Dorsa, 1995). Furthermore, a previous extensive review of neuroendocrine influences on hormones behaviour has suggested that oxytocin and testosterone may have opposite effects on brain activation in the sense that they trigger a shift in cortical and sub-cortical processing in opposite directions (Bos et al., 2012). Thus, in contrast with the previous chapter we would expect T to have a potentially opposite effect in cortico-subcortical connectivity. As part of a larger study investigating the effects of T on social behaviour we also conducted a T administration and resting-state fMRI study in collaboration with the group of Professor Jack van Honk at the University of Cape Town.

Testosterone has a well-established role in the reduction of fear and the promotion of dominance motivation and aggression in many species (Mazur & Booth, 1998; Wingfield, Hegner, Dufty Jr., & Ball, 1990). In humans, the neural mechanisms underlying these effects are not yet clear, but it has been suggested that testosterone administration can decouple the orbitofrontal cortex from subcortical threat reactivity, leading to an increase in impulse-driven

goal-directed behaviour in response to threat (Terburg, Hooiveld, Aarts, Kenemans, & van Honk, 2011; Terburg & van Honk, 2013). Direct evidence for this hypothesis is however currently lacking as acute threat reactivity in the brain and associated goal-directed behaviour have not yet been studied in relation to testosterone administration.

We do know that testosterone can reduce physiological fear responses in humans (Hermans et al., 2007; Hermans, Putman, Baas, Koppeschaar, & van Honk, 2006), and testosterone has repeatedly been linked to subcortical-cortical decoupling (Schutter & van Honk, 2004) and decoupling of the OFC from the amygdala in particular (Bos et al., 2012; van Wingen et al., 2010; Volman et al., 2016, 2011). Although the specific functions ascribed to the OFC are highly diverse (Stalnaker, Cooch, & Schoenbaum, 2015), it is generally accepted that its coupling with the amygdala serves to adjust behaviour based on the integration of top-down goal-directed action tendencies and bottom-up emotional reactivity (Kringelbach & Rolls, 2004; Milad & Rauch, 2007; Murray & Izquierdo, 2007; Zald et al., 2014).

We aimed to tap into this function by means of a functional magnetic resonance imaging (fMRI) experiment with dynamically changing situations of acute threat with goal-directed escape possibilities (Montoya, van Honk, Bos, & Terburg, 2015). We applied this experiment in a double-blind placebo-controlled testosterone administration design along with a measurement of baseline resting-state fMRI (RS-fMRI) connectivity. Using this design, we could investigate the hypothesis that testosterone's decoupling of the OFC from the amygdala is directly involved in threat and escape anticipation.

7.2 Methods

7.2.1 Participants

Thirty healthy young women were recruited to participate in the experiment. Ethical approval was granted by the Human Research Ethics Committee of the University of Cape Town (UCT). Before being invited to participate, all women were screened with self-report questionnaires for present or previous psychiatric conditions. Additional exclusion criteria, also assessed by self-report questionnaire, were: Current or recent use of psychotropic medications, use of hormonal contraceptives, pregnancy, abnormal menstrual cycle, any endocrine disorders, any other serious medical condition, left-handedness, habitual smoking, hearing problems, and colour blindness. Upon their arrival at the laboratory, all participants provided written informed consent before testing began. After recruitment, four participants were unable to complete their scans: One did not fit in the head coil, and three could not complete scans due to electricity failure at the scan facility. This left 26 participants who were included in the resting state analyses. A further four were excluded from the task-based statistical analyses: One due to excessive head movement in the scanner (40mm) during the task, one due to coil signal failure, and two due to headphone failure, meaning they did not hear the aversive noise. After these 8 exclusions, the total sample consisted of 22 participants (age range 18-37, mean age 21.3, *SD*=4.4), with 11 in each administration order (placebo in first session, or testosterone in first session). Only women were considered as participants because the parameters (quantity and time course) for inducing neurophysiological effects after a single sublingual administration of 0.5 mg of testosterone are known in women, whereas these parameters are not known in men (Tuiten et al., 2000). Each participant was paid ZAR250 for their participation.

7.2.2 Drug administration

We followed the procedure first reported by Tuiten *et al* (2000), which involves the sublingual administration of 0.5 mg of testosterone with a hydroxypropyl-β-cyclodextrin carrier (manufactured by Laboswiss AG, Davos, Switzerland) to healthy young women. Placebo samples were similar except for the omission of testosterone. This is a well-established single dose testosterone administration procedure that has been widely used for nearly two decades and has many times shown to generate behavioural effects in young women (Bos et al., 2012; van Honk et al., 2014). For the dosage chosen, no side effects have been reported in this or other studies to date.

7.2.3 Procedure/experimental design

Participants were tested on two separate days. The first and second session were separated by at least 48 hours to ensure full wash-out. Both testing days fell within the follicular phase of the participants' menstrual cycles to ensure low and stable basal levels of sex hormones (e.g. progesterone, luteinizing hormone, and follicle stimulating hormone). On both occasions, they arrived at the lab to receive the drug or placebo administration in the morning. Participants were instructed not to participate in any activity that could cause excessive fluctuations in hormone production, such as sports games, exams, or sexual activity. Four hours after administration they returned to the lab to undergo magnetic resonance imaging (MRI). This experiment was part of a larger study and all participants participated in two other fMRI tasks, not reported in this paper.

7.2.4 Threat escape task (TET)

We used an active escape paradigm that has been validated in previous pharmaco-fMRI research (Montoya et al., 2015). The task invokes different stages of threat imminence using visual images that approached (increase in size) the participant, culminating in a highly aversive noise (AN; a 1-second ~110 dB female scream), see Figure 7.1. The proximity of the threat, from furthest to nearest, can be distant (easily escapable), imminent (with effort escapable at chance level), or inescapable.

Each condition has a matched safe condition without AN presentation, which is distinguishable by a different visual stimulus. In all conditions, except for the inescapable condition, the participant can avoid AN presentation by pressing a button in time to prevent the image from reaching full-size. The speed of the approaching threat is controlled based on each participant's baseline reaction times as assessed in a practice session, and is updated based on performance during the experiment (see below). This allows for all participants, regardless of general reaction time speed, to escape from the imminent threat at the same probability, i.e. chance-level performance, resulting in a reliable 50% of these trials with actual AN presentation and thus a uniform level of threat across participants. Furthermore, this design allows for comparison of not only safe and threatening conditions, but also between proximity and escapability of threat. Finally, after the participant's scan session they indicated their consciously experienced level of fear in each of the six task conditions on a Likert scale from 1 ("not afraid at all") to 7 ("very afraid").

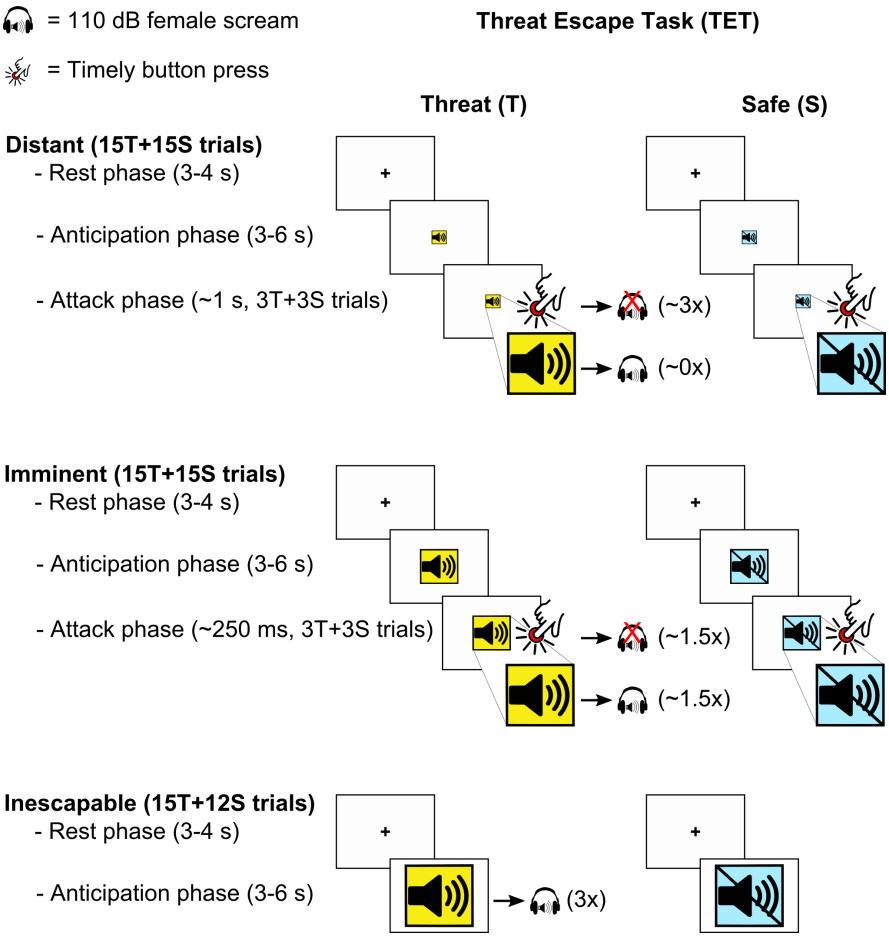

Figure 7.1: Outline of the threat escape task.

Participants are repeatedly attacked by rapidly approaching pictures. Participants can escape by pressing a button, but when they fail to do so they will be presented with a highly aversive noise (AN). The pictures are manipulated to be distant-escapable, imminent (escapable at chance-level) or inescapable, and all conditions are compared with an equivalent safe-context control condition involving the same procedure but without the threat of AN exposure.

7.2.5 Assessment of mood

In both sessions, before scanning, the participants completed the profile of mood states 2nd edition (POMS-II) to assess baseline mood differences due to drug administration. The POMS-II is a 65-item questionnaire that indexes consciously experienced anger, tension/anxiety, depression, vigour, confusion and friendliness, as well as a combined total mood score, using a 5-point Likert scale (Heuchert & McNair, 2012).

7.2.6 2D:4D measurement

Following evidence that prenatal testosterone exposure, as indexed by second-to-fourth digit ratio (2D:4D), drives the effect of testosterone on conscious but not reactive behaviour later in life (Terburg *et al*, 2013b), we also included this metric to our administration study. On one of their testing days, each participant's right hand was scanned on a flatbed scanner, which images allow for accurate measurement of the 2D:4D ratio. Digit lengths were measured in Adobe Photoshop CS5 with the ruler tool from medial finger crease to middle of fingertip (Breedlove, 2010).

7.2.7 fMRI acquisition

All scans were obtained using a 3 Tesla Magnetom Allegra Siemens dedicated head MRI scanner (Siemens Medical Systems GmBH, Erlangen, Germany) with a four-channel phased array head coil, at the Cape Universities Brain Imaging Centre. Whole brain T2* weighted 2D-Echo Planar Imaging (EPI) functional volumes were acquired with 36 ascending axial slices. The following parameters were used: EPI factor=64, TR/TE: 2s/27 ms, FA=70°, FOV (anterior-posterior, inferior-superior, left-right): 64*64*36 slices, voxel size: 3.5 x 3.5 x 4mm. Five volumes from start of the task were discarded to allow MR signal to stabilize, and 438 usable functional volumes were acquired. A T1-weighted high resolution structural scan (magnetization-prepared rapid gradient echo; MPRAGE) was obtained once for each participant using the following parameters: TR/TE: 2.53s/6.6ms, flip angle 7°, FOV 256*256*128mm, voxel size: 1 x 1 x 1.33mm, volume acquisition time: 8 min 33s.

To investigate whether the effect of testosterone on OFC coupling is specific to threat processing or context independent, this study also included a resting-state fMRI session. On the same scanner and during the same session a total of 298 functional volumes were obtained

using a standard interleaved EPI sequence using a 64*64*29 FOV, a flip angle of 70°, a TR of 1.6s, a TE of 27ms, and a voxel size of 3.75 x 3.75 x 5mm. During this 10-minute scan participants were instructed to remain awake and to try and clear their minds while looking at a fixation cross.

7.2.8 TET analysis

7.2.8.1 Preprocessing

MR scans were analysed using SPM8 (Wellcome Department of Imaging Neuroscience, London, UK). Pre-processing included; slice-time correction, motion correction of the 6 motion parameters and the sum of squared difference minimization, volume realignment to the middle volume and AC-PC realignment to improve co-registration. Functional and structural volumes were co-registered and subsequently normalized to Montreal Neurological Institute (MNI) space using unified segmentation procedure (Ashburner and Friston, 2005) and resampled into 2mm isotropic voxels using 4th degree B-spline interpolation. Finally, all images were smoothed using an 8mm FWHM Gaussian kernel.

7.2.8.2 Functional activation analysis

The effects of testosterone on brain activity related to threat anticipation were investigated within general linear models (GLM). The task was designed to measure anticipatory BOLD responses to passively undergo, or actively escape from, AN exposure. Therefore, trials without actual attacks (12 trials for each condition) were of main interest, whereas trials with attacks (3 trials for each condition excluding safe/inescapable) were treated as separate variables in the model, which ensures that the effects of motion related artefacts due to button-presses and AN

presentation do not affect our measure of interest. Thereto, in the first-level GLM for each test-session, we used twelve regressors for our trials of interest: Six for the trial-onsets (box-car function for stimulus-duration, 3-6s), and six for the trial-offsets (delta function). Trial-offset regressors were included based on a previous study into threat-offset effects (Klumpers et al., 2010) but considered of no-interest for the current study. Furthermore, ten other nuisance regressors were defined: Five for the trial-onsets for stimuli that would attack, four for the attack-onset (box-car function for attack-duration), and one for the AN-onset (box-car function for AN-duration, 1s).

These regressors were all convolved with the hemodynamic response function as implemented in the SPM8 software. In addition, realignment parameters and a discrete cosine transform high-pass filter with a 1/128Hz cut-off frequency were added to the model to reduce variance due to nuisance factors such as movement and drifts in the signal. Thus, in total twenty-nine regressors were entered in the first level statistical analysis. For each subject, and session, we computed contrast maps for onset of distant-escapable, imminent-escapable and inescapable threat and safe cues versus baseline.

For the second level analysis, these contrast maps were entered in a full-factorial 2 x 2 x 3 ANOVA design with drug (testosterone and placebo), condition (threat and safe) and distance (distant-escapable, imminent-escapable, inescapable) as within-subject factors. To evaluate our hypotheses within this GLM we first tested for threat related (de)activations in each distance condition (e.g. Inescapable[Threat < > Safe], etc.). We next tested the two crucial comparisons, which are (de)activations in anticipation of escapable versus inescapable threat (i.e. (Distant[Threat > Safe] + Imminent[Threat > Safe]) / 2 < > Inescapable[Threat > Safe]), and

(de)activations in anticipation of high versus low threat (i.e. (Imminent[Threat > Safe] + Inescapable[Threat > Safe]) / 2 < > Distant[Threat > Safe]). Finally, we compared (de)activations between all combinations of distances (e.g. Distant[Threat > Safe] < > Inescapable[Threat > Safe], etc.). This three-step approach was used for general task effects as well as for testosterone administration effects.

To identify brain (de)activation patterns we first applied whole-brain FWE-correction with a cluster-wise threshold of $p<.05$ and cluster-defining threshold $p<.001$. Next we aimed to identify anatomically specific effects in the OFC and subcortical threat network by applying FWE-correction for the region of interest (ROI) volume with a voxel-wise threshold of $p<.05$. The ROIs consisted of a bilateral midbrain mask based on the TD Lobes atlas from the WFU Pickatlas Toolbox implemented in SPM (Maldjian *et al*, 2003), a bilateral amygdala mask (Amunts et al., 2005) taken from the anatomy toolbox as implemented in SPM8 (Eickhoff et al., 2005), a bilateral hypothalamus mask created by defining an 8mm sphere around the central coordinate (MNI coordinate: x=0, y=2, z=13) of hypothalamus subregions as described by Baroncini and colleagues and Terburg et al. (Baroncini et al., 2012; Terburg & van Honk, 2013), and a bilateral OFC mask including the rectus and orbital parts of the superior, medial and middle frontal gyri as defined in the AAL template (Tzourio-Mazoyer et al., 2002). See Fig. 2 for a visualisation of these ROIs.

7.2.8.3 Functional connectivity analysis

Psycho-Physiological Interaction (PPI) analysis was performed to determine the functional connectivity of the OFC with other brain regions using the PPI module implemented in SPM8. In short, a volume of interest (VOI) was created using a 6mm sphere around the peak-voxel

coordinate of OFC activation identified in the functional activation analysis. For each participant time-course (first-eigenvariate) was extracted, and mean-corrected for general task effects. A new GLM was obtained using this time-course as regressor together with a regressor for the task-contrast of interest, and their interaction (i.e. PPI). To maintain power, we limited this analysis to the identification of connectivity differences in the overall condition contrast (threat versus safe). Finally, contrast-maps of the PPI were entered in separate full-factorial models to test for testosterone administration effects on threat-related OFC connectivity. Although this approach does not allow to test for connectivity modulations based on specific threat distances, it does provide insight into connectivity pattern modulations across dynamically changing threatening compared to safe conditions in general.

7.2.9 RS-fMRI analysis

7.2.9.1 Preprocessing

Functional and anatomical images were processed using the fMRI Signal Processing Toolbox for MATLAB (Patel et al., 2014). Anatomical images were skull-stripped. Functional image pre-processing consisted of core image processing and denoising. Core image processing started with slice timing correction with the middle slide as the reference. All frequencies except Nyquist and zero frequencies were kept. Rigid-body parameters (3 rotations and 3 translations) and their first derivatives necessary for head movement correction were calculated and all functional images were aligned to the first frame. Next, affine transformations were calculated and used to co-register the functional data to the skull-stripped anatomical image using a grey matter mask. Zeropadding temporarily added 100 zeros to the end of the time series to prevent errors in denoising the data at a later stage. The data were then transformed to the Montreal

Neurological Institute template (average of 152 brains; MNI152), T1 weighted, in standard space by non-linear warping.

Head movement during fMRI scans have been shown to affect functional connectivity measures such as decreased long-distance correlations and increased short-distance correlations (Van Dijk et al., 2012). Traditional methods can remove some artefacts, but are not able to correct for subtler artefacts, such as spike-like movements that lead to spin-history effects. We used a data-driven method that identifies, models, and removes motion artefacts by wavelet despiking (Patel et al., 2014), without the need for data scrubbing. This method first decomposes the time series into a set of scales using the Maximal Overlap Discrete Wavelet Transform (MODWT). It then identifies maximal and minimal wavelet coefficients and detects and removes chains of these coefficients. Such chains are present across multiple scales at the same point in time and represent transients of all sizes. Lastly, the time series are recomposed from the remaining coefficients using inverse MODWT (iMODWT). After wavelet despiking, motion, motion derivatives, CSF and white matter were regressed out.

7.2.9.2 Seed-based connectivity analysis

To assess OFC connectivity modulations by testosterone, the pre-processed wavelet despiked images were band-pass filtered (0.1 - 0.01Hz) and average time-series were extracted for the same OFC sphere used in the PPI analyses of the TET. Whole-brain connectivity maps were calculated based on Pearson correlations between the seed time series and the rest of the brain. The resulting connectivity maps were *z*-transformed, and these were analysed in SPM8 using a pairwise comparison and the same statistical thresholds as used in the TET analyses. To further explore connectivity modulations by testosterone, we also performed this analysis using the

three bilateral amygdala sub-nuclei seeds obtained from an anatomical connectivity derived amygdala sub parcellation (Bzdok, Laird, Zilles, Fox, & Eickhoff, 2013).

7.2.9.3 Whole-brain connectivity analysis

In addition to the hypothesis driven seed-based resting-state connectivity analysis, we also employed a data-driven independent component analysis (ICA) to explore potential whole brain effects of testosterone on functional connectivity. Seed-based analyses only focus on very specific networks and connections. In contrast, independent component analysis makes no assumptions about the underlying networks and thus allows a model-free analysis of any potential differences. Analyses were carried out using Probabilistic Independent Component Analysis (Beckmann & Smith, 2004) as implemented in MELODIC (Multivariate Exploratory Linear Decomposition into Independent Components) Version 3.14, part of FSL (FMRIB's Software Library, www.fmrib.ox.ac.uk/fsl). The following steps were applied to the pre-processed wavelet despiked data: masking of non-brain voxels; voxel-wise de-meaning of the data; normalisation of the voxel-wise variance. Pre-processed data were whitened and projected into a 35-dimensional subspace using probabilistic Principal Component Analysis where the number of dimensions was estimated using the Laplace approximation to the Bayesian evidence of the model order (Beckmann & Smith, 2004), thus resulting in 35 independent components. The whitened observations were decomposed into sets of vectors which describe signal variation across the temporal domain (time-courses), the session/subject domain and across the spatial domain (maps) by optimising for non-Gaussian spatial source distributions using a fixed-point iteration technique (Hyvärinen, 1999b). Estimated Component maps were divided by the standard deviation of the residual noise and thresholded by fitting a mixture model to the histogram of intensity values (Beckmann & Smith, 2004). Permutation testing was used to

assess potential effects of testosterone across all 35 components, using 5000 permutations and a threshold free cluster enhancement (TFCE) to control for multiple comparison as implemented in FSL's randomise tool (Winkler, Ridgway, Webster, Smith, & Nichols, 2014).

7.2.9.4 Data availability

Non-thresholded statistical maps of the main fMRI analyses can be found at the NeuroVault data repository (Gorgolewski et al., 2015): http://neurovault.org/collections/AUIXVATH/ and http://neurovault.org/collections/ISHJRKRU/. All other data are available on request from the authors.

7.3 Results

7.3.1 Subjective experience data

Participants were asked to guess which session had included the testosterone dose and they were unable to correctly guess above chance ($\chi 2$=0.2338, p=0.63). Additionally, POMS-II mood scales showed no difference on the total mood scale (Heuchert *et al*, 2012) between drug conditions ($t(22)$=0.928, p=0.364), and when looking at the separate moods this was also the case for anger, vigour, confusion, tension, and fatigue (all ps > 0.38). Depression was significantly lower in the testosterone (1.07, SD=0.12) compared to placebo (1.15, SD=0.20) condition ($t(21)$=2.791, p=0.011), but this small difference could be considered negligible as in both conditions these scores are near the absolute minimum of score '1' which in the 5-point Likert scale represents 'no depression at all'.

The fear ratings regarding the AN, rated on a 7-point Likert scale, were generally high in both drug conditions (testosterone: M=5.71, SD=1.34; placebo: M=6.12, SD=1.01) and over both

sessions (session 1: *M*=6.02, *SD*=1.02; session 2: *M*=5.82 *SD*=1.36). Paired sample *T*-tests confirmed no significant difference between the two drug conditions ($t(21)=-1.7$, $p=0.103$) or between the two sessions ($t(21)=-0.78$, $p=0.444$).

7.3.2 Threat escape task

7.3.2.1 General task effects

Statistics and results for the TET are summarized in Table 7.1, Figure 7.2, and see http://neurovault.org/collections/AUIXVATH/ for non-thresholded statistical maps. In line with previous work on acute and escapable threat (Klumpers et al., 2010; Mobbs et al., 2007; Montoya et al., 2015), we observed reliable threat-potentiated activity in the salience network of the brain (anterior insula, dorsal anterior cingulate cortex, thalamus and striatum) in all three distance conditions. Furthermore, both high threat conditions (imminent and inescapable) evoked midbrain activity, and both escapable threat conditions (distant and imminent) evoked hypothalamic reactions. Threat-related deactivations were observed in the medial prefrontal cortex, including the medial OFC (MOFC), particularly in the high threat conditions, and inescapable threat also deactivated areas in the medial temporal cortex and the angular gyrus.

As can be seen in Table 7.1 and Figure 7.2, analysis of threat level and escapability revealed that high threat evoked midbrain reactivity and deactivations in medial prefrontal. Striatal reactivity to threat was strongest when the threat was escapable. Thus, in line with previous studies (Klumpers et al., 2010; Mobbs et al., 2007; Montoya et al., 2015) an approaching threat shifts brain activity away from cortical towards subcortical processing, whereby the anticipation for an active escape response evokes striatal threat reactivity.

7.3.2.2 Testosterone administration effects

Testosterone had no direct effect on threat reactivity in the three distance conditions separately[2], but did increase activity in the left lateral OFC (LOFC) in escapable compared to inescapable threatening conditions (see Figure 7.2). Post-hoc *T*-tests showed this was due to an increase to escapable rather than a decrease to inescapable threat (see Table 7.1).

PPI-analysis (see methods) using the location of this LOFC cluster revealed that testosterone administration reduced threat-related connectivity with the midbrain, hypothalamus, left amygdala and MOFC (see Figure 7.2). More specific allocation of the midbrain cluster indicated that it corresponds to the location of the periaqueductal gray (see (Hermans, Henckens, Roelofs, & Fernández, 2013)) and the amygdala cluster corresponds to the left central-medial amygdala (CMA; see (Amunts et al., 2005)) Finally, post-hoc *T*-tests revealed that specifically in the testosterone condition left-sided LOFC-CMA coupling was reduced in threat compared to safe conditions.

7.3.2.3 2D:4D analysis

To investigate the relation between testosterone administration effects and 2D:4D, beta weights were extracted from a 6mm sphere around the LOFC peak activation identified in the

[2] This was also the case when applying a more liberal threshold; $p<.01$ as cluster-defining threshold

testosterone/TET analysis. These beta-weights were entered in a 2 (testosterone and placebo) x 2 (threat and safe) x 3 (distant, imminent and inescapable) repeated measures ANOVA with 2D:4D as covariate. The 2D:4D covariate was non-significant ($F(1,20)=0.443$, $p=.513$), which was also the case for its interactions with the within-subjects variables (all p's > .16).

Table 7.1: Functional MRI findings.

All reported clusters are activations (or deactivations, indicated with a negative *T*-value) to threat>safe contrasts. Clusters are whole-brain statistics FWE cluster-wise corrected ($p<.05$) with cluster defining threshold $p<.001$, or in case of region of interest analysis (indicated with *, and see Fig. 7.2 for a visualisation) FWE voxel-wise corrected ($p<.05$). PFC = Prefrontal Cortex, OFC = Orbitofrontal Cortex, s.c. = same cluster.

Structure	Hemisphere	Cluster size	*p*-value	Peak *T*-value	MNI-coordinate		
					X	**Y**	**Z**
Threat effects							
Inescapable							
Anterior Insula	Left	571	0.006	5.43	-32	20	4
	Right	793	0.001	5.67	34	24	-6
Anterior Cingulate Cortex	Both	1986	<.001	4.8	-6	10	38
Supplemental Motor Area	Both	s.c.					
Striatum	Both	872	0.001	4.45	-10	4	0
Thalamus	Both	s.c.					
Midbrain	Both	s.c.					
Midbrain*	Both	321	0.002	4.39	8	-14	-10
Angular Gyrus	Left	480	0.012	-4.65	-48	-60	28
	Right	508	0.01	-4.61	50	-66	32
Medial OFC	Both	3049	<.001	-4.89	-8	40	-8
Medial Temporal Cortex	Left	617	0.004	-4.69	-48	-38	0
Medial OFC*	Both	551	<.001	-4.89	-8	40	-8
Imminent							
Anterior Insula	Both	6554	<.001	7.23	32	26	-4
Striatum	Both	s.c.					
Thalamus	Both	s.c.					
Midbrain	Both	s.c.					

Anterior Cingulate Cortex	Both	2245	<.001	6.03	2	10	48
Supplemental Motor Area	Both	s.c.					
Hypothalamus*	Both	5	0.041	2.91	-2	-2	-6
Midbrain*	Both	372	<.001	4.44	6	-26	-10
Medial OFC	Both	682	0.002	-4.99	4	30	-14
Dorsomedial PFC	Left	441	0.017	-4.87	-20	32	44
Medial OFC*	Both	227	<.001	-4.99	4	30	-14
Distant							
Anterior Insula	Left	897	<.001	5.55	-36	20	4
	Right	706	0.002	5.97	36	24	4
Anterior Cingulate Cortex	Both	1612	<.001	6.53	-6	4	48
Supplemental Motor Area	Both	s.c.					
Striatum	Both	879	0.001	5.07	8	-12	4
Thalamus	Both	s.c.					
Hypothalamus*	Left	31	0.013	3.28	-6	-4	-12
Threat escapability effects							
Escapable>Inescapable							
Medial PFC	Both	1831	<.001	4.65	18	30	-4
Striatum	Both	s.c.					
Medial Temporal Cortex	Left	763	0.001	4.18	-42	-40	0
Medial OFC*	Left	11	0.017	4.1	-6	56	-18
High>Low							
Midbrain*	Left	10	0.02	3.75	-6	-26	-10
Medial OFC	Both	1607	<.001	-5.11	2	34	-16
Dorsomedial PFC	Left	367	0.033	-4.39	-14	60	18
Medial Temporal Cortex	Left	465	0.014	-4.01	-52	-56	-8
Medial OFC*	Both	373	<.001	-5.11	2	34	-16
	Left	40	0.007	-4.35	-10	52	-16
Distant>Imminent							
Medial OFC*	Both	90	0.003	4.56	4	30	-14
Imminent>Inescapable							
Striatum	Both	635	0.003	4.24	18	28	-4
Distant>Inescapable							
Medial PFC	Both	2260	<.001	4.75	10	24	-4
Striatum	Both	s.c.					
Medial Temporal Cortex	Left	1062	<.001	4.25	-40	-32	-6

Medial OFC*	Both	367	0.004	4.48	-6	56	-18
Drug, threat escapability interactions							
Testosterone>Placebo: Escapable>Inescapable							
Lateral OFC	Left	347	0.04	4.39	-28	48	-6
Lateral OFC*	Left	27	0.006	4.39	-28	48	-6
Testosterone>Placebo: Escapable							
Lateral OFC*	Left	2	0.044	3.82	-28	50	-4
Testosterone>Placebo: Distant>Inescapable)							
Lateral OFC*	Left	19	0.006	4.39	-28	48	-6
Drug, psycho-physiological interactions							
PPI of Threat>Safe with lOFC signal: Placebo>Testosterone							
Medial Temporal Cortex	Right	1539	<.001	5.44	60	-44	14
Superior Temporal Cortex	Right	785	<.001	5.33	54	-22	2
Anterior Insula	s.c.	s.c.					
Striatum	s.c.	s.c.					
Hypothalamus*	Both	67	0.012	3.58	0	-4	-18
Midbrain*	Right	13	0.018	4.14	10	-32	-12
Medial OFC*	Both	12	0.024	4.44	2	56	-10
Amygdala*	Left	45	<.001	5.33	-22	-8	-8
PPI of Threat>Safe with lOFC signal: Testosterone							
Amygdala*	Left	26	0.003	-4.64	-26	-8	-8

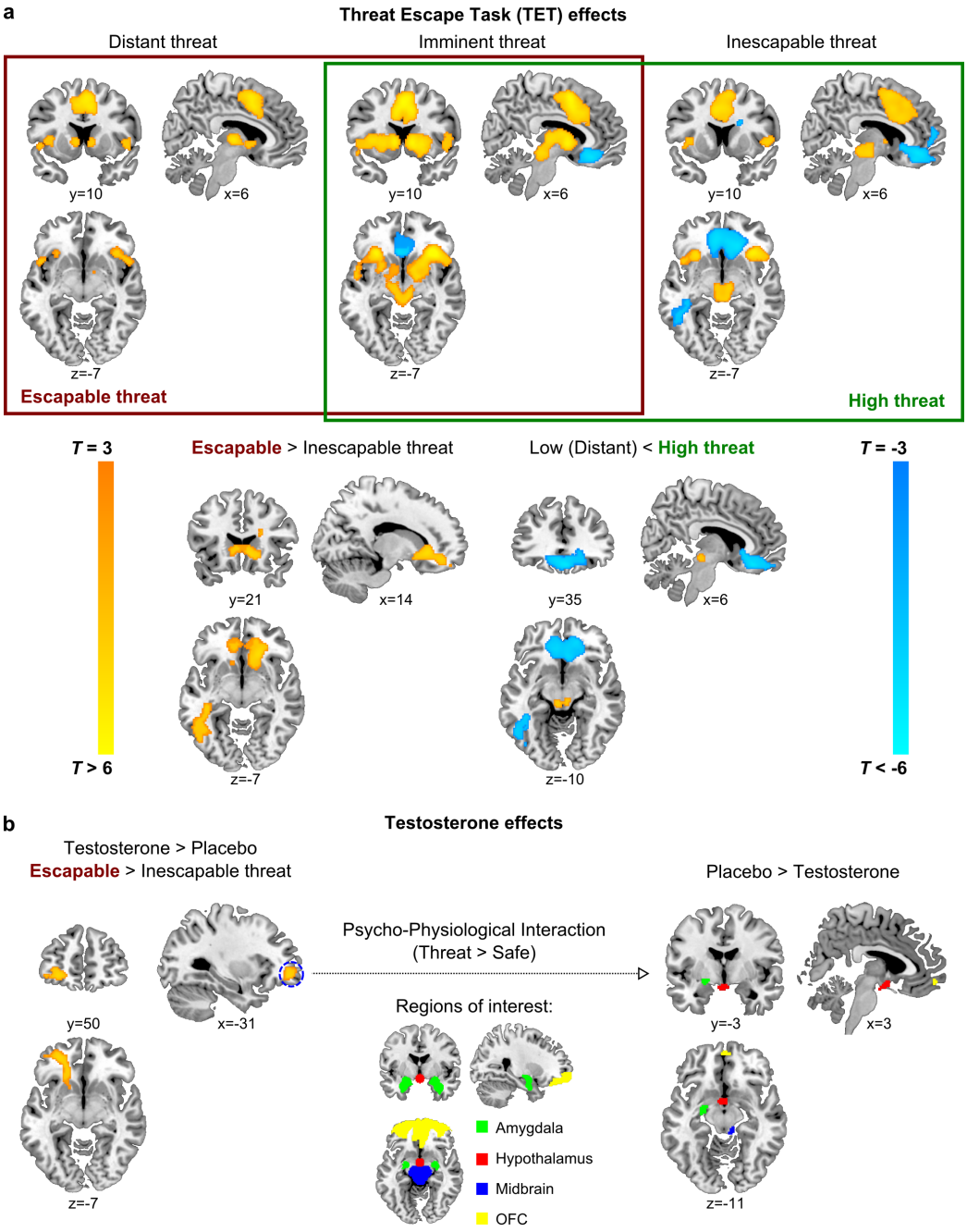

Figure 7.2: Functional MRI findings.

Only significant clusters are shown. **a**, TET effects: All three threat conditions reliably activated the brain's salience network consisting of the anterior insula, dorsal ACC, thalamus and striatum. The medial prefrontal cortex deactivated particularly when under high threat conditions, the midbrain particularly reacted to high threat, and threat evoked increased striatal activity particularly when it was escapable. **b**, Testosterone effects: Testosterone activated the left lateral OFC in response to escapable threat, and decoupled this OFC cluster from the midbrain (PAG), left amygdala (CMA), hypothalamus and medial OFC in threat compared to safe conditions.

7.3.3 RS-fMRI Results

To specifically investigate testosterone's effect during resting state, whole-brain correlation maps (based on Fischer *z*-transformed Pearson correlation maps) were computed for the LOFC seed. In both drug conditions left LOFC connectivity was particularly strong with the right OFC, bilateral striatum and anterior cingulate cortex (see Figure 7.3). Pairwise comparisons indicated no significant differences between placebo and testosterone, also when applying a more liberal threshold ($p<.01$ as cluster-defining threshold). Similarly, pairwise comparisons of the *z*-maps also indicated no significant differences between placebo and testosterone for any of the amygdala seeds (Bzdok et al., 2013) using the same liberal thresholds, and exploratory ICA analysis did not reveal any differences between drug conditions (see http://neurovault.org/collections/AUIXVATH/ for seed-based non-thresholded statistical maps and http://neurovault.org/collections/ISHJRKRU/ for the 35 identified ICA components). Details of the amygdala and whole-brain analysis are provided in the supplementary materials.

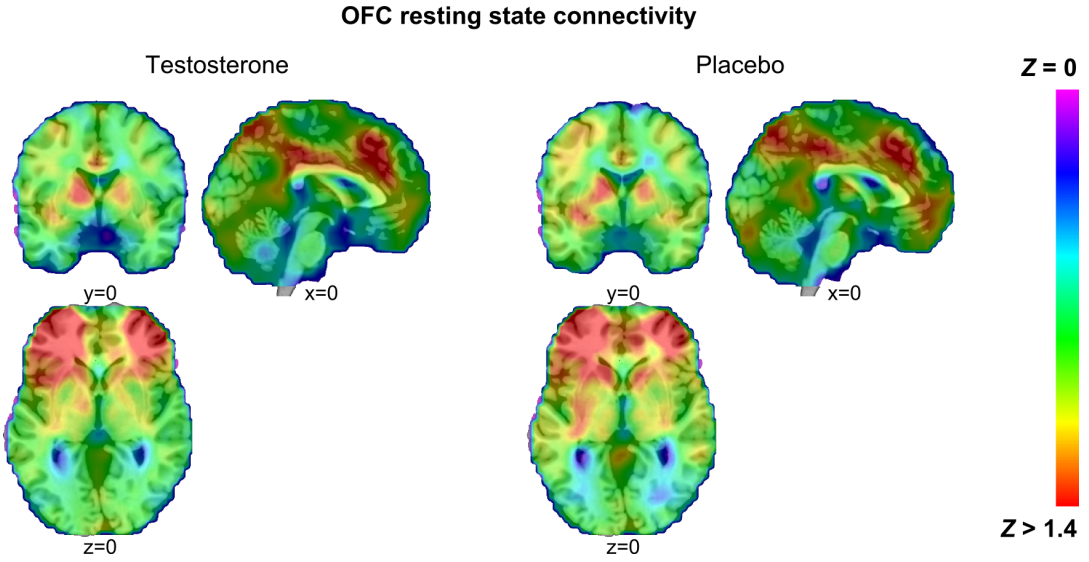

Figure 7.3: Resting state connectivity of the left lateral OFC.
Connectivity was particularly strong with the right OFC, bilateral striatum and anterior cingulate cortex. This pattern was similar after testosterone and placebo administration.

7.4 Discussion

This study provides evidence that a single administration of testosterone changes the activation and connectivity pattern of the left LOFC particularly when under acute threat. Testosterone activates the left LOFC in situations of goal-directed escape anticipation, and decouples the left LOFC from a subcortical threat network (i.e. CMA, hypothalamus and PAG) when under threat.

To start with the latter, this testosterone induced LOFC-subcortex decoupling can theoretically either constitute a loss of top-down control over the subcortical threat system, or a decrease of bottom-up input to the LOFC. We cannot assess the direction of this effect directly in the present data, but given that we find reliable threat-reactivity in this subcortical threat system, which does not change after testosterone administration, a loss of top-down control seems unlikely. Alternatively, testosterone might thus prevent subcortically generated threat reactivity to influence the OFC. Following the view that OFC-amygdala connectivity serves to adjust behaviour based on the integration of top-down goal-directed action tendencies and bottom-up affective reactivity (Kringelbach & Rolls, 2004; Milad & Rauch, 2007; Murray & Izquierdo, 2007; Zald et al., 2014), testosterone might thus push OFC processing towards goal-directed action. Further support for this view can be found in our observation that testosterone specifically boosts LOFC activity in situations that require such a goal-directed action, i.e. active escape from a threat. Although we cannot assess any behavioural benefit from this testosterone-driven LOFC activity with the present design –given that it adjusts to the behaviour of the participant to keep threat levels stable across participants–, these results do follow the hypothesis that testosterone can promote goal-directed action in case of threat (Terburg & van Honk, 2013; van Honk, Terburg, et al., 2011).

An interesting aspect of the present findings is the functional distinction between LOFC and MOFC. Both areas are structurally (Murray & Izquierdo, 2007) and functionally (Zald et al., 2014) connected to the amygdala, but in the MOFC this connection has been linked to impulse control and reward drive, whereas in the LOFC to adjustment of behaviour in case of potential punishment (Kringelbach & Rolls, 2004; Milad & Rauch, 2007). This seems to be in line with the MOFC deactivation in response to high threat observed here and in previous studies (Mobbs et al., 2007; Montoya et al., 2015). Moreover, the fact that testosterone boosts the LOFC particularly in situations of goal-directed escape anticipation seamlessly links to the LOFC's sensitivity for potentially punishing or dangerous situations.

Interestingly, testosterone has also been linked to a downregulation of MOFC activity in relation to social aggression (Mehta & Beer, 2010). The authors interpreted this effect as a reduction of impulse control from the MOFC due to testosterone, which is further emphasized by evidence that testosterone levels in adolescent boys predict reduced MOFC-amygdala connectivity, which in turn is associated with increased alcohol use (Peters, Jolles, Duijvenvoorde, Crone, & Peper, 2015). Moreover, in many other testosterone administration studies increased socially aggressive impulses have been observed (e.g. (Terburg et al., 2016; Terburg, Aarts, & van Honk, 2012; van Honk et al., 2001)), which has also been associated with an upregulation of activation in the same subcortical threat system as reported here (Goetz et al., 2014; Hermans, Ramsey, & van Honk, 2008). Together, a framework emerges wherein testosterone decouples the OFC from the amygdala resulting in reduced impulse control from the MOFC, underlying tendencies of risk taking and social aggression, and reduced input into the LOFC, underlying goal-directed behaviour in case of threat. By decoupling the OFC from

the subcortical threat system testosterone thus prepares the human brain for aggressive as well as evasive action in case of threat.

Chapter 8 Discussion

Throughout this thesis we have attempted to answer the broad question of what influences brain morphology. Specifically, we focused our attention on potential differences between typical and atypical development such as seen in autism and ADHD by taking a micro- to macro-scale approach. At the micro level we sought to disentangle how genetic influences might contribute to morphological brain differences. Then we attempted to explore differences in brain function that might arise from such altered structural developmental patterns. Subsequently, we attempted to gain a better understanding of how hormones and gender influence these processes in terms of brain function and behaviour at the macro level. Although it should be noted that the present work largely does not include direct comparisons between male and female groups (with the exception of chapter 4). The effect of gender has mainly been investigated in the context of the interaction between brain function and sex hormones and inferences about gender differences are thus more speculative than experimental at this point. Future work will look more directly at gender differences in brain morphology. There are a number of points to be taken away from this as outlined in Figure 8.1 and subsequent sections of this concluding chapter.

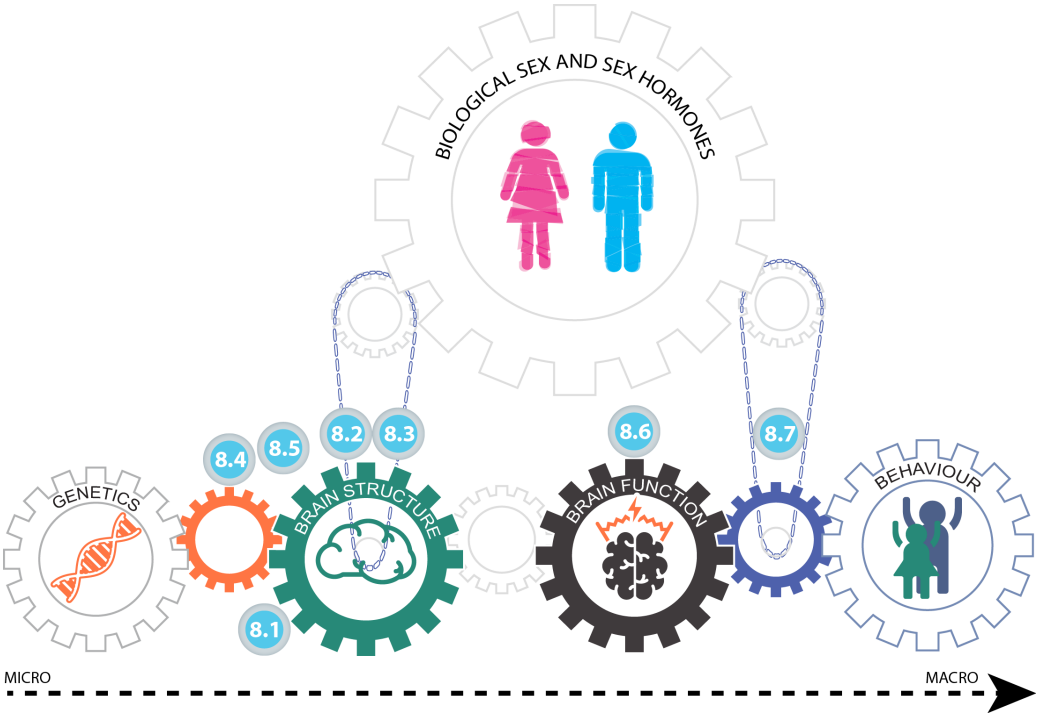

Figure 8.1: Framework

Each number refers to sections in this chapter.

8.1 Brain morphology is different in autism

First, atypical development (such as is the case in autism or ADHD) is associated with altered brain morphology (Figure 8.1 - label 8.1). Most prominently perhaps are early findings of altered developmental trajectories (Courchesne, 2002; Courchesne et al., 2001, 2011). Possibly as a result of these early broad perturbations, neuroanatomical differences later in life do not appear to be restricted to isolated brain regions. A review by Amaral and colleagues provide an overview of the wide range of brain regions that might be affected in autism and could underlie the triad of autism symptoms (Amaral, Schumann, & Nordahl, 2008). The pattern that emerges from this and other reviews (Ecker, 2016; Toal, Murphy, & Murphy, 2005) is one of heterogeneity and broad whole-brain effects. We started our analysis by quantifying these potential differences for ourselves in our own (MRC-AIMS) and publically available (ABIDE) data. Both Chapters 2

and 4 affirm the notion of altered brain morphology in autism both in children (Chapter 2) as well as later in life (Chapter 4). However, this work also emphasizes the notion that differences are extremely heterogeneous and are perhaps not truly captured by one-size-fits-all theories.

The present data only provides snapshots of brain morphology at a very specific time-point. Structural covariance is assumed to capture differences in developmental trajectories but it does not provide detailed information as to when and precisely how those trajectories change over time. Some of the differences observed in children with autism (Chapter 2) were not observed in adults with autism (Chapter 4). It is difficult to directly compare between these two datasets however. In the ABIDE data used for Chapter 2 we explicitly restricted our analyses to a very narrow age range to avoid having to regress out age as a moderating factor. It is well known that age and CT have a strong significant correlation, but we also know that developmental trajectories in autism might differ. Thus, regressing out age in the child dataset would also effectively potentially remove variance caused by these differing developmental trajectories that might be associated with the condition itself.

In the adult MRC-AIMS dataset (Chapter 4) however, age had to be regressed out because we were dealing with a large age range and thus the correlation between age and CT would have a much larger effect on the overall variability in cortical thickness. Regressing out age in this would have also likely removed some variance explained by the condition itself. However, it would have been impossible to clearly distinguish between the two and

thus two quantify how much of the variance was due to age effects and how much due to diagnosis.

In an ideal world one would be able to trace those trajectories in a longitudinal design and preferably from the same individuals. Initiatives such as EU-AIMS and even ABIDE aim to gather such data, but at present this is not available. Furthermore, as stressed throughout this thesis, structural covariance analysis at present only allows us to analyse group based covariance. Thus, individual level data is not present at the level of network analysis. Unfortunately, this prevents a detailed analysis of inter-individual variation, which we expect to be substantial in autism as well as ADHD. As methods are being developed to assess individual level morphometric covariance we will aim to apply these to the present data as well.

8.2 Biological sex modulates brain morphology in autism

Second, we know that biological sex modulates brain development and interacts with the autism phenotypic expression (Lai et al., 2014, 2015) (Figure 8.1 - label 8.2). The clearest evidence for that is the male bias in autism, with an approximate 4 to 1 ratio of males to females. The theories discussed in Chapter 4 such as the EMB (Baron-Cohen, 2002) and GI (Bejerot et al., 2012) theories capture some of the spectrums broad variability in that respect. They furthermore provide a testable framework to study sex differences in autism. For example, Lai and colleagues showed that neurobiological variation associated with autism, as captured with structural neuroimaging, showed minimal spatial overlap between sexes (Lai, Lombardo, Suckling, et al., 2013). From this it can be concluded that

autism manifests differently between sexes at a brain morphological level. Specifically, in the same study it was shown that the pattern in females with autism showed neural 'masculinization' as would be predicted by the EMB theory. Interestingly though, the study did not show a similar effect in the male autism group. Likely the difference in 'masculinization' for men was too small to be observed as an extreme of the normative sex difference. This could also be seen as evidence for the hypotheses that women in general need a higher disease burden to develop the condition (Werling & Geschwind, 2013). In Chapter 4 we sought to use the same data modality we used in Chapter 2 to test for GI or EMB patterns similar to the Lai et al. study (2013). While confirming the existence of a normative sex difference our results show evidence for both theories in different brain regions and to different extends. In general, the pattern of neurobiological differences between neurotypical adults and adults with autism was extremely heterogeneous.

One caveat of the data presented in Chapters 2 and 4 that may not have been addressed enough is the fact that structural covariance analysis by definition provides only a single data-point per group. Because the covariance is based on the groups covariance, it is not a method well suited to capture specific individual variance. In both chapters we used different approaches to navigate that problem. In Chapter 2 we permuted the underlying distribution to create a null-distribution that could be used for two-sample permutation tests. This method however was not suited to test rank-order effects as there is really no workable version of a three- (or even four) sample permutation, other than moving directly to post-doc testing of individual pairs. Thus in Chapter 4 we chose to use bootstrapping to create confidence intervals for each group and test linear rank orders on

those. It appears that in the present data the bootstrapping approach provided many more significant differences between the groups. Thus, it is possible that the bootstrapping approach was more sensitive to false positives. We are currently planning to run parts of the analyses done in Chapter 4 using permutation tests of individual group pairs and see whether the results show spatial overlap with those found on pair-wise tests of bootstrapped groups.

8.3 Sex hormones influence brain morphology

Thirdly, and strongly related to the previous point, we also know that sex hormones in general influence brain morphology and function (Figure 8.1 - label 8.3). Specifically, the hormones estradiol and testosterone have been repeatedly shown to alter brain morphology by driving sexual differentiation (McCarthy et al., 2012). This is a process that happens from birth as various studies have shown that prenatal indicators of for example testosterone have been associated with morphological differences later in life (Lombardo, Ashwin, Auyeung, Chakrabarti, Taylor, et al., 2012; Peper, Brouwer, van Baal, et al., 2009).

The effects of hormones on brain morphology (and function) are not restricted to prenatal or early development. It has been well documented for example that surging hormone levels during puberty also have profound effects on brain reorganization as well (Koolschijn et al., 2014; Peper, Brouwer, Schnack, et al., 2009; Peper et al., 2011). Given this continuous influence that hormones play on altered brain structure and functions it

is hard to pin-point their precise effects on behaviour or ascribe them a general function beyond stating that they 'masculinize' or 'feminize' the brain. If, as some authors have suggested (Baron-Cohen, 2002; Bejerot et al., 2012), sex hormones are indeed strongly intertwined with atypical development they may prove to be useful as therapeutics (Meyer-Lindenberg et al., 2011). A better understanding of their long-term effects is certainly needed. In the present work we have only highlighted some interactions between sex hormones and brain function in an acute short-term way (e.g. by looking at effects of administering these hormones) and not in a clinical or neurodevelopmental population.

In Chapter 7 we attempted to include a measure of prenatal hormones exposure (e.g. 2D-4D ratio) in our analysis as previous studies had shown that these might modulate effects later in life (van Honk, Schutter, et al., 2011). In the context of both fear modulation and resting-state connectivity we found no moderating effects of this marker for prenatal testosterone. Thus, one could hypothesize that both transient as well as prenatal effects of testosterone are likely to be context dependent. Ideally studies looking into acute effects of hormones or neurobiological effect of sex would account for hormone levels and the effect of pre- and postnatal exposure on brain morphology. Obviously this is a near impossible task given that such detailed longitudinal data is almost never available. Nonetheless, basic parameters such as digit-ratios, pubertal stage or development and behavioural patterns of 'masculinization' or 'feminization' can be included to provide better insights into the interaction hormones might play on brain morphology.

8.4 Genes modulate brain morphology

Fourth, and likely much earlier in the complex causal chain of interactions, we know that genes have a driving influence on brain morphology and ultimately on behaviour (Figure 8.1 - label 8.4). The fact that there are many genetic determinants for shaping the human brain is not new nor surprising. What is new is the ability to study the precise relationship between the two. For example Whitaker and colleagues were recently able to link transcriptional profiles from publically available AIBS data to processes of cortical myelination and brain maturation (Whitaker et al., 2016). Given that one of our most prominent measures relies on myelination (e.g. differences in CT are ultimately the result of changes in the grey-white matter ratio and profile and thus of myelination) we hypothesized that any differences in CT in individuals with autism might be driven by a transcriptional profile that should overlap with a genetic profile of autism risk genes. Thus, in Chapter 3 we investigated which risk genes for autism were associated with alterations observed in brain morphology. We showed that transcriptional modules that are downregulated in autism post-mortem cortex (both during development as well as later in life) are the strongest associated with whole-brain differences in cortical thickness.

Although the data available to disentangle this complex interaction is far from ideal and analyses largely rely on post-mortem examination, it provides the first insights into linking genetics with neurobiology and hopefully ultimately with behaviour. Perhaps the most important caveat of the results presented in Chapter 3, with regards to the link between gene expression and alterations in CT, is the time discrepancy between datasets.

The CT estimates were based on imaging data obtained from children whereas the gene expression was based on the 6 adult donors in the AIBS dataset. It is known that gene expression may change over time (Glass et al., 2013) and it is possible some of the gene modules change over time. Unfortunately, there is no spatially detailed information available on gene expression (neither from autism donors nor from neurotypical donors) that would allow any other comparison. There is less spatially detailed information available and we tried to address that issue in our analysis for Chapter 3 by also using genetic modules obtained from developmental gene-expression datasets.

Ideally however, one would be able to have age-matched samples or have both gene expression as well as cortical thickness estimates from the same individuals. In a less ideal world however one could address the question of this developmental (or time-varying) variability using longitudinal imaging data (for example, by using longitudinal studies or by proxy and use datasets that span a wider age-range). Another approach could be to assess the spatiotemporal profile of gene-expression in individuals with autism and healthy individuals to address whether there are even any baseline differences in this profile. Although not as spatially accurate, there are datasets that allow this type of time-varying analysis (Parikshak et al., 2013; Parikshak, Swarup, Belgard, Irimia, Ramaswami, Gandal, Hartl, Leppa, De, et al., 2016). As a future project we plan to investigate spatiotemporal profiles of gene-expression in these data. Specifically, we plan to look

whether autism risk genes might show more variability in modular membership across time and brain regions[3].

As another question, we are also interested to find out whether genes that are more susceptible to change might overlap more broadly with genes that explain risk for developmental conditions. For example, in a parallel study (not reported here) we found that risk genes that are associated with schizophrenia, autism and intellectual disability overlap with regions of the genome known as Human Accelerated Regions (HARs) and, as such, we hypothesized that some of these genes might in fact be under positive selection (Warrier, Bethlehem, Geschwind, & Baron-Cohen, 2017). Our rationale was that the phenotypic difficulties seen in these conditions are potentially extremes of adaptive traits that are maintained in the general population and thus likely to be part of a fairly steady genetic modular backbone. As a follow-up it would be interesting to see if these genes are also more versatile in their expression profile over time (as opposed to across species or conditions) or whether they are consistently associated with the same or similar neurobiological spatiotemporal profile.

8.5 Sex differentially expressed genes interact with autism

Fifth, although not addressed directly in this thesis but related to the previous three points, we also know that genes that are differentially expressed between sexes interacts

[3] I have been awarded an exchange fellowship with Professor Dan Geschwind and Dr Neelroop Parikshak to work on this project for a period of 8 months at UCLA.

with autism risk (Werling, Parikshak, & Geschwind, 2016) (Figure 8.1 - label 8.5). Interestingly, Werling and colleagues showed that it is not the autism risk genes per se that contribute to phenotypic risk but that sexually dimorphic genes themselves can increase or decrease the risk for autism. This further strengthens the hypotheses that basic neurobiological sex differences interact with autism. This is not a topic that we addressed experimentally in the present work. It is noteworthy however, as it again emphasizes that biological sex can be seen as an overarching influence on many aspect of neurobiology and its interaction with behaviour and neurodevelopmental conditions. As outlined above it would be interesting to see if these sex differentially expressed genes also follow altered developmental trajectories by looking at their spatiotemporal characteristics. Although at present there are no clear plans to include this in our future analysis of spatiotemporal gene co-expression it will be interesting to explore if these genes are robustly clustered together over time or whether they interact with other genes at different time-points and spatial locations.

8.6 Brain function is altered in autism

Sixth, it can also be assumed that individuals with autism show altered patterns of functional organization (Figure 8.1 - label 8.6). Numerous studies have suggested and shown that people with autism will have different patterns of connectivity (Belmonte et al., 2004; Cherkassky et al., 2006; Courchesne & Pierce, 2005; Ebisch et al., 2011; Just et al., 2004; Kana, Keller, Cherkassky, Minshew, & Just, 2006; Kana et al., 2009; Noonan, Haist, & Müller, 2009; von dem Hagen, Stoyanova, Baron-Cohen, & Calder, 2013). These disconnectivity theories and findings all have merit to them and they all explain elements

of atypical development that might underlie the neurobiology of autism. However, they again are likely to capture only subgroups or elements of the autism spectrum.

Furthermore, most studies have explored connectivity patterns in adults with autism and, given evidence for diverging developmental trajectories from previous chapters as well as the broader literature (Courchesne, 2002; Courchesne et al., 2001, 2011), the link between adult connectivity patterns and those of children is not that clearly understood. In addition, most of the studies mentioned previously have been done on high-functioning adults. The reasons for both these choices are likely both pragmatic (e.g. fMRI imaging is expensive and undoubtedly easier with people that clearly understand instructions and data quality better with individuals who are more at ease and better able to lie still) as well as based on theoretical assumptions about high functioning adult autism being less clouded by high comorbidity with other conditions such as ADHD, OCD, intellectual disability, or even normal variance in developmental trajectories. Again, in an ideal world, detailed longitudinal studies would provide a solution to deal with a lot of these problems in the long term. In the short term however it might be easier to use techniques that can at least deal with some of the pragmatic issues. EEG may provide one such solution by the simple fact that it is cheaper, less sensitive to noise from head motion and less invasive. Which makes it arguably better suited in paediatric samples.

Finally, techniques might also result in different hypotheses altogether (Vissers et al., 2012). Early indications of differences in functional connectivity largely stem from EEG research looking at high frequency gamma oscillations as measured with EEG or MEG (Brock et al., 2002). With fMRI we can only look at changes at a very low frequency and

there is a very real possibility that higher frequency network characteristics will not overlap with the low frequency networks we can image with functional MRI. EEG provides a less invasive and cheaper alternative to fMRI. Obviously the spatial resolution is not as high but it does allow more fine-grained temporal analysis and is more practical to implement. Unfortunately, there is little information in the literature on baseline differences in network topology in autism as assessed with EEG. Most studies to date have focused on spectral density asymmetries and not connectivity (Burnette et al., 2011; Stroganova et al., 2007). Thus, we decided to also add a resting-state recording to a planned EEG study to assess potential differences in functional brain organization ourselves.

Unfortunately, our results from Chapter 5 do not provide a clear answer to the question of whether autism is mostly characterized by any one specific theory of altered connectivity, and nor does it necessarily disprove any previous findings obtained with fMRI. In fact, the main picture (both from present results as from previous literature) is that people with autism show a diverse pattern of both hyper- and hypo-connectivity that is not specific for a certain type of connection, and hence are 'atypical' in a broad sense. As a classification, overall hypo- or hyper- connectivity of two subclasses of connections (long vs. short range) is certainly an oversimplification of the autistic spectrum. A recent review on brain connectivity in high functioning adults with autism reaches a similar conclusion (Vissers et al., 2012). The current models of local versus global connectivity, general hypo-connectivity or hyper- connectivity to the frontal cortex do not capture the diversity of abnormal functional connectivity. The present data does suggest some more detailed aspects of connectivity patterns that might prove a promising lead. There is for

example evidence for a different and possibly 'confused' integration of connectivity in frontal and pre-fontal cortex, where we observe some connectivity differences between both groups. Looking at the characteristics of these specific networks may give clearer answers but likely with a limited scope in terms of describing autism in general. Atypical characteristics of one specific network are at best only related to a specific aspect of the autism diagnosis and are unlikely to cover the complete spectrum of behaviours.

Of course, the present findings should be considered preliminary as data collection is still ongoing and present results are only based on a relatively small sample. Thus, at this point they should mostly be considered a proof of concept, showing that EEG can be used to measure functional brain network connectivity in individuals with autism.

8.7 Hormones: person and context matter.

Lastly, sex hormones do not solely influence brain morphology early on they also play a role later in life in their capacity to alter brain function (Bethlehem et al., 2013; Bos et al., 2012) (Figure 8.1 - label 8.7). In Chapters 6 and 7 we describe the acute effects of two prominent hormones: oxytocin and testosterone. In these chapters we show that the effects of administering these substances is very context and person dependent. For example, administering oxytocin affects individuals with high AQ scores to a higher degree than it does individuals with a low AQ score (Bethlehem, Lombardo, et al., 2017). We found a neurobiological network of cortical and subcortical brain regions that is strongly affected in a baseline rs-fMRI recording. Interestingly, this network largely covers brain regions associated with social communication, pain perception and reward

processing. Indirectly, this might be the underlying framework for effects we observed in an earlier oxytocin administration study (Auyeung et al., 2015). In that study we showed that oxytocin improves eye-contact in autistic individuals and that those who where the strongest affected (e.g. made the least eye-contact in the placebo condition) improved the most. This is of course speculative, as ideally these elements would be studied in a concurrent fashion by for example combining eye-tracking with neuroimaging to see if the same neural networks are altered in that specific context.

Furthermore, the imaging study we presented here only included individuals without a diagnosis and we can not emphasize enough that it is highly likely that these effects fluctuate with individual variability that might not necessarily be the same in individuals with an autism diagnosis. Previous literature has already shown that baseline differences in the oxytocin system of individuals with autism might be expected (Modahl et al., 1998). To study this we also recently finished collecting a smaller imaging dataset of age-matched women with a diagnosis and plan to analyse this in the same fashion. Following the exploratory positive correlation reported in Chapter 6 we expect to find an even stronger effect for women on the autism spectrum as their AQ will likely be much higher. Should this effect not exist in the autism group it could be a clear sign that there are indeed fundamental baseline differences in the oxytocin system of individuals with autism.

In addition, as outlined in Chapter 6, very little is known about the neurobiological interaction between oxytocin and biological sex let alone other hormones. In the study we presented here we controlled for menstrual cycle effects but given that there is evidence of hormone modulating effects within the autistic spectrum by other sex steroid

hormones (Auyeung et al., 2013), it would be interesting to explore whether the administration of oxytocin also has a downstream effect on other hormones directly. The study presented in Chapter 6 also collected saliva samples throughout the recording (e.g. before OT administration, 10 minutes after OT administration and at the end of the scanning session). For a future project we plan to analyse whether oxytocin interacts with testosterone (Crespi, 2016; Jaeggi, Trumble, Kaplan, & Gurven, 2015; Weisman, Zagoory-Sharon, & Feldman, 2014).

Testosterone is a hormone one might not directly associate with positive effects on social cognition however it has previously been shown that depending on the context its outcome can be positive (Van Honk et al., 2012). Furthermore, if we indeed assume that a surge in prenatal testosterone influences brain development to increase autism risk (Baron-Cohen, 2002; Baron-Cohen et al., 2015) it could be argued that individuals with autism might in fact be somewhat desensitized to testosterone later in life. This is of course very speculative, and overexposure early in life could cause both desensitization (e.g. by triggering an adaptive response of decreasing the number of androgen receptors) or trigger a hypersensitization (e.g. by triggering an increase in androgen receptors to fit the over abundance). This it not a question that can be answered within the current study. What we do however show is that testosterones effects are also very dependent on context and previous studies had already shown that its effects are also modulated by individual variability such as prenatal exposure to testosterone (Montoya et al., 2013; van Honk, Schutter, et al., 2011). Interestingly though, both in the present study (Chapter 7) as well as in previous work (Bos et al., 2016), effects on functional connectivity varied with context and appeared independent of prenatal exposure as measured with 2D-4D

digit-ratio. Clearly, more work is needed to disentangle the complex interaction between context, testosterone administration, prenatal testosterone exposure and autism. Ideally this is achieved by using longitudinal data where prenatal testosterone levels are quantified more clearly (Lombardo, Ashwin, Auyeung, Chakrabarti, Lai, et al., 2012). It would be interesting for future studies to attempt to replicate effect of testosterone administration in this cohort to get a clearer picture of the pre-natal and post-natal interaction of testosterone. At a more fundamental level one could explore the effects of testosterone exposure on gene-expression in for example animal models or iPSC work Such projects are currently being undertaken by other members of our lab.

To summarize this factor, the most we can say is that the effects of hormones influence brain function in a person- and context-dependent manner. Although both hormones show promise as potential therapeutic target (whether by increasing eye-contact or reducing an element of social anxiety/fear), at present we know too little about its person and contextual variability to provide a general conclusion about its potential broad therapeutic use. Based on the broad literature (Bartz et al., 2011; Bethlehem et al., 2014, 2013; Meyer-Lindenberg, 2008; Meyer-Lindenberg et al., 2011; Modi & Young, 2012) it seems plausible to assume that oxytocin might benefit specific individuals on the autistic spectrum in particular contexts, but these need to be defined much more clearly as research has also shown that its administration can have a less positive effect (De Dreu, 2011; De Dreu et al., 2010; De Dreu, Greer, Handgraaf, Shalvi, & Van Kleef, 2012; Miller, 2013)

8.8 Conclusions

This thesis has highlighted a few of the cogs in a complex set of mechanisms that ultimately drive human behaviour. We showed how biological sex and sex hormones sit on top of a causal chain that goes from the micro level (e.g. genes) to the macro level (e.g. behaviour) by affecting brain morphology and function. Furthermore, within this causal chain there are various interactions between those different levels of organization. For example, genes affect brain morphology, while sex affects genes and brain morphology directly as well. These effects might not even be one directional (hence their representation in the framework overview as cogs). For example, hormones that influence brain function could over time also influence brain morphology indirectly. All the interactions shown in the present work simply provide points where this causal chain may be vulnerable to lead to atypical development and highlight the need for integrative frameworks that includes different levels of analysis. However, as is the case in hormone administration studies, they will hopefully also provide windows to not only better understanding, but ultimately treatments that could help alleviate symptoms.

References

Alaerts, K., Swinnen, S. P., & Wenderoth, N. (2016). Sex differences in autism: A resting-state fMRI investigation of functional brain connectivity in males and females. *Social Cognitive and Affective Neuroscience*, *11*(6), 1002–1016. http://doi.org/10.1093/scan/nsw027

Alexander-Bloch, A., Giedd, J. N., & Bullmore, E. T. (2013). Imaging structural co-variance between human brain regions. *Nature Reviews. Neuroscience*, *14*(5), 322–36. http://doi.org/10.1038/nrn3465

Alexander-Bloch, A., Raznahan, A., Bullmore, E. T., & Giedd, J. N. (2013). The Convergence of Maturational Change and Structural Covariance in Human Cortical Networks. *Journal of Neuroscience*, *33*(7), 2889–2899. http://doi.org/10.1523/JNEUROSCI.3554-12.2013

Almeida Montes, L. G., Prado Alcantara, H., Martinez Garcia, R. B., De La Torre, L. B., Avila Acosta, D., & Duarte, M. G. (2013). Brain Cortical Thickness in ADHD: Age, Sex, and Clinical Correlations. *Journal of Attention Disorders*, *17*(8), 641–654. http://doi.org/10.1177/1087054711434351

Amaral, D. G., Schumann, C. M., & Nordahl, C. W. (2008). Neuroanatomy of autism. *Trends in Neurosciences*, *31*(3), 137–145. http://doi.org/10.1016/j.tins.2007.12.005

American Psychiatric Association. (2013). *Diagnostic and Statistical Manual of Mental Disorders. 5th ed.*. Arlington, VA: American Psychiatric Press.

Amodio, D. M., & Frith, C. D. (2006). Meeting of minds: the medial frontal cortex and social cognition. *Nature Reviews Neuroscience*, *7*(4), 268–277. http://doi.org/10.1038/nrn1884

Amunts, K., Kedo, O., Kindler, M., Pieperhoff, P., Mohlberg, H., Shah, N. J., … Zilles, K. (2005). Cytoarchitectonic mapping of the human amygdala, hippocampal region and

entorhinal cortex: Intersubject variability and probability maps. *Anatomy and Embryology*, *210*(5–6), 343–352. http://doi.org/10.1007/s00429-005-0025-5

Arsenijevic, Y., & Tribollet, E. (1998). Region-specific effect of testosterone on oxytocin receptor binding in the brain of the aged rat. *Brain Research*, *785*(1), 167–170. http://doi.org/10.1016/S0006-8993(97)01429-7

Ashburner, J., & Friston, K. J. (2000). Voxel-Based Morphometry—The Methods. *NeuroImage*, *11*(6), 805–821. http://doi.org/10.1006/nimg.2000.0582

Ashwin, E., Ashwin, C., Rhydderch, D., Howells, J., & Baron-cohen, S. (2009). Eagle-Eyed Visual Acuity: An Experimental Investigation of Enhanced Perception in Autism. *Biological Psychiatry*, *65*(1), 17–21. http://doi.org/10.1016/j.biopsych.2008.06.012

Assaf, M., Jagannathan, K., Calhoun, V. D., Miller, L., Stevens, M. C., Sahl, R., … Pearlson, G. D. (2010). Abnormal functional connectivity of default mode sub-networks in autism spectrum disorder patients. *Neuroimage*, *53*(1), 247–256. http://doi.org/10.1016/j.neuroimage.2010.05.067.Assaf

Auyeung, B., Lombardo, M. V., & Baron-cohen, S. (2013). Prenatal and postnatal hormone effects on the human brain and cognition. *Pflugers Archiv European Journal of Physiology*, *465*(5), 557–571. http://doi.org/10.1007/s00424-013-1268-2

Auyeung, B., Lombardo, M. V., Heinrichs, M., Chakrabarti, B., Sule, A., Deakin, J., … Baron-Cohen, S. (2015). Oxytocin increases eye contact during a real-time, naturalistic social interaction in males with and without autism. *Translational Psychiatry*, *5*(2), e507. http://doi.org/10.1038/tp.2014.146

Balardin, J. B., Comfort, W. E., Daly, E. M., Murphy, C. M., Andrews, D., Murphy, D. G. M., … Sato, J. R. (2015). Decreased centrality of cortical volume covariance networks in autism spectrum disorders. *Journal of Psychiatric Research*, *69*, 142–149. http://doi.org/10.1016/j.jpsychires.2015.08.003

Bale, T., & Dorsa, D. (1995). Regulation of Oxytocin Receptor Messenger Ribonucleic Acid in the Ventromedial Hypothalamus by Testosterone and Its Metabolites ". *Endocrinology*, (March), 5135–5138. Retrieved from http://press.endocrine.org/doi/abs/10.1210/endo.136.11.7588251

Baron-Cohen, S. (2002). The extreme male brain theory of autism. *Trends in Cognitive*

Sciences, *6*(6), 248–254. Retrieved from http://www.ncbi.nlm.nih.gov/pubmed/23180205

Baron-Cohen, S., Ashwin, E., Ashwin, C., Tavassoli, T., & Chakrabarti, B. (2009). Talent in autism: hyper-systemizing, hyper-attention to detail and sensory hypersensitivity. *Philosophical Transactions of the Royal Society of London. Series B, Biological Sciences*, *364*(1522), 1377–83. http://doi.org/10.1098/rstb.2008.0337

Baron-Cohen, S., Auyeung, B., Nørgaard-Pedersen, B., Hougaard, D. M., Abdallah, M. W., Melgaard, L., … Lombardo, M. V. (2015). Elevated fetal steroidogenic activity in autism. *Molecular Psychiatry*, *20*(3), 369–376. http://doi.org/10.1038/mp.2014.48

Baron-Cohen, S., Hoekstra, R. a, Knickmeyer, R., & Wheelwright, S. (2006). The Autism-Spectrum Quotient (AQ)--adolescent version. *Journal of Autism and Developmental Disorders*, *36*(3), 343–50. http://doi.org/10.1007/s10803-006-0073-6

Baron-Cohen, S., Lombardo, M. V., Auyeung, B., Ashwin, E., Chakrabarti, B., & Knickmeyer, R. (2011). Why are Autism Spectrum conditions more prevalent in Males? *PLoS Biology*, *9*(6). http://doi.org/10.1371/journal.pbio.1001081

Baron-cohen, S., Richler, J., Bisarya, D., Gurunathan, N., & Wheelwright, S. (2003). The systemizing quotient: an investigation of adults with Asperger syndrome or high-functioning autism, and normal sex differences. *Philosophical Transactions of the Royal Society B: Biological Sciences*, *358*(1430), 361–374. http://doi.org/10.1098/rstb.2002.1206

Baron-Cohen, S., & Wheelwright, S. (2004). The Empathy Quotient: An Investigation of Adults with Asperger Syndrome or High Functioning Autism, and Normal Sex Differences. *Journal of Autism and Developmental Disorders*, *34*(2), 163–175. http://doi.org/10.1023/B:JADD.0000022607.19833.00

Baron-Cohen, S., Wheelwright, S., Robinson, J., & Woodbury-Smith, M. (2005). The Adult Asperger Assessment (AAA): a diagnostic method. *Journal of Autism and Developmental Disorders*, *35*(6), 807–819. http://doi.org/10.1007/s10803-005-0026-5

Baron-Cohen, S., Wheelwright, S., Skinner, R., Martin, J., & Clubley, E. (2001). The autism-spectrum quotient (AQ): evidence from Asperger syndrome/high-functioning

autism, males and females, scientists and mathematicians. *Journal of Autism and Developmental Disorders*, *31*(1), 5–17. Retrieved from http://www.ncbi.nlm.nih.gov/pubmed/11439754

Baroncini, M., Jissendi, P., Balland, E., Besson, P., Pruvo, J.-P., Francke, J.-P., … Prevot, V. (2012). MRI atlas of the human hypothalamus. *NeuroImage*, *59*(1), 168–180. http://doi.org/10.1016/j.neuroimage.2011.07.013

Bartz, J. a, Zaki, J., Bolger, N., & Ochsner, K. N. (2011). Social effects of oxytocin in humans: context and person matter. *Trends Cogn Sci*, *15*(7), 301–309. Retrieved from http://www.ncbi.nlm.nih.gov/pubmed/21696997

Beckmann, C. F. C. F., DeLuca, M., Devlin, J. T., & Smith, S. M. (2005). Investigations into resting-state connectivity using independent component analysis. *Philosophical Transactions of the Royal Society of London. Series B, Biological Sciences*, *360*(1457), 1001–13. http://doi.org/10.1098/rstb.2005.1634

Beckmann, C. F. C. F., & Smith, S. M. (2004). Probabilistic independent component analysis for functional magnetic resonance imaging. *IEEE Transactions on Medical Imaging*, *23*(2), 137–152. http://doi.org/10.1109/TMI.2003.822821

Beery, A. K., & Zucker, I. (2011). Sex bias in neuroscience and biomedical research. *Neuroscience & Biobehavioral Reviews*, *35*(3), 565–572. http://doi.org/10.1016/j.neubiorev.2010.07.002

Bejerot, S., Eriksson, J. M., Bonde, S., Carlström, K., Humble, M. B., Eriksson, E., … Eriksson, E. (2012). The extreme male brain revisited: Gender coherence in adults with autism spectrum disorder. *British Journal of Psychiatry*, *201*(2), 116–123. http://doi.org/10.1192/bjp.bp.111.097899

Belmonte, M. K., Allen, G., Beckel-Mitchener, A., Boulanger, L. M., Carper, R. a, & Webb, S. J. (2004). Autism and abnormal development of brain connectivity. *The Journal of Neuroscience : The Official Journal of the Society for Neuroscience*, *24*(42), 9228–31. http://doi.org/10.1523/JNEUROSCI.3340-04.2004

Benjamini, Y., & Hochberg, Y. (1995). Controlling the False Discovery Rate: A Practical and Powerful Approach to Multiple Testing. *Journal of the Royal Statistical Society. Series B (Methodological)*, *57*(1), 289–300.

Bernhardt, B. C., Klimecki, O. M., Leiberg, S., & Singer, T. (2014). Structural covariance networks of the dorsal anterior insula predict females' individual differences in empathic responding. *Cerebral Cortex*, *24*(8), 2189–2198. http://doi.org/10.1093/cercor/bht072

Bernhardt, B. C., Valk, S. L., Silani, G., Bird, G., Frith, U., Singer, T., … Singer, T. (2014). Selective disruption of sociocognitive structural brain networks in autism and alexithymia. *Cerebral Cortex*, *24*(12), 3258–3267. http://doi.org/10.1093/cercor/bht182

Bethlehem, R. A. I., Baron-Cohen, S., van Honk, J., Auyeung, B., & Bos, P. A. (2014). The oxytocin paradox. *Frontiers in Behavioral Neuroscience*, *8*(February), 48. http://doi.org/10.3389/fnbeh.2014.00048

Bethlehem, R. A. I., Lombardo, M. V., Lai, M.-C., Auyeung, B., Crockford, S. K., Deakin, J., … Baron-Cohen, S. (2017). Intranasal oxytocin enhances intrinsic corticostriatal functional connectivity in women. *Translational Psychiatry*, *7*(4), e1099. http://doi.org/10.1038/tp.2017.72

Bethlehem, R. A. I., Romero-Garcia, R., Mak, E., Bullmore, E. T., & Baron-Cohen, S. (2017). Structural Covariance Networks in Children with Autism or ADHD. *Cerebral Cortex*, 1–10. http://doi.org/10.1093/cercor/bhx135

Bethlehem, R. A. I., van Honk, J., Auyeung, B., & Baron-Cohen, S. (2013). Oxytocin, brain physiology, and functional connectivity: a review of intranasal oxytocin fMRI studies. *Psychoneuroendocrinology*, *38*(7), 962–974. http://doi.org/10.1016/j.psyneuen.2012.10.011

Billeci, L., Sicca, F., Maharatna, K., Apicella, F., Narzisi, A., Campatelli, G., … Muratori, F. (2013). On the application of quantitative EEG for characterizing autistic brain: a systematic review. *Frontiers in Human Neuroscience*, *7*(August), 442. http://doi.org/10.3389/fnhum.2013.00442

Biswal, B. B., Eldreth, D. a, Motes, M. a, & Rypma, B. (2010). Task-dependent individual differences in prefrontal connectivity. *Cerebral Cortex (New York, N.Y. : 1991)*, *20*(9), 2188–97. http://doi.org/10.1093/cercor/bhp284

Blakemore, S.-J. (2010). The Developing Social Brain: Implications for Education. *Neuron*,

65(6), 744–747. http://doi.org/10.1016/j.neuron.2010.03.004

Born, J., Lange, T., Kern, W., McGregor, G. P., Bickel, U., & Fehm, H. L. (2002). Sniffing neuropeptides: a transnasal approach to the human brain. *Nature Neuroscience*, *5*(6), 514–6. http://doi.org/10.1038/nn849

Bos, P. A., Hofman, D., Hermans, E. J., Montoya, E. R., Baron-Cohen, S., & van Honk, J. (2016). Testosterone reduces functional connectivity during the "Reading the Mind in the Eyes" Test. *Psychoneuroendocrinology*, *68*, 194–201. http://doi.org/10.1016/j.psyneuen.2016.03.006

Bos, P. A., Montoya, E. R., Hermans, E. J., Keysers, C., & van Honk, J. (2015). Oxytocin reduces neural activity in the pain circuitry when seeing pain in others. *NeuroImage*, *113*, 217–224. http://doi.org/10.1016/j.neuroimage.2015.03.049

Bos, P. A., Panksepp, J., Bluthé, R.-M. M., & van Honk, J. (2012). Acute effects of steroid hormones and neuropeptides on human social-emotional behavior: a review of single administration studies. *Frontiers in Neuroendocrinology*, *33*(1), 17–35. http://doi.org/10.1016/j.yfrne.2011.01.002

Bourgeron, T. (2009). A synaptic trek to autism. *Current Opinion in Neurobiology*, *19*(2), 231–234. http://doi.org/10.1016/j.conb.2009.06.003

Bourgeron, T. (2015). From the genetic architecture to synaptic plasticity in autism spectrum disorder. *Nature Reviews Neuroscience*, *16*(9), 551–563. http://doi.org/10.1038/nrn3992

Bourgeron, T. (2016). Current knowledge on the genetics of autism and propositions for future research. *Comptes Rendus Biologies*, *339*(7), 300–307. http://doi.org/10.1016/j.crvi.2016.05.004

Breedlove, S. M. (2010). Minireview: Organizational hypothesis: Instances of the fingerpost. *Endocrinology*, *151*(9), 4116–4122. http://doi.org/en.2010-0041 [pii]10.1210/en.2010-0041

Brieber, S., Neufang, S., Bruning, N., Kamp-becker, I., Remschmidt, H., Herpertz-Dahlmann, B., … Konrad, K. (2007). Structural brain abnormalities in adolescents with autism spectrum disorder and patients with attention deficit/hyperactivity disorder. *Journal of Child Psychology and Psychiatry and Allied Disciplines*, *48*(12), 1251–1258.

http://doi.org/10.1111/j.1469-7610.2007.01799.x

Brock, J., Brown, C. C., Boucher, J., & Rippon, G. (2002). The temporal binding deficit hypothesis of autism. *Development and Psychopathology*, *14*(2), 209–24. Retrieved from http://www.ncbi.nlm.nih.gov/pubmed/12030688

Bullmore, E. T., & Sporns, O. (2009). Complex brain networks: graph theoretical analysis of structural and functional systems. *Nat Rev Neurosci*, *10*(3), 186–198. http://doi.org/10.1038/nrn2575

Burnette, C. P., Henderson, H. a, Inge, A. P., Zahka, N. E., Schwartz, C. B., & Mundy, P. C. (2011). Anterior EEG asymmetry and the Modifier Model of Autism. *Journal of Autism and Developmental Disorders*, *41*(8), 1113–24. http://doi.org/10.1007/s10803-010-1138-0

Bzdok, D., Laird, A. R., Zilles, K., Fox, P. T., & Eickhoff, S. B. (2013). An investigation of the structural, connectional, and functional subspecialization in the human amygdala. *Human Brain Mapping*, *0*(12), 3247–3266. http://doi.org/10.1002/hbm.22138

Cai, W., Chen, T., Szegletes, L., Supekar, K., & Menon, V. (2015). Aberrant cross-brain network interaction in children with attention-deficit/hyperactivity disorder and its relation to attention deficits: a multi- and cross-site replication study. *Biological Psychiatry*, 1–11. http://doi.org/http://dx.doi.org/10.1016/j.biopsych.2015.10.017

Caria, A., de Falco, S., Falco, S. De, & Caria, A. (2015). Anterior insular cortex regulation in autism spectrum disorders. *Frontiers in Behavioral Neuroscience*, *9*(March), 1–9. http://doi.org/10.3389/fnbeh.2015.00038

Chen, E. Y., Tan, C. M., Kou, Y., Duan, Q., Wang, Z., Meirelles, G. V., … Ma'ayan, A. (2013). Enrichr: interactive and collaborative HTML5 gene list enrichment analysis tool. *BMC Bioinformatics*, *14*(1), 128. http://doi.org/10.1186/1471-2105-14-128

Cherkassky, V. L., Kana, R. K., Keller, T. A., & Just, M. A. (2006). Functional connectivity in a baseline resting-state network in autism. *Neuroreport*, *17*(16), 1687–90. http://doi.org/10.1097/01.wnr.0000239956.45448.4c

Chumbley, J. R., & Friston, K. J. (2009). False discovery rate revisited: FDR and topological inference using Gaussian random fields. *NeuroImage*, *44*(1), 62–70. http://doi.org/10.1016/j.neuroimage.2008.05.021

Churchland, P. S., & Winkielman, P. (2012). Modulating social behavior with oxytocin: how does it work? What does it mean? *Hormones and Behavior*, *61*(3), 392–399. http://doi.org/10.1016/j.yhbeh.2011.12.003.Modulating

Cohen, M. X. (2014). *Analyzing Neural Time Series Data*. MIT Press.

Convit, A., Czobor, P., & Volavka, J. (1991). Lateralized abnormality in the EEG of persistently violent psychiatric inpatients. *Biological Psychiatry*, *30*(4), 363–70. Retrieved from http://www.ncbi.nlm.nih.gov/pubmed/1912127

Courchesne, E. (2002). Abnormal early brain development in autism. *Molecular Psychiatry*, *7 Suppl 2*, S21–S23. http://doi.org/10.1038/sj.mp.4001169

Courchesne, E. (2004). Brain development in autism: early overgrowth followed by premature arrest of growth. *Mental Retardation and Developmental Disabilities Research Reviews*, *10*(2), 106–11. http://doi.org/10.1002/mrdd.20020

Courchesne, E., Campbell, K., & Solso, S. (2011). Brain growth across the life span in autism: age-specific changes in anatomical pathology. *Brain Research*, *1380*, 138–45. http://doi.org/10.1016/j.brainres.2010.09.101

Courchesne, E., Carper, R. a, & Akshoomoff, N. (2003). Evidence of brain overgrowth in the first year of life in autism. *JAMA : The Journal of the American Medical Association*, *290*(3), 337–44. http://doi.org/10.1001/jama.290.3.337

Courchesne, E., Karns, C. M., Davis, H. R., Ziccardi, R., Carper, R. a, Tigue, Z. D., … Courchesne, R. Y. (2001). Unusual brain growth patterns in early life in patients with autistic disorder: an MRI study. *Neurology*, *57*(2), 245–54. Retrieved from http://www.ncbi.nlm.nih.gov/pubmed/11468308

Courchesne, E., & Pierce, K. (2005). Why the frontal cortex in autism might be talking only to itself: local over-connectivity but long-distance disconnection. *Current Opinion in Neurobiology*, *15*(2), 225–230. http://doi.org/10.1016/j.conb.2005.03.001

Courchesne, E., Pierce, K., Schumann, C. M., Redcay, E., Buckwalter, J. A., Kennedy, D. P., & Morgan, J. (2007). Mapping early brain development in autism. *Neuron*, *56*(2), 399–413. http://doi.org/10.1016/j.neuron.2007.10.016

Craig, A. D. B. (2009). How do you feel — now? The anterior insula and human awareness.

Nature Reviews Neuroscience, *10*(1), 59–70. http://doi.org/10.1038/nrn2555

Craik, F. I. M., & Bialystok, E. (2006). Cognition through the lifespan: Mechanisms of change. *Trends in Cognitive Sciences*, *10*(3), 131–138. http://doi.org/10.1016/j.tics.2006.01.007

Crespi, B. J. (2016). Oxytocin, testosterone, and human social cognition. *Biological Reviews*, *91*(2), 390–408. http://doi.org/10.1111/brv.12175

De Dreu, C. K. W. (2011). Oxytocin promotes human ethnocentrism. *Proceedings of the …*, *108*(4), 1262–1266. http://doi.org/10.1073/pnas.1015316108

De Dreu, C. K. W., Greer, L. L., Handgraaf, M. J. J., Shalvi, S., & Van Kleef, G. a. (2012). Oxytocin modulates selection of allies in intergroup conflict. *Proceedings. Biological Sciences / The Royal Society*, *279*(1731), 1150–4. http://doi.org/10.1098/rspb.2011.1444

De Dreu, C. K. W., Greer, L. L., Handgraaf, M. J. J., Shalvi, S., Van Kleef, G. a, Baas, M., … Feith, S. W. W. (2010). The neuropeptide oxytocin regulates parochial altruism in intergroup conflict among humans. *Science (New York, N.Y.)*, *328*(5984), 1408–11. http://doi.org/10.1126/science.1189047

de Jong, S. (1993). SIMPLS: An alternative approach to partial least squares regression. *Chemometrics and Intelligent Laboratory Systems*, *18*(3), 251–263. http://doi.org/10.1016/0169-7439(93)85002-X

de Leeuw, C. A., Mooij, J. M., Heskes, T., Posthuma, D., Leeuw, C. A. De, Mooij, J. M., … Posthuma, D. (2015). MAGMA: Generalized Gene-Set Analysis of GWAS Data. *PLoS Computational Biology*, *11*(4), 1–19. http://doi.org/10.1371/journal.pcbi.1004219

Dean, D. C., Travers, B. G., Adluru, N., Destiche, D. J., Samsin, D., Prigge, M. B. D., … Dean, D. C. (2016). Investigating the Microstructural Correlation of White Matter in Autism Spectrum Disorder. *Brain Connectivity*, *6*(5), 415–433. http://doi.org/10.1089/brain.2015.0385

Deco, G., Tononi, G., Boly, M., & Kringelbach, M. L. (2015). Rethinking segregation and integration: contributions of whole-brain modelling. *Nature Reviews Neuroscience*, *16*(7), 430–439. http://doi.org/10.1038/nrn3963

DeFelipe, J., & Jones, E. G. (1988). *Cajal on the Cerebral Cortex: An Annotated Translation of the Complete Writings*. Oxford University Press.

Desikan, R. S., Ségonne, F., Fischl, B., Quinn, B. T., Dickerson, B. C., Blacker, D., … Killiany, R. J. (2006). An automated labeling system for subdividing the human cerebral cortex on MRI scans into gyral based regions of interest. *NeuroImage*, *31*, 968–980. http://doi.org/10.1016/j.neuroimage.2006.01.021

Domes, G., Lischke, A., Berger, C., Grossmann, A., Hauenstein, K., Heinrichs, M., & Herpertz, S. C. (2010). Effects of intranasal oxytocin on emotional face processing in women. *Psychoneuroendocrinology*, *35*(1), 83–93. http://doi.org/10.1016/j.psyneuen.2009.06.016

Dougherty, C. C., Evans, D. W., Myers, S. M., Moore, G. J., & Michael, A. M. (2015). A Comparison of Structural Brain Imaging Findings in Autism Spectrum Disorder and Attention-Deficit Hyperactivity Disorder. *Neuropsychology Review*, 25–43. http://doi.org/10.1007/s11065-015-9300-2

Dube, J., Lafortune, M., Bedetti, C., Bouchard, M., Franc, J., Doyon, J., … Recherches, C. De. (2015). Cortical Thinning Explains Changes in Sleep Slow Waves during Adulthood. *Journal of Neuroscience*, *35*(20), 7795–7807. http://doi.org/10.1523/JNEUROSCI.3956-14.2015

Dumais, K. M., & Veenema, A. H. (2015). Vasopressin and oxytocin receptor systems in the brain: Sex differences and sex-specific regulation of social behavior. *Frontiers in Neuroendocrinology*, (May). http://doi.org/10.1016/j.yfrne.2015.04.003

Durston, S., Eickhoff, S. B., Konrad, K., & Eickhoff, S. B. (2010). Konrad K , Eickhoff SB . Is the ADHD brain wired differently ? A review on structural and functional connectivity in attention deficit hyperactivity disorder . Hum Brain Mapp 31 : 904-9 ... Is the ADHD Brain Wired Differently ? A Review on Structural and , (March 2016). http://doi.org/10.1002/hbm.21058

Ebisch, S. J. H., Gallese, V., Willems, R. M., Mantini, D., Groen, W. B., Romani, G. L., … Bekkering, H. (2011). Altered intrinsic functional connectivity of anterior and posterior insula regions in high-functioning participants with autism spectrum disorder. *Human Brain Mapping*, *32*(7), 1013–28.

http://doi.org/10.1002/hbm.21085

Ebner, N. C., Chen, H., Porges, E., Lin, T., Fischer, H., Feifel, D., & Cohen, R. A. (2016). Oxytocin's effect on resting-state functional connectivity varies by age and sex. *Psychoneuroendocrinology*, *69*, 50–59. http://doi.org/10.1016/j.psyneuen.2016.03.013

Ecker, C. (2016). The neuroanatomy of autism spectrum disorder: An overview of structural neuroimaging findings and their translatability to the clinical setting. *Autism : The International Journal of Research and Practice*, 1362361315627136-. http://doi.org/10.1177/1362361315627136

Ecker, C., Ginestet, C. E., Feng, Y., Johnston, P., Lombardo, M. V., Lai, M.-C., … MRC AIMS Consortium, for the. (2013). Brain Surface Anatomy in Adults With Autism. *JAMA Psychiatry*, *70*(1), 59. http://doi.org/10.1001/jamapsychiatry.2013.265

Ecker, C., Ginestet, C. E., Feng, Y., Johnston, P., Lombardo, M. V., Lai, M.-C., … Murphy, D. G. M. (2013). Brain surface anatomy in adults with autism: the relationship between surface area, cortical thickness, and autistic symptoms. *JAMA Psychiatry*, *70*(1), 59–70. http://doi.org/10.1001/jamapsychiatry.2013.265

Ecker, C., Ronan, L., Feng, Y., Daly, E. M., Murphy, C. M., Ginestet, C. E., … Wheelwright, S. (2013). Intrinsic gray-matter connectivity of the brain in adults with autism spectrum disorder. *Proceedings of the National Academy of Sciences of the United States of America*, *110*(32), 13222–7. http://doi.org/10.1073/pnas.1221880110

Eickhoff, S. B., Stephan, K. E., Mohlberg, H., Grefkes, C., Fink, G. R., Amunts, K., & Zilles, K. (2005). A new SPM toolbox for combining probabilistic cytoarchitectonic maps and functional imaging data. *NeuroImage*, *25*(4), 1325–1335. http://doi.org/S1053-8119(04)00792-X [pii]10.1016/j.neuroimage.2004.12.034

Eisenberg, I. W., Wallace, G. L., Kenworthy, L., Gotts, S. J., & Martin, A. (2015). Insistence on sameness relates to increased covariance of gray matter structure in autism spectrum disorder. *Molecular Autism*, 1–12. http://doi.org/10.1186/s13229-015-0047-7

Elman, J. A., Panizzon, M. S., Hagler, D. J., Fennema-Notestine, C., Eyler, L. T., Gillespie, N. A., … Kremen, W. S. (2017). Genetic and environmental influences on cortical mean

diffusivity. *NeuroImage*, *146*(November 2016), 90–99. http://doi.org/10.1016/j.neuroimage.2016.11.032

Evans, A. C. (2013). Networks of anatomical covariance. *NeuroImage*, *80*, 489–504. http://doi.org/10.1016/j.neuroimage.2013.05.054

Evans, J. W., Kundu, P., Horovitz, S. G., & Bandettini, P. A. (2015). Separating slow BOLD from non-BOLD baseline drifts using multi-echo fMRI. *NeuroImage*, *105*, 189–197. http://doi.org/10.1016/j.neuroimage.2014.10.051

Eyler, L. T., Chen, C., Panizzon, M. S., Fennema-Notestine, C., Neale, M. C., Jak, A., … Kremen, W. S. (2012). A Comparison of Heritability Maps of Cortical Surface Area and Thickness and the Influence of Adjustment for Whole Brain Measures: A Magnetic Resonance Imaging Twin Study. *Twin Research and Human Genetics*, *15*(3), 304–314. http://doi.org/10.1017/thg.2012.3

Fair, D. A., Posner, J., Nagel, B. J., Bathula, D., Costa-Dias, T. G., Mills, K. L., … Joel, T. (2010). Atypical Default Network Connectivity in Youth with ADHD. *Biological Psychiatry*, *68*(12), 1084–1091. http://doi.org/10.1016/j.biopsych.2010.07.003.Atypical

Fallani, F. D. V., Costa, L. da F., Rodriguez, F. A., Astolfi, L., Vecchiato, G., Toppi, J., … Babiloni, F. (2010). A graph-theoretical approach in brain functional networks. Possible implications in EEG studies. *Nonlinear Biomedical Physics*, *4 Suppl 1*, S8. http://doi.org/10.1186/1753-4631-4-S1-S8

Fischl, B., & Dale, A. M. (2000). Measuring the thickness of the human cerebral cortex from magnetic resonance images. *Proceedings of the National Academy of Sciences*, *97*(20), 11050–11055. http://doi.org/10.1073/pnas.200033797

Fjell, A. M., Grydeland, H., Krogsrud, S. K., Amlien, I., Rohani, D. a, Ferschmann, L., … Walhovd, K. B. (2015). Development and aging of cortical thickness correspond to genetic organization patterns. *Proceedings of the National Academy of Sciences of the United States of America*, *112*(50), 15462–15467. http://doi.org/10.1073/pnas.1508831112

Frazier, T. W., Georgiades, S., Bishop, S. L., & Hardan, A. Y. (2014). Behavioral and Cognitive Characteristics of Females and Males With Autism in the Simons Simplex Collection. *Journal of the American Academy of Child & Adolescent Psychiatry*, *53*(3), 329–340.e3.

http://doi.org/10.1016/j.jaac.2013.12.004

Friederici, A. D. (2012). The cortical language circuit: from auditory perception to sentence comprehension. *Trends in Cognitive Sciences*, *16*(5), 262–268. http://doi.org/10.1016/j.tics.2012.04.001

Friston, K. J., Frith, C. D., Liddle, P., & Frackowiak, R. S. J. (1993). Functional Connectivity: The Principal-Component Analysis of Large (PET) Data Sets. *Journal of Cerebral Blood Flow & Metabolism*, *13*(1), 5–14. http://doi.org/10.1038/jcbfm.1993.4

Frith, U., & Happé, F. (1994). Autism: beyond "theory of mind". *Cognition*, *50*(1–3), 115–32. Retrieved from http://www.ncbi.nlm.nih.gov/pubmed/8039356

Gabard-durnam, L. J., Tierney, A. L., Vogel-Farley, V., Tager-Flusberg, H. B., & Nelson, C. a. (2013). Alpha Asymmetry in Infants at Risk for Autism Spectrum Disorders. *Journal of Autism and Developmental Disorders*. http://doi.org/10.1007/s10803-013-1926-4

Gandal, M. J., Haney, J., Parikshak, N. N., Leppa, V., Horvath, S., & Geschwind, D. H. (2016). Shared molecular neuropathology across major psychiatric disorders parallels polygenic overlap. *bioRxiv*. http://doi.org/10.1101/040022

Gao, S., Becker, B., Luo, L., Geng, Y., Zhao, W., Yin, Y., … Kendrick, K. M. (2016). Oxytocin, the peptide that bonds the sexes also divides them. *Proceedings of the National Academy of Sciences of the United States of America*. http://doi.org/10.1073/pnas.1602620113

Gaugler, T., Klei, L., Sanders, S. J., Bodea, C. A., Goldberg, A. P., Lee, A. B., … Buxbaum, J. D. (2014). Most genetic risk for autism resides with common variation. *Nature Genetics*, *46*(8), 881–885. http://doi.org/10.1038/ng.3039

Glass, D., Viñuela, A., Davies, M. N. M. N., Ramasamy, A., Parts, L., Knowles, D., … Consortium, M. (2013). Gene expression changes with age in skin, adipose tissue, blood and brain. *Genome Biology*, *14*(7), R75. http://doi.org/10.1186/gb-2013-14-7-r75

Goetz, S. M., Tang, L., Thomason, M. E., Diamond, M. P., Hariri, A. R., & Carre, J. M. (2014). Testosterone rapidly increases neural reactivity to threat in healthy men: a novel two-step pharmacological challenge paradigm. *Biol Psychiatry*, *76*(4), 324–331.

http://doi.org/10.1016/j.biopsych.2014.01.016

Gong, G., He, Y., Chen, Z. J., & Evans, A. C. (2012). Convergence and divergence of thickness correlations with diffusion connections across the human cerebral cortex. *NeuroImage*, *59*(2), 1239–1248. http://doi.org/10.1016/j.neuroimage.2011.08.017

Gorgolewski, K. J., Varoquaux, G., Rivera, G., Schwarz, Y., Ghosh, S. S., Maumet, C., … Margulies, D. S. (2015). NeuroVault.org: a web-based repository for collecting and sharing unthresholded statistical maps of the human brain. *Front Neuroinform*, *9*, 8. http://doi.org/10.3389/fninf.2015.00008

Greicius, M. D., Supekar, K., Menon, V., & Dougherty, R. F. (2009). Resting-state functional connectivity reflects structural connectivity in the default mode network. *Cerebral Cortex (New York, N.Y. : 1991)*, *19*(1), 72–8. http://doi.org/10.1093/cercor/bhn059

Gupta, S., Ellis, S. E., Ashar, F. N., Moes, A., Bader, J. S., Zhan, J., … Arking, D. E. (2014). Transcriptome analysis reveals dysregulation of innate immune response genes and neuronal activity-dependent genes in autism. *Nature Communications*, *5*, 5748. http://doi.org/10.1038/ncomms6748

Haber, S. N., & Knutson, B. (2010). The Reward Circuit: Linking Primate Anatomy and Human Imaging. *Neuropsychopharmacology*, *35*(1), 4–26. http://doi.org/10.1038/npp.2009.129

Happé, F. (1999). Autism: cognitive deficit or cognitive style? *Trends in Cognitive Sciences*, *3*(6), 216–222. Retrieved from http://www.ncbi.nlm.nih.gov/pubmed/10354574

Happé, F., & Frith, U. (2006). The weak coherence account: Detail-focused cognitive style in autism spectrum disorders. *Journal of Autism and Developmental Disorders*, *36*(1), 5–25. http://doi.org/10.1007/s10803-005-0039-0

Hardan, A. Y., Libove, R. A., Keshavan, M. S., Melhem, N. M., & Minshew, N. J. (2009). A Preliminary Longitudinal Magnetic Resonance Imaging Study of Brain Volume and Cortical Thickness in Autism. *Biological Psychiatry*, *66*(4), 320–326. http://doi.org/10.1016/j.biopsych.2009.04.024

Harmon-Jones, E. (2003). Early Career Award. Clarifying the emotive functions of asymmetrical frontal cortical activity. *Psychophysiology*, *40*(6), 838–48. Retrieved from http://www.ncbi.nlm.nih.gov/pubmed/14986837

Harmon-Jones, E., & Allen, J. J. (1998). Anger and frontal brain activity: EEG asymmetry consistent with approach motivation despite negative affective valence. *Journal of Personality and Social Psychology*, *74*(5), 1310–6. Retrieved from http://www.ncbi.nlm.nih.gov/pubmed/9599445

Harmon-Jones, E., Gable, P. A., & Peterson, C. K. (2010). The role of asymmetric frontal cortical activity in emotion-related phenomena: A review and update. *Biological Psychology*, *84*(3), 451–462. http://doi.org/10.1016/j.biopsycho.2009.08.010

Harris, F. J. F. J. (1978). On the use of windows for harmonic analysis with the discrete Fourier transform. *Proceedings of the IEEE*, *66*(1), 51–83. http://doi.org/10.1109/PROC.1978.10837

Hawrylycz, M. J., Lein, E. S., Guillozet-Bongaarts, A., Shen, E. H., Ng, L., Miller, J. A., … De, L. N. Van. (2012). An anatomically comprehensive atlas of the adult human brain transcriptome. *Nature*, *489*(7416), 391–399. http://doi.org/10.1038/nature11405

Hazlett, H. C., Gu, H., Munsell, B. C., Kim, S. H., Styner, M., Wolff, J. J., … Piven, J. (2017). Early brain development in infants at high risk for autism spectrum disorder. *Nature Publishing Group*, *542*(7641), 348–351. http://doi.org/10.1038/nature21369

Hermans, E. J., Henckens, M. J., Roelofs, K., & Fernández, G. (2013). Fear bradycardia and activation of the human periaqueductal grey. *NeuroImage*, *66*, 278–287. http://doi.org/10.1016/j.neuroimage.2012.10.063

Hermans, E. J., Putman, P., Baas, J. M. P., Gecks, N. M., Kenemans, J. L., & van Honk, J. (2007). Exogenous testosterone attenuates the integrated central stress response in healthy young women. *Psychoneuroendocrinology*, *32*(8–10), 1052–1061. http://doi.org/10.1016/j.psyneuen.2007.08.006

Hermans, E. J., Putman, P., Baas, J. M. P., Koppeschaar, H. P. F., & van Honk, J. (2006). A single administration of testosterone reduces fear-potentiated startle in humans. *Biol Psychiatry*, *59*(9), 872–874. Retrieved from http://www.sciencedirect.com/science/article/B6T4S-4J616MX-7/2/ad86ebc8dc48d0ce460b50bd2425e273

Hermans, E. J., Ramsey, N. F., & van Honk, J. (2008). Exogenous testosterone enhances responsiveness to social threat in the neural circuitry of social aggression in humans.

Biol Psychiatry, *63*(3), 263–270. http://doi.org/S0006-3223(07)00476-3 [pii]10.1016/j.biopsych.2007.05.013

Herting, M. M., Gautam, P., Spielberg, J. M., Dahl, R. E., & Sowell, E. R. (2015). A longitudinal study: changes in cortical thickness and surface area during pubertal maturation. *PLoS One*, *10*(3), e0119774. http://doi.org/10.1371/journal.pone.0119774

Heuchert, J. P., & McNair, D. M. (2012). *POMS 2: Profile of Mood States 2nd Edition*.

Hibar, D. P., Stein, J. L., Renteria, M. E., Arias-Vasquez, A., Desrivières, S., Jahanshad, N., … Medland, S. E. (2015). Common genetic variants influence human subcortical brain structures. *Nature*, *520*(7546), 224–229. http://doi.org/10.1038/nature14101

Hickok, G., & Poeppel, D. (2007). The cortical organization of speech processing. *Nature Reviews Neuroscience*, *8*(5), 393–402. http://doi.org/10.1038/nrn2113

Hyvärinen, A. (1999a). Fast and Robust Fixed-Point Algorithm for Independent Component Analysis. *IEEE Trans. Neur. Net.*, *10*(3), 626–634.

Hyvärinen, A. (1999b). Fast and robust fixed-point algorithms for independent component analysis. *IEEE Transactions on Neural Networks*, *10*(3), 626–634. http://doi.org/10.1109/72.761722

Insel, T. R., & Shapiro, L. E. (1992). Oxytocin receptor distribution reflects social organization in monogamous and polygamous voles. *Proceedings of the National Academy of Sciences of the United States of America*, *89*(13), 5981–5. Retrieved from http://www.ncbi.nlm.nih.gov/pubmed/1321430

Jaeggi, A. V., Trumble, B. C., Kaplan, H. S., & Gurven, M. (2015). Salivary oxytocin increases concurrently with testosterone and time away from home among returning Tsimane' hunters. *Biology Letters*, *11*(3), 20150058–20150058. http://doi.org/10.1098/rsbl.2015.0058

Jonckheere, A. R. (1954). A distribution-free k-sample test against ordered alternatives. *Biometrika*, *41*(1/2), 133–145. http://doi.org/10.2307/2333011

Just, M. A., Cherkassky, V. L., Keller, T. A., Kana, R. K., & Minshew, N. J. (2007). Functional and anatomical cortical underconnectivity in autism: evidence from an FMRI study of an executive function task and corpus callosum morphometry. *Cerebral Cortex*

(New York, N.Y. : 1991), *17*(4), 951–61. http://doi.org/10.1093/cercor/bhl006

Just, M. A., Cherkassky, V. L., Keller, T. A., & Minshew, N. J. (2004). Cortical activation and synchronization during sentence comprehension in high-functioning autism: evidence of underconnectivity. *Brain : A Journal of Neurology*, *127*(Pt 8), 1811–1821. http://doi.org/10.1093/brain/awh199

Kähkönen, S., Komssi, S., Wilenius, J., & Ilmoniemi, R. J. (2005). Prefrontal TMS produces smaller EEG responses than motor-cortex TMS: implications for rTMS treatment in depression. *Psychopharmacology*, *181*(1), 16–20. http://doi.org/10.1007/s00213-005-2197-3

Kaiser, M. D., Yang, D. Y.-J., Voos, A. C., Bennett, R. H., Gordon, I., Pretzsch, C., … Pelphrey, K. A. (2016). Brain Mechanisms for Processing Affective (and Nonaffective) Touch Are Atypical in Autism. *Cerebral Cortex*, *26*(6), 2705–2714. http://doi.org/10.1093/cercor/bhv125

Kana, R. K., Keller, T. A., Cherkassky, V. L., Minshew, N. J., & Just, M. A. (2006). Sentence comprehension in autism: thinking in pictures with decreased functional connectivity. *Brain : A Journal of Neurology*, *129*(Pt 9), 2484–93. http://doi.org/10.1093/brain/awl164

Kana, R. K., Keller, T. A., Cherkassky, V. L., Minshew, N. J., & Just, M. A. (2009). Atypical frontal-posterior synchronization of Theory of Mind regions in autism during mental state attribution. *Social Neuroscience*, *4*(2), 135–52. http://doi.org/10.1080/17470910802198510

Katz, L. C., & Shatz, C. J. (1996). Synaptic Activity and the Construction of Cortical Circuits. *Science*, *274*(5290), 1133–1138. http://doi.org/10.1126/science.274.5290.1133

Kern, J. K., Geier, D. A., King, P. G., Sykes, L. K., Mehta, J. A., & Geier, M. R. (2015). Shared Brain Connectivity Issues, Symptoms, and Comorbidities in Autism Spectrum Disorder, Attention Deficit/Hyperactivity Disorder, and Tourette Syndrome. *Brain Connectivity*, *5*(6), 321–335. http://doi.org/10.1089/brain.2014.0324

King, L. B., Walum, H., Inoue, K., Eyrich, N. W., & Young, L. J. (2015). Variation in the Oxytocin Receptor Gene Predicts Brain Region Specific Expression and Social Attachment. *Biological Psychiatry*, (32), 1–10.

http://doi.org/10.1016/j.biopsych.2015.12.008

Klumpers, F., Raemaekers, M. A. H. L., Ruigrok, A. N. V., Hermans, E. J., Kenemans, J. L., & Baas, J. M. P. (2010). Prefrontal Mechanisms of Fear Reduction After Threat Offset. *Biological Psychiatry*, *68*(11), 1031–1038. http://doi.org/10.1016/j.biopsych.2010.09.006

Kober, H., Barrett, L. F., Joseph, J., Bliss-Moreau, E., Lindquist, K. A., & Wager, T. D. (2008). Functional grouping and cortical–subcortical interactions in emotion: A meta-analysis of neuroimaging studies. *NeuroImage*, *42*(2), 998–1031. http://doi.org/10.1016/j.neuroimage.2008.03.059

Koch, S. B. J., van Zuiden, M., Nawijn, L., Frijling, J. L., Veltman, D. J., & Olff, M. (2016). Intranasal Oxytocin Normalizes Amygdala Functional Connectivity in Posttraumatic Stress Disorder. *Neuropsychopharmacology*, *41*(8), 2041–2051. http://doi.org/10.1038/npp.2016.1

Konrad, K., & Eickhoff, S. B. (2010). Is the ADHD brain wired differently? A review on structural and functional connectivity in attention deficit hyperactivity disorder. *Human Brain Mapping*, *31*(6), 904–916. http://doi.org/10.1002/hbm.21058

Koolschijn, P. C. M. P., Peper, J. S., & Crone, E. A. (2014). The influence of sex steroids on structural brain maturation in adolescence. *PLoS ONE*, *9*(1). http://doi.org/10.1371/journal.pone.0083929

Kosmicki, J., Samocha, K., Howrigan, D., Sanders, S., Slowikowski, K., Lek, M., … Daly, M. (2016). Refining the role of de novo protein truncating variants in neurodevelopmental disorders using population reference samples. *bioRxiv*, 52886. http://doi.org/10.1101/052886

Kramer, K. M., Cushing, B. S., Carter, C. S., Wu, J., & Ottinger, M. A. (2004). Sex and species differences in plasma oxytocin using an enzyme immunoassay. *Canadian Journal of Zoology*, *82*(8), 1194–1200. http://doi.org/10.1139/z04-098

Kringelbach, M. L., & Rolls, E. T. (2004). The functional neuroanatomy of the human orbitofrontal cortex: evidence from neuroimaging and neuropsychology. *Prog Neurobiol*, *72*(5), 341–372. http://doi.org/10.1016/j.pneurobio.2004.03.006

Kuleshov, M. V, Jones, M. R., Rouillard, A. D., Fernandez, N. F., Duan, Q., Wang, Z., …

Gundersen, G. W. (2016). Enrichr: a comprehensive gene set enrichment analysis web server 2016 update. *Nucleic Acids Research*, *44*(W1), W90-7. http://doi.org/10.1093/nar/gkw377

Kundu, P., Brenowitz, N. D., Voon, V., Worbe, Y., Vértes, P. E., Inati, S. J., … Bullmore, E. T. (2013). Integrated strategy for improving functional connectivity mapping using multiecho fMRI. *Proceedings of the National Academy of Sciences of the Unites States of America*, *110*(40), 16187–16192. http://doi.org/10.1073/pnas.1301725110

Kundu, P., Inati, S. J., Evans, J. W., Luh, W.-M., & Bandettini, P. A. (2012). Differentiating BOLD and non-BOLD signals in fMRI time series using multi-echo EPI. *NeuroImage*, *60*(3), 1759–1770. http://doi.org/10.1016/j.neuroimage.2011.12.028

Lai, M.-C., Lombardo, M. V., Auyeung, B., Chakrabarti, B., & Baron-cohen, S. (2015). Sex/Gender Differences and Autism: Setting the Scene for Future Research. *Journal of the American Academy of Child and Adolescent Psychiatry*, *54*(1), 11–24. http://doi.org/10.1016/j.jaac.2014.10.003

Lai, M.-C., Lombardo, M. V., Chakrabarti, B., & Baron-Cohen, S. (2013). Subgrouping the Autism "Spectrum": Reflections on DSM-5. *PLoS Biology*, *11*(4), e1001544. http://doi.org/10.1371/journal.pbio.1001544

Lai, M.-C., Lombardo, M. V., Ecker, C., Chakrabarti, B., Suckling, J., Bullmore, E. T., … Baron-cohen, S. (2014). Neuroanatomy of Individual Differences in Language in Adult Males with Autism. *Cerebral Cortex*, (October), bhu211. http://doi.org/10.1093/cercor/bhu211

Lai, M.-C., Lombardo, M. V., Suckling, J., Ruigrok, A. N. V., Chakrabarti, B., Ecker, C., … Baron-Cohen, S. (2013). Biological sex affects the neurobiology of autism. *Brain*, *136*(9), 2799–2815. http://doi.org/10.1093/brain/awt216

Lange, N., Travers, B. G., Bigler, E. D., Prigge, M. B. D., Froehlich, A. L., Nielsen, J. A., … Lainhart, J. E. (2015). Longitudinal Volumetric Brain Changes in Autism Spectrum Disorder Ages 6-35 Years. *Autism Research*, *8*(1), 82–93. http://doi.org/10.1002/aur.1427

Lee, S. H., Ripke, S., Neale, B. M., Faraone, S. V, Purcell, S. M., Perlis, R. H., … Consortium, P. G. (2013). Genetic relationship between five psychiatric disorders estimated from

genome-wide SNPs. *Nature Genetics*, *45*(9), 984–94. http://doi.org/10.1038/ng.2711

Leitner, Y., Neuroscience, H., & Leitner, Y. (2014). The co-occurrence of autism and attention deficit hyperactivity disorder in children - what do we know? *Frontiers in Human Neuroscience*, *8*(April), 268. http://doi.org/10.3389/fnhum.2014.00268

Leng, G., & Ludwig, M. (2016). Intranasal Oxytocin: Myths and Delusions. *Biological Psychiatry*, *79*(3), 243–250. http://doi.org/10.1016/j.biopsych.2015.05.003

Lerch, J. P., Worsley, K., Shaw, W. P., Greenstein, D. K., Lenroot, R. K., Giedd, J., & Evans, A. C. (2006). Mapping anatomical correlations across cerebral cortex (MACACC) using cortical thickness from MRI. *NeuroImage*, *31*(3), 993–1003. http://doi.org/10.1016/j.neuroimage.2006.01.042

Li, X., Cao, Q., Pu, F., Li, D., Fan, Y., An, L., … Wang, Y. (2015). Abnormalities of structural covariance networks in drug-naïve boys with attention deficit hyperactivity disorder. *Psychiatry Research - Neuroimaging*, *231*(3), 273–278. http://doi.org/10.1016/j.pscychresns.2015.01.006

Lindquist, K. A., Wager, T. D., Kober, H., Bliss-Moreau, E., & Barrett, L. F. (2012). The brain basis of emotion: A meta-analytic review. *Behavioral and Brain Sciences*, *35*(3), 121–143. http://doi.org/10.1017/S0140525X11000446

Lischke, A., Gamer, M., Berger, C., Grossmann, A., Hauenstein, K., Heinrichs, M., … Domes, G. (2012). Oxytocin increases amygdala reactivity to threatening scenes in females. *Psychoneuroendocrinology*, *37*(9), 1431–8. http://doi.org/10.1016/j.psyneuen.2012.01.011

Lombardo, M. V., Ashwin, E., Auyeung, B., Chakrabarti, B., Lai, M.-C., Taylor, K., … Baron-cohen, S. (2012). Fetal programming effects of testosterone on the reward system and behavioral approach tendencies in humans. *Biological Psychiatry*, *72*(10), 839–847. http://doi.org/10.1016/j.biopsych.2012.05.027

Lombardo, M. V., Ashwin, E., Auyeung, B., Chakrabarti, B., Taylor, K., Hackett, G., … Baron-Cohen, S. (2012). Fetal testosterone influences sexually dimorphic gray matter in the human brain. *Journal of Neuroscience*, *32*(2), 674–680. http://doi.org/10.1523/jneurosci.4389-11.2012

Lombardo, M. V., Auyeung, B., Holt, R. J., Waldman, J., Ruigrok, A. N. V., Mooney, N., … Kundu, P. (2016). Improving effect size estimation and statistical power with multi-echo fMRI and its impact on understanding the neural systems supporting mentalizing. *NeuroImage*. http://doi.org/10.1016/j.neuroimage.2016.07.022

Lombardo, M. V., & Baron-Cohen, S. (2011). Neural Endophenotypes of Social Behaviour in Autism Spectrum Conditions. In J. Decety & J. T. Cacioppo (Eds.), *The Oxford Handbook of Social Neuroscience*.

Lombardo, M. V., Chakrabarti, B., Bullmore, E. T., Baron-Cohen, S., Consortium, M. R. C. A., & Baron-Cohen, S. (2011). Specialization of right temporo-parietal junction for mentalizing and its relation to social impairments in autism. *NeuroImage*, *56*(3), 1832–1838. http://doi.org/10.1016/j.neuroimage.2011.02.067

Long, Z., Duan, X., Chen, H. H., Zhang, Y., & Chen, H. H. (2016). Structural covariance model reveals dynamic reconfiguration of triple networks in autism spectrum disorder. *Applied Informatics*. http://doi.org/10.1186/s40535-016-0023-0

Lord, C., Risi, S., Lambrecht, L., Cook, E. H., Leventhal, B. L., DiLavore, P. C., … Rutter, M. (2000). The autism diagnostic observation schedule-generic: a standard measure of social and communication deficits associated with the spectrum of autism. *Journal of Autism and Developmental Disorders*, *30*(3), 205–23. Retrieved from http://www.ncbi.nlm.nih.gov/pubmed/11055457

Lord, C., Rutter, M., & Le Couteur, A. (1994). Autism Diagnostic Interview-Revised: a revised version of a diagnostic interview for caregivers of individuals with possible pervasive developmental disorders. *Journal of Autism and Developmental Disorders*, *24*(5), 659–85. Retrieved from http://www.ncbi.nlm.nih.gov/pubmed/7814313

Loth, E., Spooren, W., Ham, L. M., Isaac, M. B., Auriche-Benichou, C., Banaschewski, T., … Murphy, D. G. M. (2015). Identification and validation of biomarkers for autism spectrum disorders. *Nature Reviews Drug Discovery*, *15*(1), 70–73. http://doi.org/10.1038/nrd.2015.7

Low, L. K., & Cheng, H.-J. (2006). Axon pruning: an essential step underlying the developmental plasticity of neuronal connections. *Philosophical Transactions of the Royal Society of London. Series B, Biological Sciences*, *361*(1473), 1531–44.

http://doi.org/10.1098/rstb.2006.1883

MacDonald, E., Dadds, M. R., Brennan, J. L., Williams, K., Levy, F., & Cauchi, A. J. (2011). A review of safety, side-effects and subjective reactions to intranasal oxytocin in human research. *Psychoneuroendocrinology*, *36*(8), 1114–26. http://doi.org/10.1016/j.psyneuen.2011.02.015

MacDonald, K., & Feifel, D. (2014). Oxytocin's role in anxiety: A critical appraisal. *Brain Research*, *1580*, 22–56. http://doi.org/10.1016/j.brainres.2014.01.025

Mak, E., Colloby, S. J., Thomas, A., & O'Brien, J. T. (2016). The segregated connectome of late-life depression: a combined cortical thickness and structural covariance analysis. *Neurobiology of Aging*, *48*, 212–221. http://doi.org/10.1016/j.neurobiolaging.2016.08.013

Mazur, A., & Booth, A. (1998). Testosterone and dominance in men. *Behavioral and Brain Sciences*, *21*(3), 353–397. Retrieved from http://www.ncbi.nlm.nih.gov/entrez/query.fcgi?cmd=Retrieve&db=PubMed&dopt=Citation&list_uids=10097017

McCarthy, M. M., Arnold, A. P., Ball, G. F., Blaustein, J. D., & De Vries, G. J. (2012). Sex Differences in the Brain: The Not So Inconvenient Truth. *Journal of Neuroscience*, *32*(7), 2241–2247. http://doi.org/10.1523/JNEUROSCI.5372-11.2012

McKavanagh, R., Buckley, E., & Chance, S. A. (2015). Wider minicolumns in autism: A neural basis for altered processing? *Brain*, *138*(7), 2034–2045. http://doi.org/10.1093/brain/awv110

Mehta, P., & Beer, J. (2010). Neural mechanisms of the testosterone-aggression relation: The role of orbitofrontal cortex. *J Cogn Neurosci*, *22*(10), 2357–2368. http://doi.org/10.1162/jocn.2009.21389

Mensen, V. T., Wierenga, L. M., van Dijk, S., Rijks, Y., Oranje, B., Mandl, R. C. W. W., … Durston, S. (2016). Development of cortical thickness and surface area in autism spectrum disorder. *NeuroImage: Clinical*, *13*, 215–222. http://doi.org/10.1016/j.nicl.2016.12.003

Meyer-Lindenberg, A. (2008). Impact of prosocial neuropeptides on human brain function. *Progress in Brain Research*, *170*(January 2008), 463–470.

http://doi.org/10.1016/S0079-6123(08)00436-6

Meyer-Lindenberg, A., Domes, G., Kirsch, P., & Heinrichs, M. (2011). Oxytocin and vasopressin in the human brain: social neuropeptides for translational medicine. *Nature Reviews. Neuroscience*, *12*(9), 524–38. http://doi.org/10.1038/nrn3044

Milad, M. R., & Rauch, S. L. (2007). The role of the orbitofrontal cortex in anxiety disorders. *Annals of the New York Academy of Sciences*, *1121*, 546–561. http://doi.org/annals.1401.006 [pii]10.1196/annals.1401.006

Miller, G. (2013). The promise and perils of oxytocin. *Science*, *339*(January), 267–269. Retrieved from http://www.hammiverse.com/instructionalunits/chemical_neuralsignaling/hw/oxytocin_article.pdf

Minka, T. P. (2001). Automatic choice of dimensionality for PCA. *Advances in Neural Information Processing Systems*, (514), 598–604. http://doi.org/10.1.1.19.9545

Minshew, N. J., Goldstein, G., & Siegel, D. J. (1997). Neuropsychologic functioning in autism: profile of a complex information processing disorder. *Journal of the International Neuropsychological Society : JINS*, *3*(4), 303–16. Retrieved from http://www.ncbi.nlm.nih.gov/pubmed/9260440

Mobbs, D., Petrovic, P., Marchant, J. L., Hassabis, D., Weiskopf, N., Seymour, B., … Frith, C. D. (2007). When fear is near: Threat imminence elicits prefrontal-periaqueductal gray shifts in humans. *Science*, *317*(5841), 1079–1083. http://doi.org/10.1126/science.1144298

Modahl, C., Green, L., Fein, D., Morris, M., Waterhouse, L., Feinstein, C., & Levin, H. (1998). Plasma oxytocin levels in autistic children. *Biological Psychiatry*, *43*(4), 270–277. http://doi.org/10.1016/S0006-3223(97)00439-3

Modi, M. E., & Young, L. J. (2012). The oxytocin system in drug discovery for autism: Animal models and novel therapeutic strategies. *Hormones and Behavior*, *61*(3), 340–350. http://doi.org/10.1016/j.yhbeh.2011.12.010.The

Mogil, J. S. (2012). Sex differences in pain and pain inhibition: multiple explanations of a controversial phenomenon. *Nature Reviews Neuroscience*, *13*(12), 859–866. http://doi.org/10.1038/nrn3360

Montoya, E. R., Terburg, D., Bos, P. A., Will, G.-J., Buskens, V., Raub, W., & van Honk, J. (2013). Testosterone administration modulates moral judgments depending on second-to-fourth digit ratio. *Psychoneuroendocrinology*, *38*(8), 1362–1369. http://doi.org/10.1016/j.psyneuen.2012.12.001

Montoya, E. R., van Honk, J., Bos, P. A., & Terburg, D. (2015). Dissociated neural effects of cortisol depending on threat escapability. *Human Brain Mapping*, *36*(11), 4304–4316. http://doi.org/10.1002/hbm.22918

Morris, L. S., Kundu, P., Baek, K., Irvine, M. A., Mechelmans, D. J., Wood, J., … Voon, V. (2016). Jumping the Gun: Mapping Neural Correlates of Waiting Impulsivity and Relevance Across Alcohol Misuse. *Biological Psychiatry*, *79*(6), 499–507. http://doi.org/10.1016/j.biopsych.2015.06.009

Mostert, J. C., Shumskaya, E., Mennes, M., Onnink, A. M. H., Hoogman, M., Kan, C. C., … Arias-Vasquez, A. (2016). Characterising resting-state functional connectivity in a large sample of adults with ADHD. *Progress in Neuro-Psychopharmacology and Biological Psychiatry*, *67*, 82–91. http://doi.org/10.1016/j.pnpbp.2016.01.011

Murray, E. A., & Izquierdo, A. (2007). Orbitofrontal cortex and amygdala contributions to affect and action in primates. *Annals of the New York Academy of Sciences*, *1121*, 273–296. http://doi.org/annals.1401.021 [pii]10.1196/annals.1401.021

Nelson, H., & Wilson, J. (1991). *National Adult Reading Test (NART)*. Windsor, UK: NFER-Nelson.

Newman, M. (2006). Modularity and community structure in networks. *Proceedings of the National Academy of …*, *103*(23), 8577–82. http://doi.org/10.1073/pnas.0601602103

Newman, M. (2010). *Networks: and Introduction* (1st ed.). Oxford University Press.

Noonan, S. K., Haist, F., & Müller, R.-A. (2009). Aberrant functional connectivity in autism: evidence from low-frequency BOLD signal fluctuations. *Brain Research*, *1262*, 48–63. http://doi.org/10.1016/j.brainres.2008.12.076

Nordahl, C. W., Dierker, D., Mostafavi, I., Schumann, C. M., Rivera, S. M., Amaral, D. G., … Essen, D. C. Van. (2007). Cortical Folding Abnormalities in Autism Revealed by Surface-Based Morphometry. *The Journal of Neuroscience*, *27*(43), 11725–11735.

http://doi.org/10.1523/JNEUROSCI.0777-07.2007

Ohnishi, T., Matsuda, H., Hashimoto, T., Kunihiro, T., Nishikawa, M., Uema, T., & Sasaki, M. (2000). Abnormal regional cerebral blood flow in childhood autism. *Brain*, *123 (Pt 9*, 1838–44. http://doi.org/10.1093/brain/123.9.1838

Ortiz, E., Stingl, K., Münßinger, J., Braun, C., Preissl, H., & Belardinelli, P. (2012). Weighted Phase Lag Index and Graph Analysis: Preliminary Investigation of Functional Connectivity during Resting State in Children. *Computational and Mathematical Methods in Medicine*, *2012*, 1–8. http://doi.org/10.1155/2012/186353

Ozonoff, S., Pennington, B. F., & Rogers, S. J. (1991). Executive function deficits in high-functioning autistic individuals: relationship to theory of mind. *Journal of Child Psychology and Psychiatry, and Allied Disciplines*, *32*(7), 1081–1105. Retrieved from http://onlinelibrary.wiley.com/doi/10.1111/j.1469-7610.1991.tb00351.x/abstract

Paloyelis, Y., Krahé, C., Maltezos, S., Williams, S. C., Howard, M. A., & Fotopoulou, A. (2016). The Analgesic Effect of Oxytocin in Humans: A Double-Blind, Placebo-Controlled Cross-Over Study Using Laser-Evoked Potentials. *Journal of Neuroendocrinology*, *28*(4). http://doi.org/10.1111/jne.12347

Panizzon, M. S., Fennema-Notestine, C., Eyler, L. T., Jernigan, T. L., Prom-Wormley, E., Neale, M., … Kremen, W. S. (2009). Distinct genetic influences on cortical surface area and cortical thickness. *Cerebral Cortex*, *19*, 2728–2735. http://doi.org/10.1093/cercor/bhp026

Parikshak, N. N., Luo, R., Zhang, A., Won, H., Lowe, J. K., Chandran, V., … Geschwind, D. H. (2013). Integrative Functional Genomic Analyses Implicate Specific Molecular Pathways and Circuits in Autism. *Cell*, *155*(5), 1008–1021. http://doi.org/10.1016/j.cell.2013.10.031

Parikshak, N. N., Swarup, V., Belgard, T. G., Irimia, M., Ramaswami, G., Gandal, M. J., … Geschwind, D. H. (2016). Genome-wide changes in lncRNA, splicing, and regional gene expression patterns in autism. *Nature*, *540*(7633), 423–427. http://doi.org/10.1038/nature20612

Parikshak, N. N., Swarup, V., Belgard, T. G., Irimia, M., Ramaswami, G., Gandal, M. J., … Geschwind, D. H. (2016). regional gene expression patterns in autism. *Nature*

Publishing Group, *540*(7633), 423–427. http://doi.org/10.1038/nature20612

Patel, A. X., Kundu, P., Rubinov, M., Jones, P. S., Vértes, P. E., Ersche, K. D., … Bullmore, E. T. (2014). A wavelet method for modeling and despiking motion artifacts from resting-state fMRI time series. *NeuroImage*, *95*, 287–304. http://doi.org/10.1016/j.neuroimage.2014.03.012

Paul, L. K., Corsello, C., Kennedy, D. P., & Adolphs, R. (2014). Agenesis of the corpus callosum and autism: a comprehensive comparison. *Brain : A Journal of Neurology*, *137*(Pt 6), 1813–29. http://doi.org/10.1093/brain/awu070

Peper, J. S., Brouwer, R. M., Schnack, H. G., van Baal, G. C., van Leeuwen, M., van den Berg, S. M., … Hulshoff Pol, H. E. (2009). Sex steroids and brain structure in pubertal boys and girls. *Psychoneuroendocrinology*, *34*(3), 332–342. http://doi.org/10.1016/j.psyneuen.2008.09.012

Peper, J. S., Brouwer, R. M., van Baal, G. C. M., Schnack, H. G., van Leeuwen, M., Boomsma, D. I., … Pol, H. E. H. (2009). Does having a twin brother make for a bigger brain? *European Journal of Endocrinology*, *160*(5), 739–746. http://doi.org/10.1530/EJE-08-0915

Peper, J. S., Koolschijn, P. C. M. P., & Ce, P. (2012). Sex Steroids and the Organization of the Human Brain. *Journal of Neuroscience*, *32*(20), 6745–6746. http://doi.org/10.1523/JNEUROSCI.1012-12.2012

Peper, J. S., van den Heuvel, M. P., Mandl, R. C. W. W., Pol, H. E., & van Honk, J. (2011). Sex steroids and connectivity in the human brain: a review of neuroimaging studies. *Psychoneuroendocrinology*, *36*(8), 1101–1113. Retrieved from http://www.ncbi.nlm.nih.gov/pubmed/21641727

Peters, S., Jolles, D. J., Duijvenvoorde, A. C. K. Van, Crone, E. A., & Peper, J. S. (2015). The link between testosterone and amygdala — orbitofrontal cortex connectivity in adolescent alcohol use. *Psychoneuroendocrinology*, *53*, 117–126. http://doi.org/10.1016/j.psyneuen.2015.01.004

Pierce, K., Müller, R.-A., Ambrose, J., Allen, G., & Courchesne, E. (2001). Face processing occurs outside the fusiform “face area” in autism: evidence from functional MRI. *Brain : A Journal of Neurology*, *124*(Pt 10), 2059–73. Retrieved from

http://www.ncbi.nlm.nih.gov/pubmed/11571222

Plaisted Grant, K., Davis, G., Grant, K. P., & Davis, G. (2009). Perception and apperception in autism: rejecting the inverse assumption. *Philosophical Transactions of the Royal Society of London Series B, Biological Sciences*, *364*(1522), 1393–1398. http://doi.org/10.1098/rstb.2009.0001

Power, J. D., Barnes, K. A., Snyder, A. Z., Schlaggar, B. L., & Petersen, S. E. (2012). Spurious but systematic correlations in functional connectivity MRI networks arise from subject motion. *Neuroimage*, *59*(3), 2142–2154. http://doi.org/10.1016/j.neuroimage.2011.10.018

Quintana, D. S., Guastella, A. J., Westlye, L. T., & Andreassen, O. A. (2016). The promise and pitfalls of intranasally administering psychopharmacological agents for the treatment of psychiatric disorders. *Molecular Psychiatry*, *21*(1), 29–38. http://doi.org/10.1038/mp.2015.166

Rane, P., Cochran, D., Hodge, S. M., Haselgrove, C., Kennedy, D. N., & Frazier, J. A. (2015). Connectivity in Autism: A Review of MRI Connectivity Studies. *Harvard Review of Psychiatry*, *23*(4), 223–44. http://doi.org/10.1097/HRP.0000000000000072

Rash, J. A., Aguirre-Camacho, A., & Campbell, T. S. (2013). Oxytocin and Pain. *The Clinical Journal of Pain*, 1. http://doi.org/10.1097/AJP.0b013e31829f57df

Ray, S., Miller, M., Karalunas, S., Robertson, C., Grayson, D. S., Cary, R. P., … Fair, D. A. (2014). Structural and functional connectivity of the human brain in autism spectrum disorders and attention-deficit/hyperactivity disorder: A rich club-organization study. *Human Brain Mapping*, *35*(12), 6032–6048. http://doi.org/10.1002/hbm.22603

Raznahan, A., Lerch, J. P., Lee, N., Greenstein, D., Wallace, G. L., Stockman, M., … Giedd, J. N. (2011). Patterns of coordinated anatomical change in human cortical development: a longitudinal neuroimaging study of maturational coupling. *Neuron*, *72*(5), 873–84. http://doi.org/10.1016/j.neuron.2011.09.028

Riem, M. M. E., Ijzendoorn, M. H. Van, Tops, M., Boksem, M. a S., Rombouts, S. A. R. B., Bakermans-Kranenburg, M. J., … Bakermans-Kranenburg, M. J. (2012). No Laughing Matter: Intranasal Oxytocin Administration Changes Functional Brain Connectivity

during Exposure to Infant Laughter. *Neuropsychopharmacology*, *37*(9), 2174–2174. http://doi.org/10.1038/npp.2012.27

Rilling, J. K., Demarco, A. C., Hackett, P. D., Chen, X., Gautam, P., Stair, S., … Pagnoni, G. (2013). Sex differences in the neural and behavioral response to intranasal oxytocin and vasopressin during human social interaction. *Psychoneuroendocrinology*. http://doi.org/10.1016/j.psyneuen.2013.09.022

Rohlfs, P., & Ramírez, J. M. (2006). AGGRESSION AND BRAIN ASYMMETRIES: A THEORETICAL REVIEW. *Aggression and Violent Behavior*, *11*(3), 283–297.

Romero-garcia, R., Atienza, M., Clemmensen, L. H., & Cantero, J. L. (2012). Effects of network resolution on topological properties of human neocortex. *NeuroImage*, *59*(4), 3522–3532. http://doi.org/10.1016/j.neuroimage.2011.10.086

Romme, I. A. C. C., de Reus, M. A., Ophoff, R. A., Kahn, R. S., van den Heuvel, M. P., Reus, M. A. De, & Heuvel, M. P. Van Den. (2016). Connectome Disconnectivity and Cortical Gene Expression in Patients With Schizophrenia. *Biological Psychiatry*, *81*(6), 1–8. http://doi.org/10.1016/j.biopsych.2016.07.012

Rommelse, N. N. J. J., Franke, B., Geurts, H. M., Hartman, C. A., Buitelaar, J. K., Geurts, H. M., & Hartman, C. A. (2010). Shared heritability of attention-deficit/hyperactivity disorder and autism spectrum disorder. *European Child & Adolescent Psychiatry*, *19*(3), 281–295. http://doi.org/10.1007/s00787-010-0092-x

Rommelse, N. N. J. J., Geurts, H. M., Franke, B., Buitelaar, J. K., & Hartman, C. A. (2011). A review on cognitive and brain endophenotypes that may be common in autism spectrum disorder and attention-deficit/hyperactivity disorder and facilitate the search for pleiotropic genes. *Neuroscience & Biobehavioral Reviews*, *35*(6), 1363–1396. http://doi.org/10.1016/j.neubiorev.2011.02.015

Rubenstein, J. L., & Merzenich, M. (2003). Model of autism: increased ratio of excitation/inhibition in key neural systems. *Genes, Brain and Behavior*, *2*, 255–267. http://doi.org/10.1046/j.1601-183X.2003.00037.x

Rubinov, M., & Sporns, O. (2010). Complex network measures of brain connectivity: Uses and interpretations. *NeuroImage*, *52*, 1059–69. http://doi.org/10.1016/j.neuroimage.2009.10.003

Ruigrok, A. N. V., Salimi-Khorshidi, G., Lai, M.-C., Baron-Cohen, S., Lombardo, M. V., Tait, R. J., & Suckling, J. (2014). A meta-analysis of sex differences in human brain structure. *Neuroscience & Biobehavioral Reviews*, *39*, 34–50. http://doi.org/10.1016/j.neubiorev.2013.12.004

Rybak, M., Crayton, J. W., Young, I. J., Herba, E., & Konopka, L. M. (2006). Frontal alpha power asymmetry in aggressive children and adolescents with mood and disruptive behavior disorders. *Clinical EEG and Neuroscience*, *37*(1), 16–24. Retrieved from http://www.ncbi.nlm.nih.gov/pubmed/16475480

Salmi, J., Roine, U., Glerean, E., Lahnakoski, J., Nieminen-Von Wendt, T., Tani, P., … Sams, M. (2013). The brains of high functioning autistic individuals do not synchronize with those of others. *NeuroImage: Clinical*, *3*, 489–497. http://doi.org/10.1016/j.nicl.2013.10.011

Sanders, S. J., He, X., Willsey, A. J., Ercan-Sencicek, A. G., Samocha, K. E., Cicek, A. E., … State, M. W. (2015). Insights into Autism Spectrum Disorder Genomic Architecture and Biology from 71 Risk Loci. *Neuron*, *87*(6), 1215–1233. http://doi.org/10.1016/j.neuron.2015.09.016

Schaer, M., Ottet, M.-C., Scariati, E., Dukes, D., Franchini, M., Eliez, S., & Glaser, B. (2013). Decreased frontal gyrification correlates with altered connectivity in children with autism. *Frontiers in Human Neuroscience*, *7*(November), 750. http://doi.org/10.3389/fnhum.2013.00750

Schmitt, J. E., Lenroot, R. K., Ordaz, S. E., Wallace, G. L., Lerch, J. P., Evans, A. C., … Giedd, J. N. (2009). Variance decomposition of MRI-based covariance maps using genetically informative samples and structural equation modeling. *NeuroImage*, *47*(1), 56–64. http://doi.org/10.1016/j.neuroimage.2008.06.039

Schutter, D. J. L. G., de Weijer, A. D., Meuwese, J. D. I., Morgan, B., & van Honk, J. (2008). Interrelations between motivational stance, cortical excitability, and the frontal electroencephalogram asymmetry of emotion: a transcranial magnetic stimulation study. *Human Brain Mapping*, *29*(5), 574–80. http://doi.org/10.1002/hbm.20417

Schutter, D. J. L. G., & van Honk, J. (2004). Decoupling of midfrontal delta-beta oscillations after testosterone administration. *International Journal of Psychophysiology*, *53*(1),

71–73. http://doi.org/10.1016/j.ijpsycho.2003.12.012S0167876003002794 [pii]

Seeley, W. W., Crawford, R. K., Zhou, J., Miller, B. L., & Greicius, M. D. (2009). Neurodegenerative Diseases Target Large-Scale Human Brain Networks. *Neuron*, *62*(1), 42–52. http://doi.org/10.1016/j.neuron.2009.03.024

Seung, H. (2011). Towards functional connectomics. *Nature*, *471*, 170–171.

Sharda, M., Khundrakpam, B. S., Evans, A. C., & Singh, N. C. (2014). Disruption of structural covariance networks for language in autism is modulated by verbal ability. *Brain Structure & Function*. http://doi.org/10.1007/s00429-014-0953-z

Shaw, P., Eckstrand, K., Sharp, W., Blumenthal, J., Lerch, J. P., Greenstein, D., … Rapoport, J. L. (2007). Attention-deficit/hyperactivity disorder is characterized by a delay in cortical maturation. *Proceedings of the National Academy of Sciences of the United States of America*, *104*(49), 19649–54. http://doi.org/10.1073/pnas.0707741104

Silva, F. H. L. da. (1999). Dynamics of EEGs as signals of neuronal populations: models and theoretical considerations. In E. Niedermeyer & F. H. L. da Silva (Eds.), *Electroencephalography: Basic Principles, Clinical Applications and Related Fields* (4th ed., pp. 76–92). Baltimore: Williams and Wilkins.

Singer, T., Snozzi, R., Bird, G., Petrovic, P., Silani, G., Heinrichs, M., & Dolan, R. J. (2008). Effects of oxytocin and prosocial behavior on brain responses to direct and vicariously experienced pain. *Emotion*, *8*(6), 781–791. http://doi.org/10.1037/a0014195

Smith, A. L., Barnhart, T., Ahlers, E., Abbott, D., Freeman, S. M., Young, L. J., & Goodman, M. M. (2013). Investigation of three PET ligands as oxytocin receptor biomarkers in marmoset models. *J Nucl Med*, *54*(1752).

Smith, A. L., Freeman, S. M., Voll, R. J., Young, L. J., & Goodman, M. M. (2013). Investigation of an F-18 oxytocin receptor selective ligand via PET imaging. *Bioorganic & Medicinal Chemistry Letters*, *23*(19), 5415–20. http://doi.org/10.1016/j.bmcl.2013.07.045

Smith, E., Thurm, A., Greenstein, D., Farmer, C., Swedo, S., Giedd, J. N., & Raznahan, A. (2016). Cortical thickness change in autism during early childhood. *Human Brain Mapping*, *37*(7), 2616–2629. http://doi.org/10.1002/hbm.23195

Smith, S. M., Nichols, T. E., Vidaurre, D., Winkler, A. M., Behrens, T. E. J., Glasser, M. F., … Miller, K. L. (2015). A positive-negative mode of population covariation links brain connectivity, demographics and behavior. *Nature Neuroscience*, *18*(11), 1565–1567. http://doi.org/10.1038/nn.4125

Smith, S. M., Vidaurre, D., Beckmann, C. F. C. F., Glasser, M. F., Jenkinson, M., Miller, K. L., … Van Essen, D. C. (2013). Functional connectomics from resting-state fMRI. *Trends in Cognitive Sciences*, *17*(12), 666–682. http://doi.org/10.1016/j.tics.2013.09.016

Somel, M., Guo, S., Fu, N., Yan, Z., Hu, H. Y. H., Xu, Y., … Khaitovich, P. (2010). MicroRNA, mRNA, and protein expression link development and aging in human and macaque brain. *Genome Research*, *20*(9), 1207–1218. http://doi.org/10.1101/gr.106849.110

Soreq, L., Rose, J., Soreq, E., Hardy, J., Trabzuni, D., Cookson, M. R., … Ule, J. (2017). Major Shifts in Glial Regional Identity Are a Transcriptional Hallmark of Human Brain Aging. *Cell Reports*, *18*(2), 557–570. http://doi.org/10.1016/j.celrep.2016.12.011

Sowell, E. R., Peterson, B. S., Kan, E., Woods, R. P., Yoshii, J., Bansal, R., … Toga, A. W. (2007). Sex differences in cortical thickness mapped in 176 healthy individuals between 7 and 87 years of age. *Cerebral Cortex (New York, N.Y. : 1991)*, *17*(7), 1550–60. http://doi.org/10.1093/cercor/bhl066

Sporns, O. (2011). *Networks of the Brain*. Cambridge: MIT Press.

Sporns, O., Tononi, G., & Kötter, R. (2005). The Human Connectome: A Structural Description of the Human Brain. *PLoS Computational Biology*, *1*(4), e42. http://doi.org/10.1371/journal.pcbi.0010042

Sripada, C. S., Phan, K. L., Labuschagne, I., Welsh, R., Nathan, P. J., & Wood, A. (2013). Oxytocin enhances resting-state connectivity between amygdala and medial frontal cortex. *The International Journal of Neuropsychopharmacology / Official Scientific Journal of the Collegium Internationale Neuropsychopharmacologicum (CINP)*, *16*(2), 255–60. http://doi.org/10.1017/S1461145712000533

Stalnaker, T. A., Cooch, N. K., & Schoenbaum, G. (2015). What the orbitofrontal cortex does not do. *Nat Neurosci*, *18*(5), 620–627. http://doi.org/10.1038/nn.3982

Stam, C. J., Nolte, G., & Daffertshofer, A. (2007). Phase lag index: Assessment of functional connectivity from multi channel EEG and MEG with diminished bias from common

sources. *Human Brain Mapping*, *28*(11), 1178–1193. http://doi.org/10.1002/hbm.20346

Stam, C. J., & Reijneveld, J. C. (2007). Graph theoretical analysis of complex networks in the brain. *Nonlinear Biomedical Physics*, *1*(1), 3. http://doi.org/10.1186/1753-4631-1-3

Steiger, J. H. (1980). Test for comparing elements of a correlation matrix. *Psychological Bulletin*, *87*(2), 245–251.

Sterling, T. D. (1959). Publication Decisions and Their Possible Effects on Inferences Drawn from Tests of Significance--Or Vice Versa. *Journal of the American Statistical Association*, *54*(285), 30. http://doi.org/10.2307/2282137

Stessman, H. A. F., Xiong, B., Coe, B. P., Wang, T., Hoekzema, K., Fenckova, M., … Eichler, E. E. (2017). Targeted sequencing identifies 91 neurodevelopmental-disorder risk genes with autism and developmental-disability biases. *Nature Genetics*, (January). http://doi.org/10.1038/ng.3792

Striepens, N., Kendrick, K. M., Hanking, V., Landgraf, R., Wüllner, U., Maier, W., & Hurlemann, R. (2013). Elevated cerebrospinal fluid and blood concentrations of oxytocin following its intranasal administration in humans. *Scientific Reports*, *3*, 3440. http://doi.org/10.1038/srep03440

Stroganova, T. a, Nygren, G., Tsetlin, M. M., Posikera, I. N., Gillberg, C., Elam, M., & Orekhova, E. V. (2007). Abnormal EEG lateralization in boys with autism. *Clinical Neurophysiology : Official Journal of the International Federation of Clinical Neurophysiology*, *118*(8), 1842–54. http://doi.org/10.1016/j.clinph.2007.05.005

Tang, G., Gudsnuk, K., Kuo, S. H., Cotrina, M. L., Rosoklija, G., Sosunov, A., … Sulzer, D. (2014). Loss of mTOR-Dependent Macroautophagy Causes Autistic-like Synaptic Pruning Deficits. *Neuron*, *83*(5), 1131–1143. http://doi.org/10.1016/j.neuron.2014.07.040

Terburg, D., Aarts, H., & van Honk, J. (2012). Testosterone affects gaze aversion from angry faces outside of conscious awareness. *Psychological Science*, *23*(5), 459–63. http://doi.org/10.1177/0956797611433336

Terburg, D., Hooiveld, N., Aarts, H., Kenemans, J. L., & van Honk, J. (2011). Eye tracking

unconscious face-to-face confrontations: dominance motives prolong gaze to masked angry faces. *Psychological Science*, *22*(3), 314–9. http://doi.org/10.1177/0956797611398492

Terburg, D., Syal, S., Rosenberger, L. A., Heany, S. J., Stein, D. J., & van Honk, J. (2016). Testosterone abolishes implicit subordination in social anxiety. *Psychoneuroendocrinology*, *72*, 205–211. http://doi.org/10.1016/j.psyneuen.2016.07.203

Terburg, D., & van Honk, J. (2013). Approach–avoidance versus dominance–submissiveness: A multilevel neural framework on how testosterone promotes social status. *Emotion Review*, *5*(3), 296–302. http://doi.org/10.1177/1754073913477510

Tewarie, P., van Dellen, E., Hillebrand, A., & Stam, C. J. (2015). The minimum spanning tree: An unbiased method for brain network analysis. *NeuroImage*, *104*, 177–188. http://doi.org/10.1016/j.neuroimage.2014.10.015

Thatcher, R. W., Krause, P. J., & Hrybyk, M. (1986). Cortico-cortical associations and EEG coherence: a two-compartmental model. *Electroencephalography and Clinical Neurophysiology*, *64*(2), 123–43. Retrieved from http://www.ncbi.nlm.nih.gov/pubmed/2424729

Tick, B., Bolton, P., Happé, F., Rutter, M., & Rijsdijk, F. (2016). Heritability of autism spectrum disorders: a meta-analysis of twin studies. *Journal of Child Psychology and Psychiatry, and Allied Disciplines*, *57*(5), 585–95. http://doi.org/10.1111/jcpp.12499

Toal, F., Murphy, D. G. M., & Murphy, K. C. (2005). Autistic-spectrum disorders: lessons from neuroimaging. *The British Journal of Psychiatry*, *187*(5), 395–397. http://doi.org/10.1192/bjp.187.5.395

Tomasi, D., & Volkow, N. (2012). Abnormal functional connectivity in children with attention-deficit/hyperactivity disorder. *Biological Psychiatry*, *71*(5), 443–450. http://doi.org/10.1016/j.biopsych.2011.11.003.Abnormal

Tuiten, A., van Honk, J., Koppeschaar, H. P. F., Bernaards, C., Thijssen, J., & Verbaten, R. (2000). Time course of effects of testosterone administration on sexual arousal in women. *Archives of General Psychiatry*, *57*(2), 146–149. Retrieved from

http://www.ncbi.nlm.nih.gov/pubmed/10665617

Tzourio-Mazoyer, N., Landeau, B., Papathanassiou, D., Crivello, F., Etard, O., Delcroix, N., … Joliot, M. (2002). Automated anatomical labeling of activations in SPM using a macroscopic anatomical parcellation of the MNI MRI single-subject brain. *NeuroImage*, *15*(1), 273–289. http://doi.org/10.1006/nimg.2001.0978S1053811901909784 [pii]

Uddin, L., Supekar, K., & Menon, V. (2010). Typical and atypical development of functional human brain networks: insights from resting-state FMRI. *Frontiers in Systems Neuroscience*, *4*(May), 21. http://doi.org/10.3389/fnsys.2010.00021

van Diessen, E., Numan, T., van Dellen, E., van der Kooi, A. W. W., Boersma, M., Hofman, D., … Stam, C. J. (2014). Opportunities and methodological challenges in EEG and MEG resting state functional brain network research. *Clinical Neurophysiology : Official Journal of the International Federation of Clinical Neurophysiology*. http://doi.org/10.1016/j.clinph.2014.11.018

Van Dijk, K. R. a, Sabuncu, M. R., & Buckner, R. L. (2012). The influence of head motion on intrinsic functional connectivity MRI. *NeuroImage*, *59*(1), 431–8. http://doi.org/10.1016/j.neuroimage.2011.07.044

van Honk, J., Bos, P. A., & Terburg, D. (2014). Testosterone and Dominance in Humans: Behavioral and Brain Mechanisms. *New Frontiers in Social Neuroscience*, 201–214.

Van Honk, J., Montoya, E. R., Bos, P. a., Vugt, M. Van, Terburg, D., van Honk, J., … Terburg, D. (2012). New evidence on testosterone and cooperation. *Nature*, *485*(7399), E4–E5. http://doi.org/10.1038/nature11136

van Honk, J., Schutter, D. J., Bos, P. A., Kruijt, A.-W., Lentjes, E. G., & Baron-Cohen, S. (2011). Testosterone administration impairs cognitive empathy in women depending on second-to-fourth digit ratio. *Proceedings of the National Academy of Sciences*, *108*(8), 3448–3452. http://doi.org/10.1073/pnas.1011891108

van Honk, J., Terburg, D., Bos, P. A., Honk, J. Van, Terburg, D., Bos, P. A., … Bos, P. A. (2011). Further notes on testosterone as a social hormone. *Trends in Cognitive Sciences*, *15*(7), 291–292. http://doi.org/10.1016/j.tics.2011.05.003

van Honk, J., Tuiten, A., Hermans, E. J., Putman, P., Koppeschaar, H. P. F., Thijssen, J., … van

Doornen, L. (2001). A single administration of testosterone induces cardiac accelerative responses to angry faces in healthy young women. *Behavioral Neuroscience*, *115*(1), 238–242. Retrieved from http://www.ncbi.nlm.nih.gov/entrez/query.fcgi?cmd=Retrieve&db=PubMed&dopt=Citation&list_uids=11256447

van Wijk, B. C. M., Stam, C. J., Daffertshofer, A., Wijk, B. C. M. Van, Stam, C. J., & Daffertshofer, A. (2010). Comparing brain networks of different size and connectivity density using graph theory. *PLoS ONE*, *5*(10). http://doi.org/10.1371/journal.pone.0013701

van Wingen, G., Mattern, C., Verkes, R. J., Buitelaar, J. K., & Fernández, G. (2010). Testosterone reduces amygdala-orbitofrontal cortex coupling. *Psychoneuroendocrinology*, *35*(1), 105–113. http://doi.org/10.1016/j.psyneuen.2009.09.007

Vinck, M., Oostenveld, R., Van Wingerden, M., Battaglia, F., & Pennartz, C. M. A. A. (2011). An improved index of phase-synchronization for electrophysiological data in the presence of volume-conduction, noise and sample-size bias. *NeuroImage*, *55*(4), 1548–1565. http://doi.org/10.1016/j.neuroimage.2011.01.055

Vissers, M. E., Cohen, M. X., & Geurts, H. M. (2012). Brain connectivity and high functioning autism: a promising path of research that needs refined models, methodological convergence, and stronger behavioral links. *Neuroscience and Biobehavioral Reviews*, *36*(1), 604–25. http://doi.org/10.1016/j.neubiorev.2011.09.003

Voineagu, I., Wang, X., Johnston, P., Lowe, J. K., Tian, Y., Horvath, S., … Geschwind, D. H. (2011). Transcriptomic analysis of autistic brain reveals convergent molecular pathology. *Nature*, *474*(7351), 380–384. http://doi.org/10.1038/nature10110

Volman, I., Toni, I., Verhagen, L., & Roelofs, K. (2011). Endogenous testosterone modulates prefrontal-amygdala connectivity during social emotional behavior. *Cerebral Cortex*, *21*(10), 2282–2290. http://doi.org/10.1093/cercor/bhr001

Volman, I., von Borries, A. K., Bulten, B. H., Verkes, R. J., Toni, I., Roelofs, K., … Jan, R. (2016). Testosterone Modulates Altered Prefrontal Control of Emotional Actions in Psychopathic Offenders(1,2,3). *Eneuro*, *3*(1). http://doi.org/10.1523/ENEURO.0107-15.2016

von dem Hagen, E., Stoyanova, R. S., Baron-Cohen, S., & Calder, A. J. (2013). Reduced functional connectivity within and between "social" resting state networks in autism spectrum conditions. *Social Cognitive and Affective Neuroscience*, *8*(6), 694–701. http://doi.org/10.1093/scan/nss053

Von Economo, C., & Koskinas, G. N. (2008). *Atlas of Cytoarchitectonics of the Adult Human Cerebral Cortex*. (L. C. Triarhou, Ed.) (1st ed.). Thessaloniki: Karger.

Wager, T. D., Atlas, L. Y., Lindquist, M. A., Roy, M., Woo, C.-W., & Kross, E. (2013). An fMRI-Based Neurologic Signature of Physical Pain. *New England Journal of Medicine*, *368*(15), 1388–1397. http://doi.org/10.1056/NEJMoa1204471

Wager, T. D., Keller, M. C., Lacey, S. C., & Jonides, J. (2005). Increased sensitivity in neuroimaging analyses using robust regression. *NeuroImage*, *26*(1), 99–113. http://doi.org/10.1016/j.neuroimage.2005.01.011

Walum, H., Waldman, I. D., & Young, L. J. (2016). Statistical and Methodological Considerations for the Interpretation of Intranasal Oxytocin Studies. *Biological Psychiatry*, *79*(3), 251–257. http://doi.org/10.1016/j.biopsych.2015.06.016

Wang, J., Barstein, J., Ethridge, L. E., Mosconi, M. W., Takarae, Y., & Sweeney, J. A. (2013). Resting state EEG abnormalities in autism spectrum disorders. *Journal of Neurodevelopmental Disorders*, *5*(1), 1–14. http://doi.org/10.1186/1866-1955-5-24

Warrier, V., Bethlehem, R. A. I., Geschwind, D., & Baron-Cohen, S. (2017). Genetic overlap between educational attainment, schizophrenia and autism. *bioRxiv*. http://doi.org/doi.org/10.1101/093575

Watanabe, T., Abe, O., Kuwabara, H., Yahata, N., Takano, Y., Iwashiro, N., … Yamasue, H. (2013). Mitigation of Sociocommunicational Deficits of Autism Through Oxytocin-Induced Recovery of Medial Prefrontal Activity. *JAMA Psychiatry*, *71*(2), 166–75. http://doi.org/10.1001/jamapsychiatry.2013.3181

Watanabe, T., Kuroda, M., Kuwabara, H., Aoki, Y., Iwashiro, N., Tatsunobu, N., … Yamasue, H. (2015). Clinical and neural effects of six-week administration of oxytocin on core symptoms of autism. *Brain*, *138*(11), 3400–3412. http://doi.org/10.1093/brain/awv249

Wechsler, D. (1999). *Wechsler Abbreviated Scale of Intelligence.* New York, NY: The

Psychological Corporation: Harcourt Brace & Company.

Weisman, O., Zagoory-Sharon, O., & Feldman, R. (2014). Oxytocin administration, salivary testosterone, and father-infant social behavior. *Progress in Neuro-Psychopharmacology & Biological Psychiatry*, *49*, 47–52. http://doi.org/10.1016/j.pnpbp.2013.11.006

Werling, D. M., & Geschwind, D. H. D. H. (2013). Sex differences in autism spectrum disorders. *Current Opinion in Neurology*, *26*(2), 146–153. http://doi.org/10.1097/WCO.0b013e32835ee548.Sex

Werling, D. M., Parikshak, N. N., & Geschwind, D. H. (2016). Gene expression in human brain implicates sexually dimorphic pathways in autism spectrum disorders. *Nature Communications*, *7*, 10717. http://doi.org/10.1038/ncomms10717

Whitaker, K. J., Vértes, P. E., Romero-Garcia, R., Váša, F., Moutoussis, M., Prabhu, G., … Bullmore, E. T. (2016). Adolescence is associated with genomically patterned consolidation of the hubs of the human brain connectome. *Proceedings of the National Academy of Sciences*, *113*(32), 9105–9110. http://doi.org/10.1073/pnas.1601745113

Wilke, M. (2012). An alternative approach towards assessing and accounting for individual motion in fMRI timeseries. *NeuroImage*, *59*(3), 2062–72. http://doi.org/10.1016/j.neuroimage.2011.10.043

Wingfield, J. C., Hegner, R. E., Dufty Jr., A. M., & Ball, G. F. (1990). The "Challenge Hypothesis": Theoretical Implications for Patterns of Testosterone Secretion, Mating Systems, and Breeding Strategies. *The American Naturalist*, *136*(6), 829–846. Retrieved from http://www.jstor.org/stable/2462170

Winkler, A. M., Ridgway, G. R., Webster, M. A., Smith, S. M., & Nichols, T. E. (2014). Permutation inference for the general linear model. *NeuroImage*, *92*, 381–397. http://doi.org/10.1016/j.neuroimage.2014.01.060

Wittfoth-Schardt, D., Gründing, J., Wittfoth, M., Lanfermann, H., Heinrichs, M., Domes, G., … Waller, C. (2012). Oxytocin modulates neural reactivity to children's faces as a function of social salience. *Neuropsychopharmacology : Official Publication of the American College of Neuropsychopharmacology*, *37*(8), 1799–807.

http://doi.org/10.1038/npp.2012.47

Wold, S., Sjöström, M., & Eriksson, L. (2001). PLS-regression: A basic tool of chemometrics. *Chemometrics and Intelligent Laboratory Systems*, *58*(2), 109–130. http://doi.org/10.1016/S0169-7439(01)00155-1

Wolosin, S. M., Richardson, M. E., Hennessey, J. G., Denckla, M. B., & Mostofsky, S. H. (2009). Abnormal cerebral cortex structure in children with ADHD. *Human Brain Mapping*, *30*(1), 175–184. http://doi.org/10.1002/hbm.20496

Yang, D. Y.-J., Beam, D., Pelphrey, K. A., Abdullahi, S., & Jou, R. J. (2016). Cortical morphological markers in children with autism: a structural magnetic resonance imaging study of thickness, area, volume, and gyrification. *Molecular Autism*, *7*, 11. http://doi.org/10.1186/s13229-016-0076-x

Yang, D. Y.-J., Rosenblau, G., Keifer, C., & Pelphrey, K. A. (2015). An integrative neural model of social perception, action observation, and theory of mind. *Neuroscience & Biobehavioral Reviews*, *51*, 263–275. http://doi.org/10.1016/j.neubiorev.2015.01.020

Yarkoni, T., Poldrack, R. A., Nichols, T. E., Van Essen, D. C., & Wager, T. D. (2011). Large-scale automated synthesis of human functional neuroimaging data. *Nature Methods*, *8*(8), 665–670. http://doi.org/10.1038/nmeth.1635

Yatawara, C. J., Einfeld, S. L., Hickie, I. B., Davenport, T. A., & Guastella, A. J. (2015). The effect of oxytocin nasal spray on social interaction deficits observed in young children with autism: a randomized clinical crossover trial. *Molecular Psychiatry*. http://doi.org/10.1038/mp.2015.162

Young, L. J. (2015). Oxytocin, social cognition and psychiatry. *Neuropsychopharmacology : Official Publication of the American College of Neuropsychopharmacology*, *40*(1), 243–4. http://doi.org/10.1038/npp.2014.186

Yuen, R. K., Merico, D., Cao, H., Pellecchia, G., Alipanahi, B., Thiruvahindrapuram, B., … Scherer, S. W. (2016). Genome-wide characteristics of de novo mutations in autism. *Npj Genomic Medicine*, *1*(1), 16027. http://doi.org/10.1038/npjgenmed.2016.27

Zagni, E., Simoni, L., & Colombo, D. (2016). Sex and Gender Differences in Central Nervous System-Related Disorders. *Neuroscience Journal*, *2016*, 1–13.

http://doi.org/10.1155/2016/2827090

Zald, D. H., McHugo, M., Ray, K. L., Glahn, D. C., Eickhoff, S. B., & Laird, A. R. (2014). Meta-analytic connectivity modeling reveals differential functional connectivity of the medial and lateral orbitofrontal cortex. *Cereb Cortex*, *24*(1), 232–248. http://doi.org/10.1093/cercor/bhs308

Zielinski, B. A., Anderson, J. S., Froehlich, A. L., Prigge, M. B. D., Nielsen, J. A., Cooperrider, J. R., … Lainhart, J. E. (2012). scMRI Reveals Large-Scale Brain Network Abnormalities in Autism. *PloS One*, *7*(11). http://doi.org/10.1371/journal.pone.0049172

Zielinski, B. A., Gennatas, E. D., Zhou, J., & Seeley, W. W. (2010). Network-level structural covariance in the developing brain. *Proceedings of the National Academy of Sciences*, *107*(42), 18191–18196. http://doi.org/10.1073/pnas.1003109107

Zielinski, B. a., Prigge, M. B. D. D., Nielsen, J. a., Froehlich, A. L., Abildskov, T. J., Anderson, J. S., … Lainhart, J. E. (2014). Longitudinal changes in cortical thickness in autism and typical development. *Brain*, *137*(6), 1799–1812. http://doi.org/10.1093/brain/awu083

Zilles, K., & Amunts, K. (2012). Segregation and Wiring in the Brain. *Science*, *335*(6076), 1582–1584. http://doi.org/10.1126/science.1221366

Zunhammer, M., Geis, S., Busch, V., Greenlee, M. W., & Eichhammer, P. (2015). Effects of Intranasal Oxytocin on Thermal Pain in Healthy Men. *Psychosomatic Medicine*, *77*(2), 156–166. http://doi.org/10.1097/PSY.0000000000000142

Zuo, X.-N., Di Martino, A., Kelly, C., Shehzad, Z. E., Gee, D. G., Klein, D. F., … Milham, M. P. (2010). The oscillating brain: complex and reliable. *NeuroImage*, *49*(2), 1432–45. http://doi.org/10.1016/j.neuroimage.2009.09.037

Appendix A Supplementary Material chapter 1

A.1 Appendix A: Graph theory

The opening quote of this thesis was made over 500 years ago by Leonardo Da Vinci and neatly summarizes a key scientific concept that is rapidly gaining appreciation across a wide variety of scientific disciplines: network theory. The principle idea behind network theory is that it is possible to mathematically describe how different elements are interconnected. Studying the art of these networks can, in a sense, teach us to see and discriminate patterns in seemingly chaotic interactions and systems. Consequently, network theory has been used to describe and subsequently optimize a wide variety of complex systems. The most prominent examples are perhaps; social networks, communication networks, shipping networks, neural networks and even regulatory networks describing gene interactions. Although there are numerous ways to quantify and describe properties of networks, one very prominent method is called graph theory.

The foundation for graph theory dates back to the 18th century to a mathematical problem called the Seven Bridges of Königsberg. In this problem the challenge is to visit different parts of the city of Königsberg (now Kalinigrad), which are connected by seven bridges, by visiting each bridge exactly once. Around 1736 Leonhard Euler in essence founded graph theory by pointing

out, and later proving it mathematically, that the geographic starting point is irrelevant to solve the problem. Instead, one has to look at the exact way the elements are interconnected. By describing each part of the city as an element and the bridges as their connections he effectively described the mathematical structure that is now called a graph. In mathematical formulation elements are usually termed vertices or nodes and connections are termed edges, together making up a graph or network. Thus, in Euler's original graph each bridge was represented by an edge and each landmass as a node. Traversing through a network while visiting each node and only using each connection once is now known as an Euler walk. Now, Euler showed that these walks are only possible if all nodes are connected and exactly zero or two of the nodes have an odd degree. Thus, in historical Kalinigrad no Euler walk would be possible. Once a graph is constructed or a network is known there are a number of different measures that can be used to describe its properties. The simplest type of graph or network is a binary one, where all vertices are either connected or not but the strength of their connection is irrelevant. For simplification, weighted or non-binary networks are often thresholded to create a binary or unweighted graph.

In the studies presented in this thesis, functional and structural magnetic resonance imaging were used to reconstruct the functional and structural covariance networks respectively. Pearson correlation was used to estimate connectivity between different regions of the brain. Thus, in graph theoretical terms, brain regions represent the networks nodes and the correlational relation between them represents the connection of path between these nodes.

A.2 Graph metrics

As an initial step the most commonly used graph metrics were investigated as described below. Note that in mathematical notation, nodes are commonly referred to as vertices and relations between vertices as paths. These metrics are all implemented in the aforementioned Brain Connectivity Toolbox (Rubinov & Sporns, 2010) and are described in more detail elsewhere (Stam & Reijneveld, 2007) and (Newman, 2015). Some measures are computed at a global level (e.g. as an overall network property), some are computed at a local level (e.g. for each network node individually) and some are computed at both levels.

A.2.1 Global Measures

Path length (L) is a measure that does not describe any actual physical path length but rather a virtual representation of the minimal number of edges that are on average needed to connect two vertices. For every vertex the average number of edges necessary to reach all other vertices constitute its path length ($d_{i,j}$) and is thus determined by:

$$L = \frac{1}{N(N-1)} \sum_{i,j \in N, i \neq j} d_{i,j}$$

Modularity (Q) indicates the extent to which the network is subdivided into modules of highly interconnected nodes, with relatively few connections between modules (Bullmore &

Sporns, 2009; Mej Newman, 2006). Randomised networks contain fewer modules and thus have lower modularity.

Assortativity is represented by correlation coefficients between the degrees of all nodes on two opposite ends of an edge. A positive assortativity coefficient indicates that nodes tend to link to other nodes with the same or similar degree, i.e. high-degree nodes tend to connect to nodes that also have high degrees. Random networks have lower assortativity. Assortativity is a special case of modularity

Transitivity (T) is a metric that is largely adopted from analysis of social network. A relation is said to be transitive if it implies that *a*[relation]*b* and *b*[relation]*c* automatically means a[relation]c. In network analysis the relation is a connection between nodes. Thus there is a transitive connection if vertex *a* connects to vertex *b*, vertex *b* connects to vertex *c* and vertex *a* connects to vertex *c*. In essence these 3 elements form a fully connected (triangular) subgraph. The metric is provided by taking the ratio of triangles (e.g. fully connected pairs of 3) against triplets (e.g. only partially connected pairs of 3), the number of triangles is multiplied by a factor 3 do incorporate the fact that there are always three nodes involved. It should be noted that transitivity is a special case of the clustering coefficient described in more detail below.

$$\mathrm{T}^{\Delta} = \frac{3 * number\ of\ triangles}{number\ of\ paths\ with\ length\ 2}$$

Small-world coefficient (σ) determines whether the studied network shows the characteristics of small-world networks: high clustering, but low path length. The small-world efficient was calculated as follows:

$$\sigma(G) = \frac{C_G / C_R}{L_G / L_R}$$

In this formula, G is the network studied and R a corresponding random network. A network is considered small-world (Alexander-Bloch et al., 2010; Humphries, Gurney, & Prescott, 2006) if $\sigma > 1$. As random networks have both a lower clustering coefficients and a shorter path length, the resulting small world coefficient is also lower.

Efficiency can be defined as local or global efficiency. Thresholding graphs can sometimes lead to parts of the network becoming disconnected. Local efficiency is then the efficiency of certain parts of the entire network and global efficiency is the overall efficiency of the network. When there are no isolated parts in the network local and global efficiency are the same. Sometimes however different modules can be defined based on path length and clustering coefficient. In this case local efficiency of the different modules can also be determined. The way to calculate efficiency for a certain set of vertices is almost the same as how average path length is determined. It is done by using the inverse of the distance:

$$E = \frac{1}{N(N-1)} \sum_{i,j \in N, i \neq j} \frac{1}{d_{i,j}}$$

Cost-efficiency is calculated by subtracting the cost from the global efficiency, which results in a measure of the trade-off between cost and efficiency. As mentioned above, cost was defined as the number of existing edges as a fraction of all possible edges.

A.2.2 Local Measures

Degree is perhaps the most fundamental metric in graph theory along with path length as most other measures are based on these two components. Degree is simply the number of of connections that a node has. The degree distribution (e.g. the probability distribution of degrees) is sometimes used as a global metric to determine if networks obtained from different groups show an overall shift in characteristic nodal connectivity.

Clustering coefficient (C) Clustering coefficients are the number of nearest neighbours or connections (e_i) of a vertex (i) relative to the maximum possible number of connections in the network:

$$C_i = \frac{2e_i}{v_i(v_i - 1)}$$

where:

$$2e_i = \sum_{j,m} a_{i,j} a_{j,m} a_{m,i}$$

In this case $a_{i,j}$ is what is called the adjacency matrix that lists whether an edge exists between vertex *i* and *j*. The numerator ($2e_i$) in this formula thus represents the number of existing edges between a vertex *i* and all of its possible neighbours (*j* and *m*). This also includes the

connections between the neighbours themselves. The numerator ($2e_i$) thus represents the number of 'clusters' around vertex *i*. The denominator ($v_i(v_i - 1)$) represents the degree of a vertex *i*, which is simply the maximum number of possible edges between *i* and its neighbours. The clustering coefficient is thus the ratio of the number of clusters to the number of edges.

Betweenness centrality is the fraction of all shortest paths in the network that pass through a certain node The betweenness of a vertex is normally defined as the number of shortest paths between pairs of other vertices that run through that vertex (Freeman, 1977). The betweenness of a vertex is thus calculated by taking a ratio of all shortest paths between two specific vertices that run through that specific vertex ($n_{j,k}(i)$) to all shortest paths between those two vertices ($n_{j,k}$). For the entire network an average of all vertices is computed.

$$B_i = \sum_{j,k \in N, j \neq k} \frac{n_{j,k}(i)}{n_{j,k}}$$

Eigenvector centrality is a measure used to determine the relative contribution of a node to the network. Nodes that have a high eigenvector centrality connect to other nodes that have high eigenvector centrality. In essence the nodes with the highest eigenvector centrality contribute most to the networks structure. This is a particularly interesting measure for brain network analysis as it might allow investigating of potentially important brain regions based on their embededness in the overall network structure.

Nodal efficiency or local efficiency is the global efficiency calculated for the neighbourhood of a specific node. Thus, it considers all directly connected nodes for a single node a separate network and computes the efficiency for this nodal centered ‘subgraph’.

Appendix B Supplementary Material chapter 2

B.1 Supplementary Material chapter 2

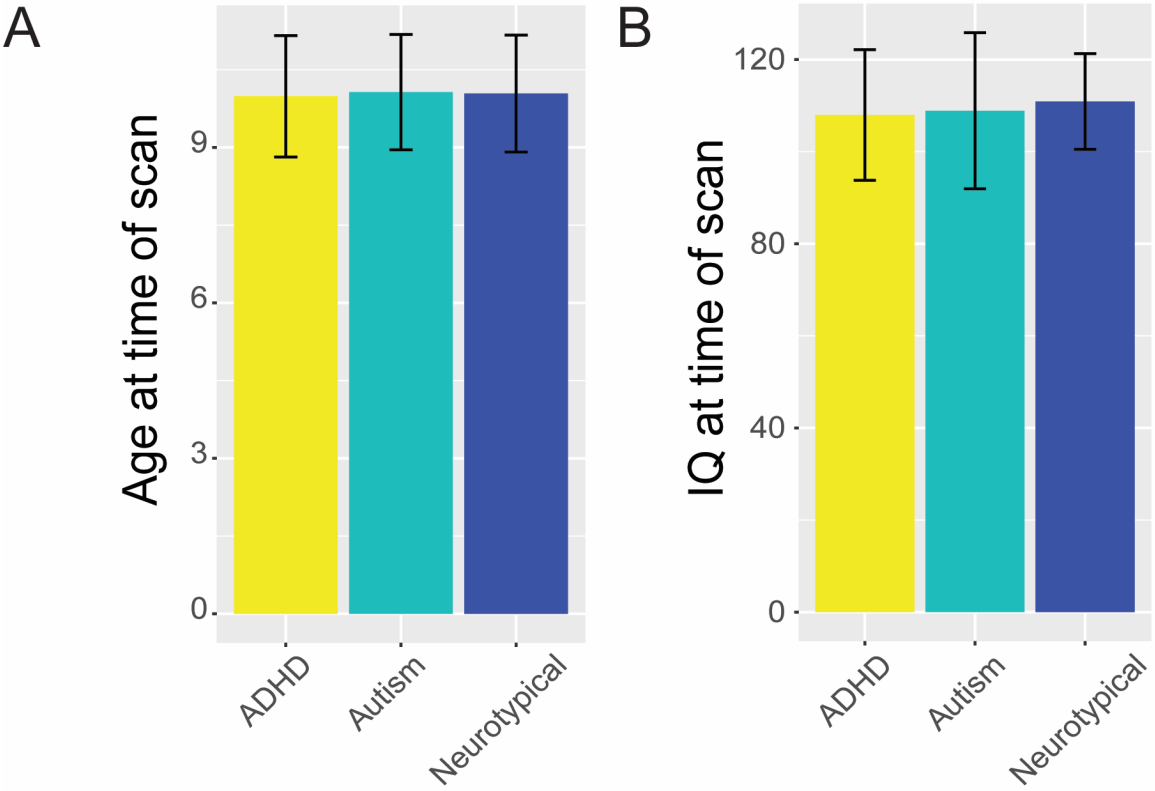

Fig. B.1: Age and IQ of all three matched groups.

Panel A shows the mean age at time of scan, panel B shows mean IQ for each group. Error bars indicate standard deviation from the mean.

Table B.1: Information on scanner site and matching

All scans were visually inspected by two independent researchers and only when both researchers agreed were subjects included in subsequent analyses. After this initial quality control variance in cortical thickness across all subjects was also analysed and subjects that had a whole-brain variance in cortical thickness that was more than 3 standard deviations from the sample mean were also removed from subsequent analysis. After this quality control step there were a few sites that only contained 2 or fewer subjects (MaxMun, Olin, Pitt, Stanford and Trinity), in order to minimize the effect of regressing out site, these sites were removed from subsequent analyses. Secondly, two sites had more than 10 subjects selectively from only one group (Washington University and Peking), as regressing out these sites would effectively also remove potential group effects these sites were removed from further analyses. This left a total of 218 subjects; ADHD (*n=69, age = 9.99 ±1.17, IQ = 107.95 ±14.18*), autism (*n=62 age=10.07 ±1.11, IQ = 108.86 ±16.94*) and NT (*n=87, age = 10.04 ±1.13, IQ = 110.89 ±10.39*). Within the ADHD group subdivisions could be made between presentation types, namely; ADHD-Combined (n=38), ADHD-Hyperactive/Impulsive (n =9) and ADHD-Inattentive (n=22)

		Scanner Site													
		KKI	MaxMun	NYU	OHSU	Olin	Peking	Pitt	Stanford	Trinity	UCLA	UM	USM	WashU	Yale
Before QC	NT	50	0	22	0	0	0	0	12	0	0	13	3	13	7
	ADHD	12	0	52	22	0	35	0	0	0	0	0	0	0	0
	ASD	13	5	27	6	4	0	1	12	1	15	17	1	0	5
		KKI	MaxMun	NYU	OHSU	Olin	Peking	Pitt	Stanford	Trinity	UCLA	UM	USM	WashU	Yale
After QC	NT	3	0	4	0	0	0	0	12	0	0	3	0	3	0
	ADHD	0	0	13	5	0	5	0	0	0	0	0	0	0	0
	ASD	3	3	2	0	2	0	0	11	0	5	11	0	0	1
		KKI	MaxMun	NYU	OHSU	Olin	Peking	Pitt	Stanford	Trinity	UCLA	UM	USM	WashU	Yale
After matching and minimizing site effects	NT	47	0	18	0	0	0	0	0	0	0	12	3	0	7
	ADHD	12	0	40	17	0	0	0	0	0	0	0	0	0	0
	ASD	10	0	25	6	0	0	0	0	0	10	6	1	0	4

B.2 Subcortical Volumetric and Covariance Differences

We found a significant volume difference between the Neurotypical and ADHD group in the left putamen, left amygdala and right amygdala (p-value <0.025, uncorrected; only the right amygdala survived FDR correction). See also figure B1. We also found a volumetric difference

between the ADHD and Autism groups in left amygdala and right amygdala, p-value <0.025, uncorrected; here only left amygdala survived FDR correction). The construction of a brain covariance network that included both cortical and subcortical structures was not suitable given that subcortical structures have a large variability of volume compared with the homogeneity of cortical regions with the same area as obtained from our parcellation scheme. However, we have explored the potential volume covariance of subcortical structures among groups (Figures B3 and B4). Here, we found that the autism group had, compared with neurotypical individuals, a significantly reduced covariance between right amygdala and left & right thalamus and between right amygdala and left Pallidum. Interestingly, the amygdala had a significantly reduced degree in the autism group compared to the control group. The ADHD group showed a significant correlation reduction between left & right cerebellum and left & right putamen, between left caudate and right thalamus and between left accumbens and right accumbens. Comparing the autism and ADHD groups revealed significant differences between left putamen and left & right cerebellum and between left pallidum and right amygdala. However, due to the large number of comparison these differences did not survived FDR corrections. The notion of altered subcortical and cortical processing fits with the idea of network alterations being dependent on the specific network (B. A. Zielinski et al., 2012). Specifically, reduced Involvement of amygdala and thalamic regions in the autism group might contribute to the underconnectivity of the salience network reported by Zalienski and collesgues (2012). Furthermore, although this can not be thoroughly assessed with the present approach (e.g. due the nature of the parcellation at the cortical level) it would seem reasonable to assume that these subcortical alterations in both volume and covariance could contribute to alterations in cortical-

subcortical coupling, specifically of the amygdala and striatal regions (Eisenberg, Wallace, Kenworthy, Gotts, & Martin, 2015).

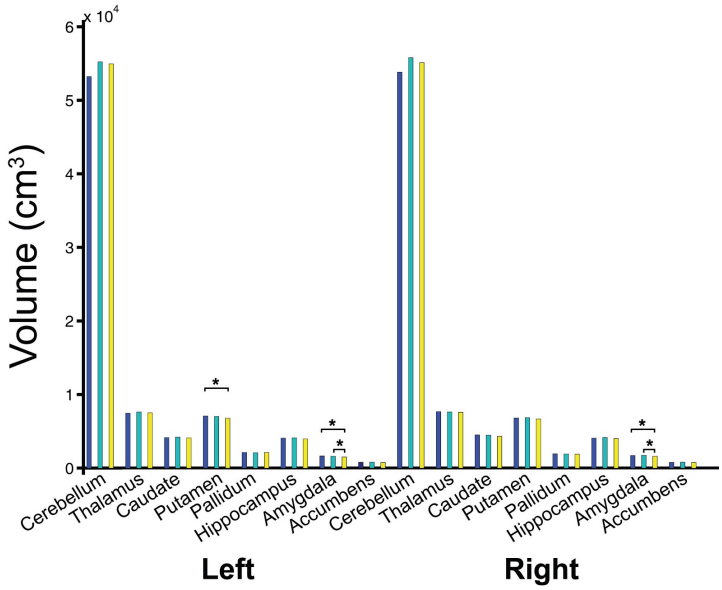

Fig. B.2 Volumetric differences

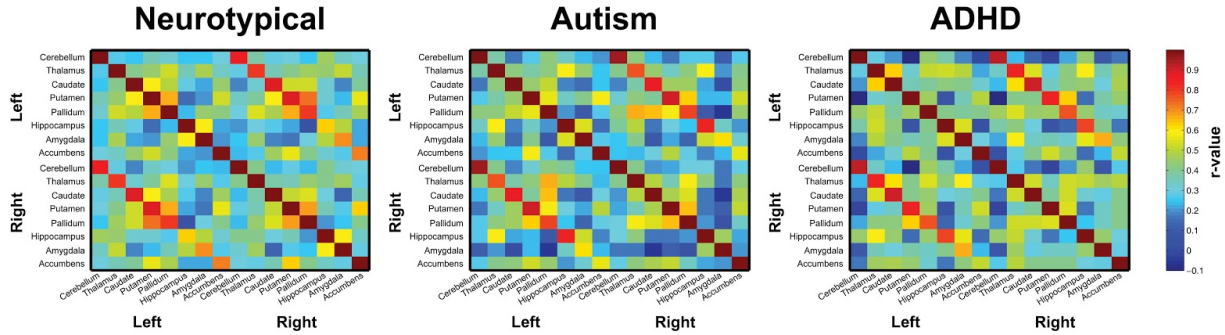

Fig. B.3: Subcortical structural covariance networks

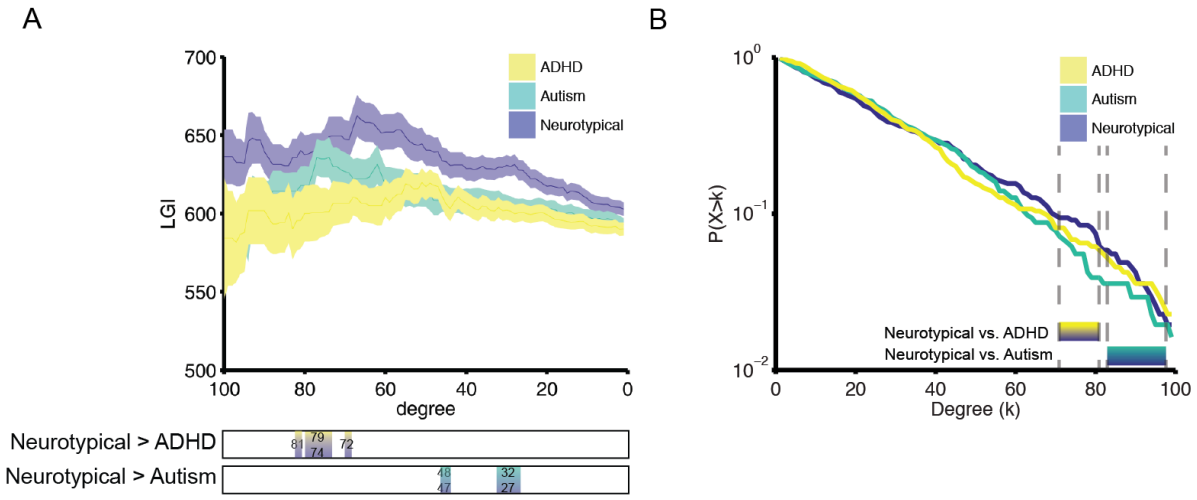

Fig. B.4: Gyrification index and degree distribution

Panel A shows gyrification as a function of degree. Bars below the figure show the degree ranges where there is a significant difference between the respective groups. Panel B shows the cumulative degree distribution of the covariance network based on gyrification. Lines represent the proportion of nodes in the network with a degree higher than k (hubs) in each group. Bars below the figure represent the areas where there is a significant difference between the groups.

Appendix C Supplementary Material chapter 3

C.1 1. Neuroimaging Data

C.1.1 Discovery dataset

Overview

A description of the dataset is provided in detail elsewhere (Bethlehem et al., 2017). Briefly, structural T1-weighted MPRAGE images were collected from two publicly available datasets: ABIDE (http://fcon_1000.projects.nitrc.org/indi/abide/) and ADHD-200 (http://fcon_1000.projects.nitrc.org/indi/adhd200/). From these datasets, we selected a subset of 3 diagnostic groups (autism, ADHD and neurotypical individuals) of males between the ages of 8 and 12 years old. The initial sample consisted of 348 eligible individuals (see below for details on sample matching and quality control). The structural T1-MPRAGE data were pre-processed using Freesurfer *v5.3* to estimate regional cortical thickness. The cortical thickness maps were automatically parcellated into 308 equally sized cortical regions of 500 mm^2 that were constrained by the anatomical boundaries defined in the Desikan-Killiany atlas (Desikan et al., 2006; Romero-garcia et al., 2012). Individual parcellation templates were created by warping this standard template containing 308 cortical regions to each individual MPRAGE image in native space. A key advantage of warping of the segmentation map to the native space relates to the attenuation of possible distortions from warping images to a standard space that is normally needed for group comparisons. Lastly, average cortical thickness was extracted for each of the 308 cortical regions in each individual participant.

C.1.2 Quality control and matching

Details of the quality control and matching are described in detail elsewhere (Bethlehem et al., 2017). In short, scans were visually checked by two independent researchers. When both researchers independently agreed subjects were included in the final sample. Variance in cortical thickness across all subjects was also analysed and subjects with variance in global cortical thickness that was more than 3 standard deviations from the sample mean were removed from subsequent analysis. After this last step, there were a few sites that only contained 2 or fewer subjects (MaxMun, Olin, Pitt, Stanford and Trinity) and, to minimize the effect of regressing out site, these sites were removed from subsequent analyses. Secondly, two sites had more than 10 subjects selectively from only one group (Washington University and Peking), as regressing out these sites would effectively also remove potential group effects these sites were removed from further analyses. This left a total sample size of 218 subjects: ADHD *(n=69, age = 9.99 ±1.17, IQ = 107.95 ±14.18)*, autism *(n=62 age=10.07 ±1.11, IQ = 108.86 ±16.94)* and controls *(n=87, age = 10.04 ±1.13, IQ = 110.89 ±10.39)*.

C.1.3 Validation Dataset

In order to validate our findings, we used two independent datasets of children with and without autism in a similar age range from the second release of ABIDE (http://fcon_1000.projects.nitrc.org/indi/abide/abide_II.html). Specifically, we utilized the data collected at Georgetown University (Validation 1) and Kennedy Krieger Institute (Validation 2) that were not included in the first release of ABIDE and consists of a young cohort of children with and without autism. Structural T1-weighted MPRAGE images were

pre-processed with the same pipeline as described above. Subjects that had an overall variance in CT that was more than 3 standard deviations from the group mean were removed from further analysis. The final sample for validation consisted of 102 subjects for Validation 1 [autism (*n=48, age=10.97±1.53*) and controls (*n=54, age=10.43±1.71*)] and 21o subjects for Validation 2 [autism (*n=56, age=10.32±1.51*) and controls (*n=154, age=10.34±1.20*)].

C.2 PLSR analysis

C.2.1 Overview

The following describes a simplified overview of PLSR and the difference between the SIMPLS and the NIPALS algorithm.

Partial least squares regression or PLSR is a data reduction technique closely related to principal component analysis (PCA) and ordinary least squares (OLS) regression. Here we use the SIMPLS algorithm (de Jong, 1993), where the independent variable matrix (X) and the dependent variable (Y) is centred giving rise to X_0 and Y_0 respectively. The first component is then weighted by w_1 and q_1 to calculate factor scores (or component scores) T_1 and U_1.

This T1 is the weighted sum of the centred independent variable:

$$T_1 = X_0 w_1 + E_1 \qquad \text{(eqn 1)}$$

And U1 is the weighted sum of the centred dependent variable:

$U_1 = Y_0 q_1 + E_2$ (eqn 2)

The weights and the factors scores are calculated to ensure the maximum covariance between T_1 and U_1, which is a departure from regular PCA where the scores and loadings are calculated to explain the maximum variance in X_0.

$So\ U_1 \sim T_1$ (eqn 3)

Or,

$U_1 = B_0 + B_1 T_1 + E_4$ (eqn 4)

Or,

$U_1 = B_0 + B_1(X_0 w_1) + E_5$ (eqn 5)

In the SIMPLS algorithm provides an alternative where the matrices are not deflated by the weights when calculating the new components, and, as a result, it is easier to interpret the components based on the original centred matrices.

As the components are calculated to explain the maximum covariance between the dependent and independent variable, the first component need not explain the maximum variance in the dependent variable. However, as the number of components calculated increases, they progressively tend to explain lesser variance in the dependent variable.

Here we present the rationale for choosing genes with both positive and negative weights:

From equations 2 and 5 above, we know that:

$$Y_0 q_1 = B_0 + B_1(X_0 w_1) + E_5 \quad \text{(eqn 6)}$$

This can be rewritten as:

$$Y_0 q_1 \sim B_1(X_0 w_1) \quad \text{(eqn 7)}$$

And if both B_1 and q_1 are positive which is the case in our analyses, then,

$$Y_0 \sim X_0 w_1 \quad \text{(eqn 8)}$$

In our dataset:

Y_0 is a px1 vector of ΔCT with positive and negative values.

q_1 is a 1x1 vector of weight for the first PLSR component.

B1 is the regression coefficient.

X_0 is a pxn matrix of gene expression, where p is the number of cortical regions, and n is the number of genes for which gene expression is calculated. This has been scaled and normalized to have positive and negative values. Positive values indicate that the gene is overexpressed compared to the mean gene expression, and negative values indicate that the gene is underexpressed compared to the mean gene expression.

w1 is a nx1 vector of weights for the first PLSR component.

Y_0 can be both positive or negative (ΔCT is both positive or negative, as some regions are thicker in individuals with autism compared to controls and vice versa). Similarly, both X_0 and w_1 are positive or negative.

This gives us the following possibilities:

1. For a negative value in Y_0, either the equivalent X_0 value or the equivalent w_1 value must be negative.
2. For a positive value in Y_0, both the equivalent values in X_0 and w_1 must be either positive or negative.

In other words, if the weight of the gene is positive, having a higher than average gene expression (positive X_0) contributes to positive ΔCT (i.e. greater CT in autism compared to controls), whereas having a lower than average gene expression (negative X_0) contributes to negative ΔCT. Similarly, if the weight of the gene is negative, having a higher than average gene expression contributes to negative ΔCT, whereas having a lower than average gene expression contributes to positive ΔCT. So, the sign of the weights alone cannot tell us if the gene contributes to thicker or thinner cortex in autism compared to controls. It is the combination of both the weights and the gene expression level that can be informative. However, as gene expression and ΔCT varies considerably across the regions tested, we used genes with both positive and negative weights, that were significant FDR correction in our enrichment analyses.

C.3 PLSR Analysis: Autism Data

C.3.1 Discovery dataset

Details of the PLSR analysis are described in the main manuscript, Supplementary Table S1 below lists the descriptive cross-validation statistics of the full 35-component model and Supplementary Figure S1 shows the amount of explained variance for each component included in the final analysis. Only the first component showed a significant effect ($p = 0.009$). We also conducted KEGG pathway enrichment analysis, details of which are provided in Supplementary Table C.2.

Table C.1: 35 component cross-validation

COMP	PRESS	RSS	Q2	Q2cum	RMSE
1	2.97E+02	3.07E+02	0.0336	0.0336	0.9984
2	2.65E+02	2.69E+02	0.0165	0.0496	0.9350
3	2.08E+02	2.32E+02	0.1003	0.1449	0.8673
4	1.65E+02	1.79E+02	0.0813	0.2145	0.7633
5	1.35E+02	1.45E+02	0.0736	0.2722	0.6867
6	1.17E+02	1.25E+02	0.0629	0.3180	0.6376
7	8.84E+01	9.84E+01	0.1013	0.3871	0.5652
8	6.88E+01	6.90E+01	0.0031	0.3890	0.4732
9	4.66E+01	5.20E+01	0.1033	0.4521	0.4109
10	4.15E+01	4.28E+01	0.0303	0.4687	0.3726
11	3.09E+01	3.24E+01	0.0474	0.4939	0.3243
12	2.51E+01	2.63E+01	0.0457	0.5170	0.2921
13	2.09E+01	2.16E+01	0.0300	0.5315	0.2647
14	1.58E+01	1.56E+01	-0.0157	0.5241	0.2248
15	1.11E+01	1.08E+01	-0.0268	0.5114	0.1876
16	7.76E+00	7.68E+00	-0.0107	0.5062	0.1579
17	6.18E+00	5.97E+00	-0.0356	0.4886	0.1392

18	4.44E+00	4.43E+00	-0.0027	0.4872	0.1199
19	3.41E+00	3.32E+00	-0.0252	0.4743	0.1039
20	2.71E+00	2.67E+00	-0.0158	0.4659	0.0931
21	2.11E+00	1.83E+00	-0.1505	0.3856	0.0772
22	1.53E+00	1.31E+00	-0.1671	0.2829	0.0653
23	9.77E-01	8.81E-01	-0.1093	0.2045	0.0535
24	7.11E-01	6.07E-01	-0.1703	0.0690	0.0444
25	4.14E-01	3.71E-01	-0.1157	-0.0386	0.0347
26	2.77E-01	2.71E-01	-0.0244	-0.0640	0.0296
27	1.99E-01	1.79E-01	-0.1095	-0.1805	0.0241
28	1.31E-01	1.13E-01	-0.1599	-0.3692	0.0191
29	8.53E-02	6.65E-02	-0.2834	-0.7572	0.0147
30	5.07E-02	4.42E-02	-0.1459	-1.0136	0.0120
31	4.12E-02	3.10E-02	-0.3285	-1.6751	0.0100
32	2.83E-02	2.04E-02	-0.3876	-2.7119	0.0081
33	1.81E-02	1.41E-02	-0.2831	-3.7627	0.0068
34	1.24E-02	9.81E-03	-0.2688	-5.0428	0.0056
35	7.48E-03	5.97E-03	-0.2536	-6.5753	0.0044

For each component the Predictive Error Sum of Squares (PRESS), Residual Sum of Squares (RSS), cross validated PRESS (Q2), the cumulative Q2 and the Root Mean Square of the Error (RMSE) are provided.

Figure C.1: Variance in gene expression explained by components in the Discovery dataset

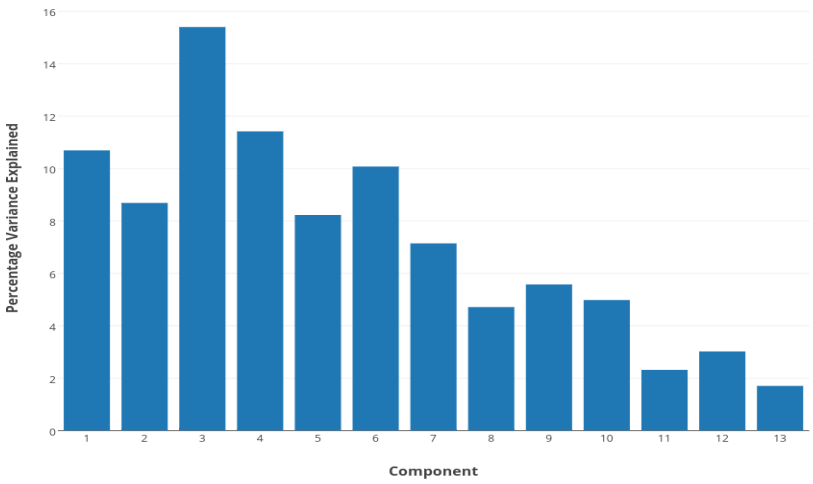

Variance explained for all 13 components included in the final model. Only components 1, 3, 4 and 6 explained more than 10% of the total variance individually, and were thus selected for further analyses. Of these 4 only component 1 explained a significant proportion of the variance in ΔCT.

Table C.2: Kegg 2016 Pathway analysis for PLSR1

Term	Overlap	P-value	Adjusted P-value	Z-score
Retrograde endocannabinoid signaling	29/101	8.64092E-07	0.000121837	-1.912944439
GABAergic synapse	27/88	4.79644E-07	0.000121837	-1.856183708
Adrenergic signaling in cardiomyocytes	36/148	3.5192E-06	0.000330805	-1.809256835
Morphine addiction	25/91	1.13401E-05	0.000799478	-1.774306875
Dopaminergic synapse	29/129	0.00013772	0.006472825	-1.761079175
HIF-1 signaling pathway	25/103	0.000107567	0.006066762	-1.73577233
Nicotine addiction	13/40	0.000234762	0.009457564	-1.56949222
Serotonergic synapse	25/112	0.000432338	0.015239928	-1.69105338
Circadian entrainment	22/95	0.000547828	0.01716529	-1.71333288
Oxytocin signaling pathway	31/158	0.001019701	0.028755556	-1.73576073
Renin secretion	16/64	0.001271626	0.032599873	-1.522988352
Pathways in cancer	62/397	0.003043863	0.053648094	-1.709378099

C.3.2 Validation dataset

For the two validation datasets, we conducted the same analysis. For Validation1, the cross-validation analysis identified that 15 components provide the best model fit. For validation 2, the cross-validation analysis identified that 16 components provide the best model fit. Only the first component explained a significant amount of variance ($P< 10^{-14}$) in both the validation datasets, and was thus analyzed further. As was the case in the discovery dataset the first component in both the datasets was significantly associated with the GO term "Synaptic Transmission". The Variance explained by the first six components in both the validation datasets are provided in Supplementary Figure C.2.

Figure C.2: Variance in gene expression explained by the first six components in the two Validation datasets

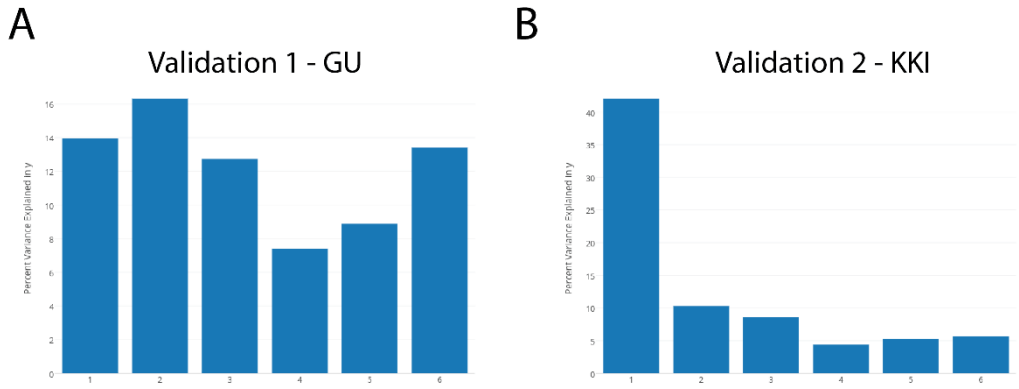

Only the first component in both the datasets significantly explained variance in ΔCT. Subsequent components all explained less than 10% of the variance in gene expression.

In comparison with the Discovery dataset, both the validation datasets also had a high, significant correlations in the gene loadings (Supplementary Figure C.3)

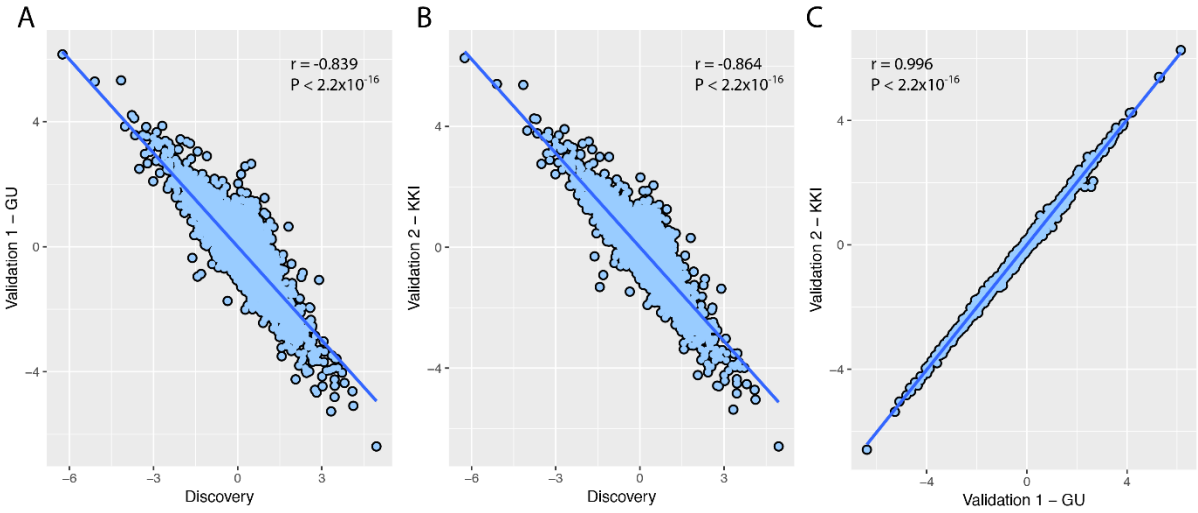

Figure C.3: Correlations between gene loadings in all three datasets

Correlations between the gene loadings provided for all three datasets. Panel A provides the correlations between the Discovery and Validation 1 datasets. Panel B provides the correlations between the Discovery and Validation 2 datasets. Panel C provides the correlation between the two validation datasets. Only the correlations in ΔCT between the two validation datasets was significant and positive, explaining the negative correlation in gene loadings between the Discovery and two validation datasets.

We also conducted KEGG based pathway enrichment for the two validation datasets using Enrichr. Details are provided in Supplementary Tables C.4 and C.5.

Table C.3: Top 10 pathways (Validation 1)

Term	Overlap	P-value	Adjusted P-value	Z-score
Adrenergic signaling in cardiomyocytes	72/148	1.142E-04	0.0331	-1.8592
Oxytocin signaling pathway	73/158	7.157E-04	0.0899	-1.9448
Long-term potentiation	35/66	9.300E-04	0.0899	-1.8231
MAPK signaling pathway	109/255	1.521E-03	0.1103	-1.9214
Glioma_Homo sapiens	33/65	3.279E-03	0.1310	-1.9054
Retrograde endocannabinoid signaling	48/101	2.699E-03	0.1310	-1.8263
mTOR signaling pathway	31/60	3.048E-03	0.1310	-1.7946
cAMP signaling pathway	85/199	4.792E-03	0.1310	-1.7119
Taste transduction	40/83	4.315E-03	0.1310	-1.6758
Morphine addiction	43/91	4.970E-03	0.1310	-1.5714

Table C.4: Top 10 pathways (Validation 2)

Term	Overlap	P-value	Adjusted P-value	Z-score
Retrograde endocannabinoid signaling	78/101	1.34E-05	0.00	-1.94
Rap1 signaling pathway	149/211	2.15E-05	0.00	-1.94
Oxytocin signaling pathway	114/158	4.36E-05	0.00	-1.92
Glutamatergic synapse	84/114	1.31E-04	0.01	-1.86
Circadian entrainment	71/95	2.06E-04	0.01	-1.80
Long-term potentiation	52/66	1.47E-04	0.01	-1.75
Thyroid hormone signaling pathway	86/118	2.07E-04	0.01	-1.70
Glioma	50/65	5.60E-04	0.01	-1.75
cAMP signaling pathway	136/199	5.03E-04	0.01	-1.74
Adrenergic signaling in cardiomyocytes	104/148	4.77E-04	0.01	-1.68

Tables C.3 and C.4 provide the top 10 pathways for the Validation analyses. We find an enrichment for similar neural pathways between the three datasets (Oxytocin signalling pathway, retrograde endocannabinoid signalling, morphine addiction, circadian entertainment, and different neurotransmitter signalling pathways).

C.3.3 Male only analysis

We also investigated if the including only males in either of the two Validation cohort will improve the correlations in ΔCT, gene scores, and gene loadings between the Discovery and the Validation. We conducted this analysis using Validation 2 (KKI) as it had more number of male participants than the Validation 1 dataset. We note that the correlations in ΔCT, gene scores, and gene loadings between the Discovery and the males-only ΔCT were similar to the correlations when males and females were included in Validation 2 (Supplementary Figure C.4). Hence, the inclusion of females does not seem to alter the results.

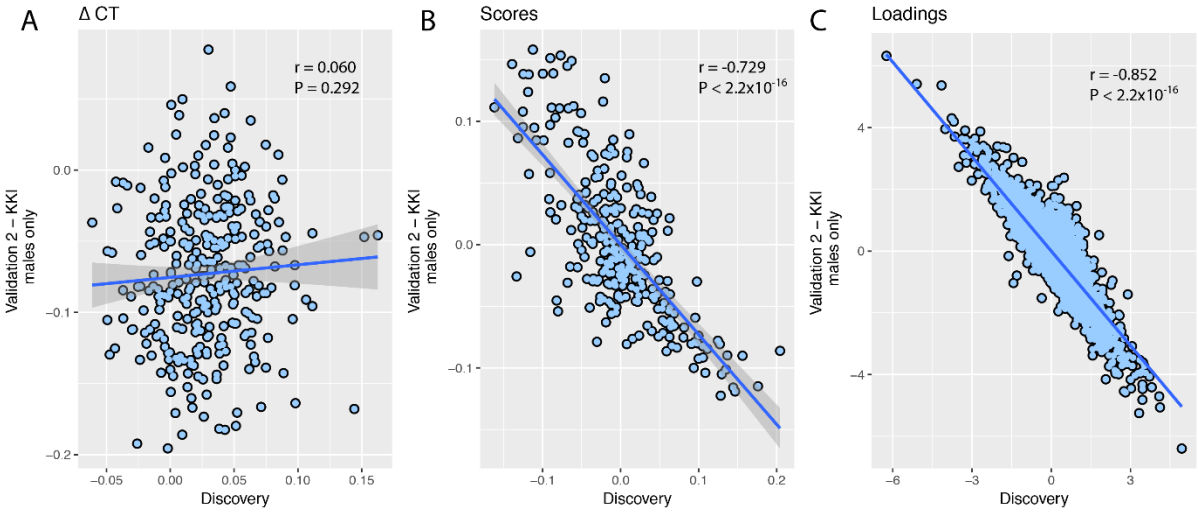

Figure C.4: Correlations between ΔCT, gene scores and gene loadings between the Discovery and the males-only Validation 2

C.4 Von Economo profiling

The spatial profile of the transcriptionally downregulated genes in the autism were examined using a regional map based on the cytoarchitectonic criterion of Von Economo (Von Economo and Koskinas, 2008). In his seminal work, Von Economo described five fundamental types of

cortical structures: granular primary motor cortex (class 1), frontal granular association cortex (class 2), parietal homotypical association cortex (class 3), dysgranular secondary sensory cortex (class 4), agranular primary sensory cortex (class 5). Allocortex (class 6) and insular cortex (class 7) were added due to their particular cytoarchitectonical characteristics (Whitaker et al., 2016; Zilles and Amunts, 2012). The average expression of all significant genes in the first PLSR component was calculated for each class (FDR adjusted P-values < 0.05). A non-parametric permutation test was applied to assess whether gene expression values were different from 0 in each class. A reference distribution was created by computing the gene expression values across Von Economo classes for a random subset of genes (10,000 permutations). The two tails of the resulting distribution were used to retain or reject the null hypothesis of an average gene expression equal to 0. Von Economo profiling analysis for the two validation datasets are provided in Supplementary Figure C.5.

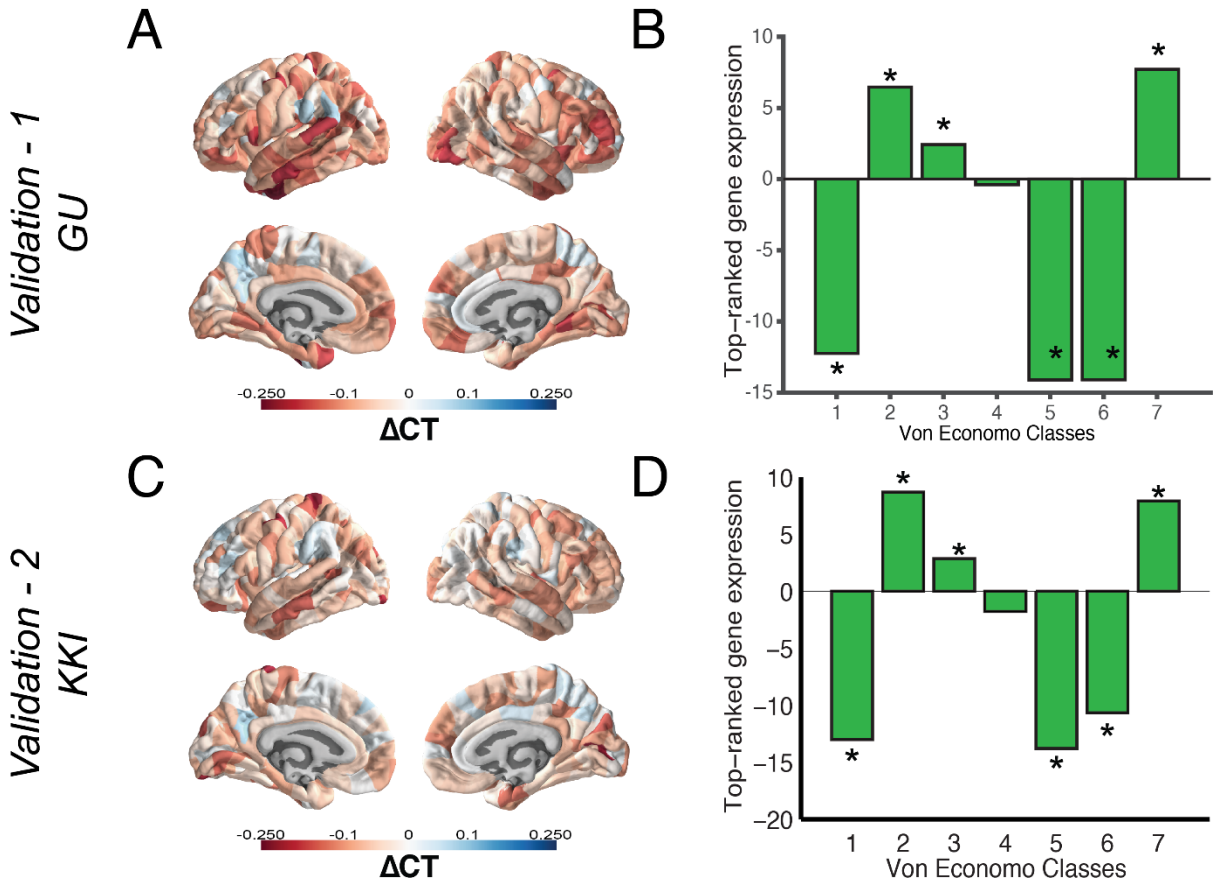

Figure C.5: Von Economo Expression Z-Scores of the two validation datasets

Von Economo expression profiles largely resemble the pattern of over-expression in association cortices observed in the discovery dataset. The validation datasets reveals a significant over-expression of the PLSR1 in classes 2 and 3 (association cortices), as well as in the insular cortex (class 7). On the other hand, Class 1 and 5 (primary cortices) and Class 6 (limbic regions) show a significant PLSR1 under-expression.

C.5 PLSR Analysis: ADHD data

To investigate if our results were autism specific we also performed a PLSR analysis on the cortical thickness difference between a matched group of children with ADHD (matched on age, IQ and scanner site across all three groups) and the same neurotypical control group used in the main study. We used the exact same pipeline as described in the main manuscript. Cross-

validation results of the initial 35-component PLSR model are listed in Supplementary Table C.6. It is immediately clear that this model does not provide a good fit for the ADHD ΔCT as the cross-validated cumulative Q2 does not show a clear peak. Although there are three components that explain more than 10% of the variance each none of these components are significantly associated with the ΔCT. For a full comparison, we nonetheless performed pathway and ontology analyses for those three components revealed no significant pathways or biological processes associated with genes that passed FDR correction in each PLSR component. We did not proceed with further enrichment analyses.

Table C.5: PLS 35 component model for the ADHD-controls CT difference

COMP	PRESS	RSS	Q2	Q2cum
1	3.14E+02	3.07E+02	-0.0239	-0.0239
2	2.98E+02	2.84E+02	-0.0481	-0.0732
3	2.66E+02	2.57E+02	-0.0384	-0.1144
4	1.89E+02	2.04E+02	0.0744	-0.0314
5	1.56E+02	1.65E+02	0.0570	0.0273
6	1.36E+02	1.43E+02	0.0529	0.0787
7	1.26E+02	1.18E+02	-0.0634	0.0203
8	8.28E+01	7.89E+01	-0.0492	-0.0278
9	6.62E+01	6.87E+01	0.0356	0.0087
10	6.54E+01	6.11E+01	-0.0700	-0.0606
11	5.03E+01	5.36E+01	0.0603	0.0033
12	4.29E+01	4.35E+01	0.0120	0.0153
13	4.01E+01	3.84E+01	-0.0423	-0.0264
14	3.02E+01	2.87E+01	-0.0548	-0.0826
15	2.51E+01	2.39E+01	-0.0517	-0.1385
16	2.06E+01	1.88E+01	-0.0949	-0.2466
17	1.58E+01	1.51E+01	-0.0463	-0.3044
18	1.30E+01	1.23E+01	-0.0620	-0.3852
19	1.05E+01	9.71E+00	-0.0819	-0.4986
20	7.50E+00	6.74E+00	-0.1126	-0.6673
21	5.64E+00	5.49E+00	-0.0268	-0.7120

22	4.64E+00	3.96E+00	-0.1713	-1.0052
23	3.28E+00	3.06E+00	-0.0720	-1.1496
24	2.51E+00	2.01E+00	-0.2496	-1.6861
25	1.63E+00	1.31E+00	-0.2463	-2.3476
26	1.04E+00	9.13E-01	-0.1341	-2.7965
27	7.33E-01	6.50E-01	-0.1273	-3.2798
28	5.68E-01	4.95E-01	-0.1480	-3.9132
29	4.07E-01	3.23E-01	-0.2594	-5.1879
30	2.67E-01	2.36E-01	-0.1313	-6.0006
31	2.01E-01	1.53E-01	-0.3138	-8.1973
32	1.16E-01	9.63E-02	-0.2034	-10.0677
33	5.71E-02	5.02E-02	-0.1358	-11.5707
34	3.41E-02	2.96E-02	-0.1514	-13.4742
35	1.85E-02	1.67E-02	-0.1073	-15.0269

For each component the Predictive Error Sum of Squares (PRESS), Residual Sum of Squares (RSS), cross validated PRESS (Q2) and the cumulative Q2 are provided.

C.6 Gene modules and enrichment analyses

C.6.1 Transcriptional dataset and adult gene co-expression modules

The following describes the analyses conducted in Parikshak et al., 2016. We also outline our rationale for using these datasets in the present study.

Briefly, rRNA-depleted RNA sequencing was conducted using cortical brain tissue samples from 48 autism donors and 49 neurotypical controls. Differential gene expression (DGE) identified 1143 dysregulated genes in the autism cortex samples compared to the control cortex samples of which 584 genes were upregulated and 558 genes were downregulated in the autism cortex. This dataset comprises of 13 autism donors and 14 control donors that overlap with

Gandal et al., 2016 due to the inclusion of data from Voineagu et al., 2011. DGE analyses were performed using gene expression levels that have been normalized for gene length, library size, and G+C content. DGE was calculated using a linear mixed effects regression model where individual donor identifier was treated as a random effect, and age, sex, brain region, and diagnosis were treated as fixed effects. Genes were said to be differentially expressed if they had a Benjamini-Hochberg FDR corrected $P < 0.05$. In our analyses, we used genes and associated P-values and fold difference from Supplementary Table 2 from Parikshak et al., 2016 using the cortex-only dataset. We defined genes as being transcriptionally dysregulated if they had a Benjamini-Hochberg FDR corrected P-value < 0.05. In this subset of significant genes, genes were downregulated if they had a log2(Fold-change) < 0, and similarly, they were upregulated if they had a log2(Fold-change) > 0. Downregulated genes were significantly enriched for pathways involved in synaptic transmission and genes expression in neurons.

Weighted gene co-expression modules were constructed using the R package weighted gene co-expression network analyses (WGCNA) (https://labs.genetics.ucla.edu/horvath/CoexpressionNetwork/Rpackages/WGCNA/) after bootstrapping 100 times. Modules significantly associated with a diagnosis of autism were identified using a linear mixed effects regression analyses, using the first principal component of each module against diagnosis, age, sex, and brain region. WGCNA is an excellent data-reduction technique, that utilizes gene co-expression patterns to construct weighted co-expression network modules. This identifies clusters of genes with similar expression that are usually enriched for specific biological pathways. Here we

focussed on six gene co-expression modules constructed from the entire cortical gene-expression profile that are associated with autism: M9, M19, and M20 that are enriched for upregulated genes in autism, and M4, M10, and M16 that are enriched for downregulated genes in autism. All six modules show significant cell-type enrichment. Further, the downregulated modules are all enriched for synaptic function and neuronal genes and the upregulated modules are enriched for inflammatory pathway and glial function. As we had identified a significant enrichment of synaptic function in the significant PLSR1 genes we hypothesized that genes would be enriched for the three downregulated modules. This further supported the enrichment of the PLSR1 genes for the transcriptionally dysregulated genes in the autism post-mortem cortex.

C.6.2 Validation Transcriptional dataset

The following describes the analyses conducted in Gandal et al., 2016.

DGE analysis was conducted using raw microarray gene expression data from cortical samples from 33 autism donors and 38 control donors. Three autism microarray datasets were used from three different studies: (Chow et al., 2012; Garbett et al., 2008; Voineagu et al., 2011). Samples from the Voineagu et al., 2011 overlapped with the Parikshak et al., 2016 dataset, making this a quasi-independent dataset. DGE was calculated using the log fold change values using the Limma package after accounting for biological covariates (age, sex, brain region) and technical covariates (such as experimental batch, post-mortem interval, pH etc) for each study separately. Finally, meta-analysis of the log fold change values were conducted using a random effects

model. Approximately 10,000 genes were retained after filtering for genes that were present across all three studies. As mentioned above, we identified genes as being downregulated if they had a log(Fold-change) < 0, and an Benjamini-Hochberg FDR corrected P-value < 0.05. We identified 830 transcriptionally dysregulated genes, and 464 genes that were downregulated in the autism postmortem cortex.

C.6.3 Developmental gene co-expression modules

The following describes the analyses conducted in Parikshak et al., 2013.

WGCNA network analyses were conducted using RNA sequencing based gene expression data from BrainSpan whole-genome transcriptomic data. The authors used only data from brain samples spanning 8 weeks post-conception to 12 months after birth. WGCNA identified a total of 17co-expresion modules. Five of these modules are associated with different risks for autism. Modules Mdev 13, Mdev16, and Mdev17 are enriched for transcriptionally dysregulated genes in the autism post-mortem cortex. Whereas modules Mdev2 and Mdev3 are enriched for rare genetic variants associated with autism. Modules Mdev13, Mdev16, and Mdev17 are enriched for the GO term 'Synaptic transmission' and are all upregulated. Mdev16 is upregulated first (Post-conception week - PCW 10), followed by Mdev17 (PCW 13) and finally Mdev13 (PCW 16). The developmental trajectories of all three modules are closely aligned but are sequential. In contrast, Mdev2 and Mdev3 are enriched for pathways associated with DNA binding and transcriptional regulation.

C.6.4 Rare de novo genetic variants

The following describes the analyses conducted in Sanders et al., 2015.

Genes harbouring rare, de novo variants associated with autism were identified from Sanders et al., 2015. A total of 65 genes associated with autism (FDR adjusted P-value < 0.1) were identified using exome sequencing data and small de novo CNV detection largely using genotyping data. This was conducted after integrating data from multiple different studies from more than 10,220 individuals from 2,591 families recruited as a part of the Simon's Simplex Collection.

C.6.5 Common genetic variants

Genome-wide association data of the latest data freeze of the autism spectrum disorder working group of the Psychiatric Genomics Consortium was downloaded from the PGC website (http://www.med.unc.edu/pgc/results-and-downloads). This dataset consists of 5,305 cases and 5,305 pseudocontrols (i.e. the non-transmitted haplotypes of the parents) of European ancestry. A total of 553,795,981 SNPs were tested for association. SNP based P-values were converted to gene-based P-values using a hg19 genome build using MAGMA (de Leeuw et al., 2015), which accounts for linkage disequilibrium between SNPs when calculating gene-based P-values. The Benjamini-Hochberg FDR corrected gene-based P-values were used as the independent variable to test for enrichment analyses using a regression model (explained below).

C.6.6 Regression analyses

Usually, enrichment analyses are conducted using Fisher's exact test or hypergeometric test (equivalent to a one-sided Fisher's exact test). However, these tests do not incorporate potential covariates that may arise with the different methods used to identify significant genes (for example, comparing enrichment of genes identified using exome sequencing in a list of genes identified using RNA expression). One significant covariate for enrichment analyses is gene length. To correct for the gene length bias we used a logistic regression analyses with gene length included as a covariate.

This can be written as:

$$Y = B_0 + B_1x_1 + B_2x_2 + E$$

Where Y is the odds that the gene is significant after FDR correction for the PLSR module (1 if the gene is significant, 0 if the gene is not significant); x1 is the independent variable in the autism dataset tested; x2 is the gene length. Regression analyses were conducted in R. For all enrichment analyses, the dependent variable (Y) was if the gene was significant after FDR correction in the PLSR component. If the gene was significant, i.e. FDR-adjusted P-value < 0.05, this gene was given a membership of 1, and a membership of 0 if the gene failed to reach significant. The independent varied between the analyses. For the transcriptionally regulated gene lists, the independent variable was the absolute fold-change of the gene if the gene was significant after FDR correction (P_corrected < 0.05). For gene co-expression module analyses, the kME for all the genes which measures the module membership of the gene. For the common

variants, we used the Z scores of the gene-based P-values. Finally, for the rare-variant analyses, if the gene was one of the 65 genes harbouring rare de novo variants (Sanders et al., 2015), the gene was given a membership of 1, and if not a membership of 0. Results of the enrichment analysis are provided in Supplementary Table C.6

Table C.6: Results of the gene enrichment analyses

Discovery (ABIDE 1)						
Category	**Dataset**	**OR**	**Upper CI (95%)**	**Lower CI (95%)**	**P**	**P_corrected**
Autism transcription	Dysregulated	1.21	1.23	1.19	2.00E-16	2.81E-15
Autism transcription	Downregulated	1.87	1.94	1.8	6.74E-13	3.55E-16
Autism transcription	Upregulated	1.01	1.02	1	4.99E-01	4.99E-01
Adult co-expression modules	Mod4	1.08	1.08	1.07	2.00E-16	3.55E-16
Adult co-expression modules	Mod10	1.07	1.08	1.07	2.00E-16	3.55E-16
Adult co-expression modules	Mod16	1.08	1.08	1.07	2.00E-16	3.55E-16
Adult co-expression modules	Mod9	0.93	0.94	0.92	2.01E-14	2.92E-14
Adult co-expression modules	Mod19	0.93	0.94	0.92	2.00E-16	3.55E-16
Adult co-expression modules	Mod20	0.97	0.97	0.96	6.22E-05	7.66E-05
Common variants	Common variants	1	1.01	1	2.75E-01	2.93E-01
Rare variants	Rare variants	0.96	0.99	0.93	2.42E-01	2.76E-01
Fetal co-expression modules	Moddev2	0.97	0.97	0.96	1.28E-11	1.70E-11
Fetal co-expression modules	Moddev3	0.96	0.97	0.96	2.00E-16	3.55E-16
Fetal co-expression modules	Moddev13	1.04	1.04	1.04	2.00E-16	3.55E-16
Fetal co-expression modules	Moddev16	1.06	1.06	1.05	2.00E-16	3.55E-16
Fetal co-expression modules	Moddev17	1.04	1.05	1.04	2.00E-16	3.55E-16
Validation 1 (GU)						
Category	**Dataset**	**OR**	**Upper CI (95%)**	**Lower CI (95%)**	**P**	**P_corrected**

Autism transcription	Downregulated	1.24	1.31	1.18	4.05E-03	4.62E-03
Adult co-expression modules	Mod4	1.06	1.07	1.04	2.49E-05	3.32E-05
Adult co-expression modules	Mod10	1.05	1.06	1.04	2.02E-05	3.23E-05
Adult co-expression modules	Mod16	1.07	1.08	1.06	2.81E-10	5.62E-10
Fetal co-expression modules	Moddev13	1.05	1.06	1.05	8.85E-11	2.36E-10
Fetal co-expression modules	Moddev16	1.07	1.08	1.06	3.47E-12	1.39E-11
Fetal co-expression modules	Moddev17	1.07	1.07	1.06	2.25E-14	1.80E-13
Validation 2 (KKI)						
Category	**Dataset**	**OR**	**Upper CI (95%)**	**Lower CI (95%)**	**P**	**P_corrected**
Autism transcription	Downregulated	1.3	1.45	1.15	6.35E-04	1.10E-03
Adult co-expression modules	Mod4	1.02	1.04	0.99	1.95E-01	1.95E-01
Adult co-expression modules	Mod10	1.04	1.06	1.01	2.48E-03	3.00E-03
Adult co-expression modules	Mod16	1.02	1.04	1	3.16E-02	3.60E-02
Fetal co-expression modules	Moddev13	1.06	1.07	1.04	6.20E-11	4.34E-10
Fetal co-expression modules	Moddev16	1.05	1.05	1.05	1.69E-06	3.94E-06
Fetal co-expression modules	Moddev17	1.05	1.07	1.04	3.04E-09	1.06E-08
Validation_transcription						
Dataset1	**Dataset2**	**OR**	**Upper CI (95%)**	**Lower CI (95%)**	**P**	**P_corrected**
Discovery MRI	Downregulated genes	1.4	1.45	1.34	6.19E-08	1.86E-07
Validation1 MRI	Downregulated genes	1.35	1.44	1.27	3.68E-03	5.00E-03
Validation2 MRI	Downregulated genes	1.3	1.52	1.08	1.97E-02	1.90E-02

C.7 Rank-rank hypergeometric overlap (RRHO) analysis

RRHO is a threshold-free algorithm that is used to identify overlap between two separate gene lists (Plaisier et al., 2010). The algorithm parses two separate ranked lists and identifies overlap at various step sizes as it steps through the lists. It is useful for addressing two problems. First, RRHO is threshold-free, and hence, we do not need to define a statistical threshold for investigating overlap between two gene lists. Second, it is more robust to the size of the gene list. For the Z-scores of the PLSR1 genes in the discovery and validation MRI cohort, we ranked the genes, with the genes having the highest negative Z score having the highest rank. To account for the negative correlation in the ΔCT between the two datasets, and consequently, the negative correlation in gene weights and the Z-scores, we conducted rank- inverse rank overlap, where we inverted the rank of the Z-scores in the validation MRI cohort. RRHO was performed on the online server (http://systems.crump.ucla.edu/rankrank/rankranksimple.php) using a step size of 100 as recommended. We identified a significant overlap in the Z-scores of the PLSR1 genes between the discovery MRI dataset and the validation MRI dataset, after correcting for multiple testing correction using Benjamini-Yekutieli based FDR correction.

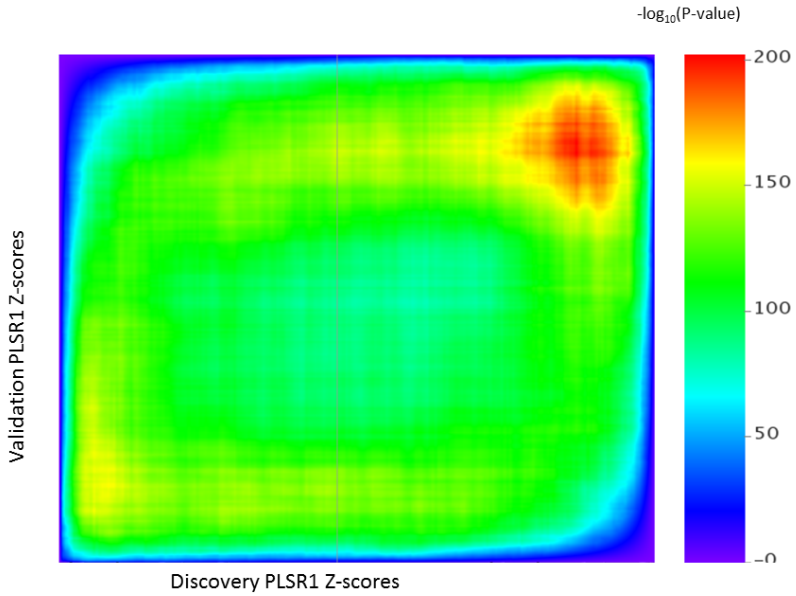

Figure C.7: Rank-rank hypergeometric overlap between the PLSR1 Z-scores of the discovery and validation autism MRI cohorts.

Appendix D Supplementary Material chapter 6

D.1 Procedure and participants

Participants were recruited via online advertisements, the Cambridge Psychology database, local newspaper advertisements and posters spread across Cambridge. None of our participant had a diagnosis of autism or Asperger or related disorder and all participants were of Caucasian origin. Participants were instructed to abstain from alcohol and caffeine on the day of testing and from food and drink, except water, for 2 hours before spray administration. On arrival all participants were informed about the nature of the study and were given the opportunity to ask any questions for clarification. Written informed consent was obtained from all participants. Prior to the first session participants completed the Autism Spectrum Quotient (AQ) (Baron-Cohen et al., 2001) and the Empathy Quotient (EQ) (Baron-Cohen & Wheelwright, 2004). At the start of the first session, participants were administered the Wechsler Abbreviated Scale of Intelligence (WASI; (Wechsler, 1999)) and National Adult Reading Test (NART; (Nelson & Wilson, 1991)). Descriptive statistics on these measures are provided in table D.1.

Before administration of the nasal spray a medical examination including measurements of blood pressure, heart rate, general wellbeing and short medical history was conducted by a GMC registered medical doctor. A pregnancy test was also administered to avoid any potential effects of OXT. A medical professional provided a prescription and remained in attendance to manage any potential adverse effects from the spray. The participants received either the active

or placebo nasal spray (three puffs per nostril, alternating between sides 4IU, 6.72 μg each). Heart rate and blood pressure were also continually monitored during scanning. One participant reported feeling slightly light-headed after the first MRI session. Post-hoc un-blinding revealed that this occurred during the placebo condition. No other side effects were reported. After administration of the nasal spray participants were prepared for MRI scanning and the anatomical MRI commenced approximately 30 minutes after administration, followed by the resting-state sequence 40 minutes after oxytocin administration. This study was part of a larger project and subjects subsequently (e.g. the resting-state was always acquired first) performed 3 short computerized tasks in the scanner that are not reported here. After scanning participants were asked to judge in which order they thought they had received the sprays. None of the participants were confident in their judgment and when pressed 11 out of 25 guessed correctly.

D.2 Image processing

Multi-echo functional images were pre-processed and denoised using the AFNI integrated multi-echo independent component analysis (ME-ICA, meica.py v3, beta1; http://afni.nimh.nih.gov) pipeline (Kundu et al., 2013). This pipeline included: skull-stripping of the anatomical MPRAGE image and warping it to the MNI anatomical template, co-registration of the first TE functional data to compute motion correction and for anatomical-functional co-registration, deobliquing of functional data, 12-paramater affine anatomical-functional co-registration using the local Pearson correlation and T2* weights (lp-t2s) cost function. Each TE functional dataset was slice-time corrected and spatially aligned through application of the anatomically derived alignment matrix using nonlinear warping to MNI

space (MNI152 template) with AFNI 3dQwarp. No temporal filtering or smoothing was applied to the data.

Next, functional data were decomposed into independent components (ICs) as part of the ME-ICA pipeline. Subsequently, ICs were categorized as BOLD or non-BOLD based on their weightings measured by Kappa and Rho values, respectively. Because BOLD signal changes are linearly dependent on echo time (TE), a characteristic of the T2* decay, TE dependence of BOLD signal is used to dissociate BOLD from non-BOLD signal using the pseudo-*F*-statistic, Kappa. ICs that scale strongly with TE have high Kappa scores (Kundu et al., 2013). Conversely, non-BOLD ICs are identified by TE independence measured by the pseudo-*F*-statistic, Rho. By removing non-BOLD ICs, data are denoised for motion, physiological and scanner artefacts in a robust manner based on physical principles (J. W. Evans, Kundu, Horovitz, & Bandettini, 2015; Kundu et al., 2013). One session for one subject had to be excluded due to technical difficulties in the realignment procedure. This subject was removed from subsequent analyses.

D.3 Between-Component Connectivity Analysis

Time courses for each component and subject were used to model between-component connectivity during placebo and oxytocin administration. This was achieved by constructing a correlation matrix of the 22 non-noise components for each subject. Connectivity strength in this correlation matrix was measured as the correlation coefficient after running robust regression (Wager et al., 2005) (https://github.com/canlab/RobustToolbox), to mitigate bias

from outlier time points. We then tested for difference in connectivity strength for placebo versus oxytocin with a paired-sample t-test for each between-component connection. Correction for multiple comparisons was achieved via Bonferroni correction at a family-wise error rate of 5%. For component pairs that survived multiple comparison correction, we computed a difference score between oxytocin and placebo on the Fisher z-transformed correlation statistics (Steiger, 1980). This difference score indicates the size of oxytocin-related connectivity enhancement, with larger scores indicating larger enhancement of connectivity from oxytocin, whereas scores near 0 indicate no difference in connectivity between oxytocin and placebo. To report an effect size for any oxytocin-related effects on connectivity, we computed effect size as the mean of the difference score divided by the standard deviation of the difference score. This effect size is analogous to Cohen's d and indicates the magnitude of effect above a null effect of 0 in units of standard deviation. To get an indication of how variable such an effect size estimate is, we used bootstrapping (1 million resamples) to identify the 95% bias-accelerated bootstrap confidence intervals around our actual effect size estimate. We also used this difference score to test for association with autistic traits as measured by the AQ using robust regression. In past work we have observed that oxytocin tends to have larger effects on individuals have higher levels of autistic traits (Auyeung et al., 2015). Therefore, we made the directional prediction that oxytocin-related effects on connectivity would be positively correlated with autistic traits.

Table D.1: Descriptive statistics on participant sample from administration study

This table show the mean, standard deviations and range of the questionnaire scores obtained during this study. Normality was assessed using the Shapiro-Wilk test of normality and indicated that the assumption against normality should be rejected, in subsequent test we thus used parametric tests (i.e. to assess the correlation of our main outcome measure with AQ).

	Mean	Standard Deviations	Range		Normality	
			Min	Max	W	*p*
WASI	115.3	13.19	90	148	0.956	0.347
NART	118.1	5.04	107	127	0.960	0.411
AQ	14.4	7.32	3	33	0.963	0.475
EQ	55.6	14.53	19	77	0.955	0.330

Table D.2: Descriptive statistics for OXTR expression in females

Descriptive statistics for all female data from the GTEx and BrainSpan datasets. RNAseq data was summarized to RPKM and all descriptives and inferential statistics are based on these RPKM values. Two different one-sample t-tests were performed to compare OXTR expression to 0 and to non-brain (skin) tissue. These tests were performed within a permutation test (1000 permutations) to derive p-values.

	Expression Descriptives				Compared to 0		Compared to skin tissue expression		
Region	n	mean	sd	median	T	P	T	P	Mean Difference
Caudate (basal ganglia)	32	2.51	3.27	1.27	4.33	1.43E-04	4.12	3.64E-04	2.38
Nucleus accumbens (basal ganglia)	34	4.52	3.58	3.60	7.37	1.81E-08	7.17	4.56E-08	4.40
Frontal Cortex (BA9)	31	1.32	1.27	0.88	5.76	2.70E-06	5.23	1.74E-05	1.19
Putamen (basal ganglia)	28	1.98	1.56	1.38	6.73	3.13E-07	6.32	1.20E-06	1.86
Hypothalamus	25	3.23	2.77	2.88	5.82	5.26E-06	5.60	1.14E-05	3.10
Spinal cord (cervical c-1)	28	2.11	2.43	1.22	4.61	8.68E-05	4.34	2.37E-04	1.99
Anterior cingulate cortex (BA24)	23	1.29	0.78	1.05	7.96	6.36E-08	7.21	3.48E-07	1.17
Substantia nigra	24	6.65	10.84	3.92	3.01	6.29E-03	2.95	8.36E-03	6.53
Hippocampus	29	1.12	0.90	0.86	6.69	2.91E-07	5.96	2.75E-06	1.00
Amygdala	22	1.23	0.69	0.96	8.39	3.83E-08	7.55	2.13E-07	1.11
primary motor cortex (area M1, area 4)	8	1.78	0.79	1.43	6.39	3.72E-04	2.83	1.81E-02	1.65
dorsolateral prefrontal cortex	8	1.57	0.81	1.43	5.48	9.28E-04	2.83	1.81E-02	1.45
posterior (caudal) superior temporal cortex (area 22c)	9	1.44	0.85	1.16	5.08	9.49E-04	2.36	3.58E-02	1.32
primary visual cortex (striate cortex, area V1/17)	9	1.37	0.52	1.64	7.85	4.99E-05	2.36	3.58E-02	1.24
anterior (rostral) cingulate (medial prefrontal) cortex	7	1.46	0.51	1.45	7.60	2.70E-04	3.37	9.29E-03	1.33
orbital frontal cortex	8	1.41	0.68	1.26	5.88	6.11E-04	2.83	1.81E-02	1.29
inferolateral temporal cortex (area TEv, area 20)	9	1.69	0.69	1.60	7.29	8.44E-05	2.36	3.58E-02	1.56
primary somatosensory cortex (area S1, areas 3,1,2)	8	1.63	0.82	1.73	5.66	7.70E-04	2.83	1.81E-02	1.51
ventrolateral prefrontal cortex	9	1.69	1.07	1.30	4.75	1.44E-03	2.36	3.58E-02	1.57
cerebellar cortex	9	1.09	0.48	1.10	6.78	1.40E-04	2.36	3.58E-02	0.97
primary auditory cortex (core)	8	1.88	0.63	2.11	8.36	6.89E-05	2.83	1.81E-02	1.75
mediodorsal nucleus of thalamus	8	1.19	0.59	1.20	5.70	7.35E-04	2.83	1.81E-02	1.07
posteroventral (inferior) parietal cortex	9	1.42	0.78	1.15	5.47	5.93E-04	2.36	3.58E-02	1.30

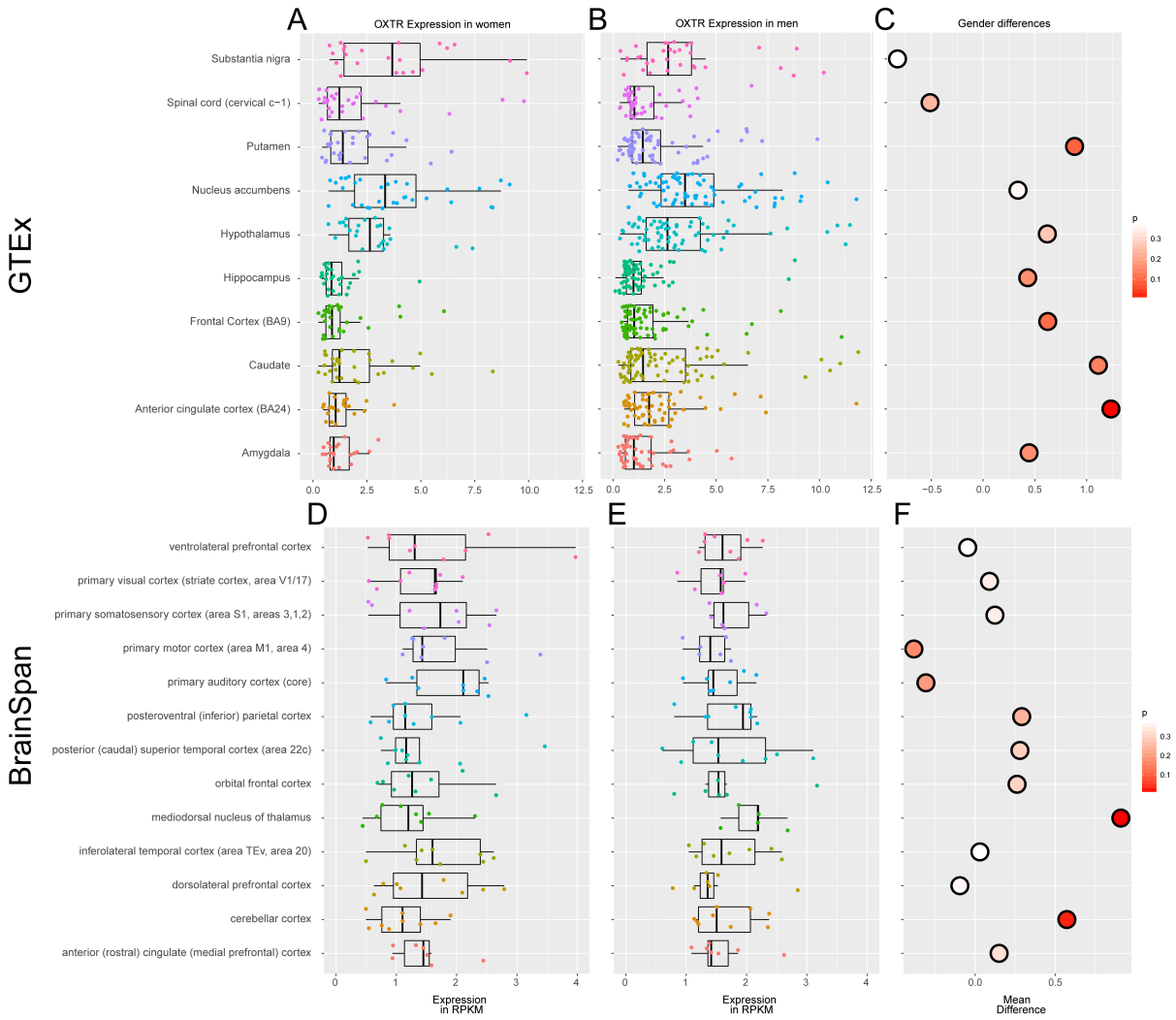

Fig. D.1**:** Gender comparison of OXTR expression

Although our main expression and imaging analyses focused on the oxytocin system in women, we also performed exploratory analyses on potential gender differences in OXTR expression in the same gene expression data-sets. Panels **A** and **D** show the RPKM expression values of OXTR for women, panels **B** and **E** show expression in the same brain regions for men. Panels **C** and **F** show the gender differences. Only the anterior cingulate, medial nucleus of the thalamus and the cerebellar cortex showed significant gender differences ($p<0.05$). In all cases where there was a significant difference men showed slightly higher expression on average. These findings should be considered exploratory as the samples are not matched, the BrainSpan datasets is limited in terms of sample size and there is in general a lot of variability in the expression of the oxytocin receptor.

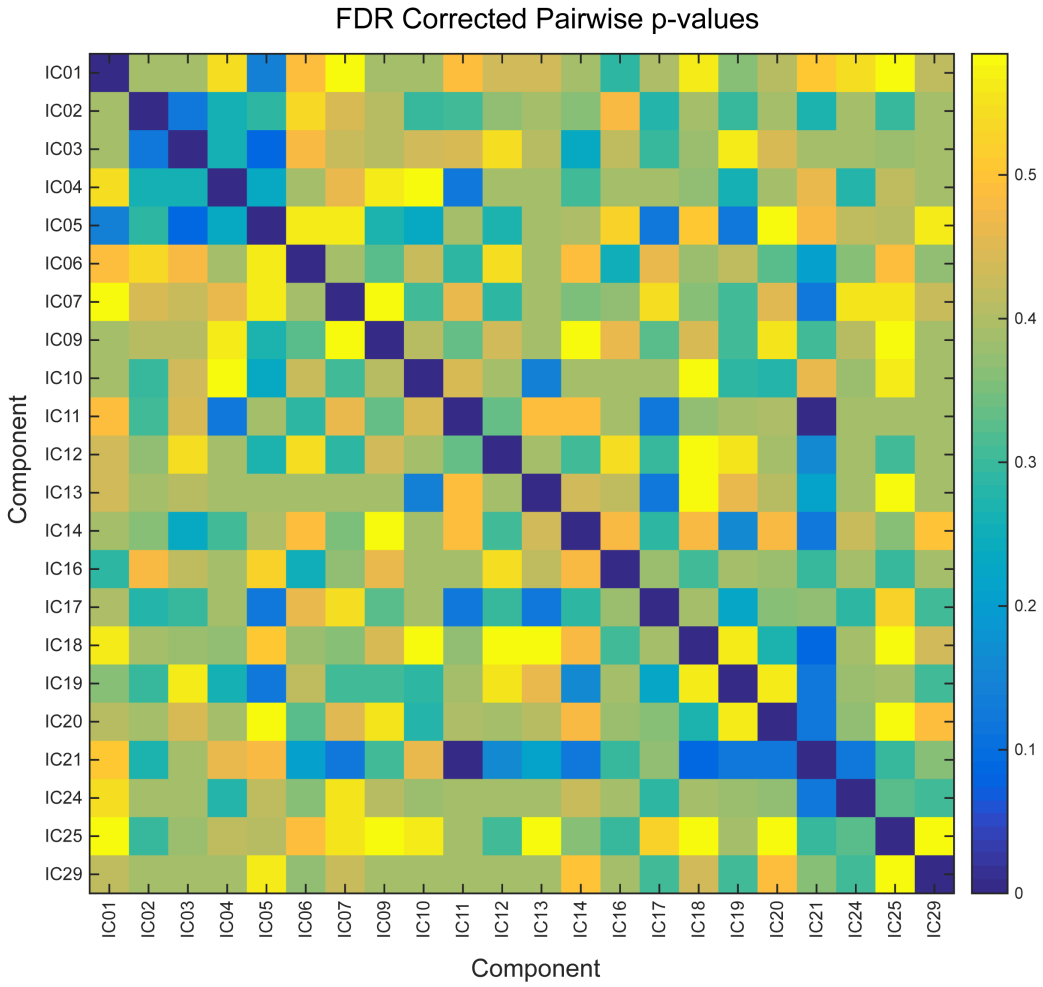

Fig. D.2**:** FDR corrected pairwise comparisons of all components

Only the component pair IC11-IC21 survived multiple comparison corrections, none of the other pairs were significant at $p < 0.05$.

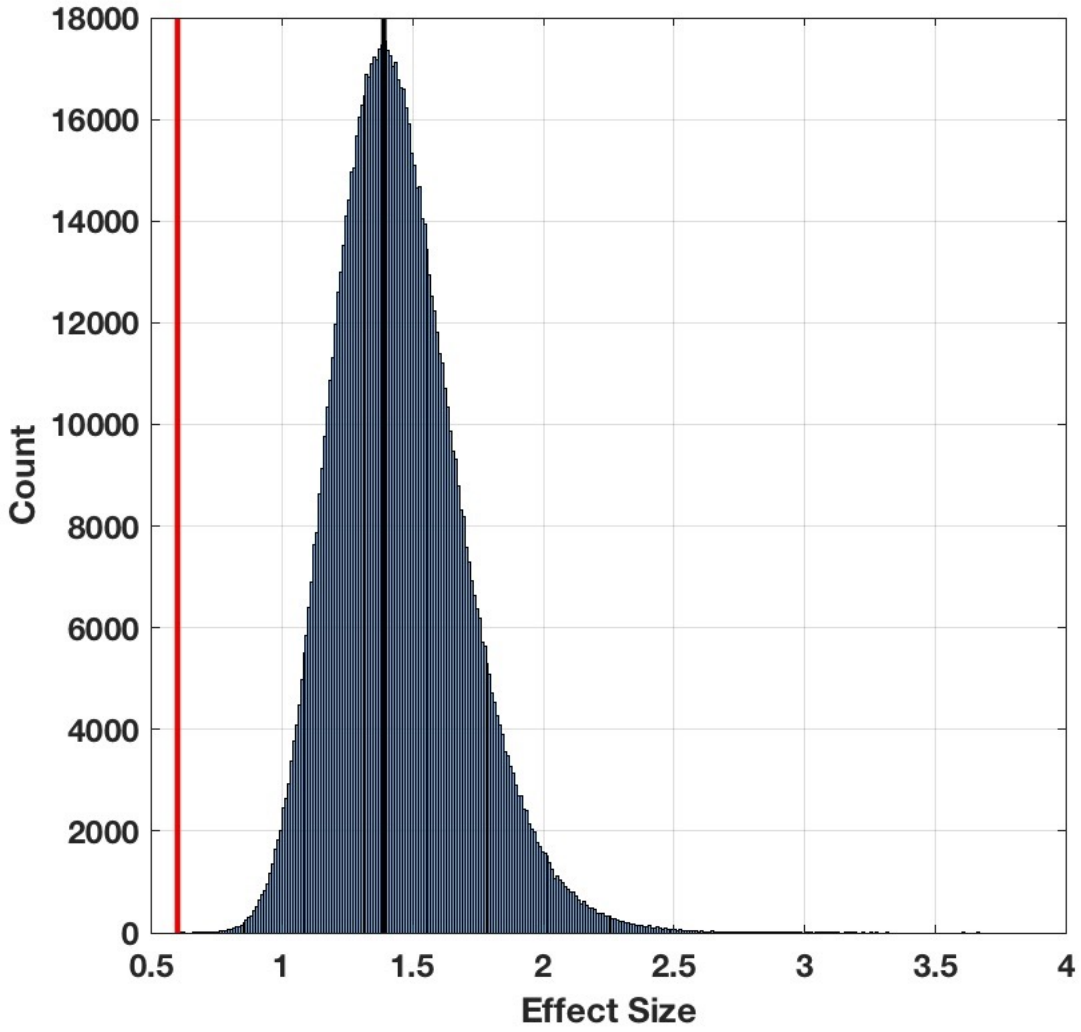

Fig. D.3: Bootstrap effect size distribution for IC11-IC21 effect.

Shows the distribution of effect size estimates calculated after bootstrapping (1 million resamples). The actual estimate is shown with the black vertical line. The red line shows the minimum effect size (d = 0.6) for achieving 80% power at an alpha of 0.05 and n=24.

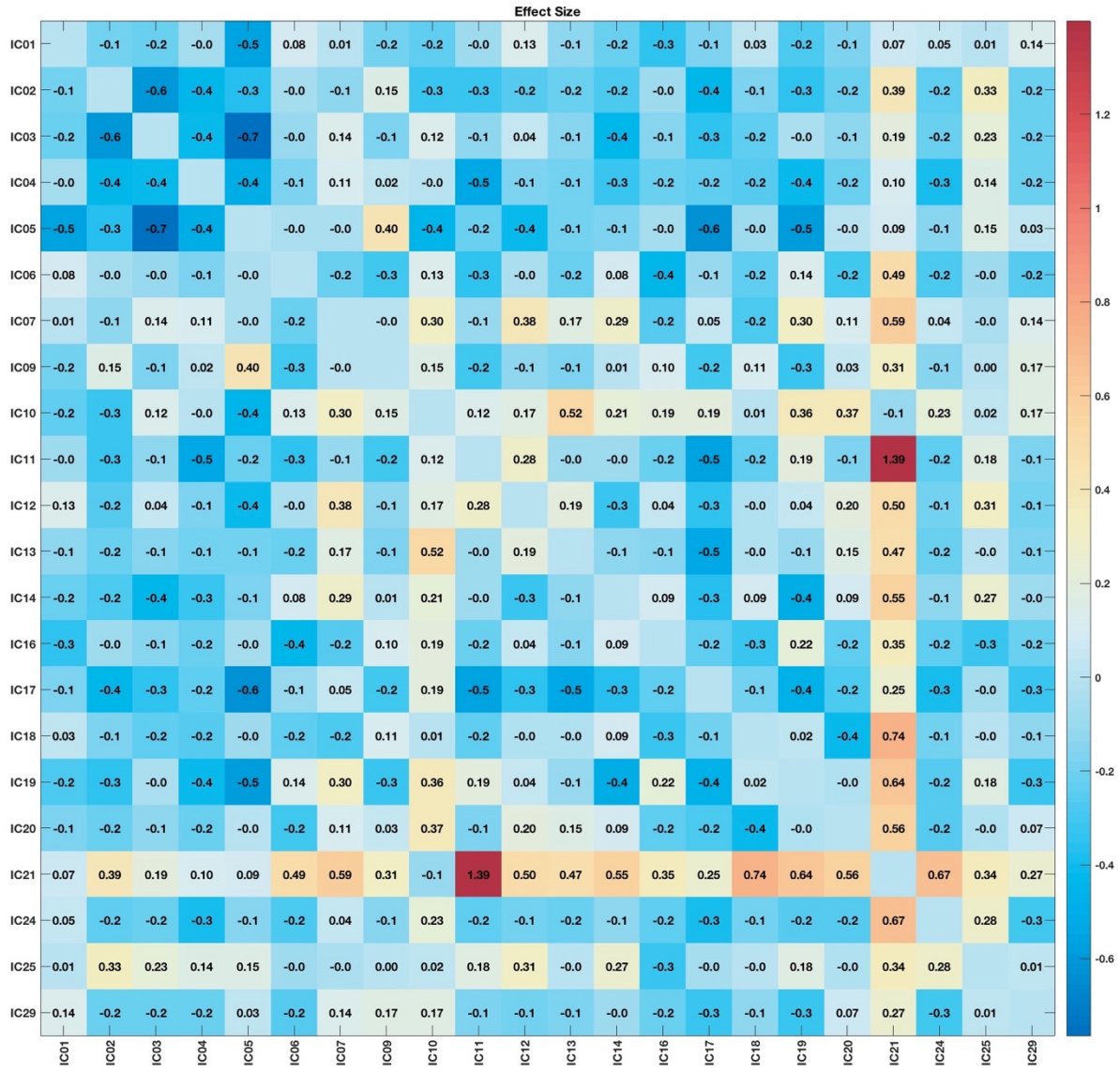

Fig. D.4**:** Effect size estimates for all pairwise comparisons.

Effect size is computed as the mean of the difference score (e.g., oxytocin – placebo) divided by the standard deviation of the difference score. This effect size is analogous to Cohen's d and indicates the magnitude of effect above a null effect of 0 in units of standard deviation.

Appendix E Supplementary Material chapter 7

E.1 Whole-brain effects

In addition to the hypothesis driven resting-state connectivity analysis, we also employed a data-driven approach to investigate potential whole brain effects of testosterone on functional connectivity. Seed-based analyses only focus on very specific networks and connections. In contrast, independent component analysis makes no assumptions about the underlying networks and thus allows a model-free analysis of any potential differences. Analyses were carried out using Probabilistic Independent Component Analysis (Beckmann & Smith, 2004) as implemented in MELODIC (Multivariate Exploratory Linear Decomposition into Independent Components) Version 3.14, part of FSL (FMRIB's Software Library, www.fmrib.ox.ac.uk/fsl). The following steps were applied to the pre-processed wavelet despiked data: masking of non-brain voxels; voxel-wise de-meaning of the data; normalisation of the voxel-wise variance. Pre-processed data were whitened and projected into a 35-dimensional subspace using probabilistic Principal Component Analysis where the number of dimensions was estimated using the Laplace approximation to the Bayesian evidence of the model order (Beckmann & Smith, 2004; Minka, 2001), thus resulting in 35 independent components. The whitened observations were decomposed into sets of vectors which describe signal variation across the temporal domain (time-courses), the session/subject domain and across the spatial domain (maps) by optimising for non-Gaussian spatial source distributions using a fixed-point iteration technique (Hyvärinen, 1999a). Estimated Component maps were

divided by the standard deviation of the residual noise and thresholded by fitting a mixture model to the histogram of intensity values (Beckmann & Smith, 2004). Permutation testing was used to assess potential effects of testosterone across all 35 components, using 5000 permutations and a threshold free cluster enhancement (TFCE) to control for multiple comparison as implemented in FSL's randomise tool (Winkler et al., 2014). No significant clusters were found across any of the 35 identified components.

E.2 Seed-based connectivity effects

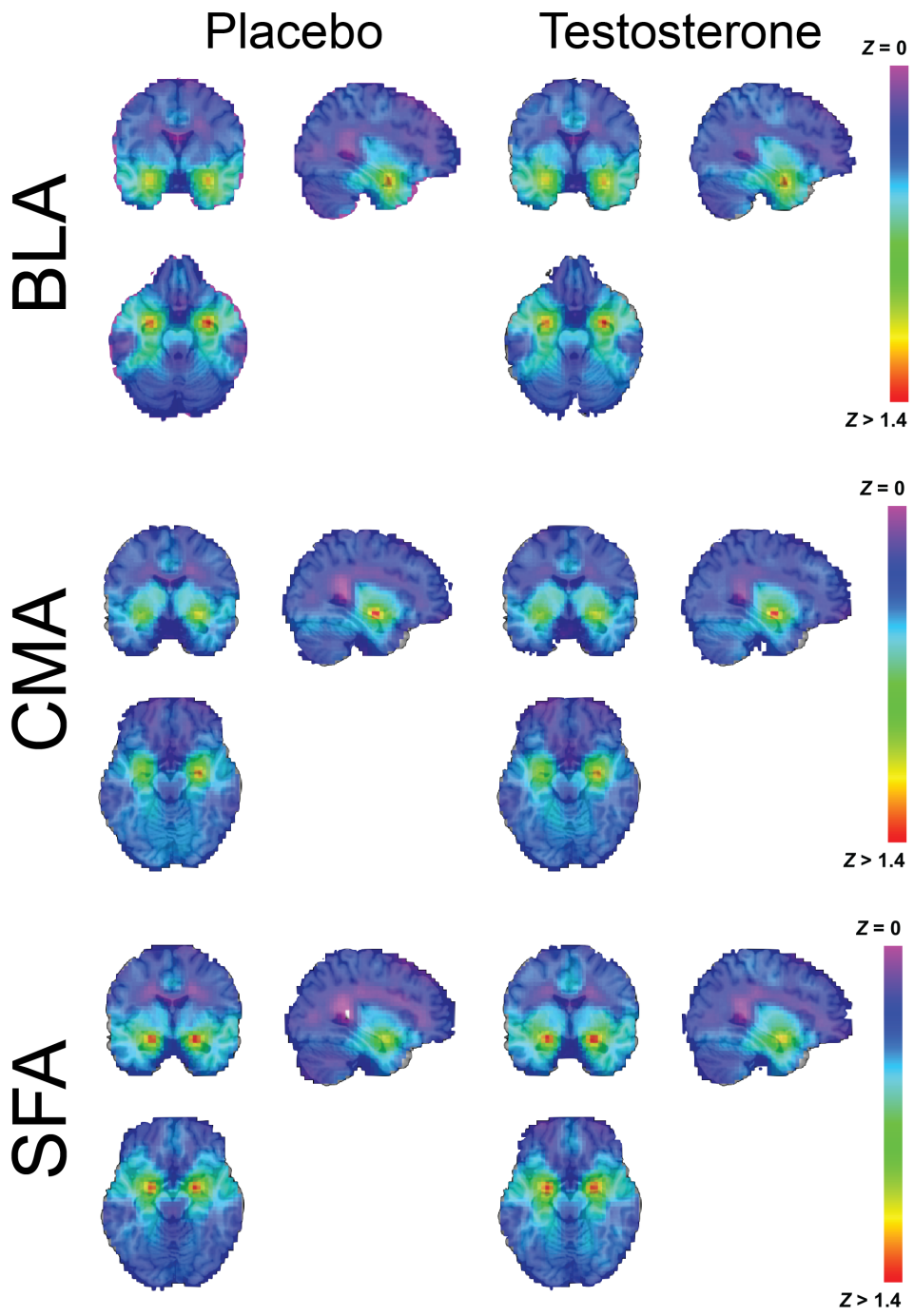

Fig. E.1 Seed-based functional connectivity of the amygdala